Corrections

p6 Scheme 1.3: cytosine should read cytidine, thymosine should read thymidine.

p15 Scheme 1.9

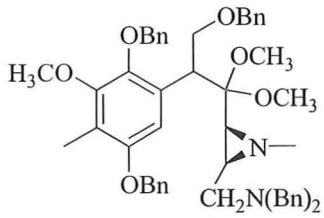

1.51

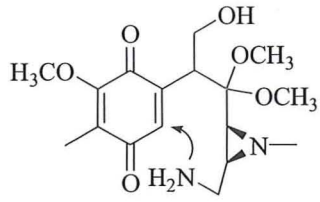

1.52

p24 line 4: Van der Waal

p38 line 5: …which can be carried <u>out</u> using Friedel Crafts….

p42 line 20: *N*-sulfonylindoles **<u>2.2</u>** and 2.46 respectively….

p46 line 4: …in <u>conjunction</u> with the acid chloride….

p51

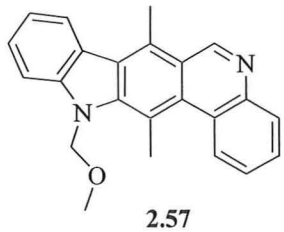

2.57

p68 line 8: …<u>facilitate</u> a population shift….

p71 line 19: …the <u>yield</u> of the desired product was greatly improved

p71 line 21: …triphenylphosphine <u>were</u> utilized….

p74 line 4: …through a +R effect **[Figure 3.3]**.

p163 line 28: **Analytical** Anal. Calcd for <u>$C_{15}H_8N_2O_2$</u>: C, 72.58; H, 3.25; N, 11.28. Found: C, 71.95; H, 3.49; N, 11.25.

THE AUSTRALIAN NATIONAL UNIVERSITY

Synthesis and Structure-Activity Relationship Studies of the Calothrixins and Other Redox-Active Compounds

A thesis presented for the degree of

Doctor of Philosophy

of the

The Australian National University

By

Paul Huntington Bernardo

Department of Chemistry
The Australian National University
Canberra, Australia

December 2004

THE AUSTRALIAN
LIBRARY
NATIONAL UNIVERSITY

Author's Statement

The work described in this thesis is original and has not been submitted for a degree or diploma at any other university. To my knowledge, it does not contain material previously published or presented by any other person except where otherwise acknowledged. The work presented is my own.

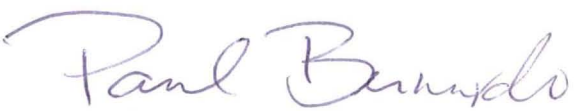

Paul H. Bernardo

10 December 2004

Acknowledgements

I would like to thank all the wonderful people who have made this work possible and have made valuable contributions to my research. First and foremost, I would like to thank my father, Dr. Vicente S. Bernardo, for all the support he has given me these years. A doctor in the family is a powerful influence, and I would like to acknowledge the paramount role my father has in my choice of research.

I would like to thank my supervisor, Dr. Christina L.L. Chai, for all the patience and encouragement she has shown through the years. I think it has been proven that I'm more difficult to work with than most people! I would also like to thank Dr. Paul Waring for all the assistance with the biological assays and theories, and for shedding light on the importance of the results we have obtained. I am very grateful to Prof. John Elix for his kind assistance with HPLC, as well as for useful discussions on organic syntheses. Dr. Geoffrey Smith has also contributed generously to our understanding of the calothrixins, and I would also like to acknowledge his gift of authentic calothrixin A to compare with our own supply of synthetic material. Prof. Rodney Rickards also kindly provided a sample of authentic calothrixin B for comparison as well. Dr. Pauline Junankar very kindly provided us with HeLa cells required to grow our own cultures and offered useful advice on cell culturing.

Among the Chai Group, certain individuals deserve special mention. Felicity Moore, for her great editorial skills in the light of my dismal prose, and commiseration for the ordeals one must go through in the course of a PhD. Paul Huleatt, for heaps of laughs and wide knowledge of useful synthetic procedures, and a passion for coffee second to none! I would also like to acknowledge Maurice LeGuen and Bronwyn Wilkes, whose results complement many of my own findings.

I would like to acknowledge the kindness and hospitality from the staff of the Department of Chemistry, Department of Biology and Molecular Biology, and the Research School of Chemistry. To the technical staff: Geoff, Vance, Mark, Fiona, and Jodie—thanks for all the help with the undergraduates and making the teaching experience bearable! I would like to thank Warren for invaluable advice on PCs—I

think throwing them out the window is still the best way to go! I would like to acknowledge the UNMRC staff, especially Chris Blake for all his help with the 500MHz NMR machine. Special thanks to the Banwell Group at the RSC-- Jasmine, Gwion, and Dan for the wonderful chemistry debates and conversations.

And to all my friends, who have kept me sane these past few years with their lively support and optimistic views. I especially thank Yekta "Mike" Mustafa and Zuraidah Zachariah, my best friends in all of Australia, for all their hospitality and kindness. I would also like to thank my friends Cathleen, Shobha, Lana, Ira, Rick, Magne and Shizuka, Ana, and Priyesh for all the laughs over the years.

And to the incomparable Irina, who has made my last few weeks here in Canberra the most memorable in all the five years I've been here!

Paul Huntington Bernardo
10 December 2004

Abstract

Calothrixin A and B are novel pentacyclic quinones that have been isolated from the *Calothrix* cyanobacteria. The calothrixins exhibit antiproliferative activity against chloroquine resistant strains of *Plasmodium falciparum*, the deadliest causative agent of malaria. Furthermore, these compounds have potent and selective activity against a range of human cancer cell lines. These biological properties have led to the identification of the calothrixins as lead compounds for drug development. A brief review of the calothrixins and other quinones, as well as an overview of Structure-Activity (SAR) and Quantitative SAR studies is presented in Chapter 1.

This thesis details the methodology for the synthesis of the calothrixins and a number of related carbazolediones. A *de novo* synthesis of the quinones was carried out using a combination of metallation and Friedel-Crafts acylation approaches. Calothrixin derivatives were also synthesized for Structure-Activity Relationship (SAR) studies in order to determine the pharmacophore required for biological activity. These synthetic studies are described in Chapter 2.

A combinatorial approach to the synthesis of calothrixin B was also attempted as described in Chapter 3. The strategy utilizes phenanthridine-7,10-dione as a template for further elaboration to calothrixin B. In principle, this synthetic route can be employed in the synthesis of a large number of calothrixin B analogues and/or derivatives.

Chapter 4 describes the SAR and QSAR studies of the calothrixins and related carbazolediones. The antiproliferative activity of the calothrixins and related carbazolediones was measured against HeLa cervical cancer cells using the colorimetric MTT assay. The results obtained in the SAR studies of the carbazolediones were used to elucidate the pharmacophore required for biological activity. QSAR studies were also carried out in order to determine the physicochemical properties of these carbazolediones that are required for biological activity. In particular, the reduction potentials as well as lipophilicity of the carbazolediones were measured and compared to the antiproliferative activities.

The ability of calothrixin A to undergo one-electron reduction to the semiquinone radical anion led to the hypothesis that calothrixin A may accumulate in cells. This mechanism of redox-driven accumulation of compounds was first observed in our SAR and QSAR studies of the epidithiopiperazine-2,5-diones (ETP compounds). These studies have led to the proposal that there is a relationship between the reduction potential of ETP compounds and the intracellular concentration of these toxins leading to redox-driven biological accumulation of the ETP compounds. To determine if the cellular accumulation of calothrixin A is driven by a similar process, uptake studies were carried out. This work is described in detail in Chapter 5.

The details of the procedures for experiments carried out in Chapters 2 to 5 are given in Chapter 6, along with the relevant data used to characterize the synthetic compounds.

List of Publications and Presentations

Some of the work reported here has been published in the literature, or presented as a poster at a conference.

Publications

Bernardo, P. H., C. L. L. Chai, et al. (2002). "A simple and concise route to calothrixin B." Tetrahedron Lett. **43**: 2939-2940.

Bernardo, P. H., N. Brasch, et al. (2003). "A Novel Mechanism for the Gluatathione Dependent Reversible Uptake of a Fungal Toxin in Cells." J. Biol. Chem. **278**(47): 46549-46555.

Bernardo, P. H. and C. L. L. Chai (2003). "Friedel-Crafts Acylation and Metalation Strategies in the Synthesis of Calothrixins A and b." J. Org. Chem **68**: 8906-8909.

Bernardo, P. H., C. L. L. Chai, et al. (2004). "Synthesis, Electrochemistry, and Bioactivity of the Cyanobacterial Calothrixins and Related Quinones." J. Med. Chem. **47**: 4958-4963.

Posters

"Chemical and Biological Properties of 3,6-Epidithiopiperazine-2,5-diones." Presented at the World Chemistry Congress, Brisbane, Australia 2001.

"Synthesis of Calothrixins and Related Analogues." Presented at the 14th International Conference on Organic Synthesis, Christchurch, New Zealand 2002.

Table of Contents

Title page i
Author's Statement ii
Acknowledgements iii
Abstract v
Publications and Poster vii
Table of Contents viii
Abbreviations xii

Chapter 1

1.1 Background 1
1.2 Biological Modes of Action of the Quinones 4
1.3 The Calothrixins and Related Alkaloids 8
1.4 Literature Syntheses of Quinones and Carbazolediones 12
1.5 Structure-Activity Relationship (SAR) Studies 18
1.6 Physicochemical Parameters and Quantitative Structure-Activity Relationship Studies 21
1.7 Project Aims and Objectives 26
1.8 Bibliography 27

Chapter 2

2.1 Introduction 32
2.2 Synthesis of Quinoline-3,4-anhydride 38
2.3 Investigation of Methods for the Acylation of Indole 41
2.3.1 Friedel-Crafts Acylation of N-Protected Indoles 42
2.3.2 Friedel-Crafts Acylation of Unprotected Indole 43
2.3.3 Model Studies in the Metallation of the Indolic C3-Position 44
2.3.4 *N*-Metallation of Indole and Coupling to Acid Chlorides 46
2.4 *N*-Protection of the Aryl Ketone and Cyclization 46
2.5 Removal of the *N*-Methoxymethyl Group 49
2.6 Synthesis of Calothrixin Derivatives and Carbazoledione Analogues 50
2.6.1 Synthesis of N12-Substituted Calothrixin B 51

2.6.2 Synthesis of 9-Methoxy-*N*-methoxymethyl Calothrixin B 53
2.7 Conclusion 57
2.8 Bibliography 59

Chapter 3

3.1 Introduction 61
3.2 Synthesis of the Phenanthridine-7,10-dione Template 66
3.3 Model Studies on the Reactivity of the Phenanthridine-7,10-dione Template and Related Quinones 73
3.4 Synthesis of the 8-Bromophenanthridine-7,10-dione Template 80
3.5 Conclusion 83
3.6 Bibliography 84

Chapter 4

4.1 Introduction 85
4.1.1 The Role of Redox Potentials in the Biological Activity of Quinones 85
4.1.2 The Role of Steric Parameters in the Biological Activity of Quinones 86
4.1.3 The Role of Lipophilicity in the Biological Activity of Quinones 87
4.2 Antiproliferative Activity of the Calothrixins and Related Quinones Against HeLa Cells 89
4.2.1 Antiproliferative Properties of Calothrixin B and Related Carbazolediones 91
4.2.2 Antiproliferative Activity of Calothrixin B Derivatives 92
4.3 Electrochemistry of the Carbazolediones and Correlation of Electrochemical Results to Biological Activity 96
4.3.1 Comparison of $E_{1/2}^{I}$ Values of the Calothrixins and Related Carbazolediones 100
4.3.2 Comparison of $E_{1/2}^{II}$ Values of the Calothrixins and Related Carbazolediones 104
4.3.3 Comparison of lnK Values of the Calothrixins and Related Carbazolediones 105
4.3.4 Comparison of the Overall Reduction Potential of the Calothrixins and Related Carbazolediones 107
4.4 Lipophilicity and Correlation of LogP Values to Biological Activity 109
4.5 Conclusion 115

Chapter 5

5.1 Introduction 120
5.2 Measurement of the Lipophilicities of the ETP Compounds 123
5.3 Measurement of ETP Reduction Potentials via Thiol-Disulfide Exchange Reactions 125
5.4 Biological Accumulation of Calothrixin A 130
5.5 Conclusions 133
5.6 Bibliography 135

Chapter 6

6.1 General Experimental 137
6.2 Experimental Procedures and Data for Chapter 2 139
6.2.1 Procedures for the Synthesis of Quinoline-3,4-anhydride 139
6.2.2 General Procedure for the Methanolysis of Anhydrides 140
6.2.3 Procedure for the Preparation of Indole Derivatives 142
6.2.4 General Procedure for the Preparation of Acid Chlorides 143
6.2.5 Procedures for the Coupling of Indole Derivatives to Acid Chlorides 144
6.2.6 General Procedure for the *N*-MOM Protection of the Indole Derivatives 150
6.2.8 General Lithiation of *N*-MOM Protected Quinone Precursors 155
6.2.9 Procedures for the Synthesis of N-Unsubstituted Carbazolediones 158
6.2.10 Synthesis of Calothrixin A 164
6.2.11 Preparation of N-Substituted Calothrixins from Calothrixin B 164
6.2.12 Deuterium Labeling Studies of Metallated Indoles 168
6.3 Experimental Procedures and Data for Chapter 3 170
6.3.1 Procedures for the Synthesis of 3-Bromo-2, 5-Dimethoxybenzaldehyde 170
6.3.2 Procedures for the Synthesis of 2,5-Dimethoxybenzoic Acid and 3-Bromo-2,5-dimethoxybenzoic Acid 171
6.3.3 Preparation of Secondary Benzamides 172
6.3.4 Preparation of Tertiary Benzamides 174
6.3.5 Palladium-Mediated Cyclization of Tertiary Benzamides 176
6.3.6 Preparation of 7,10-Dimethoxyphenanthridine 177
6.3.7 Preparation of Phenanthridine-7,10-dione 178

6.3.8 Preparation of Anilinophenanthridine-7,10-dione and Palladium-Catalyzed Cyclization to Calothrixin B and Iso-calothrixin B 179
6.4 Experimental Procedures and Data for Chapter 4 181
6.4.1 Lipophilicity Measurements via High Performance Liquid Chromatography 181
6.4.2 Experimental Protocols for Biological Experiments 181
6.5 Experimental Procedures for Chapter 5 183
6.5.1 Thiol-Disulfide Exchange Studies for the ETP Compounds via HPLC 183
6.5.2 Uptake Studies of Calothrixin A Measured by HPLC 186

Appendices

Appendix A: QSAR Output from SigmaPlot 189
Appendix B: Selected NMR Spectra of Synthetic Intermediates and Products 195

Abbreviations

Å	angstrom units
Anal.	Analysis
Aq.	aqueous
n-BuLi	*normal*-butyl lithium
s-BuLi	*secondary*-butyl lithium
t-BuLi	*tertiary*-butyl lithium
°C	degrees centigrade
Calcd	calculated
CAN	cerium (IV) ammonium nitrate
^{13}C-NMR	carbon-13 Nuclear Magnetic Resonance spectroscopy
$CDCl_3$	deuterated chloroform
cm^{-1}	wavenumber, per centimeter
m-CPBA	*meta*-chloroperbenzoic acid
CySH	L-cysteine
CySSCy	cystine
DCM	dichloromethane, CH_2Cl_2
DMD	double-mixed disulfide
DMF	*N,N*-dimethylformamide
d-DMSO	deuterated dimethylsulfoxide, $(CD_3)_2SO$
DMSO	dimethyl sulfoxide
DNA	deoxyribonucleic acids
DTT	dithiothreitol
EC_{50}	Effective Concentration to inhibit cell proliferation by 50%
EDTA	ethylenediaminetetraacetic acid
EIMS	Electron Impact Mass Spectrometry
F	Faraday's constant
FMO	Frontier Molecular Orbital
FTIR	Fourier-Transform Infrared spectroscopy
GSH	glutathione
GSSG	oxidized glutathione
h	hour(s)
^{1}H-NMR	proton Nuclear Magnetic Resonance spectroscopy
HMBC	Heteronuclear Multiple Bond Correlation

HMQC	Heteronulcear Multiple Quantum Correlation
HOMO	Highest Occupied Molecular Orbital
HPLC	High Performance Liquid Chromatography
HRMS	High-resolution mass spectrometry
Hz	frequency in Hertz
IR	infrared spectrum
L	litres
LHMDS	lithium hexamethyldisilazide
LDA	lithium diisopropylamide
LiTMP	lithium 2,2,6,6-tetramethylpiperazide
ln	natural logarithm
log	logarithm, base-10
LUMO	Lowest Unoccupied Molecular Orbital
M	molarity, mol/L
min	minute(s)
MMD	mono-mixed disulfide
MTT	3-(4,5-dimethylthiazol-2-yl)-2,5-diphenyl-2*H*-tetrazolium bromide
m/z	mass to charge ratio
mol	moles
NaH	sodium hydride
MeMgCl	methyl magnesium chloride
MOMCl	methoxymethyl chloride
MP	melting point
OAc	acetate
PBS	phosphate-buffered saline
P(*o*-tolyl)$_3$	tris(*ortho*-tolyl)phosphine
PPh_3	triphenylphosphine
ppm	part per million
QSAR	Quantitative Structure-Activity Relationship
R	universal gas constant
R_f	retardation factor
RNA	ribonucleic acids
ROS	reactive oxygen species
SAR	Structure-Activity Relationship

T	temperature, in Kelvin (K) units for thermodynamic equations
TLC	thin-layer chromatography
THF	tetrahydrofuran
TMEDA	*N,N,N'N'*-tetramethylethylenediamine
TMS	tetramethylsilane
UV Vis	Ultraviolet and Visible wavelength spectroscopy
V	Volts

Chapter 1

1.1 Background

Living organisms must compete against other organisms in order to survive. To aid in their survival, these organisms may produce a wide range of natural products. These natural products include the primary metabolites which are essential to the basic functions of growth and reproduction. Primary metabolites are utilized in intracellular processes for the production of energy and cellular materials which are necessary to sustain life.[1] In addition to primary metabolites, different organisms may produce unique chemicals whose functions are less clearly delineated, but which are presumed to play a role in chemical defense mechanisms. These secondary metabolites often display selective toxicity towards foreign organisms, and provide the original host with a comparative advantage in the struggle for survival.[1] Secondary metabolites are therefore of great interest to organic chemists and medicinal chemists due to the interesting biological properties that these compounds may possess.[2]

Many of these secondary metabolites have been identified and utilized in modern medicine. Penicillin G (**1.1**) has been isolated from various *Penicillium* species and represents one of the most important classes of antibiotics, the β-lactam antibiotics.[3] The bacteriocidal properties of the latter is due to the strained β-lactam ring which interferes with the biosynthesis of the bacterial cell wall.[4] The discovery of penicillin was a landmark in medical history which led to a dramatic decrease in post-surgical deaths caused by bacterial infection. Artemisinin (**1.2**), from the Chinese herb Qinghaosu (wormwood, *Artemesia annua L. Compositae*),[5] has shown potent activity against the *Plasmodium* parasite which causes malaria, a leading cause of death in Third World countries.[6,7] It has recently been approved for Phase II clinical trials in the USA for the treatment of malaria.[7] The marine alkaloid cytarabine (**1.3**), first isolated from the Carribean sponge, *Cryptotethia crypta*, has been employed as a chemotherapeutic agent against acute leukemia and lymphomas.[8,9] Cytarabine is often used in conjuction with other chemotherapeutic drugs to prevent the remission of cancers, often with remarkably high success rates.[10] The naphthoquinone lapachol (**1.4**), from the South American tree *Tabeburia impetiginosa*, has been used against a range of cancers including lung, breast and colon cancer. Although the National Cancer Institute deemed lapachol too toxic for clinical trials, this quinone has been used in South America for over a century to treat fevers and skin disorders.[11]

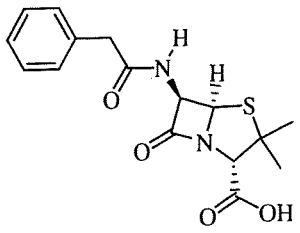

1.1

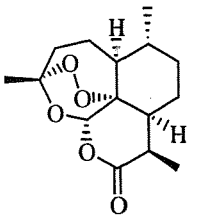

1.2

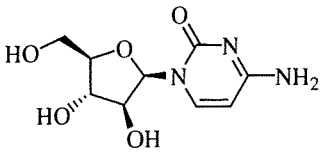

1.3

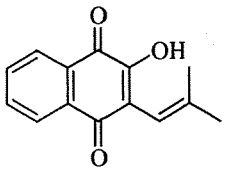

1.4

In general, the quinones are a remarkable class of bioactive compounds, and many are known to possess anticancer, anti-oxidant, and anti-inflammatory properties. Quinones are classified as *ortho*-quinones (**1.5**) which contain the cyclohexa-3,5-diene-1,2-dione moiety, or *para*-quinones (**1.6**) which possess the cyclohexa-2,5-diene-1,4-dione moiety.[12]

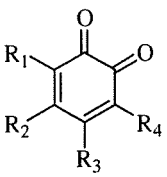

1.5

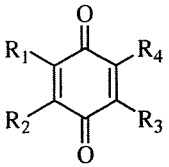

1.6

Several quinones have been approved for medicinal purposes. The anthracyclic quinone daunomycin (**1.7**), from the fungus *Streptomyces peucetius*,[13] is known for its potent and selective cytotoxicity towards cancer cells.[14] The anticancer property of daunomycin has led to its developments as an important chemotherapeutic drug in the treatment of acute leukemia.[15,16] The fungal metabolite mitomycin C (**1.8**), isolated from *Streptomyces caespitosus* in the 1950s, is an antitumor as well as antibiotic quinone which has proven efficacy against a wide range of human cancer cell lines such as WiDr colon, 2780 ovarian, and MCF-7 breast cancer cells.[17-19] Although mitomycin C has been approved for clinical use as an anticancer agent, its high toxicity makes it difficult to administer to patients.[17,20]

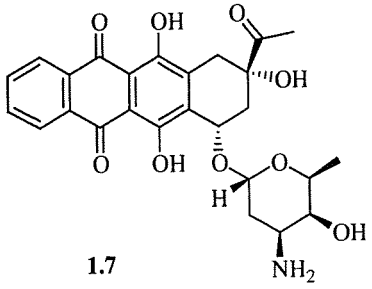

1.7

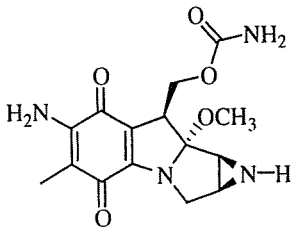

1.8

The acute toxicity of some natural products often limits their pharmacological applications. These compounds have a low therapeutic index, which is a measure of the safety of a particular drug. The therapeutic index is calculated as the ratio between the toxic (lethal) dose level in 50% of the cases studied (LD_{50}) and the effective (beneficial) dosage in 50% of the cases studied (ED_{50}) [therapeutic index=LD_{50}/ED_{50}]; therefore, a large therapeutic index reflects an effective treatment at low doses and a lethal effect at higher doses. A large therapeutic index thus reflects a low risk of undesirable side effects. In cases where the natural products are too toxic, these secondary metabolites can be used as lead compounds for drug discovery in order to develop a derivative or analogue with a higher therapeutic index.[2,21]

Several quinones have been identified as lead compounds for drug discovery. Streptonigrin (**1.9**), from the fungus *Streptomyces flocculus*, has potent antineoplastic activity against several cancer cell lines[22] as well as antiviral properties.[23] The phenanthrenequinone denbinobin (**1.10**) from the plant *Dendrobium moniliforme* has powerful antitumor and anti-inflammatory activity.[24,25] Perfragilin B (**1.11**) is a marine metabolite isolated from the bryozoan (sponge), *Membranipora perfragilis*.[26] This compound has shown potent cytotoxicity towards murine P388 leukemia, renal, and breast cancer cells.[27] It is therefore evident that naturally occurring quinones provide medicinal chemists with many opportunities for drug discovery and development.

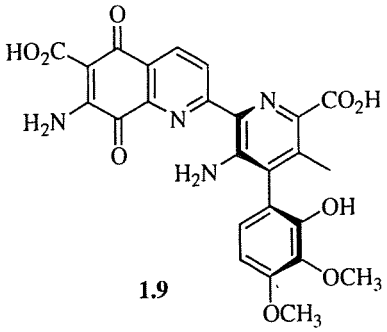

1.9

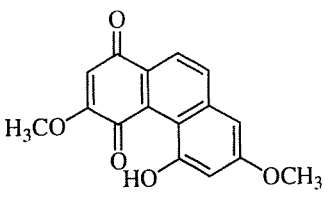

1.10

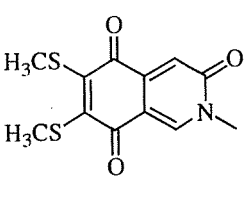

1.11

1.2 Biological Modes of Action of the Quinones

Several mechanisms have been proposed to account for the observed biological activities of the quinones.[28,29] The redox cycling mechanism, outlined in **Scheme 1.1**, is of particular importance. The first step in this process is triggered by the reduction of the quinone **1.6** by cellular reductants to the semiquinone radical **1.12**, followed by a second one-electron reduction to the hydroquinone **1.13**. Alternately, the two-electron reduction of the quinone to the hydroquinone is also known to occur in the presence of NADH and an appropriate enzyme such as the quinone reductase, DT-diaphorase.[29-31] Molecular oxygen is subsequently reduced by the hydroquinone to yield the superoxide radical anion ($O_2^{\cdot-}$) with the concomitant formation of the semiquinone radical anion **1.12,** which in turn may reduce another molecule of oxygen to yield another equivalent of the superoxide radical anion and regenerate the quinone **1.6**. The quinone **1.6** can then be reduced and the process repeated. Under normal cellular conditions, small amounts of the superoxide radical anion are detoxified through enzymatic processes.[32] In the first enzymatic process, the superoxide radical anion is converted by superoxide dismutase (SOD) to hydrogen peroxide H_2O_2. In the second enzymatic process, hydrogen peroxide is converted to water and molecular oxygen by the enzyme catalase, thus negating its toxic effects.[33] However, when hydrogen peroxide accumulates in the cell, it can react with the superoxide radical anion via the Haber-Weiss reaction to yield the hydroxide anion (HO^-), hydroxyl radical ($HO^{\cdot}$), and molecular oxygen. It has also been demonstrated that hydrogen peroxide can react directly with Fe(II) to yield the hydroxide anion (HO^-), hydroxyl radical ($HO^{\cdot}$) and Fe(III) via the Fenton reaction.

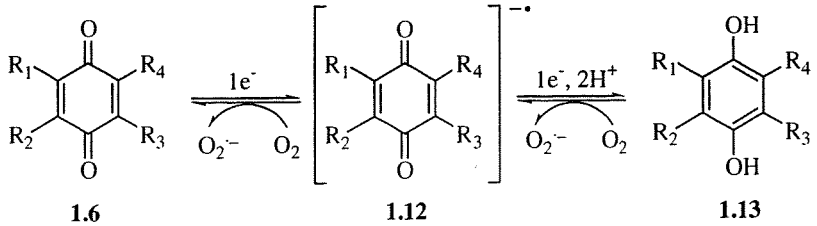

1.6 **1.12** **1.13**

$$O_2^{\cdot-} \xrightarrow{SOD} H_2O_2$$

$$2\,H_2O_2 \xrightarrow{catalase} 2\,H_2O + O_2$$

$$H_2O_2 + O_2^{\cdot-} \longrightarrow HO^- + HO^{\cdot} + O_2 \quad [\text{Haber-Weiss Reaction}]$$

$$H_2O_2 + Fe(II) \longrightarrow HO^- + HO^{\cdot} + Fe(III) \quad [\text{Fenton Reaction}]$$

Scheme 1.1

The superoxide radical anion, hydrogen peroxide, and hydroxyl radical are examples of reactive oxygen species (ROS), which in large concentrations are deleterious to the cell. The hydroxyl radical is particularly reactive and has been implicated in the destructive oxidization of a number of cellular molecules, thereby abrogating their function. For example, hydroxyl radicals have been involved in lipid peroxidation, oxidative DNA damage, and the oxidation of protein thiol (SH) residues.[28]

Michael addition reactions are another mechanism by which quinones exert their biological effects **[Scheme 1.2]**.[28] Quinones with unsubstituted α-positions are excellent Michael acceptors for various nucleophiles.[34] The reduction of the quinone to its quinol form is accomplished by the addition of a nucleophile to the α-position of the quinone. For example, menadione **1.14** is reduced by cellular glutathione **1.15** (GSH, γ-glutamyl-cysteinyl-glycine) to give the thioether **1.16**.[29,35] These adducts are formed within the cell as a means to detoxify foreign substances (xenobiotics) via thioalkylation and subsequent excretion of the adduct from the cell.[36] However, large concentrations of xenobiotic quinones may deplete cellular glutathione which in turn may lead to cell death.[28,37,38] Quinones have been shown to react with the nucleophilic residues in proteins such as cysteine thiols (SH), serine hydroxyls (OH), and free amine (NH_2) residues thus altering the normal protein function.[28,39] Furthermore, reduction of the quinone via thioether formation gives the quinol **1.16**, which can then react with molecular oxygen and induce redox cycling within the cell.[28,29,35,40]

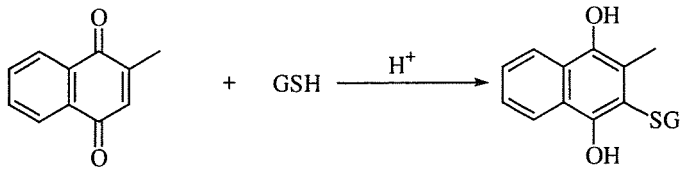

1.14 **1.16**

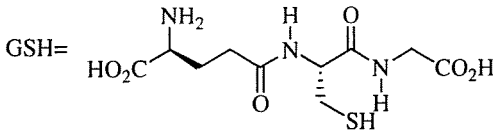

1.15

Scheme 1.2

The intercalation of quinones with DNA accounts for the third mechanism of bioactivity.[41] The insertion of polycyclic quinones such as the anthraquinone **1.17** into

the minor or major grooves of supercoiled DNA is known to produce stable quinone-DNA complexes through the resulting π-stacking interactions between the quinone and the DNA bases.[42] Studies have demonstrated that the resulting DNA complex interferes with topoisomerases thus preventing DNA transcription and translation.[16,28,42,43] Once the cell has lost its ability to produce the DNA-encoded templates required for protein synthesis, cellular growth is arrested and cell death may ensue. Furthermore, the DNA-intercalated quinone may undergo redox cycling to generate ROS in close proximity to this important biomolecule, and the hydroxyl radicals produced can oxidize the nucleotide guanosine to 8-oxo-2'-deoxyguanosine (**1.18**). Generally, the guanosine nucleotide is base-paired with cytosine. However, oxidation of guanosine to **1.18** results in a preferential base-pairing of **1.18** with adenosine instead of cytosine which may lead to potentially deadly mutations **[Scheme 1.3]**.[41,44] Furthermore, the hydroxyl radicals generated also cause oxidative damage leading to DNA strand scission. These interactions of quinones with DNA may thereby result in cytotoxic activity.[16,41,44]

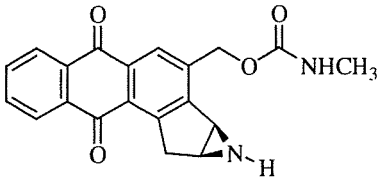

1.17

Normal Base-Pairing *via* Hydrogen Bonding in DNA

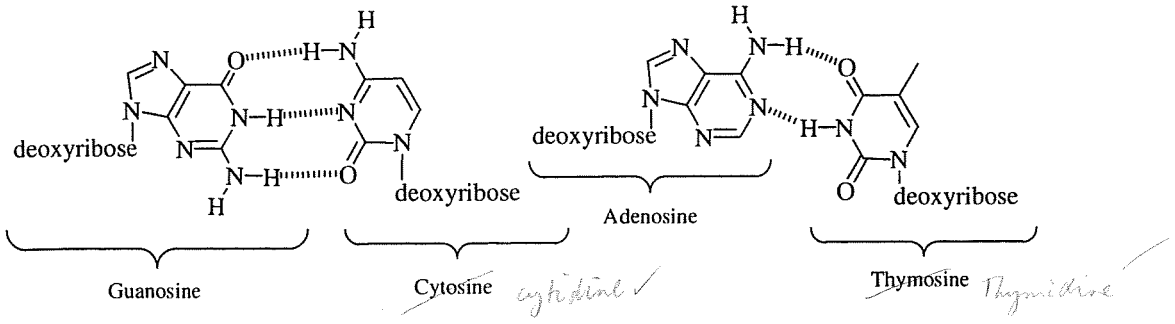

Mismatched Base-Pairing in DNA by 8'-oxo-2-deoxyguanosine

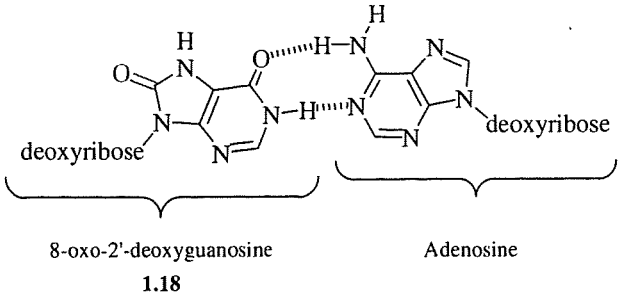

1.18

Scheme 1.3

It has been demonstrated that many quinones act through one or a combination of these three main mechanisms. In addition to these primary mechanisms, some quinones may act through novel mechanistic pathways. Mitomycin C, for example, has been shown to intercalate with DNA and react with cellular reductants to form the quinol **1.19**, and may induce redox cycling within the cell. [45] Furthermore, as **Scheme 1.4** illustrates, the intramolecular nucleophilic displacement of the C9a-methoxy substituent from the quinol **1.19** is known to give the reactive intermediate **1.20**. The reactive intermediate is attacked by nucleophiles at the C1-position thus giving rise to the mitosene derivative **1.21** which can undergo further nucleophilic attack at the C10-position with the concomitant displacement of carbamic acid to give the adduct **1.22**.[46] Since the quinone is confined to the proximity of DNA bases by π-stacking interactions, the incipient nucleophiles are generally nucleotide bases thus resulting in covalent crosslinking of the complementary DNA strands.[47,48] The covalent modification of DNA could inhibit DNA replication and transcription which may lead to cell growth arrest and ultimately, cell death. [19,45,46]

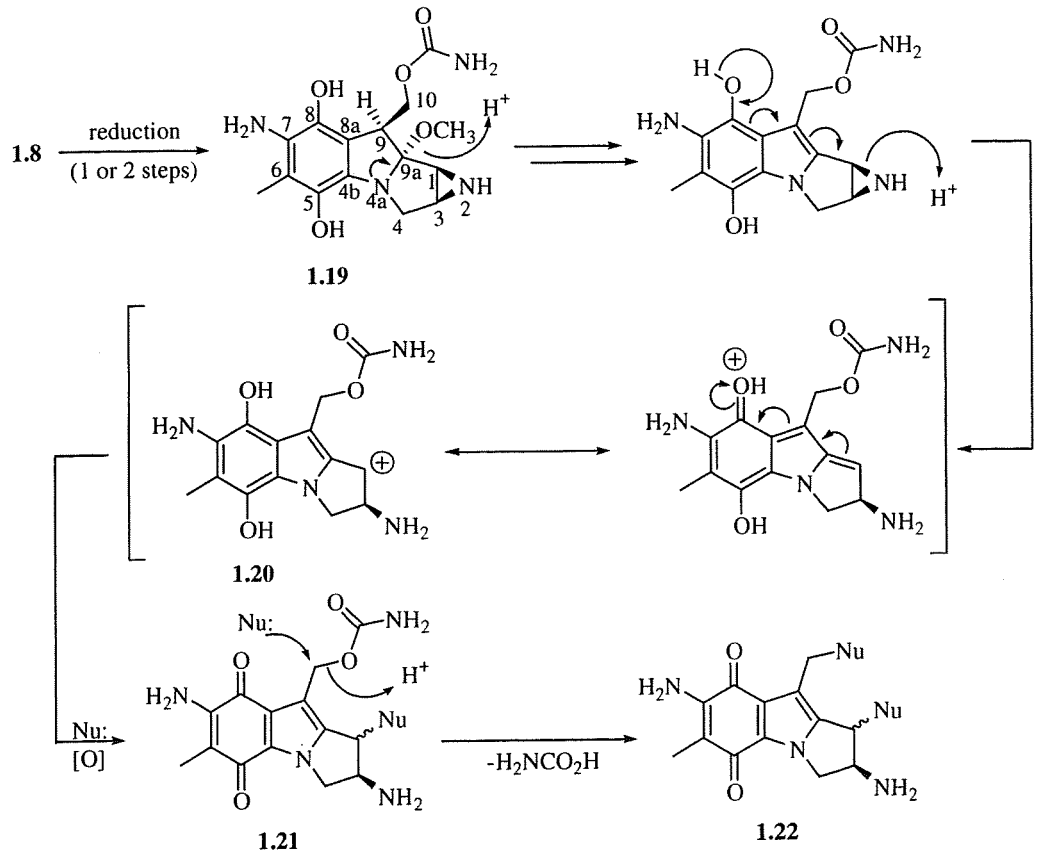

Scheme 1.4

The polymodal mechanisms of biological activity for daunomycin (**1.7**) have also been investigated extensively. In addition to DNA intercalation and the redox-cycling process,[49,50] daunomycin has been shown to eliminate the arabinose moiety to form a reactive electrophilic methide species **1.23** following the initial reduction of the quinone **1.7** to the quinol **1.24**.[16] The methide **1.23** is then attacked by nucleophiles to give the adduct **1.25**. This mechanism tethers the quinone to DNA where it can undergo redox cycling to generate ROS as mentioned earlier, thus giving rise to the cytotoxic effects observed.[16]

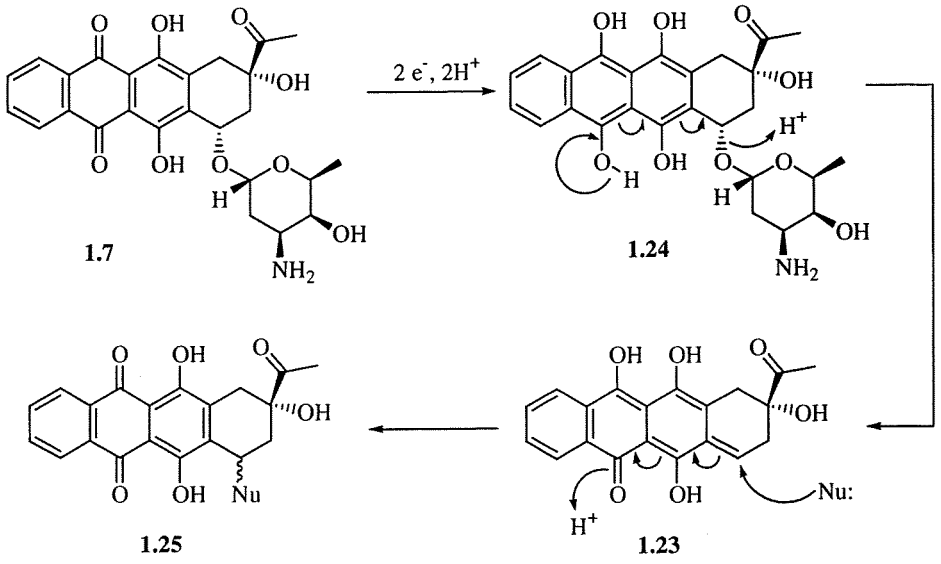

Scheme 1.5

It is often difficult to determine which mechanism(s) is involved in the primary mode of action of a particular quinone. As the examples of mitomycin C (**1.8**) and daunomycin (**1.7**) have shown, different quinones may have their own unique interactions with biological systems that are governed by their structure and reactivity. Our own interest in quinones began with the serendipitous discovery of a new class of bioactive quinones, calothrixins A and B.

1.3 The Calothrixins and Related Alkaloids

The indolophenanthridinediones calothrixins A (**1.26**) and B (**1.27**) were first isolated in 1999 by Rickards *et al.* from *Calothrix* cyanobacteria.[51] These novel metabolites were the first compounds found to incorporate the indole, quinone and quinoline moieties.

Early biological testing of these natural products indicated that these compounds were potent antitumor agents as well as effective cytotoxins against chloroquine-resistant strains of the malarial parasite *Plasmodium falciparum*.

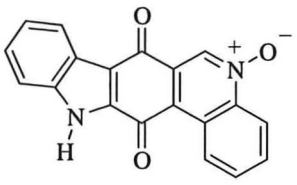

1.26

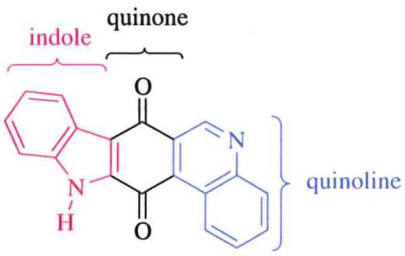

1.27

Detailed biological studies by Smith and coworkers revealed the selective biological modes of action of the calothrixins.[52-54] In one study, calothrixin A **(1.26)** was shown to be cytotoxic against Gram-positive bacteria such as *Bacillus subtilis*, *Bacillus cereus*, and the infectious *Staphylococcus aureus*. Calothrixin A, however, was inactive towards Gram-negative bacteria such as *Escherichia coli*, *Proteus mirabilis*, and *Klebsiella pneumonia*. The key difference between Gram-positive and Gram-negative bacteria is the presence of the lipopolysaccharide (LPS) layer in the latter **[Figure 1.1]**.[55,56] Thus the lack of activity of calothrixin A against Gram-negative bacteria may result from the poor diffusion of calothrixin A across the lipopolysaccharide membrane. In contrast, the rapid diffusion of calothrixin A across the peptidoglycan layer and inner membrane of Gram-positive bacteria may account for the observed selectivity.

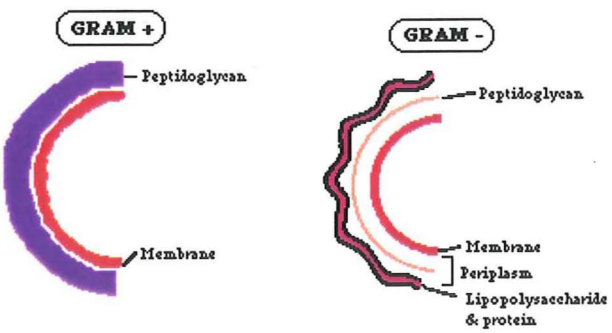

Figure 1.1

Calothrixin A was not significantly active against fungi, cyanobacteria, and green algae, and showed no cytotoxic effects against murine hepatocytes.[53] These studies indicated

that there is a high level of selectivity in the mode of action of calothrixin A, and suggests that this quinone has potential as a treatment for invasive cancers.

Enzymatic studies were also carried out in cell-free systems to determine the mode of action of calothrixin A. These studies showed that calothrixin A directly inhibits RNA polymerase, preventing the RNA chain elongation required for protein synthesis which in turn may lead to cell death.[54] The subsequent *in vitro* studies conducted showed that calothrixin A induced apoptosis, a programmed form of cell death, in Jurkat cancer cells.

Apoptosis is a highly-regulated mechanism of cell death; in contrast, the sudden death of a cell induced by gross injury is known as necrosis. During apoptosis, cellular signals activate enzymes known as caspases which systematically destroy intracellular organelles and proteins. As the apoptotic process progresses, morphological changes become apparent as shown in **Figure 1.2**. These changes include the disintegration of the nuclear envelope and endoplastic reticulum, condensation of the chromatin and enzymatic cleavage of DNA strands, culminating in the blebbing of the cellular membrane into small spherules for removal via phagocytosis.[57] In contrast, necrotic cells are characterized by a breach of the cellular membrane, resulting in the leakage of the cytoplasmic contents which may contain whole organelles and active proteins **[Figure 1.3]**.[58,59] Such leakage may be detrimental to nearby cells as the cytoplasm may contain active enzymes.

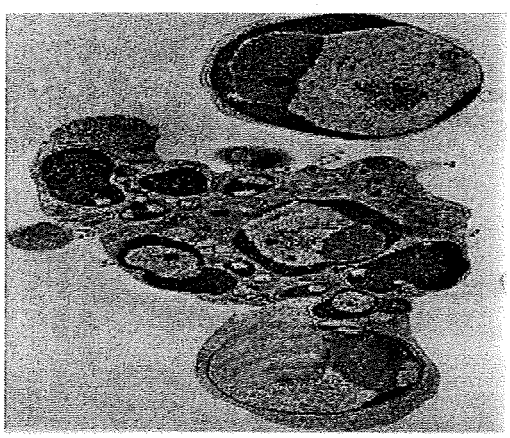

Figure 1.2 Apoptosis

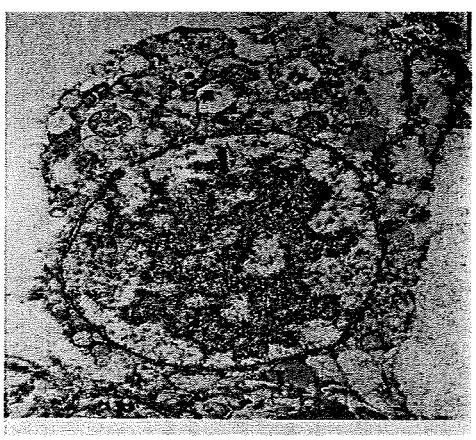

Figure 1.3 Necrosis

Calothrixin A was also shown to induce DNA damage through redox cycling in a cell-free system. It has been hypothesized that calothrixin A may intercalate with DNA and undergo redox cycling, thus inducing DNA damage which may induce apoptosis.[52] However, attempts to observe the intercalation of calothrixin A with DNA using circular dichroism studies have so far been inconclusive.[60]

The calothrixins bear structural similarities to several known compounds. These structural motifs have previously been discovered in other biologically active compounds such as the anti-tumor indole alkaloid vinblastine **(1.28)**,[61,62] and the antimalarial Cinchona quinoline alkaloid quinine **(1.29)**.[63] The calothrixins belong to a class of compounds known as the carbazolediones. The carbazolediones include clausenaquinone A **(1.30)**,[64] pyrayaquinone A **(1.31)**,[65] as well as the synthetic quinones benzocarbazoledione **(1.32)** and ellipticine quinone **(1.33)**.[66]

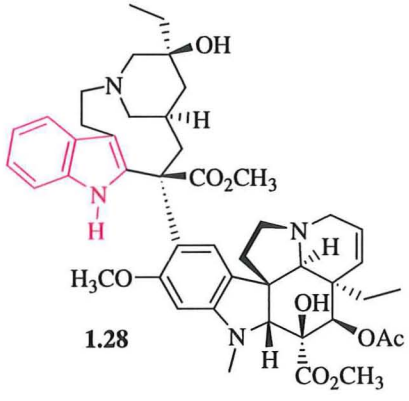

1.28

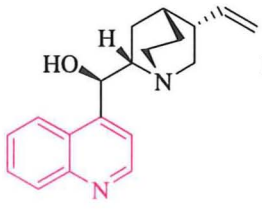

1.29

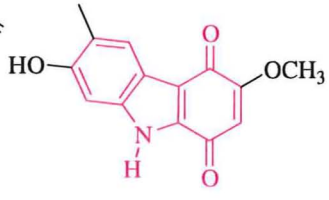

1.30

1.31

1.32

1.33

The similarities between the calothrixins and these carbazolediones can also be exploited for structure-activity relationship (SAR) studies. Knowledge of how the structure of the calothrixins affects biological activity may be useful in determining the pharmacophore which imparts the desired biological properties. SAR studies would also be useful in developing a model for the pharmacological properties of these compounds. The synthetic strategies employed for the synthesis of quinones and carbazolediones

may be applied in the synthesis of the calothrixins due to their similarities. We thus review the synthesis of a number of quinones and carbazolediones.

1.4 Literature Syntheses of Quinones and Carbazolediones

Quinones constitute a class of compounds with important biological and commercial applications.[12] Investigations into the synthesis of quinones is thus a continuous and vibrant area of research. Recent reviews by Thomson,[67] Knölker and Reddy,[65] as well as Moody,[68] and Bouaziz *et al.*[69] outline numerous strategies and methodologies that have been developed over the years to provide expedient routes towards these valuable compounds. These synthetic strategies can be divided into two general categories: synthesis of complex quinones by the elaboration of an existing quinone structure, or *de novo* synthesis of quinones from non-quinone precursors.

The *p*-benzoquinone moiety is an excellent building block for the synthesis of quinones of increasing structural complexity. In general, the elaboration of the quinone motif can be accomplished via numerous chemical techniques including radical reactions, nucleophilic addition and substitution reactions, as well as cycloaddition reactions. For example, simple 2,5-disubstituted-1,4-benzoquinones (**1.34**) can be prepared via the Michael addition of soft nucleophiles such as thiols and amines to *p*-benzoquinone **[Scheme 1.6]**.[34,70]

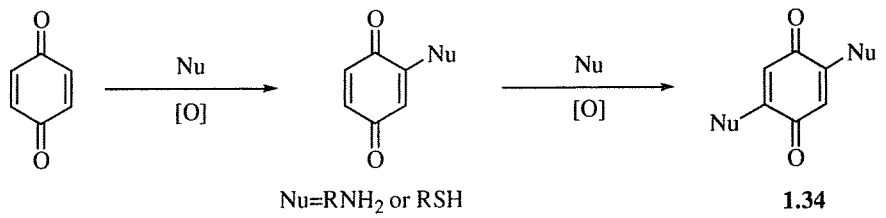

Nu=RNH_2 or RSH **1.34**

Scheme 1.6

This methodology of employing *p*-benzoquinone as a substrate for synthesizing complex quinones has been successfully utilized to install the indole moiety of carbazolediones. The general procedure involves a Michael addition reaction between aniline and a *p*-benzoquinone substrate followed by the palladium (II) mediated cyclization of the resulting adduct to give the desired carbazoledione framework. For example, the synthesis of pyrayaquinone A (**1.31**) developed by Yogo[71] shown in

Scheme 1.7 utilizes this general approach. The first step in this synthesis involved the Michael addition of the aniline **1.35** with 2-methyl-1,4-benzoquinone **(1.36)** to afford the anilinobenzoquinone **1.37**. The anilinobenzoquinone **1.37** was then converted to pyrayaquinone **1.31** through a palladium-mediated cyclization reaction. The mechanism for this cyclization reaction involves the insertion of the palladium (II) reagent into the aromatic carbon-hydrogen bond *ortho* to the amine substituent of the anilinobenzoquinone **1.37**. The resulting σ-complex **1.38** then coordinates and inserts into the carbon-carbon double bond on the quinone moiety, thus giving rise to the tetracyclic compound **1.39**. The reductive elimination of palladium (0) from the tetracyclic compound **1.39** then results in the formation of the carbazoledione **1.31**.

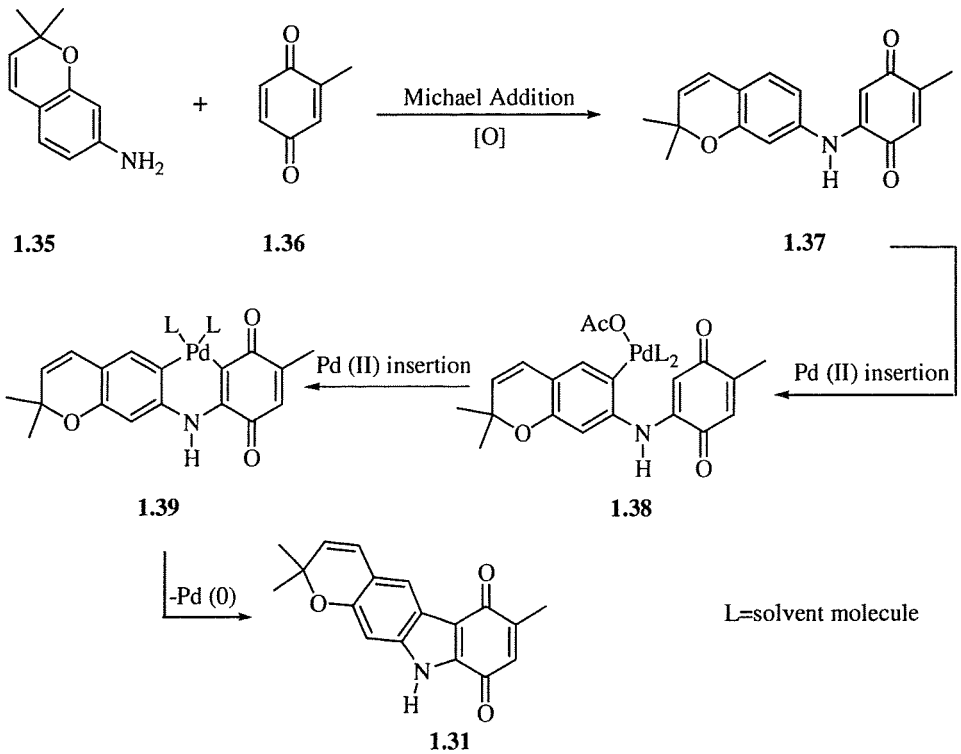

1.35 1.36 1.37 1.39 1.38 1.31

Scheme 1.7

This synthetic approach has also been successfully employed in the synthesis of other carbazolediones including the natural products such as murrayaquinone A **(1.40)**[71] and clausenaquinone A **(1.30)**.[64]

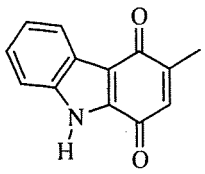

1.40

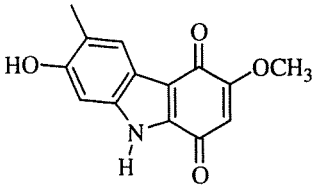

1.30

Another strategy towards the synthesis of highly functionalized quinones involves the use of non-quinonoid substrates to construct the basic framework of the molecule. The quinone moiety is then introduced in the later stages of the synthesis. These *de novo* syntheses of quinones can circumvent the problems associated with the reactivity of the quinone functionality. Bauta *et al.*[72] developed a synthetic approach towards a variety of carbazolediones via a regioselective cycloaddition reaction between indolyl carbene complexes such as **1.41** and **1.42** and substituted acetylenes **[Scheme 1.8]**. The annulation reaction between the carbenes **1.41** and **1.42** and acetylene derivative gave the quinol monomethyl ethers **1.43** and **1.44** with the smallest substituent R_S adjacent to the methoxy group. The quinol monomethyl ethers can be oxidized to afford the quinones **1.45** and **1.46**.

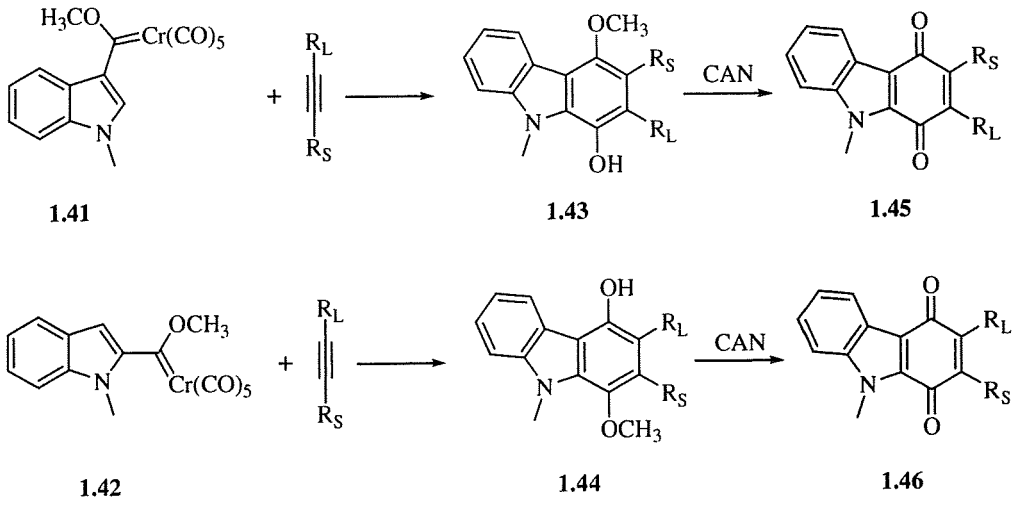

1.41 1.43 1.45

1.42 1.44 1.46

R_L=larger substituent
R_S=smaller substituent

Scheme 1.8

A second approach towards the synthesis of structurally complex quinones employs quinol ethers. These masked quinones are usually more robust than the corresponding quinones, allowing for the use of a much wider range of reaction conditions. For example, the total synthesis of the mitomycins reported by Kishi[73] provides an excellent

example of the use of quinol ethers in the synthesis of quinone natural products **[Scheme 1.9]**. In this synthesis, the *O*-alkylation of 2,4-dimethoxy-3-methylphenol (**1.47**) was carried out under basic conditions using allyl bromide (**1.48**), and the subsequent allylic rearrangement yielded the intermediate alkene **1.49**. A series of chemical transformations was then carried out to give the protected quinol dibenzyl ether **1.50**. The alkene group of the quinol dibenzyl ether **1.50** was further elaborated to give the intermediate **1.51**. Hydrogenolytic removal of the benzyl protecting groups of the compound **1.51** followed by aerial oxidation gave the quinone **1.52** *in situ*, which underwent intramolecular Michael addition with the free amine group to give the compound **1.53**. Treatment of the compound **1.53** with hydrogen tetrafluoroborate and perchloric acid yielded the indoloquinone **1.54**. The primary alcohol functionality of the indoloquinone **1.54** was then converted to the carbamate thus producing *N*-methylmitomycin A (**1.55**).

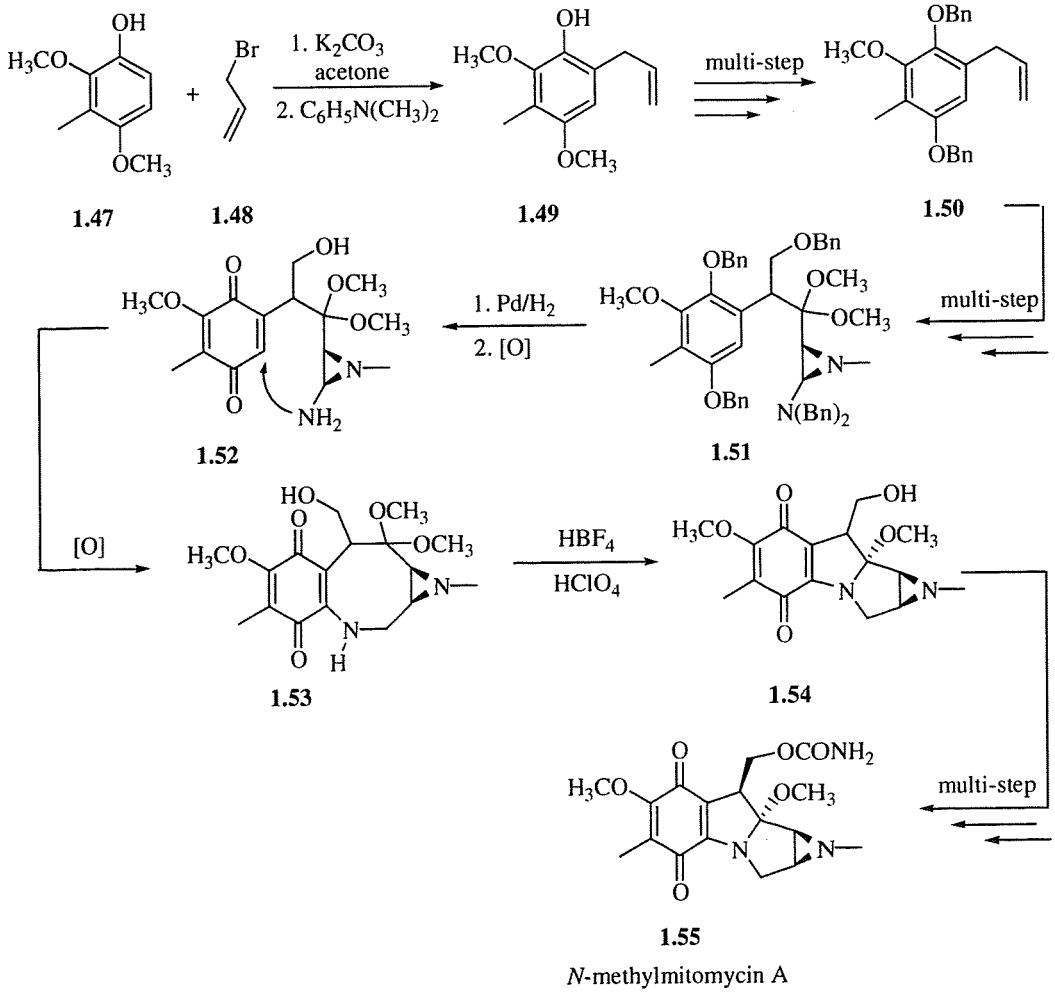

1.47 **1.48** **1.49** **1.50**

1.52 **1.51**

1.53 **1.54**

1.55

N-methylmitomycin A

Scheme 1.9

This synthetic approach can also be used to prepare mitomycins A (**1.56**), B (**1.57**) and C (**1.8**) , and porfiromycin (**1.58**).[46,73]

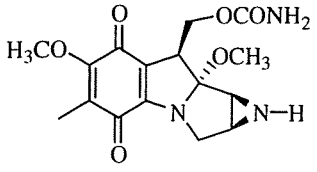

1.56

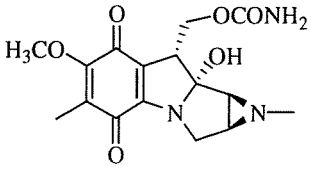

1.57

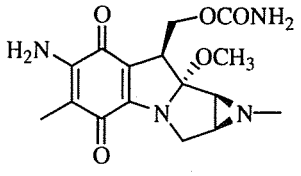

1.58

Swenton and Raynolds[74] reported an interesting *de novo* synthesis of the anthraquinone (±)-7,9-deoxydaunomycinone (**1.59**), an advanced intermediate in the synthesis of daunomycin (**1.7**). The synthesis employs a quinol ether substrate for structural elaboration, and the quinone moiety is installed in the final steps of the synthesis. In their synthesis, outlined in **Scheme 1.10**, the key substrate 3-bromo-2,5-dimethoxybenzaldehyde (**1.60**) underwent a Knoevenagel condensation with dimethyl malonate (**1.61**) to yield the alkene **1.62**. The alkene **1.62** was reduced with *tris*(*s*-butyl)borohydride and alkylated with methyl 2-bromoacetate to give the triester **1.63**. The triester was converted to the dicarboxylic acid via base-catalyzed hydrolysis and decarboxylation. Treatment of the dicarboxylic acid with acetic anhydride gave the anhydride **1.64**, which then underwent acid-catalyzed intramolecular electrophilic addition reaction to yield the bicyclic compound **1.65**, which comprises the A and B-rings of daunomycinone **1.59**. The compound was then converted to the acetal **1.66** in three steps. The quinone moiety was then constructed at this stage of the reaction sequence as follows:

Lithiation of the acetal **1.66** with *n*-butyl lithium followed by the addition of the diester dimethyl 3-methoxyphthalate (**1.67**) gave the adduct **1.68**. The adduct **1.68** was then subjected to base-catalyzed hydrolysis of the methyl ester, and the crude product was heated in the presence of methanesulfonic acid to yield the quinone **1.69**. With the tetracyclic ring systems in place, the advanced intermediate **1.59** was obtained via oxidative cleavage of the methyl ethers. Further functional group transformations would thus yield daunomycin (**1.7**).

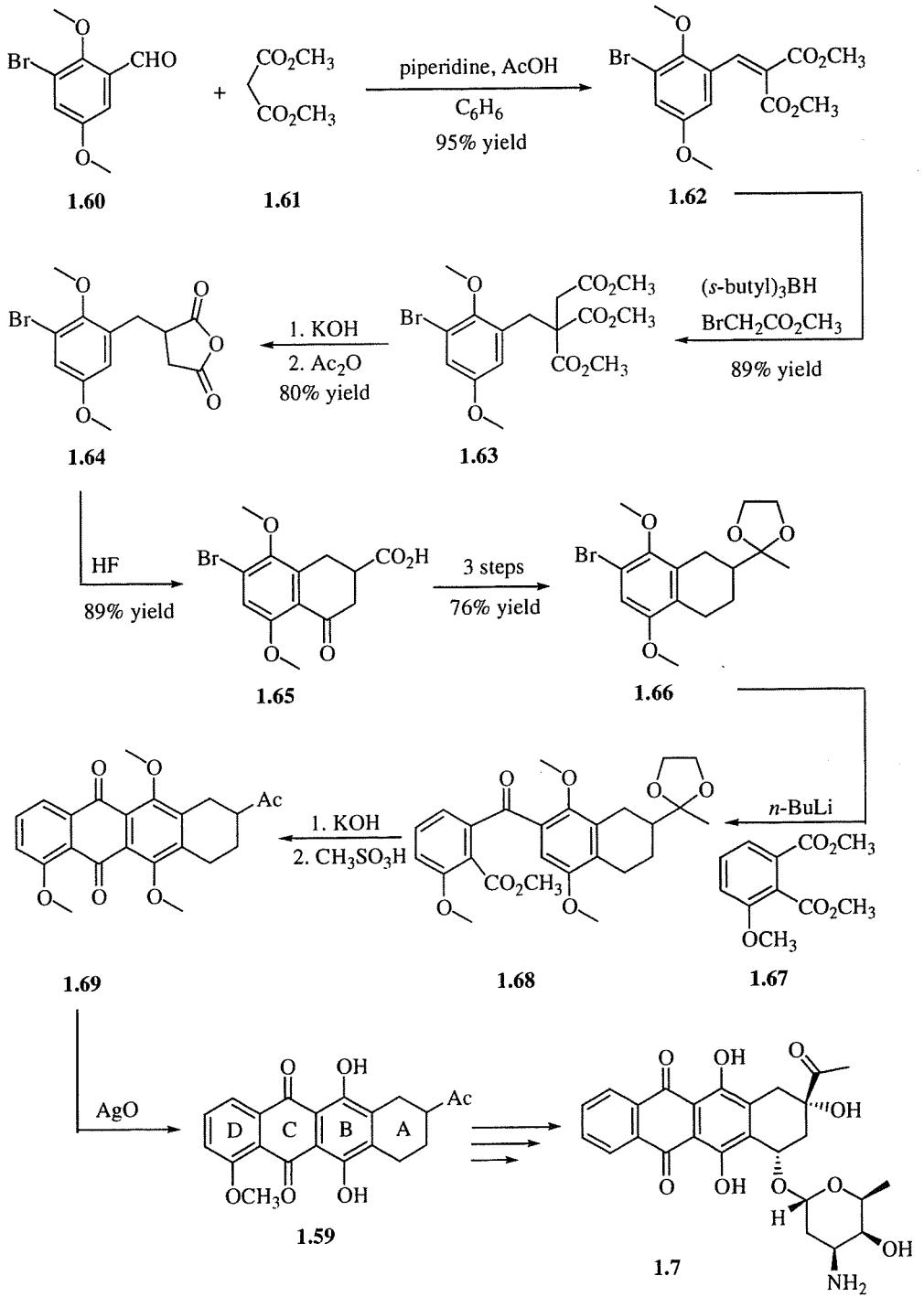

Scheme 1.10

These examples thus illustrate the wealth of synthetic transformations at our disposal for the synthesis of our target compounds. Once the target compounds are in hand, SAR studies can be carried out in order to elucidate the pharmacophore of the calothrixins.

1.5 Structure-Activity Relationship (SAR) Studies

The SAR study of a lead compound and its simpler analogues can be used to determine the substituents and functional groups which are necessary for biological activity. The functionality essential for biological activity is known as the pharmacophore. Once the pharmacophore has been established, modifications can be made to the rest of the molecule and the impact of these changes on biological activity can be measured. These studies can provide general information on the effect of substituents on the observed biological activity and toxicity.[75,76] Furthermore, the information gained through SAR studies can be used to identify new drug candidates with better biological activity and lower toxicity than the lead compound.[21] SAR investigations are therefore useful tools in the development of pharmaceutical drugs. [2]

SAR studies were essential to the development of pharmaceutical drugs based on the lead compound ellipticine **(1.70)**, a carbazole alkaloid with potent anticancer properties. Ellipticine was first isolated from the leaves of *Ochrosia elliptica*, a common tropical evergreen plant.[77] The selective antineoplastic properties of ellipticine **(1.70)** led to numerous studies culminating in two commercial drugs, 9-hydroxy-2-ellipticinium acetate **(1.71)** and 9-methoxyellipticinium lactate **(1.72)**.[78] A third compound, 9-hydroxy-2-ethyl(diethylamine)ellipticinium **(1.73)**, is currently in phase II clinical trials in the USA.[79]

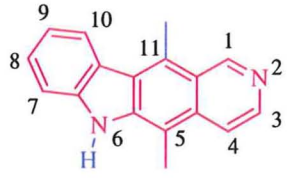

1.70

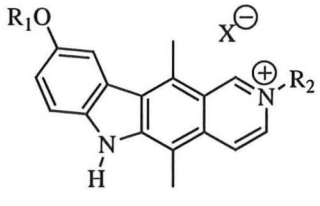

1.71: R_1=H, R_2=CH_3, X=CH_3CO_2
1.72: R_1=CH_3, R_2=H, X=$CH_2(OH)CO_2$

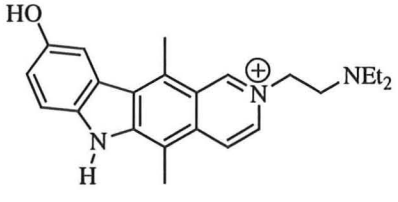

1.73

In SAR studies carried out by Meunier *et al.*,[80] fifteen ellipticine derivatives with various substituents on the tetracyclic core were assessed for their biological activity against murine P388 cells and L1210 murine leukemia cells. The studies revealed that the essential pharmacophore for biological activity is the 5-methyl-6*H*-pyrido[4,3-*b*]carbazole system shown in red in parent structure ellipticine **(1.70)**. It was

demonstrated that the antitumor activity was attenuated by the absence of any one of the functional features within this pharmacophore. Furthermore, it was found that the presence of an oxygen functionality such as OH or OCH_3 at the C9-position of ellipticine enhances the biological activity relative to the parent compound.[81] In contrast, the presence of an alkyl substituent at the C9-position of ellipticine abrogated the antitumor activity relative to the parent compound.[78] The bioactivity observed was attenuated by N6-substitution with respect to the parent ellipticine.

These observations were rationalized through the use of Quantitative SAR (QSAR) studies. In the QSAR studies, the effects of varying physicochemical properties were examined in order to determine their role in the biological activity of these ellipticine analogues and derivatives. Of the physicochemical parameters measured, the biochemical oxidation potentials appeared to have the greatest influence on biological activity. The biochemical oxidation potential is a measure of the relative ease of oxidation of the test compound by hydrogen peroxide in the presence of horse radish peroxidase (HRP). The enzyme HRP catalyzes the C9-hydroxylation of ellipticine (**1.70**) to 9-hydroxyellipticine (**1.74**), and subsequent oxidation of hydroxyellipticine **1.74** by hydrogen peroxide to form the quinone-imine derivative **1.75** as shown in **Scheme 1.11**. The ease of biochemical oxidation is reflected by the consumption of hydrogen peroxide, and the results are reported as the turnover number (μmol H_2O_2 consumed/min per μmol HRP). A high turnover number reflects the ease of biochemical oxidation to the quinone-imine.[80]

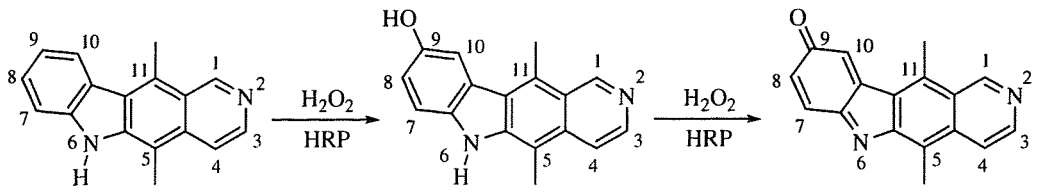

1.70 **1.74** **1.75**

Scheme 1.11

The results showed that the most active ellipticine derivatives were readily oxidized by hydrogen peroxide in the presence of HRP to give the quinone-imine, and thus these compounds had high turnover numbers. Since the C9-hydroxy derivatives already have the requisite oxygen functionality in place, oxidation can occur readily and therefore

these derivatives have a higher turnover number than the parent compound. The C9-methoxy derivatives likewise have higher turnover numbers than the deoxygenated parent compounds due to the ease of which the methoxy ether undergoes oxidative demethylation to the quinone in the presence of HRP.[82] These observations led to the theory that ellipticine (**1.70**) was a prodrug which underwent biological activation within the cell to form reactive a quinone-imine, which in turn could induce redox cycling within the cell, or act as a cellular alkylating agent by trapping nucleophiles at the C8 or C10-positions.[80,83] Thus alkylation of the C9-position of ellipticine prevents the formation of the quinone-imine, resulting in the loss of activity. Alkylation of the C10-position of ellipticine also diminishes activity, as studies have shown that Michael additions to the quinone-imine occurs preferentially at the C10-position.[78] However, these C10-alkylated ellipticines can still undergo reduction to the quinone-imine and exert their biological influence through the redox cycling mechanism.

The study by Meunier *et al.*[80] illustrates both the strengths and weaknesses of the SAR approach in determining the relationship between structure and biological activity of bioactive compounds. While SAR studies can be useful in determining the structural requirements necessary for a compound to elicit a biological response, they cannot predict the biological activity of new compounds. On the other hand, QSAR studies enable the determination of the physicochemical properties that influence biological activity. In the case of the ellipticines, the key parameter for biological activity is the ease of biooxidation which generates the biologically-active quinone-imine intermediate. Although the QSAR study of ellipticine derivatives showed that biooxidation was an important parameter for biological activity, it is important to note that no direct correlation was observed between the turnover numbers and biological activity. However, the more active compounds displayed a turnover number greater than 11000μmol H_2O_2 consumed/min per μmol HRP. From the result of the QSAR analysis, it is possible to determine if new ellipticine derivatives will be biologically active by measuring their relative ease of biooxidation. However, due to the complexity of cellular processes, biooxidation alone cannot be used to predict the magnitude of the biological activity of ellipticines.

1.6 Physicochemical Parameters and Quantitative Structure-Activity Relationship Studies

QSAR analysis is a powerful tool for developing new drug candidates based on a lead compound. QSAR studies by Hansch,[84] Tute,[85,86] and Topliss[87] have provided valuable information for the optimization of the pharmacological properties of several classes of bioactive compounds. It should be noted, however, that developing a QSAR analysis can be very difficult and may take years, and that "QSAR remains more of a challenge than an achievement."[88]

The Hansch Analysis is one of the most widely used QSAR methods for correlating physicochemical parameters and biological activity. The basis of the Hansch Analysis is the theory that the biological activity of a compound is reflected by an equilibrium reaction within the cell, and this equilibrium is governed by the laws of thermodynamics.[84-86] Thus the reaction equilibrium is defined by the equation $\Delta G_{reaction}$=-RTlnK, where ΔG is the Gibbs Free Energy of the reaction, R is the universal gas constant, T is temperature (K), and lnK is the natural logarithm of the equilibrium constant. Therefore, the various physicochemical parameters (P1, P2, ...,Pn) of a compound can be reduced to linear free energy terms as shown:

$$\Delta G_{total} = \Delta G_{P1} + \Delta G_{P2} + \ldots + \Delta G_{Pn}$$

The aim of the Hansch Analysis is to determine which physicochemical parameters have the greatest influence on biological activity, and to reduce the correlation to a mathematical formula. This is essentially a statistical approach to predicting biological activity, and as such the rules of statistics must be applied. In general, the results of a QSAR study must specify the variable n (number of data points or compounds tested), *R* (correlation coefficient) or R^2 (covariance), *P* (probability), *s* (standard error) and *F* (Fischer's Test, which shows the significance of the regression model).

One of the key parameters which has been shown to play an essential role in biological activity of quinones is the reduction potential (E), which can be expressed as single-electron reduction potentials ($E_{1/2}^{I}$ and $E_{1/2}^{II}$),[89,90] or a two-electron reduction potential ($E_{Q/Q2\text{-}}$).[29] Reduction potentials are linear free energy terms related to the Gibbs free

energy by the equation $\Delta G=-n\Delta EF$ where n is the number of electrons involved in reduction, and F is Faraday's constant. The importance of the reduction potential of quinones towards biological activity is thought to relate to the reductive activation of quinone prodrugs.[91] A large number of biologically active quinones have reduction potentials that are greater (more positive) than –0.5V with respect to the standard hydrogen electrode, which allows electron transfer to occur from biomolecules to the compound under physiological conditions.[92] Due to the complexity of redox mechanisms within the cell, linear correlations between reduction potential and biological activity are generally not observed, yet threshold values are noted.[90,93]

The lipophilic nature of a compound constitutes another important parameter in determining biological activity. Lipophilicity is a measure of the relative solubility of a drug in aqueous and lipid phases, and as such it is a free energy term proportional to the free energy of solvation (ΔG_{Solv}). The ratio of the equilibrium concentrations of the drug between the aqueous and lipid phase is called the partition coefficient P, which is generally expressed as a logarithm (logP). For a series of related compounds, such as substituted phenols (**1.76**), the substituent constant π can be used in place of logP values. The constant π is defined by the equation $\pi=\log P_X - \log P_H$ where P_X is the partition coefficient of a derivative **1.76** and P_H is the partition coefficient of the parent compound **1.77**.[94]

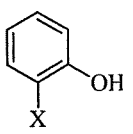

1.76
X=F, LogP_X=1.74

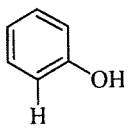

1.77
LogP_H=1.46

$\pi=\text{LogP}_X-\text{logP}_H$
=(1.74-1.46)
=0.25

The lipophilicity of a given compound influences both drug transport as well as drug-receptor interactions. In general terms, drug transport can be envisioned as the diffusion of the compound from the aqueous extracellular enviroment into the lipophilic cell membrane. In this model as illustrated in **Figure 1.4A**, the diffusion of the drug into the cell membrane would be directly proportional to the lipophilicity of the drug. Such a linear correlation between logP and biological activity has been noted by Meyer and Overton in their study of general anesthetics that exert their biological activity by diffusing into the cell membrane resulting in membrane expansion.[86,95] The resulting

increase in cellular volume and surface area of the membrane results in anesthesia, the lack of somatic sensation in the treated organs.[87]

However, most drugs do not act on the cellular membrane, and thus a more complex diffusion mechanism must be considered. For the diffusion of a compound into the cellular cytoplasm, the compound must pass from the extracellular aqueous environment into the lipid membrane and finally into the aqueous cytoplasm. This results in the compartmentalization of the compound in all three layers or partitions as shown in **Figure 1.4B**. The diffusion mechanism is further complicated when transport into cellular vesicles and organelles must be taken into account. In order to determine the concentration of the test compound in each compartment, it is necessary to solve a set of differential equations. Hansch[84] showed that the solutions to these differential equations predict that for a finite number of partitions employed, the logarithm of the concentration at a given partition and at a given point in time is inversely proportional to the square of the logP value. The result is a parabolic relationship between logC and logP.[84] Since the induction of biological activity is dependent on the drug reaching its target site, the biological activity measured should display an inverse parabolic relationship to logP. Log P is also essential in drug-receptor interactions as the receptor site can be regarded as the last compartment or partition in the diffusion mechanism.[85]

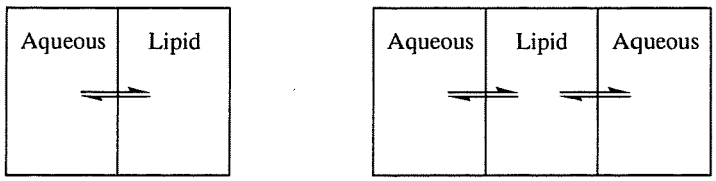

A. Diffusion across 2 partitions B. Diffusion across 3 partitions

Figure 1.4

Drug-receptor interactions are also influenced by stereoelectronic parameters such as the Taft and Verloop steric parameters, and the Hammett electronic parameter.[86] The Taft steric parameter (E_S) influences the binding of a molecule to a specific site, and is therefore related to the binding free energy $\Delta G_{binding}$. The E_S may also denote intra- or intermolecular hindrance to a chemical reaction as well as binding. Historically, the Taft steric parameter was determined experimentally for each substituent R. This was accomplished by measuring the rate of the acid-catalyzed hydrolysis of a substituted methyl acetate ($R\text{-}CH_2CO_2CH_3$) relative to methyl acetate ($CH_3CO_2CH_3$) such that E_{SR}=

$logk_R$-$logk_H$,where $logk_R$ and $logk_H$ are the logarithms of the rate constant for the substituted methyl acetate and parent compound ($CH_3CO_2CH_3$) respectively. Similarly, the Verloop steric parameter is a measure of molecular bulk of a compound based on the atomic dimensions defined by bond angles and Van der Waal radii. A third steric parameter, molar refractivity (MR), measures the volume and polarizability of a molecule or substituent.[87]

The last parameter to consider is the Hammett parameter (σ) which is a measure of the electronic effects of a substituent on chemical reactivity. Hammett correlations quantitatively express the relationship between chemical reactivity and the electron-donating or electron-accepting nature of a substituent.[87] The Hammett constant σ_X was originally defined to measure the effect of various substituents (X) on the dissociation constant of benzoic acid such that $\sigma_X = logK_X - logK_H$, where K_X and K_H are the dissociation constants for the substituted benzoic acid and the parent benzoic acid respectively.[96] The Hammett parameter is related to the free energy of the reaction by the equation $\Delta G_{reaction} = -RTlnK$. The Hammett parameter incorporates both inductive and resonance electronic effects on chemical reactivity.[87]

Combining these physicochemical parameters into one equation gives:

$$Log(1/EC_{50}) = a + bE + clogP^2 + dlogP + eE_S + f\sigma$$

where a, b, c, d, e, and f are experimentally-determined constants.

These physicochemical parameters can provide valuable insights on the biological activity of a test compound and its derivatives. Furthermore, the data obtained may also aid in the elucidation of the mode of transport and mechanism of action of these compounds. The results of the QSAR studies can be used to develop a model for predicting the biological activity of new derivatives based on the test compound.

A study by Prakash and Hodnett illustrates the use of a multiparameter QSAR for analyzing the biological activity of substituted naphthoquinones (**1.78**).[97] Twenty-seven naphthoquinone derivatives were tested for the ability to inhibit the growth of ascitic sarcoma 180 in mice which was reported as a percentage of tumor weight inhibition (%TWI). Attempts were made to correlate the parameters π, MR, and $E_{1/2}{}^1$ (reduction

potential of the quinone to semiquinone radical) to the biological activity as measured by %TWI. The results showed that moderately active compounds (*i.e.*, %TWI is less than 20) are defined by the equation

$$(\%TWI) = -0.28\pi + 9.81MR + 9.44\pi^2 - 455E_{1/2}^{I} - 71.1$$

Furthermore, the six out of the seven most active compounds (*i.e.*, %TWI is greater than 20) are defined by the equation

$$(\%TWI) = -18.6\pi + 7.30MR + 6.30\pi^2 + -392\ E_{1/2}^{I} - 52.8$$

These results can be used to model new naphthoquinone derivatives with desirable biological activity.

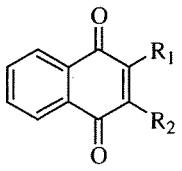

1.78

QSAR studies have been used to study the interaction between small molecules and receptors. For example, Hartmann *et al.* synthesized a number of disubstituted hexestrol derivatives (**1.79**) to test the binding affinity of these compounds to the estrogen receptor.[98,99] Their studies showed an excellent correlation between the relative binding affinities (RBA) and two physicochemical parameters, the Hammett coefficient (σ_X) and molar refractivity substituents at the C2- and C3-positions (MR_{2X} and MR_{3X}) of the derivatives. The results were summarized in the equation $Log(RBA) = -0.65\sigma_X - 1.01MR_{2X} - 1.40MR_{3X} + 1.41$ [n=20, R^2=0.91, s=0.281], where n is the number of compounds tested, R^2 is the covariance and s is the standard deviation. Similar studies have been widely employed in the development of clinical drugs which bind to the estrogen receptor.[100]

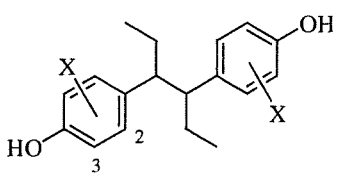

1.79

QSAR studies may therefore prove useful for correlating various physicochemical parameters with the biological activity of the calothrixins and related carbazolediones. This in turn may lead to a model for predicting the biological activity of new derivatives for drug development.

1.7 Project Aims and Objectives

The biological activity of the calothrixins has led to their identification as lead compounds for drug development. In order to study these compounds in detail, we first developed a convenient and efficient synthesis of the calothrixins and their derivatives, as well as related carbazoledione analogues. These target compounds were then subjected to biological testing in order to elucidate the pharmacophore which imparts the desired biological properties. Finally, SAR and QSAR studies were carried out to evaluate the role of physicochemical properties on biological activity with the aim of obtaining a model for predicting the biological activity of new calothrixin derivatives.

1.8 Bibliography

(1) Hanson, J. R. *Natural Products: The Secondary Metabolites*; The Royal Society of Chemistry: Cambridge, 2003; Vol. 17.

(2) Patrick, G. L. *An Introduction to Medicinal Chemistry*; 2nd ed.; Oxford University Press: Oxford, 2001.

(3) Nagarajan, R. In *Cephalosporins and Penicillins*; Flynn, E. H., Ed.; Academic Press, Inc.: New York, 1972, p 636-661.

(4) O'Callaghan, C. H.; Muggleton, P. W. In *Cephalosporins and Penicillins*; Flynn, E. H., Ed.; Academic Press, Inc.: New York, 1972, p 439-496.

(5) Colegate, S. M.; Molyneux, R. J. *Bioactive Natural Products: Detection, Isolation, and Structural Determination*; CRC Press, Inc.: Boca Raton, 1993.

(6) Yadav, J. S.; Babu, R. S.; Sabitha, G. *Tetrahedron Lett.* **2003**, *44*, 387-389.

(7) Robert, A.; Dechy-Cabaret, O.; Cazelles, J.; Meunier, B. *Acc. Chem. Res.* **2002**, *35*, 167-174.

(8) Jha, R. K.; Xu, Z.-r. *Mar. Drugs* **2004**, *2*, 123-146.

(9) Menger, F. M.; Rourk, M. J. *J. Org. Chem* **1997**, *62*, 9083-9088.

(10) Gökbuget, N.; Hoelzer, D. *Leukemia Res.* **2002**, *26*, 473-476.

(11) Hodnett, E. M.; Wongwiechintana, C.; Dunn III, W. J.; Marrs, P. *J. Med. Chem.* **1983**, *26*, 570-574.

(12) Thomson, R. H. In *Naturally Occuring Quinones*; Thomson, R. H., Ed.; Academic Press Inc.: London, 1971, p 1-38.

(13) Ginalska, G.; Bancerz, R.; Kornillowicz-Kowalska, T. *J. Ind. Microbiol. Biotechnol.* **2004**, *31*, 177-182.

(14) Remers, W. A. *The Chemistry of Antitumor Antibiotics*; John Wiley & Sons, Inc., 1979; Vol. 1.

(15) Masquelier, M.; Vitols, S. *Biochem. Pharmacol.* **2004**, *67*, 1639-1646.

(16) Barton, D.; Nakamishi, K. In *Comprehensive Natural Products Chemistry*; Barton, D. H. R., Nakamishi, K., Eds. UK, 1999; Vol. 7, p 527-536.

(17) Tomasz, M. *Chem. Biol.* **1995**, *2*, 575-579.

(18) Kunz, K. R.; Iyengar, B. S.; Dorr, R. T.; Alberts, D. S.; Remers, W. A. *J. Med. Chem.* **1991**, *34*, 2281-2286.

(19) Sami, S. M.; Iyengar, B. S.; Tarnow, S. E.; Remers, W. A.; Bradner, W. T.; Schurig, J. E. *J. Med. Chem.* **1984**, *27*, 701-708.

(20) Bradner, W. T. *Cancer Treat. Rev.* **2001**, *27*, 35-50.

(21) Thomas, G. *Medicinal Chemistry: An Introduction*; 1st ed.; John Wiley & Sons, Ltd.: Chichester, 2000.

(22) Bringmann, G.; Reichert, Y.; Kane, V. V. *Tetrahedron* **2004**, *60*, 3539-3574.

(23) Hafuri, Y.; Takemori, E.; Oogose, K.; Inouye, Y.; Nakamura, S. *J. Antibiot.* **1988**, *41*, 1471-1478.

(24) Lin, T.-H.; Chang, S.-J.; Chen, C.-C.; Wang, J.-P.; Tsao, L.-T. *J. Nat. Prod.* **2001**, *64*, 1084-1086.

(25) Kraus, G. A.; Zhang, N. *Tetrahedron Lett.* **2002**, *43*, 9597-9599.

(26) Choi, Y.-H.; Park, A.; Schmitz, F. J. *J. Nat. Prod.* **1993**, *56*, 1431-1433.

(27) Ferreira, V. F.; Park, A.; Schmitz, F. J.; Valeriote, F. A. *Tetrahedron* **2003**, *59*, 1349-1357.

(28) Bolton, J. L.; Trush, M. A.; Penning, T. M.; Dryhurst, G.; Monks, T. J. *Chem. Res. Toxicology* **2000**, *13*, 135-160.

(29) Brunmark, A.; Cadenas, E. *Free Radical Biol. Med.* **1989**, *7*, 435-477.

(30) Gutierrez, P. L. *Free Radical Biol. Med.* **2000**, *29*, 263-275.

(31) Lind, C.; Cadenas, E.; Hochstein, P.; Ernster, L. In *Methods in Enzymology*; Packer, L., Glazer, A. N., Eds.; Academic Press Inc.: San Diego, 1990; Vol. 186, p 92-105.

(32) Dinkova-Kostova, A. T.; Talalay, P. *Free Radical Biol. Med.* **2000**, *29*, 231-240.

(33) Matés, J. M.; Perez-Gomez, C.; De Castro, I. N. *Clin. Biochem.* **1999**, *32*, 595-603.

(34) Kutyrev, A. A. *Tetrahedron* **1991**, *47*, 8043-8065.

(35) Takahashi, N.; Schreiber, J.; Fischer, V.; Mason, R. P. *Arch. Biochem. Biophys.* **1987**, *252*, 41-48.

(36) Wieland, T. In *Glutathione: A Symposium*; Colowick, S., Ed.; Academic Press Inc.: New York, 1954, p 45-56.

(37) Flowers-Geary, L.; Bleczinski, W.; Harvey, R. G.; Penning, T. M. *Chem.-Biol. Interact.* **1996**, *99*, 55-72.

(38) Powis, G. *Free Radical Biol. Med.* **1989**, *6*, 63-101.

(39) Kovacic, P.; Osuna Jr., J. A. *Curr. Pharm. Design* **2000**, *6*, 277-309.

(40) Monks, T. J.; Hanzlik, R. P.; Cohen, G. M.; Ross, D.; graham, D. G. *Toxicol. Appl. Pharmacol.* **1992**, *112*, 2-16.

(41) Weiner, L. M. In *Methods in Enzymology*; Packer, L., Ed.; Academic Press Inc.: San Diego, 1994; Vol. 233, p 92-105.

(42) Kim, J. Y.; Su, T.-L.; Chou, T.-C.; Koehler, B.; Scarborough, A.; Ouerfelli, O.; Watanabe, K. A. *J. Med. Chem.* **1996**, *39*, 2812-2818.

(43) Chen, H.; Liu, X. M.; Patel, D. J. *J. Mol. Biol.* **1996**, *258*, 457-459.

(44) Sartorius, J.; Schneider, H. *J. Chem. Soc., Perkin Trans.* **1997**, *2*, 2319-2327.

(45) Paz, M. M.; Das, A.; Palom, Y.; He, Q.-Y.; Tomasz, M. *J. Med. Chem.* **2001**, *44*, 2834-2842.

(46) Danishefsky, S. J.; Schkeryantz, J. M. *Synlett* **1995**, 475-490.

(47) Hoey, B. M.; Butler, J.; Swalow, A. J. *Biochemistry* **1988**, *27*, 2608-2614.

(48) Tomasz, M.; Lipman, R.; Verdine, G. L.; Nakanishi, K. *J. Am. Chem. Soc.* **1985**, *107*, 6120-6121.

(49) Chaires, J. B. *Biophys. Chem.* **1990**, *35*, 191-202.

(50) Davies, K. J. A.; Doroshow, J. H. *J. Biol. Chem.* **1986**, *261*, 3060-3067.

(51) Rickards, R. W.; Rothschild, J. M.; Willis, A. C.; de Chazal, N. M.; Kirk, J.; Kirk, K.; Saliba, K. J.; Smith, G. D. *Tetrahedron* **1999**, *55*, 13513-13520.

(52) Chen, X.; Smith, G. D.; Waring, P. *J. Appl. Phycol.* **2003**, *15*, 269-277.

(53) Doan, N. T.; Rickards, R. W.; Rothschild, J. M.; Smith, G. D. *J. Appl. Phycol.* **2000**, *12*, 409-416.

(54) Doan, N. T.; Stewart, P. R.; Smith, G. D. *FEMS Microbiol. Lett.* **2001**, *196*, 135-139.

(55) Nikaido, H.; Vaara, M. *Microb. Rev.* **1985**, *49*, 1-32.

(56) Kaback, H. R.; Hong, J.-S. In *CRC Crit. Rev. Microbiol.*; CRC Press Inc.: Boca Raton, 1973, p 333-376.

(57) Kerr, J. F. R.; Searle, J.; Harmon, B. V.; Bishop, C. J. In *Perspectives on Mammalian Cell Death*; Potten, C. S., Ed.; Oxford University Press: New York, 1987, p 93-128.

(58) Dean, R. T. In *Perspectives on Mammalian Cell Death*; Potten, C. S., Ed.; Oxford University Press: New York, 1987, p 18-38.

(59) Robertson, J. D.; Orrenius, S. *Crit. Rev. Toxicol.* **2000**, *30*, 609-627.

(60) Le Guen, M. Honours Thesis, The Australian National University, 2003.

(61) Kruczynski, A.; Hill, B. T. *Crit. Rev. Oncol. Hematol.* **2001**, *40*, 159-173.

(62) Bau, R.; Jin, K. K. *J. Chem. Soc., Perkin Trans. 1* **2000**, 2079-2082.

(63) Karle, J. M. *Antimicrob. Agents Chemother.* **1997**, *41*, 791-794.

(64) Wu, T.-S.; Huang, S.-C.; Wu, P. L.; Lee, K.-H. *Bioorg. Med. Chem. Lett.* **1994**, *4*, 2395-2398.

(65) Knölker, H.-J.; Reddy, K. R. *Chem. Rev.* **2002**, *102*, 4303-4427.

(66) Taylor, D. A.; Baradarani, M. M.; Martinez, S. J.; Joule, J. A. *J. Chem. Res. (M)* **1979**, 4801-4817.

(67) Thomson, R. H. In *Total Synthesis of Natural Products*; ApSimon, J., Ed.; John Wiley & Sons, Inc.: New York, 1992; Vol. 8, p 311-531.

(68) Moody, C. J. *Synlett* **1994**, 681-688.

(69) Bouaziz, Z.; Nebois, P.; Poumaroux, A.; Fillion, H. *Heterocycles* **2000**, *52*, 977-999.

(70) Martynoff, M.; Tsatsas, G. *Bull. Soc. Chim. France* **1947**, 52-57.

(71) Yogo, M.; Ito, C.; Furukawa, H. *Chem. Pharm. Bull.* **1991**, *39*, 328-334.

(72) Bauta, W. E.; Wulff, W. D.; Pavkovic, S. F.; Zaluzec, E. J. *J. Org. Chem* **1989**, *54*, 3249-3252.

(73) Kishi, Y. *J. Nat. Prod.* **1979**, *42*, 549-568.

(74) Swenton, J. S.; Raynolds, P. W. *J. Am. Chem. Soc.* **1978**, *100*, 6188-6195.

(75) Schultz, T. W.; Cronin, M. T. D.; Walker, J. D.; Aptula, A. O. *J. Mol. Struct. (Theochem)* **2003**, *622*, 1-22.

(76) Schultz, T. W.; Cronin, M. T. D.; Netzeva, T. I. *J. Mol. Struct. (Theochem)* **2003**, *622*, 23-38.

(77) Goodwin, S.; Smith, A. F.; Horning, E. C. *J. Am. Chem. Soc.* **1959**, *81*, 1903-1908.

(78) Gribble, G. W. In *The Alkaloids*; Brossi, A., Ed.; Academic Press, Inc.: San Diego, 1990; Vol. 39, p 239-352.

(79) Diaz, M.; Cobas, A.; Guitian, E.; Castedo, L. *Eur. J. Chem.* **2001**, 4543-9.

(80) Meunier, G.; de Montauzon, D.; Bernadou, J.; Grassy, G.; Bonnafous, M.; Cros, S.; Meunier, B. *Mol. Pharmacol.* **1988**, *33*, 93-102.

(81) Anderson, W. K.; Gopalsamy, A.; Reddy, P. S. *J. Med. Chem.* **1994**, *37*, 1955-1963.

(82) Meunier, G.; Meunier, B. *J. Biol. Chem.* **1985**, *260*, 10576-10582.

(83) Kansal, V. K.; Potier, P. *Tetrahedron* **1986**, *42*, 2389-2408.

(84) Hansch, C. *J. Am. Chem. Soc.* **1969**, *2*, 232-239.

(85) Tute, M. S. *Advances in Drug Research* **1971**, *6*, 1-77.

(86) Tute, M. S. In *Comprehensive Medicinal Chemistry*; Sammes, P. G., Taylor, J. B., Eds.; Pergamon Press: Oxford, 1990; Vol. 4, p 1-31.

(87) Blankley, C. J. In *Quantitative Structure-Activity Relationships of Drugs*; Topliss, J. G., Ed.; Academic Press Inc.: New York, 1983; Vol. 19, p 1-21.

(88) Martin, Y. C. *J. Med. Chem.* **1981**, *24*, 229-237.

(89) Inbaraj, J. J.; Gandhidasan, R.; Murugesan, R. *Free Radical Biol. Med.* **1999**, *26*, 1072-1078.

(90) Macías-Ruvalcaba, N.; Cuevas, G.; González, I.; Aguilar-Martínez, M. *J. Org. Chem* **2002**, *67*, 3673-3681.

(91) Jaffar, M.; Phillips, R. M.; Williams, K. J.; Mrema, I.; Cole, C.; Wind, N. S.; Ward, T. H.; Stratford, I. J.; Patterson, A. V. *Biochem. Pharmacol.* **2003**, *66*, 1199-1206.

(92) De Abreu, F. C.; Ferraz, P. A. d. L.; Goulart, M. O. F. *J. Braz. Chem. Soc.* **2002**, *13*, 19-35.

(93) Siraki, A. G.; Chan, T. S.; O'Brien, P. J. *Toxicol. Sci.* **2004**, *81*, 148-159.

(94) Fujita, T.; Iwasa, J.; Hansch, C. *J. Am. Chem. Soc.* **1964**, *86*, 5175-5180.

(95) Albert, A. *Selective Toxicity*; 3rd ed.; The Broadwater Press Limited: Herts, 1965.

(96) Hansch, C.; Leo, A.; Taft, R. W. *Chem. Rev.* **1991**, *91*, 165-195.

(97) Prakash, G.; Hodnett, E. M. *J. Med. Chem.* **1978**, *21*, 369-374.

(98) Hartmann, R. W.; Schwarz, H.; Schonenberger, H. *J. Med. Chem.* **1983**, *26*, 1137-1144.

(99) Hartmann, R. W.; Heindl, A.; Schonenberg, H. *J. Med. Chem.* **1984**, *27*, 577-585.

(100) Selassie, C. D.; Garg, R.; Mekapati, S. *Pure Appl. Chem.* **2003**, *75*, 2363-2373.

Chapter 2

2.1 Introduction

The calothrixins A (**1.26**) and B (**1.27**) are the first indolophenanthridinediones isolated from nature. These compounds show potent activity against certain cancer cell lines as well as against the malarial parasite *P. falciparum*.[1-3] As further biological studies are required to assess the selectivity and potency of these compounds, a ready source of the calothrixins is needed. However, to date the isolation of the calothrixins from cultures of *Calothrix* cyanobacteria has proven to be difficult. In view of this problem, synthetic strategies to access the calothrixins are highly desired.

Prior to devising our synthetic route, we surveyed the literature and found that the structure of calothrixin B is remarkably similar to the tetracyclic ellipticine quinone (**1.33**), a precursor in the synthesis of ellipticine (**1.70**) which was first reported by Taylor *et al.* in 1979.[4] The key difference in the structures of calothrixin B and ellipticine quinone is the presence of a fifth fused benzene ring in the former. In view of this, we envisaged that the literature methods for synthesizing ellipticine quinone may provide potential synthetic routes to the calothrixins.

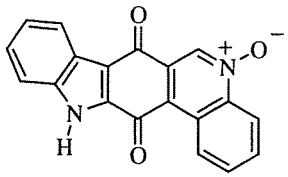

1.26

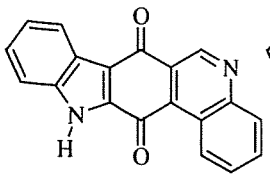

1.27

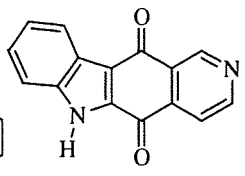

1.33

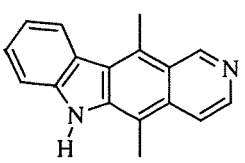

1.70

Taylor's synthesis of ellipticine quinone (**1.33**) is summarized in **Scheme 2.1**. The first step of the synthesis involved the preparation of the C2-lithiated species (**2.1**) from *N*-phenylsulfonylindole (**2.2**), followed by the addition of pyridine lactone (**2.3**) to give the C2-substituted ketone **2.4**. The primary alcohol functionality in the ketone **2.4** was then oxidized to the aldehyde **2.5** to enable intramolecular electrophilic aromatic substitution of the deprotected indole onto the aldehyde group. However, deprotection of the indole nitrogen under basic conditions in the presence of the reactive aldehyde group led to the concomitant formation of the oxepinoindole **2.6**. To prevent this premature reaction of the aldehyde functionality, the aldehyde group was protected as the acetal **2.7** prior to the deprotection of the *N*-phenylsulfonyl group. Subsequent treatment of the acetal **2.8**

with hot aqueous acid led to the hydrolytic cleavage of the acetal functionality. The resulting aldehyde then underwent intramolecular electrophilic aromatic substitution with the indole moiety at the C3 position to form the tetracyclic ring system **2.9**. *In situ* aerial oxidation of **2.9** then led to the formation of ellipticine quinone **1.33** but the overall yield was only 36%.[4]

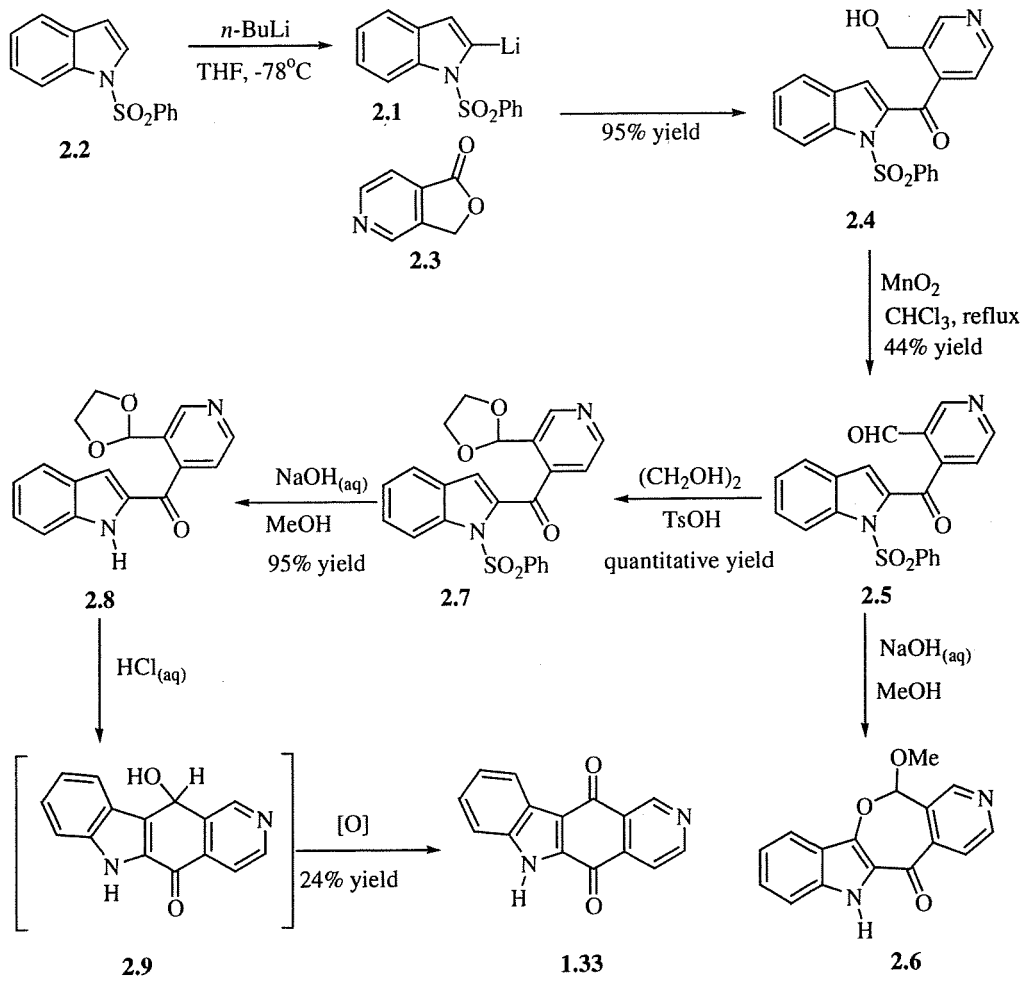

Scheme 2.1

Similar strategies for the synthesis of ellipticine quinone were later reported by Gribble and coworkers. The first method reported by Gribble *et al.*, shown in **Scheme 2.2**, employed analogous conditions to the C2-lithiation reaction of *N*-phenylsulfonylindole (**2.2**) reported by Taylor.[5] The synthesis differs from Taylor's work in the choice of commercially available pyridine-3,4-anhydride **2.10** as the electrophile in lieu of the lactone **2.3**. Regioselective attack of the lithiated indole **2.1** onto the anhydride **2.10** resulted in the formation of the indole **2.11** as the major product. Several attempts were

subsequently made to effect an intramolecular Friedel-Crafts acylation reaction by converting the acid functionality in the indole **2.11** to the acid chloride. However, this resulted in undesired side reactions such as the C3 chlorination of the indole **2.11**. The failure of the intramolecular Friedel-Crafts acylation reaction of **2.11** was attributed to the electron withdrawing properties of the *N*-phenylsulfonyl group which attenuates the reactivity of the indole towards electrophilic attack. In order to facilitate the Friedel-Crafts reaction, indole **2.11** was treated with base to cleave the *N*-phenylsulfonyl group. This was then followed by treatment with acetic anhydride to activate the carboxylic acid group in **2.11** by conversion to the reactive mixed anhydride. Unfortunately, nucleophilic attack of the indole nitrogen onto the mixed anhydride led to the formation of the lactam **2.12**. Fortunately, subsequent treatment of the lactam **2.12** with aqueous base resulted in the rearrangement of the lactam to the desired ellipticine quinone **1.33** in quantitative yield.

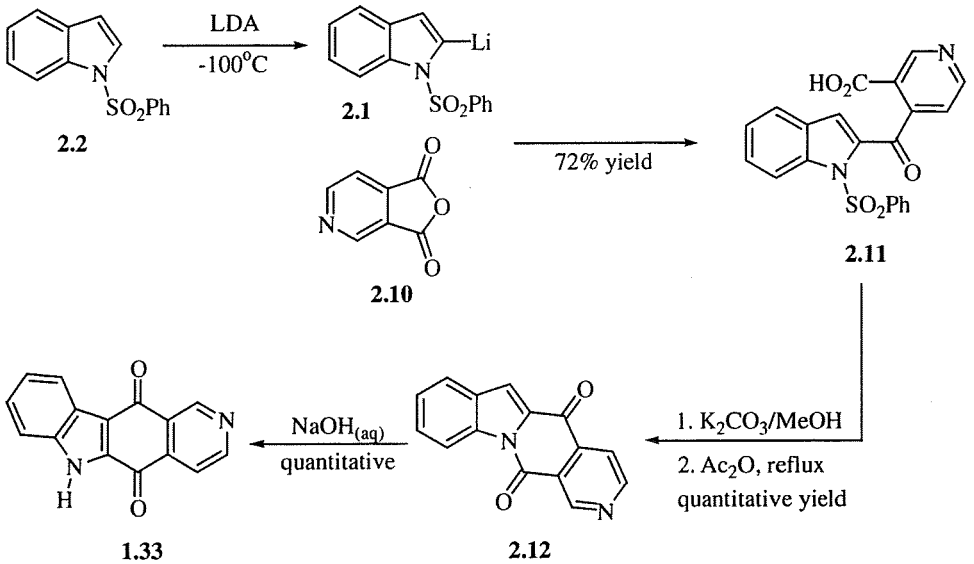

Scheme 2.2

The second method reported by Gribble, outlined in **Scheme 2.3**, was developed to provide a convenient two-step synthesis of ellipticine quinone from *N*-phenylsulfonylindole **2.2** and 3-chlorocarbonyl-4-methoxycarbonylpyridine (**2.13**).[6] The authors reported that the regioselective ring opening of commercially available pyridine-3,4-anhydride (**2.10**) could be accomplished using sodium methoxide to obtain the desired keto acid **2.14.** The requisite acid chloride **2.13** was then prepared by reacting the keto acid **2.14** with thionyl chloride. The Friedel-Crafts acylation reaction

between the acid chloride **2.13** and the indole **2.2** led to the formation of the keto ester **2.15** in fair yields. Subsequent treatment of the keto ester **2.15** with LHMDS gave the C2-lithiated intermediate which then cyclized to the desired ellipticine quinone **1.33** with concomitant removal of the *N*-phenysulfonyl group. Although the overall yield is only 23% with respect to the indole **2.2**, the procedure is relatively simple and in theory it can be carried out on a multigram scale.

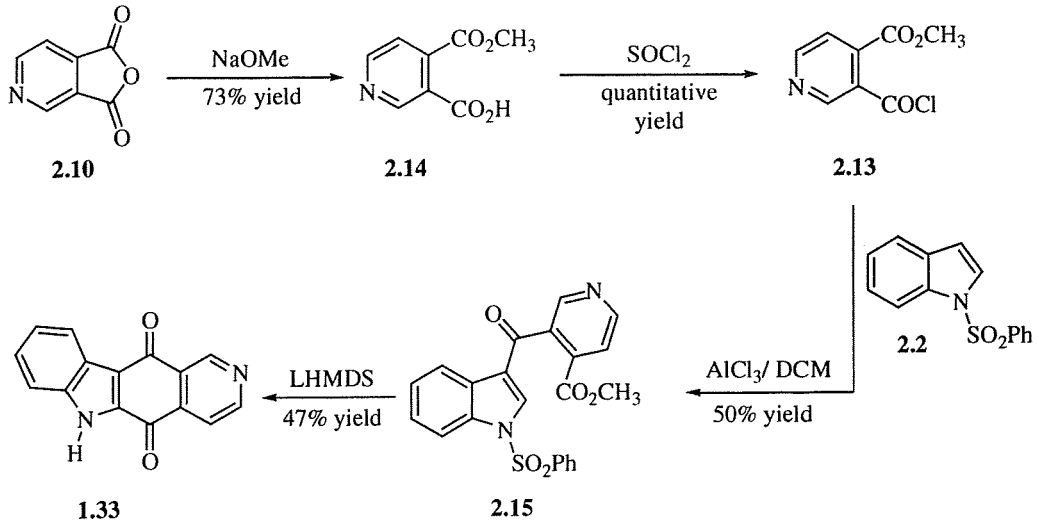

Scheme 2.3

A different approach to the synthesis of ellipticine quinone utilized a sequence of lithiation reactions in a one pot procedure as shown in **Scheme 2.4**. Treatment of 4-(*N,N*-diethylcarbonyl)pyridine (**2.16**) with *s*-BuLi generated the C3-anion **2.17**. The anion then attacked the formyl group of the protected indole **2.18** to form the alkoxide **2.19** *in situ*. Subsequent addition of more *s*-BuLi led to the formation of *N*-MOM protected quinol **2.20** which underwent facile aerial oxidation to give the product *N*-MOM ellipticine quinone **2.21** in 26% yield. Although the synthesis is quite short, the low yields obtained make this strategy uneconomical.[7]

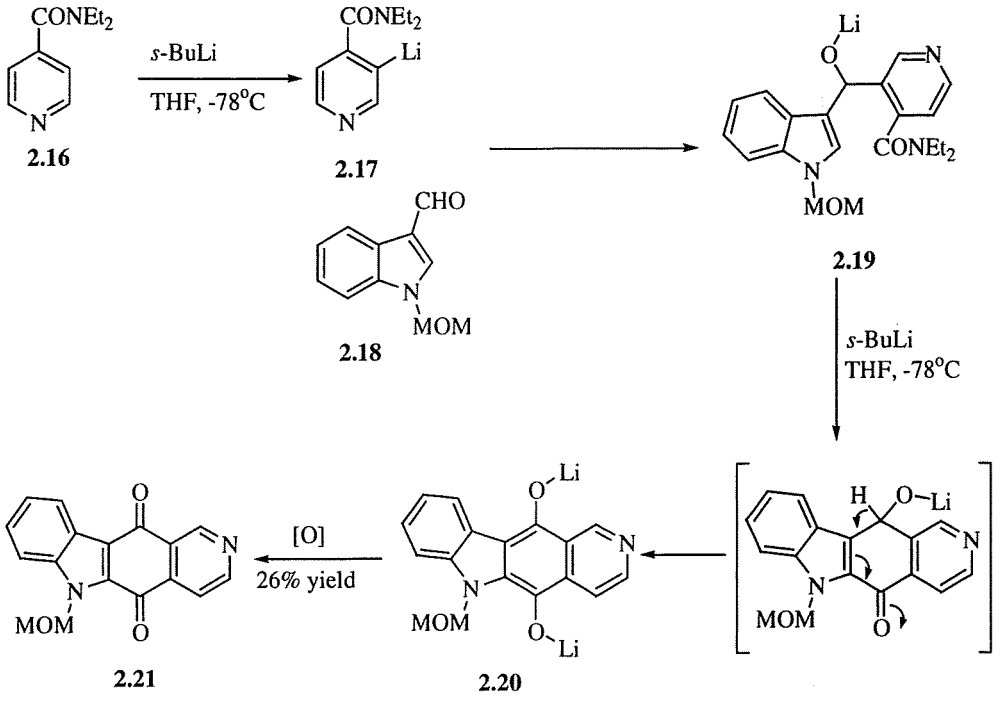

Scheme 2.4

The first synthesis of the calothrixins reported by Kelly *et al.*[8] was achieved using the one pot methodology discussed above for the synthesis of *N*-MOM ellipticine quinone. The synthesis outlined in **Scheme 2.5** was by no means trivial, and several problems were encountered. The use of alkyl lithiums (*s*-BuLi, *t*-BuLi) as metallating agents of 4-(*N,N*-diethylcarbonyl)quinoline **2.22** met with failure. Instead, the use of a lithium amide such as LiTMP was essential to ensure the successful lithiation of the quinoline **2.22**. When the lithiated quinoline **2.23** was treated with TMSCl, formation of the TMS quinoline amide **2.24** was noted to proceed at a very slow rate. This TMSCl trapping experiment indicated that only a small concentration of the lithiated quinoline **2.23** was present due to the equilibrium between the reactant quinoline **2.22** and LiTMP.[8]

After careful optimization, treatment of the quinoline **2.22** with a four-fold excess of LiTMP followed by the addition of *N*-MOM-3-formylindole **2.18** gave the desired *N*-MOM calothrixin B **2.25** in 26% yield. In the penultimate step, acid hydrolysis of the MOM group gave the desired calothrixin B (**1.27**) in 74% yield. In the final step, oxidation of the quinoline nitrogen atom of calothrixin B was achieved using *m*-CPBA to yield calothrixin A (**1.26**) in 71% yield.[8]

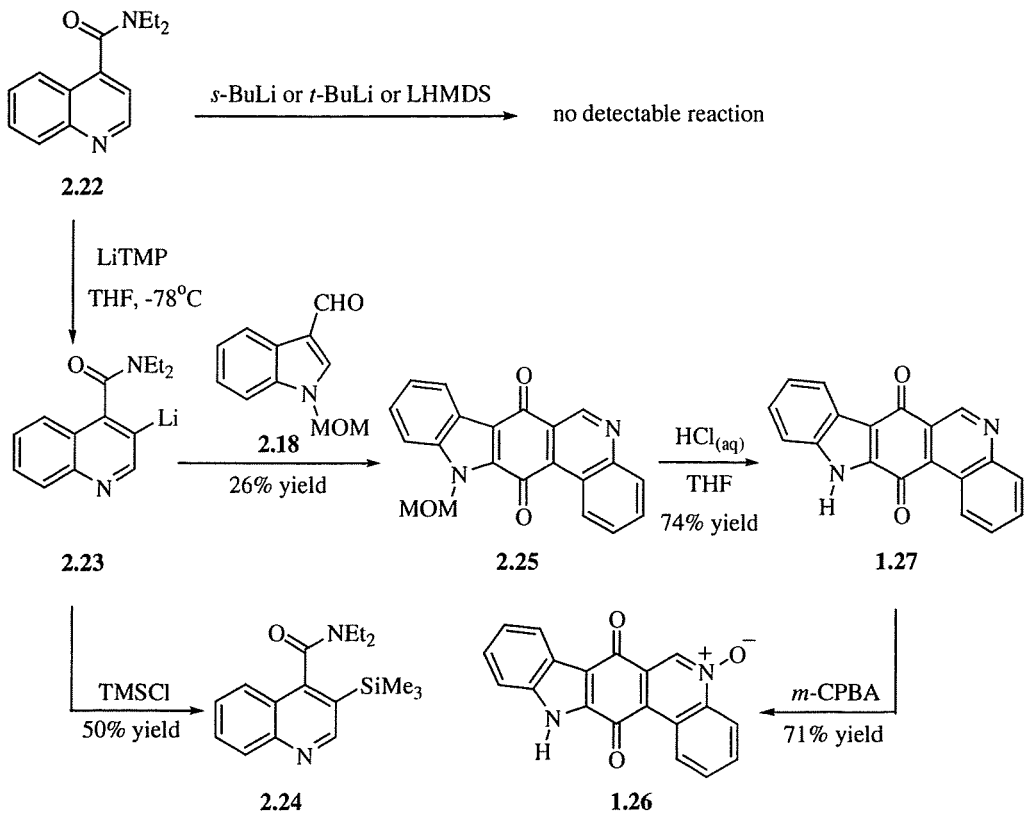

Scheme 2.5

Although Kelly's synthesis of the calothrixins is quite simple, the route suffers from a number of serious drawbacks. First of all, the starting materials employed are costly and thus the route is unsuitable for large scale syntheses. Secondly, the lithiation step of the quinoline **2.22** was problematic and led to a complex mixture of products. In addition, the synthetic route is not amenable to the rapid synthesis of structural variants or analogues due to the difficulty in effecting the key lithiation step. Despite attempts to optimize the reaction conditions, the yields reported by Kelly were quite low (12% overall yield with respect to the indole **2.18**). In view of this, a new and more versatile synthetic route was devised.

Our retrosynthetic strategy shown in **Scheme 2.6** employs an initial disconnection at the C12a-C13 bond of calothrixin B (**1.27**). A second disconnection can be made at the C7a-C7 bond of the aryl ketone **2.26**, giving reactants that correspond to indole (**2.27**) and the acid chloride **2.28**. The acid chloride **2.28** can be synthesized from the corresponding 3-carboxyl-4-methoxycarbonylquinoline **2.29**, which in turn is prepared from quinoline-3,4-anhydride **2.30**. From a synthetic point of view, the regioselective

ring opening of the anhydride **2.30** yields the mixed acid **2.29** which in turn can be converted to the acid chloride **2.28**. Our first approach utilizes the strategy reported by Gribble *et al.* for the synthesis of ellipticine quinone **1.33** previously shown in **Scheme 2.3**.[6,9] The key step in our synthesis is the coupling of commercially available indole (**2.27**) to the acid chloride **2.28** which can be carried using Friedel-Crafts acylation strategies to yield the aryl ketone **2.26**. The final step in our method is the cyclization of the aryl ketone **2.26** by lithiation or other similar strategies. We therefore began our investigation with the synthesis of the quinoline-3,4-anhydride **2.30**, the essential precursor for the requisite acid chloride **2.28.**

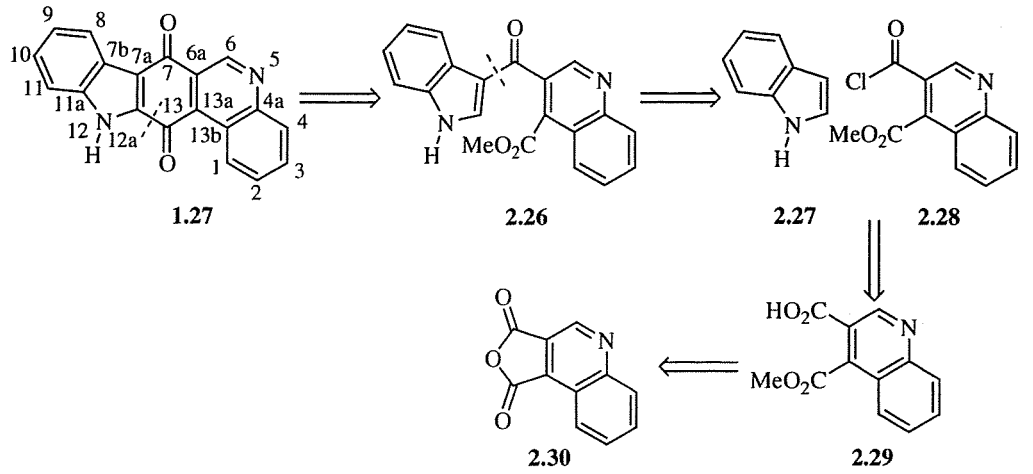

Scheme 2.6

2.2 Synthesis of Quinoline-3,4-anhydride (2.30)

The synthesis of 3-chlorocarbonyl-4-methoxycarbonylquinoline (**2.28**), the key intermediate in our synthetic strategy, began with the synthesis of quinoline-3,4-anhydride (**2.30**). The synthesis of the anhydride **2.30** has been reported in the literature and employs cheap, readily available starting materials such as isatin (**2.31**) and the acetal 1,1-dimethoxy-3-butanone (**2.32**).[10]

The reaction between isatin (**2.31**) and the acetal **2.32** proceeded via the Pfitzinger reaction as shown in **Scheme 2.7**. The reaction utilized a sequence of basic and acidic media to control the outcome of the reactions. For example, the first reaction step required concentrated aqueous KOH to effect the ring opening of isatin to produce isatic

acid (**2.33**). Under strongly basic conditions, an aldol reaction between the enolate **2.34** generated from the acetal and the keto group of isatic acid can ensue to yield the unwanted 2-methyl-3-formyl-4-carboxyquinoline (**2.35**).[10] To avoid this reaction, the pH of the isatic acid solution was adjusted to a pH of 9. Under these conditions, it is presumed that the enol ether 4-methoxy-3-buten-2-one (**2.36**) is formed from the acetal **2.32** *in situ*.[11] Subsequent addition of the amino group of isatic acid to the enol ether **2.36** followed by the acid-catalyzed elimination of methanol precipitated the enamine **2.37** as a bright yellow solid. Upon treatment with base, the enamine **2.37** rapidly underwent intramolecular cyclization to give the product 3-acetyl-4-carboxyquinoline (**2.38**) in 94% yield. The cyclization of the enamine **2.37** to the acetyl quinoline **2.38** can be monitored by ^{1}H NMR spectroscopy. The ^{1}H NMR spectrum of the acetyl quinoline **2.38** showed a characteristic singlet proton resonance at δ9.27 in the aromatic region for the C-H adjacent to the nitrogen atom while the enamine **2.37** showed a distinct singlet proton resonance for the C-H adjacent to the nitrogen atom at δ9.62. The melting point of the acetyl quinoline **2.38** was in good agreement with the value reported in the literature.[10]

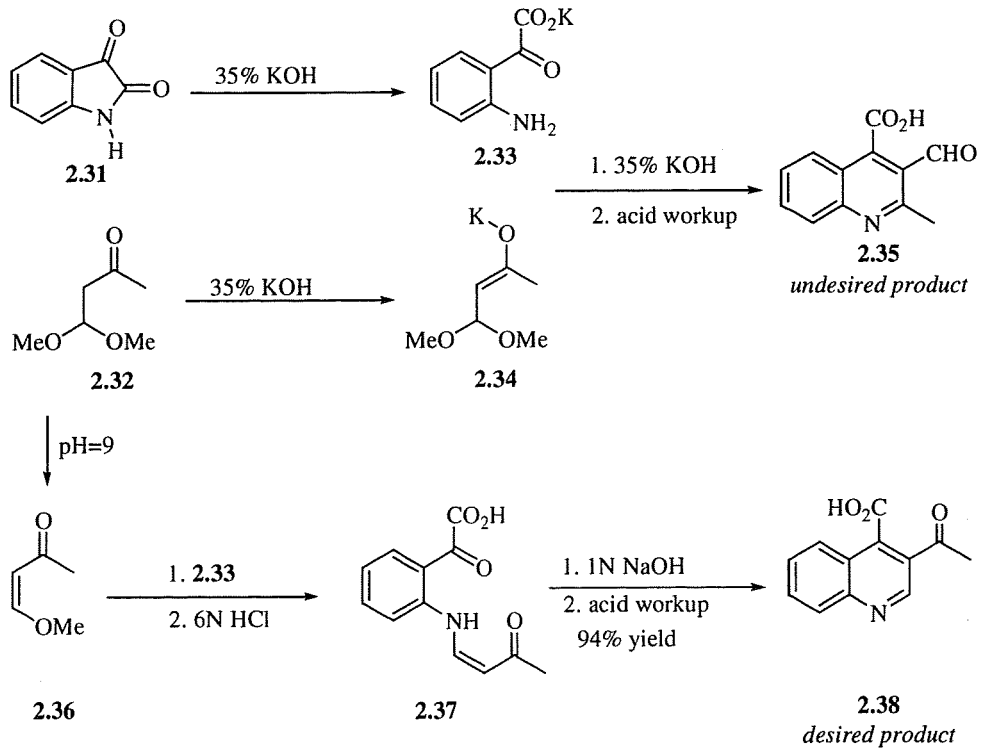

Scheme 2.7

Scheme 2.8 outlines the transformations required to convert the acetyl quinoline **2.38** to the desired anhydride **2.30**. The first transformation involved the oxidation of the acetyl group of acetyl quinoline **2.38** to the carboxyl functionality via the haloform reaction using sodium hypochlorite as the oxidant.[12] The quinoline-3,4-dicarboxylic acid **2.39** was obtained as a fine white powder in 93% yield with a melting point identical to the value reported in the literature.[10] The anhydride **2.30** was then obtained by refluxing the acid **2.39** in acetic anhydride.

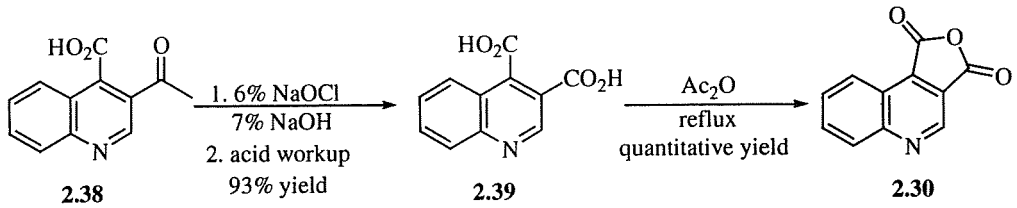

2.38 **2.39** **2.30**

Scheme 2.8

With anhydride **2.30** in hand, we were poised to synthesize the acid chloride **2.28**. Our first task was to effect the regioselective ring opening of the anhydride **2.30**. We specifically required nucleophilic attack at the C=O group attached to the C4-position of the anhydride **2.30** in order to obtain the C3-carboxylic acid. To our knowledge there is only one report of the ring opening reactions of quinoline anhydride with a nucleophile. Specifically, Godard reported that quinoline-3,4-anhydride undergoes selective ring opening in the presence of ammonia to give 4-aminocarbonyl-3-carboxylquinoline.[13] Encouraged by this report and armed with the knowledge that selective ring opening of pyridine-3,4-anhydride **2.10** was effected with NaOMe,[9] we treated the quinoline anhydride **2.30** with sodium methoxide. However, only a disappointing 1:1 mixture of the regioisomers **2.29** and **2.40** was obtained. In our hands, a 1:1 mixture of the desired keto acid **2.14** and its regioisomer was also obtained when pyridine-3,4-anhydride **2.10** was treated with NaOMe under the specified conditions. The discrepancies in these observations with that reported in the literature are not easily rationalized. Fortunately, when dry refluxing methanol was used to effect the ring opening of the quinoline anhydride **2.30**, greater regioselectivity (5:1 of 4-methylester versus 3-methylester) was observed as shown in **Scheme 2.9**. In this manner, the desired mixed acid **2.29** was obtained in 70% yield from the anhydride **2.30**.

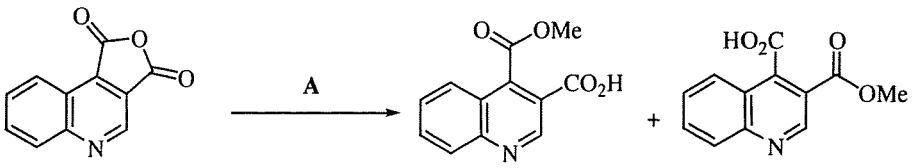

2.30 2.29 2.40

A. Reaction conditions	(2.29:2.40)
1. NaOMe, dry MeOH, -70°C to r.t.	1:1
2. dry MeOH, reflux	5:1

Scheme 2.9

With the desired mixed acid **2.29** in hand, we were able to prepare the acid chloride **2.28** in quantitative yields using thionyl chloride. As the acid chloride **2.28** was unstable, we were only able to characterize the crude product by ^{1}H and ^{13}C NMR spectroscopy. The ^{1}H NMR spectrum of the acid chloride clearly shows a methyl peak signal at δ4.20 as expected for the mixed acid. More importantly, the ^{13}C NMR spectrum shows two C=O peaks at δ163.0 and δ163.1. To prove conclusively that the compound obtained was indeed the acid chloride and not the *bis*-quinoline anhydride **2.41**, the acid chloride was treated with methanol and the crude product was analyzed via ^{1}H NMR spectroscopy. The ^{1}H NMR spectrum confirmed that the only product formed was the quinoline diester **2.42**, and therefore confirmed the identity of the desired compound as the acid chloride **2.28.**

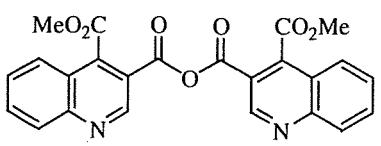

2.41

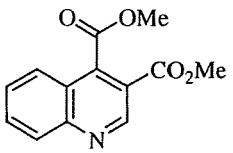

2.42

2.3 Investigation of Methods for the Acylation of Indole

The next step in our synthesis was to couple the acid chloride **2.28** to the C3-position of indole to obtain the aryl ketone **2.26**, a crucial synthetic intermediate in our proposed calothrixin B synthesis. As there are various literature procedures for the regioselective acylation of indole, different methodologies were attempted in order to establish the most efficient conditions for the coupling reaction.

2.3.1 Friedel-Crafts Acylation of *N*-Protected Indoles

In view of the literature precedence for the synthesis of the related ellipticine quinone **1.33** shown earlier in **Scheme 2.3**, our initial attempt at coupling the acid chloride **2.28** to indole utilized the Friedel-Crafts acylation reaction. This reaction is the most widely used method for the preparation of aryl ketones such as **2.26** due to the range of reaction conditions that can be employed to improve the efficiency and selectivity in the chemical transformation. In the general reaction shown in **Scheme 2.10**, an acid chloride is activated towards nucleophilic attack by the addition of a Lewis acid such as $AlCl_3$ to yield a tight ion pair consisting of an acyl cation **2.43** and an anion such as aluminum tetrachloride. For substrates which are degraded by $AlCl_3$, weaker Lewis acids such as $FeCl_3$, $ZnCl_2$ and even $BF_3(OEt_2)$ have been successfully employed to generate the acyl cation *in situ*.[14] The acyl cation formed can then react with an electron-rich substrate such as indole. However, acylation of indole can yield a mixture of C3 and/or N1 monoacylated as well as N1,C3-diacylated products.[15] The competing *N*-acylation reaction may be avoided by using *N*-protected indoles in the Friedel-Crafts reactions.

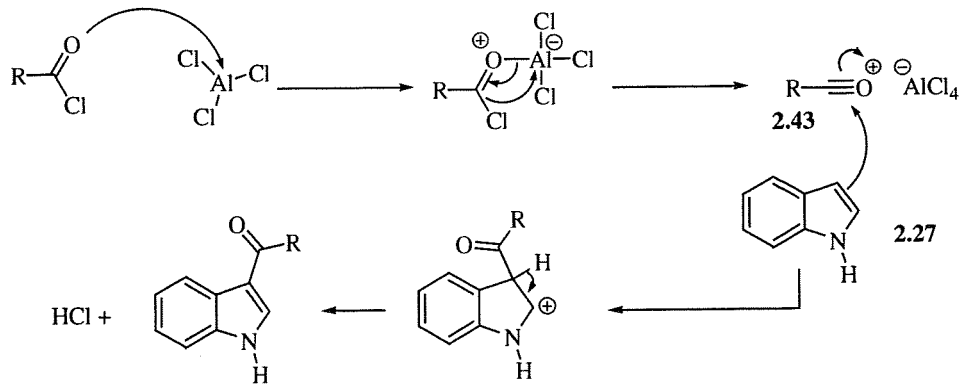

Scheme 2.10

A survey of the literature shows that acylation reactions can be readily carried out on *N*-phenylsulfonylindole (**2.2**).[9] With this consideration in mind, we prepared *N*-phenylsulfonylindole following the literature procedure as shown in **Scheme 2.11**.[16] The treatment of indole (**2.27**) with KOH in a benzene/H_2O bilayer followed by the addition of sulfonyl chlorides **2.44** and **2.45** gave the desired *N*-sulfonylindoles **2.1** and **2.46** respectively in high yields. 2.2

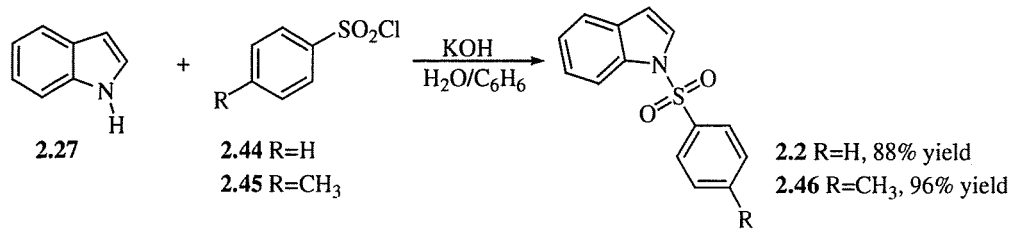

2.27 **2.44** R=H, **2.45** R=CH_3 **2.2** R=H, 88% yield, **2.46** R=CH_3, 96% yield

Scheme 2.11

We first tested the Friedel-Crafts acylation reaction by treating *N*-tosylindole (**2.46**) with acetic anhydride in the presence of $AlCl_3$ to obtain a modest 51% yield of *N*-tosyl-3-acetylindole. Encouraged by this result, Friedel-Crafts acylation of *N*-tosylindole with the acid chloride **2.28** was then attempted in the presence of $AlCl_3$. To our dismay, no product formation was observed and only unreacted *N*-tosylindole was recovered.

This failed reaction suggested that the acid chloride **2.28** is less reactive than acetic anhydride. In addition, the reactivity of the indole is attenuated by the electron withdrawing *N*-tosyl group. To overcome these problems, we attempted the reaction of *N*-tosylindole with the acid chloride **2.28** in the presence of the stronger Lewis acid $TiCl_4$, but again none of the desired product was formed and *N*-tosylindole was recovered. Refluxing the reaction mixture likewise failed to yield the desired product. To circumvent this problem, attempts were made to react unprotected indole (**2.27**) with the acid chloride **2.28**.

2.3.2 Friedel-Crafts Acylation of Unprotected Indole

The selective coupling of acid chlorides to unprotected indole has been demonstrated by Okauchi *et al.*[17] It has been noted that the use of $AlCl_3$ led to dimerization of indole while dialkyl aluminum chlorides and trialkyl aluminum catalysts gave 3-acylindoles in good yields. To our delight, the addition of the acid chloride **2.28** to indole in the presence of Et_2AlCl yielded the desired aryl ketone **2.26** as a pale yellow solid in 27% yield **[Scheme 2.12]**. ^{1}H NMR spectroscopy of the product revealed characteristic peaks at δ3.72 due to the methoxy hydrogens and at δ9.20 due to the aromatic hydrogen adjacent to the quinoline nitrogen which were indicative of the successful coupling reaction. Low resolution EIMS showed a molecular ion peak at 330 *m/z* which was confirmed by HRMS. However, as the yields were low, other coupling methods were considered.

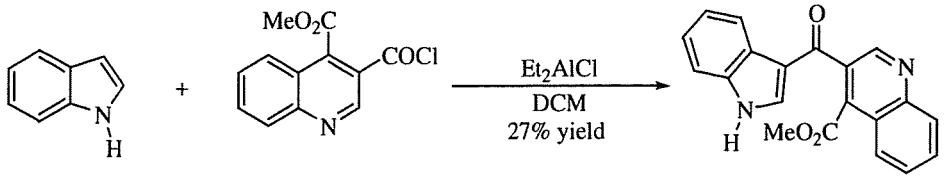

2.27 **2.28** **2.26**

Scheme 2.12

2.3.3 Model Studies in the Metallation of the Indolic C3-Position

There is much literature precedence for the metallation at the C3-position of *N*-sulfonylindoles. For example, the halogen-metal exchange reaction of *N*-tosyl-3-iodoindole (**2.47**) can be readily carried out using *n*-BuLi to give the C3-metallated compound **2.48** *in situ* [**Scheme 2.13**]. The addition of an acid chloride or alkyl halide to the reaction mixture is reported to yield the 3-substituted compound. This lithiation must be carried out at temperatures below –100°C to prevent rearrangement of *N*-tosyl-3-lithioindole **2.48** to the more stable *N*-tosyl-2-lithioindole **2.49**.[18] However, when we attempted to couple the acid chloride **2.28** to the C3-lithiated *N*-tosylindole **2.48** under these conditions, the desired product was not obtained and *N*-tosylindole (**2.46**) was recovered [**Scheme 2.14**].

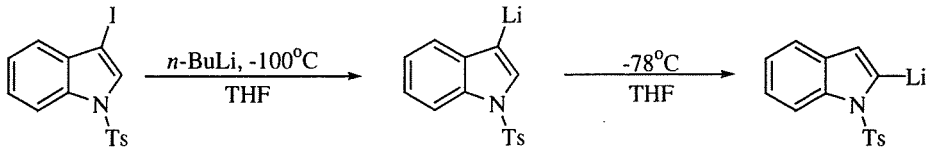

2.47 **2.48** **2.49**

Scheme 2.13

In order to understand the reasons for the failure of this reaction, deuterium-labeling studies were carried out. In these studies, *N*-tosyl-3-iodoindole (**2.47**) was treated with an excess of *n*-BuLi to generate the lithioindole species. D_2O was then added to the reaction mixture in lieu of the acid chloride **2.28** and the reaction mixture was analyzed via ^1H NMR spectroscopy. Integration of the ^1H NMR signals showed 75% D incorporation at the C3-position and only 25% D incorporation at the C2-position of *N*-tosylindole (**2.46**). The results suggest that the failure to obtain the desired product was due to the low reactivity of the acid chloride **2.28** at –100°C and not due to the inability to generate the lithiated species. Thus to facilitate the coupling reaction between the acid chloride and *N*-tosyl-3-iodoindole **2.47**, higher temperatures were required. As the

N-tosyl-3-lithioindole (**2.48**) was not stable at temperatures above -100°C, it was necessary to convert the indole **2.47** to *N*-tosyl-3-(chloromagnesium)indole **2.50** by halogen-magnesium exchange at -30°C as shown in **Scheme 2.14**. Subsequent deuterium-labeling studies followed by removal of the tosyl group showed 100% D incorporation at the C3-position of the indole **2.27**, but unfortunately the analogous reaction with the acid chloride **2.28** did not yield the desired product.

We had so far failed to effect the coupling reaction between indole and the acid chloride **2.28** at temperatures below 0°C. To achieve higher reaction temperatures, the lithioindole species **2.48** was transmetallated with $ZnCl_2$ to give the more stable *N*-tosyl-3-(chlorozinc)indole **2.51**.[19] To our delight, subsequent addition of the acid chloride to the reaction mixture at room temperature followed by chromatography gave the desired aryl ketone **2.26** in 47% yield with respect to the indole **2.47**. Interestingly, the tosyl group was cleaved from the aryl ketone **2.26** in the course of the reaction or subsequent workup. The results, however, confirmed the hypothesis that the reactivity of the acid chloride **2.28** towards various C3-metallated indoles was attenuated at lower temperatures.

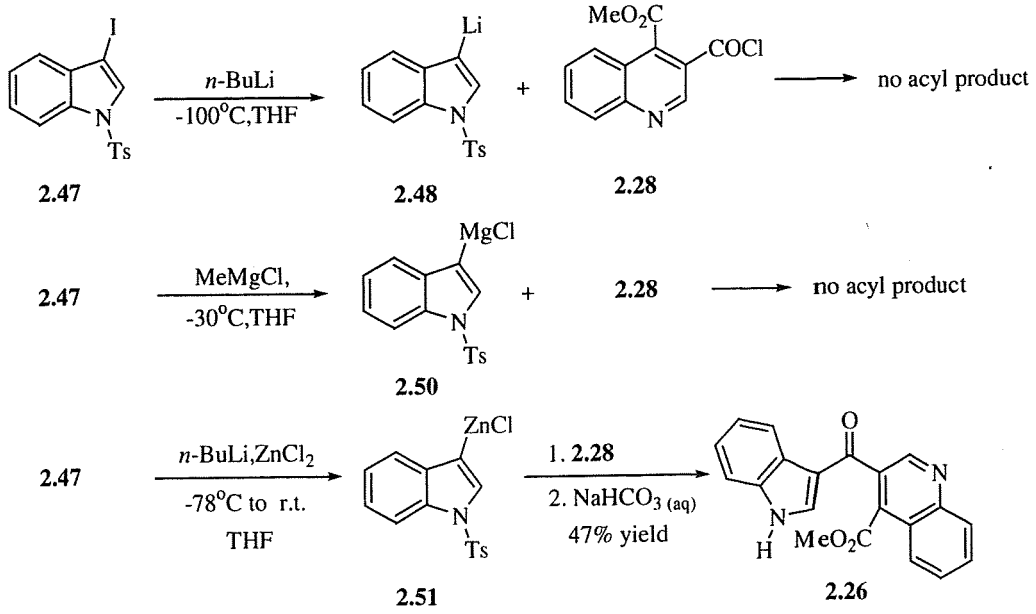

Scheme 2.14

2.3.4 *N*-Metallation of Indole and Coupling to Acid Chlorides

Our studies so far have shown that the aryl ketone **2.26** can be synthesized following two different procedures at room temperature. The first procedure utilized the unprotected indole and Et_2AlCl in conjuction with the acid chloride **2.28** whereas the second method utilized the reaction between the *N*-tosyl-3-(chlorozinc)indole (**2.51**) and the acid chloride **2.28**. The simplicity of the first method was offset by the low yields obtained, and while the second method offered better yields, this was still too low for our purposes. Further consideration of the literature suggested that a third method for coupling indole to acid chlorides may be relatively easy to effect at room temperature with high yields in return.

Report by Bergman as well as Yang *et al.* have shown that Friedel-Crafts acylation can be carried out regioselectively using acid chlorides and *N*-(chlorozinc)indole (**2.52**) to give the desired 3-acylindoles in good yields.[20,21] Following the methodology of Yang, indole (**2.27**) was reacted with MeMgCl in the presence of $ZnCl_2$ to yield *N*-(chlorozinc)indole **2.52** as shown in **Scheme 2.15**. The addition of the acid chloride **2.28** and $AlCl_3$ gave the desired aryl ketone **2.26** in 79% yield. Further optimizations showed that the absence of $AlCl_3$ in the reaction mixture gave much better yields of the aryl ketone **2.26**. Thus the new route provided the best yields (typically 90%) for the acylation of indole with the acid chloride **2.28**, and the reaction was therefore scaled up to obtain gram quantities of the aryl ketone **2.26**.

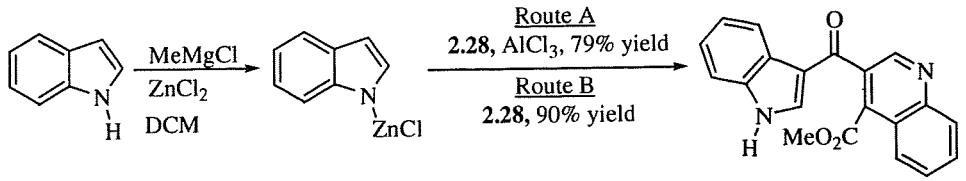

2.27 **2.52** **2.26**

Scheme 2.15

2.4 *N*-Protection of the Aryl Ketone 2.26 and Cyclization

With the key synthetic precursor **2.26** in hand, the success of the final carbon-carbon bond forming step to install the quinone moiety of calothrixin B (**1.27**) now relied on the choice of a suitable *N*-protecting group. It was envisaged that the protecting group must be stable to the harsh basic conditions required for lithiation but should be readily

removed under mild acidic conditions. With this consideration and in view of the literature precedence established by Gribble[9] and Kelly[8], a number of *N*-protected derivatives of **2.26** were synthesized.

The *N*-protected derivatives of the aryl ketone **2.26** were prepared using general literature methods for the *N*-protection of indoles as shown in **Scheme 2.16**. The general procedure for nitrogen protection involved treatment of the aryl ketone **2.26** with NaH to generate the N1-anion *in situ*, which was then quenched by the addition of the appropriate electrophile.[16,22]

The initial attempt focused on the synthesis of the *N*-acetyl ketone **2.53** following the general procedure outlined above. The ^{1}H NMR spectrum of the crude reaction mixture showed that the starting material was completely converted to the *N*-acetylated product as noted by the shift in the methoxy signal of the ester moiety from δ3.75 to δ3.72 as well as the presence of the acetyl protons at δ2.63. In addition, the ^{13}C NMR spectrum as well as EIMS and HRMS of the isolated compound were consistent with the identity of the derivative. However, the purification of the *N*-acetyl ketone proved to be difficult as purification by column chromatography on silica resulted in the cleavage of the *N*-acetyl group. Only a low yield (18%) of the purified *N*-acetyl ketone **2.53** was obtained along with the recovery of the aryl ketone **2.26**.

The second strategy was to protect the indole nitrogen of the aryl ketone **2.26** as the *N*-phenylsulfonyl ketone **2.54**. Following the outlined procedure, *N*-phenylsulfonyl ketone **2.54** was obtained in high yields as a bright yellow compound which was stable to purification on silica. However, attempts to cyclize the *N*-phenylsulfonyl ketone under various basic conditions (LDA, LDA and TMEDA, LHMDS and TMEDA, *t*-BuLi) failed to give the desired *N*-phenylsulfonyl calothrixin B, and in all cases the reaction and workup conditions led to the recovery of the aryl ketone **2.26**.

The third strategy was to synthesize the *N*-methoxymethyl (MOM) aryl ketone **2.55**. The alkylation of the aryl ketone **2.26** with MOMCl gave the desired product as a pale yellow solid in high yields (typically 90%).

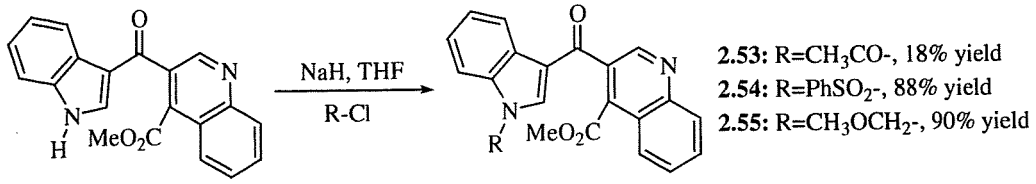

2.26

Scheme 2.16

With the *N*-MOM ketone **2.55** in hand, the intramolecular cyclization via the C2-lithiated indole species was attempted. The early attempts to effect the cyclization using a number of strong bases (*t*-BuLi, LHMDS) were unsuccessful due to the poor solubility of the *N*-MOM ketone **2.55** when diethyl ether was used as the solvent. Likewise, the cyclization reaction did not proceed when THF replaced ether as the solvent despite the improved solubility of the *N*-MOM ketone **2.55** in THF. It has been noted in the literature that strong bases such as LHMDS exist as dimers in solution, and the use of additives dissociates these dimers into the more reactive monomeric units.[23] Thus when the cyclization reaction was carried out in THF using LDA (or alternatively LHMDS) with the addition of a stoichiometric amount of TMEDA, the reaction proceeded smoothly to yield the desired *N*-MOM calothrixin B (**2.25**). Further optimizations led to the best yields when the base was added to the ketone **2.55** in THF at -78°C and the mixture was slowly warmed to 0°C and kept at 0°C for 2 hours. The reaction was then quenched at 0°C, and purification of the reaction mixture by column chromatography followed by recrystallization from ether and *n*-hexane gave *N*-MOM calothrixin B (**2.55**) as amorphous orange flakes in 92% yield.

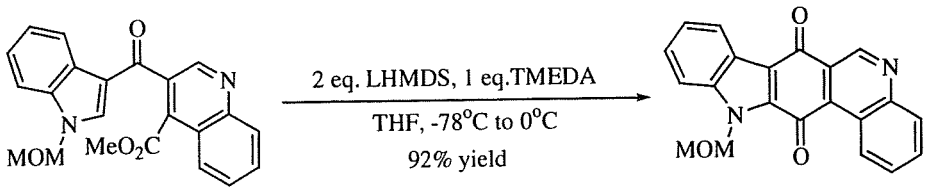

2.55 2.25

Scheme 2.17

The identity of the *N*-MOM calothrixin B synthesized was confirmed by ^{1}H NMR spectroscopy and comparison to the literature melting point. However, small differences in the ^{13}C NMR spectrum were noted (± 0.1-0.3 ppm) in comparison to the values reported by Kelly.[8] Further confirmation of the structure was obtained using EIMS, HRMS, and elemental analysis.

2.5 Removal of the *N*-Methoxymethyl Group

In order to access calothrixin A (**1.26**) and B (**1.27**), the deprotection of the *N*-MOM group of **2.25** was required. Our initial attempts at the deprotection of *N*-MOM calothrixin B utilized the conditions reported by Kelly.[8] However, in our hands, after 2 days of refluxing *N*-MOM calothrixin B (**2.25**) in a solution of HCl and THF, only unreacted starting material was recovered. When the reaction conditions were modified to employ a DMSO-HCl mixture, hydrolysis of the *N*-MOM group was observed but the yields of the desired calothrixin B (**1.27**) were difficult to reproduce and complex reaction mixtures were often obtained. The efficacy of BF_3OEt_2/LiBr for the removal of indolic *N*-MOM groups had been reported by Sundberg[24], but our attempts failed to give calothrixin B. The use of $AlCl_3$ to deprotect *N*-MOM calothrixin B only gave complex reaction mixtures. Clean and facile removal of the *N*-MOM group was finally achieved using a slight excess of BBr_3 in DCM as shown in **Scheme 2.18**.[25] Following treatment with BBr_3, the reaction mixture was then heated in saturated $NaHCO_3$ at 60°C, and subsequent workup gave the desired calothrixin B (**1.27**) as a red solid in 85% yield. We had thus concluded a total synthesis of the natural product calothrixin B in 4 steps with respect to the acid chloride in 63% overall yield, a considerable improvement over Kelly's method.

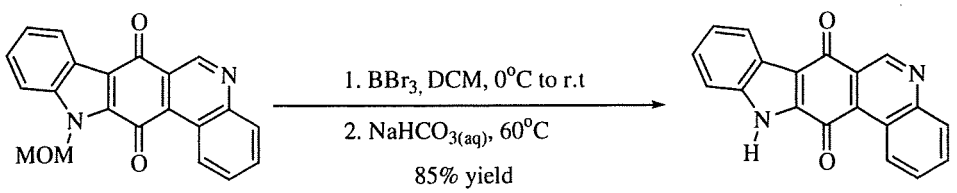

2.25 **1.27**

Scheme 2.18

The ^1H NMR spectrum of the synthetic calothrixin B (**1.27**) matched the spectrum reported by Rickards *et al.*[1] for the natural product. The EIMS and HRMS data were also consistent with the literature data for the natural product. Furthermore, co-spotting with authentic calothrixin B (**1.27**) followed by analysis via thin-layer chromatography showed that the synthetic compound was identical to the authentic natural product. There were small differences in the ^{13}C NMR spectrum (±0.1 to 0.3 ppm) of the synthetic material when compared to the literature data. These differences in carbon chemical shifts have been attributed to the presence of water in the *d*-DMSO.[8,26]

The synthesis of calothrixin A (**1.26**) from calothrixin B (**1.27**) was readily achieved using the method reported by Kelly.[8] Oxidation of calothrixin B was carried out using *m*-CPBA to yield calothrixin A as a deep red solid in 72% yield. The ^{1}H NMR spectrum and melting point for the synthetic material were identical to data for the natural product. Thin-layer chromatography via co-spotting with authentic calothrixin A also showed that the natural and synthetic compounds were identical.

2.6 Synthesis of Calothrixin Derivatives and Carbazoledione Analogues

With the success of our synthetic methodology, we were now poised to synthesize a range of compounds for Structure-Activity Relationship studies. Our paramount interest was to determine which structural features of the calothrixin molecule are essential for bioactivity. For example, in order to design better drugs based on the lead structure of the calothrixin B, it is important to assess the contribution of the different ring systems on the observed biological activity. In addition, as calothrixins A and B were now readily accesible by synthetic methods, the derivatives of the calothrixins will enable studies to examine the importance of *N*-substitution of the indole ring on biological activity.

The indolophenanthrenedione **2.56** was previously synthesized in our group for SAR studies to determine if the presence of the quinoline nitrogen on calothrixin B (**1.27**) was necessary for biological activity. Preliminary studies in our group have also shown that the indolophenanthrenedione **2.56** is less active than the quinoline-based calothrixin B (**1.27**).[27] To corroborate those results and to examine the contribution of the fifth aromatic ring to the bioactivity of these carbazolediones, the compounds ellipticine quinone (**1.33**) and benzocarbazoledione (**1.32**) were targeted for synthesis and biological studies.

It is interesting to note that although quinones are a well-established class of compounds which display biological activity, the role of the quinone ring in the bioactivation of the calothrixins A (**1.26**) and B (**1.27**) has not been assessed. The closely related compound, ellipticine (**1.70**), is an important anticancer compound which does not possess the

quinone moiety. Thus, to determine if the quinone moiety is essential for bioactivity, attempts were made to synthesize the ellipticine analogue 5-methoxymethyl-7,13-dimethyl-12*H*-5,12-diaza-indeno[1,2-*b*]-phenanthrene **2.57**.

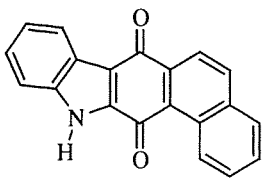

2.56

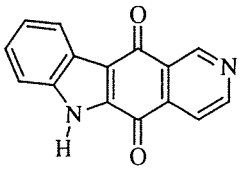

1.33

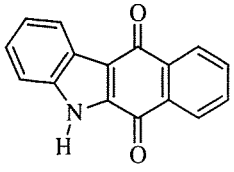

1.32

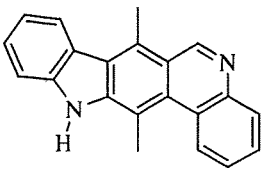

2.57

2.6.1 Synthesis of N12-Substituted Calothrixin B

The first goal was to synthesize some N12-substituted calothrixin B derivatives. The biological activity of these compounds would then be determined in order to assess the effect of *N*-substitution of the indole ring of calothrixin B. **Scheme 2.19** outlines the synthesis of these target compounds.

The initial synthesis employed the method used for the installation of the *N*-protecting groups for the aryl ketone **2.26**. In a trial reaction, the treatment of calothrixin B (**1.27**) with NaH and benzyl bromide in THF gave the desired *N*-benzyl calothrixin B (**2.58**) in only 38% yield, with unreacted calothrixin B also being isolated. The poor conversion of calothrixin B (**1.27**) to *N*-benzyl calothrixin B (**2.58**) is likely to be due to the poor solubility of calothrixin B in THF. When DMF replaced THF as the solvent, yields of 88% of *N*-benzyl calothrixin B (**2.58**) were obtained and no unreacted calothrixin B was observed. The procedure was then applied towards the synthesis of *N*-ethyl (**2.59**), *N*-methyl (**2.60**), *N*-acetyl (**2.61**), and *N*-phenylsulfonyl (**2.62**) calothrixin B derivatives.

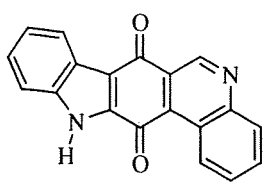

1.27

1. NaH, DMF, 0°C
2. R-X
   R-X=BnBr
   R-X=EtBr
   R-X=MeI
   R-X=AcCl
   R-X=$PhSO_2Cl$

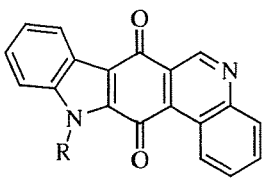

2.58: R=Bn, 88% yield
2.59: R=Et, 54% yield
2.60: R=Me, 0% yield
2.61: R=Ac, 47% yield
2.62: R=$PhSO_2$, 0% yield

Scheme 2.19

Treatment of calothrixin B (**1.27**) with NaH in DMF followed by the addition of ethyl bromide gave *N*-ethyl calothrixin B (**2.59**) as a dark red solid in 54% yield. The product was poorly soluble in organic solvents such as CH_2Cl_2, $CHCl_3$, and DMSO. Analysis of the ^1H NMR spectrum showed characteristic ethyl proton resonances at δ1.62 and 4.80 due to the methyl and methylene group respectively. To confirm the identity of the product, the EIMS of the compound was obtained and a molecular ion peak was observed at 326*m/z*, which was confirmed by HRMS. The melting point of the new compound was observed at 269-270°C.

When calothrixin B was treated with NaH in DMF followed by the addition of methyl iodide, a pale yellow solid was obtained in 88% yield. Analysis by ^1H NMR spectroscopy, however, showed that the product obtained was not the desired *N*-methyl calothrixin B (**2.60**), but the *N,N'*-dimethyl calothrixin salt **2.63 [Scheme 2.20]**. The product **2.63** is presumably formed by further methylation of the intermediate *N*-methyl calothrixin B (**2.60**) at the quinoline nitrogen position. The identity of the product was confirmed by EIMS and HRMS.

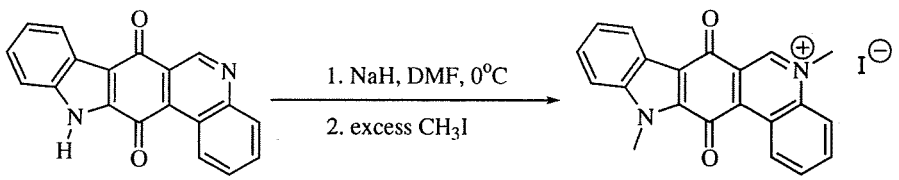

1.27 **2.63**
88% yield

Scheme 2.20

An attempt was made to synthesize *N*-acetyl calothrixin B (**2.61**) following the general procedure in **Scheme 2.19**. *N*-Acetyl calothrixin B was obtained as an orange solid in 47% yield confirmed by the ^1H NMR spectrum which displayed an acetyl peak at δ2.88. However, the product obtained was highly susceptible to hydrolysis by traces of water, and thus degradation occurred to give calothrixin B.

An attempt was also made to synthesize *N*-phenylsulfonyl calothrixin B (**2.62**). Analysis of the reaction mixture by thin-layer chromatography showed no traces of the starting material, calothrixin B (**1.27**). Upon workup, the crude product was obtained as a pale yellow solid which turned dark red upon standing. However, the ^1H NMR spectrum of

the red solid was that of calothrixin B, suggesting that *N*-phenylsulfonyl calothrixin B (**2.62**) is unstable and rapidly hydrolyses to calothrixin B and phenylsulfonic acid. Due to its instability, the preparation of this compound was abandoned.

2.6.2 Synthesis of 9-Methoxy-*N*-methoxymethyl Calothrixin B (2.64)

The indolic *N*-substituted calothrixin derivatives synthesized so far display poor solubility in both aqueous and organic solvents. The poor solubility of these compounds may pose a problem for future biological studies as the aqueous medium required for cell cultures may cause the compounds to precipitate from the solution. The synthesis of 9-methoxy-*N*-methoxymethyl calothrixin B (**2.64**) was therefore carried out in the hope of obtaining a calothrixin derivative with a more desirable solubility profile.

The synthesis of this target compound follows the procedure for our synthesis of *N*-MOM calothrixin B. In the first synthetic step, the coupling of 5-methoxy-*N*-chlorozincindole (**2.65**) to the acid chloride (**2.28**) proceeded smoothly to give the ketone **2.66** in 94% yield [**Scheme 2.21**]. The ^{1}H NMR spectrum of the ketone **2.66** displayed similar characteristics to that of the previously synthesized aryl ketone **2.26**, but was further characterized by the presence of a second methoxy peak at δ3.32. Further evidence for the successful coupling reaction was provided by EIMS and HRMS which confirmed a molecular ion peak at 359.9 *m/z* for the desired ketone.

The ketone was then treated with sodium hydride and methoxymethyl chloride in THF to yield the *N*-methoxymethyl ketone **2.67** as a white powder in 98% yield. The ^{1}H NMR spectrum clearly showed three methoxy peaks at δ3.28, δ3.78 and δ3.94 for the *N*-MOM derivative. It is interesting to note that this compound displayed better solubility in diethyl ether than the aryl ketone **2.26**. Subsequent lithiation of the *N*-MOM protected ketone **2.67** was then carried out using LHMDS and TMEDA in Et_2O, and the desired 9-methoxy-N12-methoxymethyl calothrixin B (**2.64**) was obtained as a deep red solid in quantitative yield.

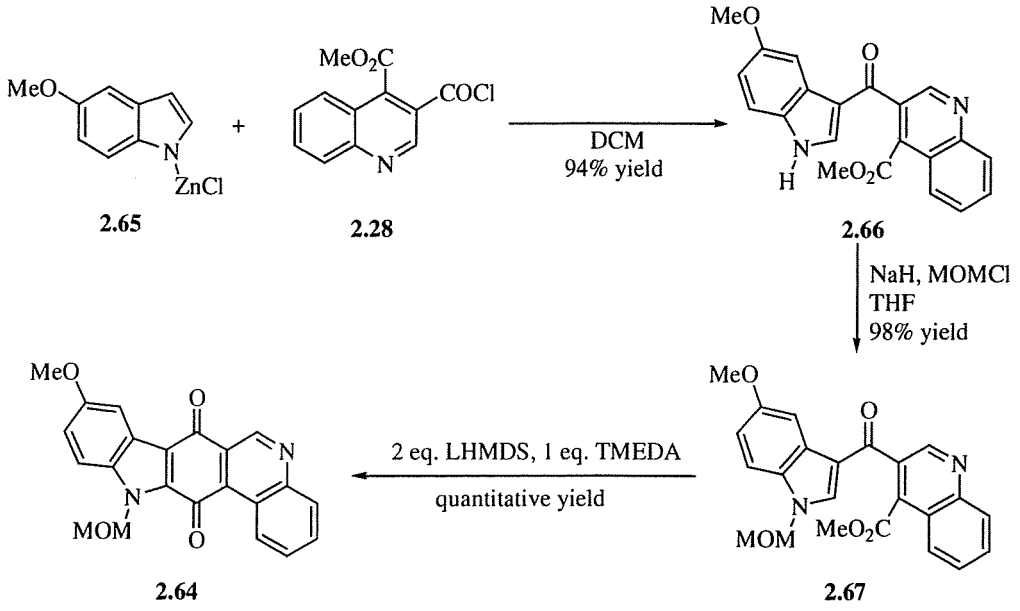

Scheme 2.21

The calothrixin derivative **2.64**, however, was poorly soluble in organic solvents and this made the acquisition of ^{1}H and ^{13}C NMR spectra difficult even in deuterated DMSO. The ^{1}H NMR data acquired at 100°C showed two characteristic methoxy peaks at δ3.38 and δ3.90 indicative of the calothrixin derivative **2.64**. The ^{13}C NMR spectrum of this compound could not be obtained due to the poor solubility. Fortunately, further evidence for the desired product was obtained by EIMS and HRMS which both showed a strong molecular ion peak at 372.1 *m/z*. The poor solubility of this derivative was exploited in the purification step as the product was easily recrystallized as dark red needles from ether and *n*-hexane.

2.6.3 Synthesis of Ellipticine Quinone and Benzocarbazoledione

To test the versatility of the methodology used to synthesize calothrixins B, the syntheses of ellipticine quinone (**1.33**) and benzocarbazoledione (**1.32**) were carried out following the general reaction scheme shown in **Scheme 2.22**.

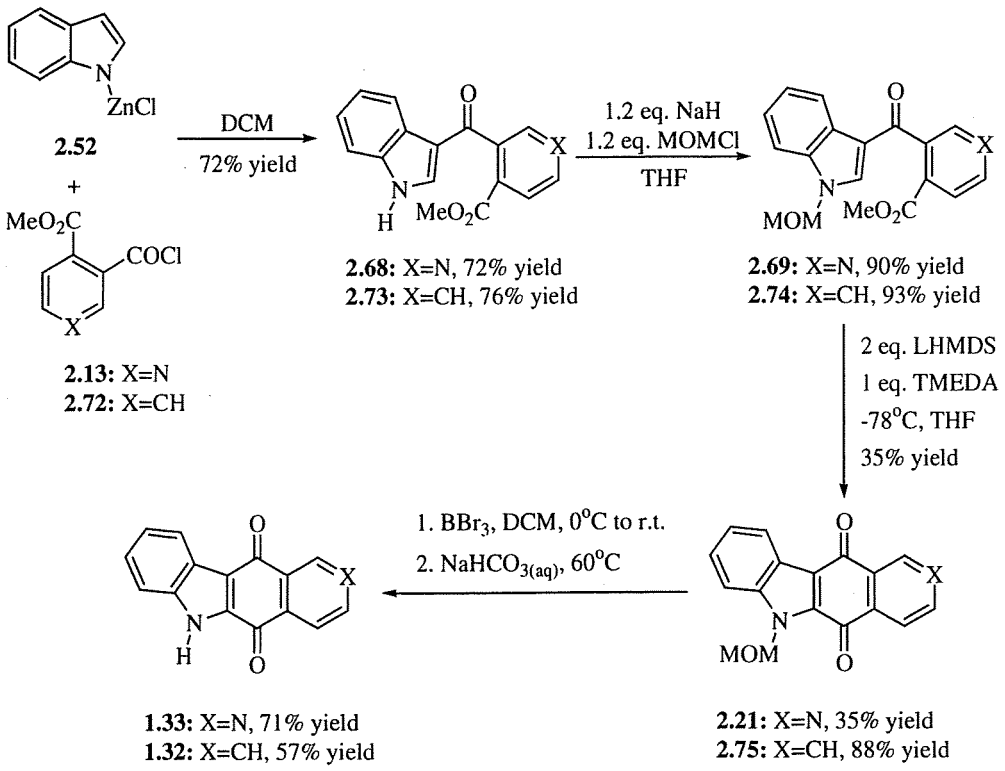

Scheme 2.22

In order to synthesize ellipticine quinone, the acid chloride **2.13** was required. The acid chloride **2.13** was prepared by refluxing dry methanol with pyridine-3,4-anhydride **2.10** to yield the mixed acid **2.14** in quantitative yield. Treatment of the mixed acid **2.14** with thionyl chloride gave the desired acid chloride **2.13** in quantitative yield. The coupling reaction between *N*-chlorozincindole **2.52** and 3-chlorocarbonyl-4-methoxycarbonylpyridine **2.13** was then carried out and a moderate yield (72%) of the coupled product **2.68** was obtained. The ^{1}H NMR spectrum of the purified product clearly showed a characteristic methoxy peak at δ3.44 indicative of the desired compound **2.68**.

Studies carried out in our group had demonstrated that the ketone **2.68** could be converted to the *N*-phenylsulfonyl ketone **2.15**. The cyclization of this compound to ellipticine quinone using LHMDS and TMEDA, however, was found to occur in low yields of 47%. To obtain better yields, the indole nitrogen was protected as the *N*-MOM derivative. Subsequent treatment of the ketone **2.68** with sodium hydride and methoxymethyl chloride gave the desired *N*-MOM ketone **2.69** in 90% yield.

Lithiation of the *N*-MOM ketone **2.69** was carried out using the standard conditions described previously. To our delight, quantitative conversion of the *N*-MOM ketone **2.69** to the desired *N*-MOM ellipticine quinone **2.21** was observed by TLC and ^{1}H NMR spectroscopy. However, purification proved to be difficult and only 35% of analytically pure material could be obtained. The *N*-MOM ellipticine quinone thus obtained displayed identical ^{1}H NMR data to that reported by Snieckus.[7] The melting point of our compound (184-185°C, corrected) however showed a large discrepancy to that reported in the literature (196-197°C, uncorrected).[7] Despite this melting point discrepancy, elemental analysis confirmed the identity and purity of our sample.

Cleavage of the *N*-MOM group of *N*-MOM ellipticine quinone **(2.21)** was easily achieved using our standard conditions. Treatment of *N*-MOM ellipticine quinone **2.21** with a slight excess of BBr_3 followed by warming in saturated $NaHCO_3$ gave ellipticine quinone **(1.33)** as an orange solid in 71% yield. The melting point of ellipticine quinone (315-316°C) was in excellent agreement with the data reported by Taylor *et al.*[4]

For the synthesis of benzocarbazoledione **(1.32)**, the acid chloride **2.72** was obtained by methanolysis of phthalic anhydride **(2.70)** to obtain the mixed acid **2.71**. Treatment of the mixed acid **2.71** with thionyl chloride gave the desired acid chloride **2.72**. The coupling of *N*-chlorozincindole and 2-chlorocarbonyl-1-methoxycarbonylbenzene **(2.72)** was then carried out under standard conditions **[Scheme 2.22]**. Trituration of the crude product with hot ether afforded the ketone **2.73** as a white solid in 76% yield. The ketone **2.73** was only moderately soluble in organic solvents, and precipitated as a white solid from halogenated solvents such as $CHCl_3$. The ^{1}H NMR spectrum displayed a characteristic methoxy singlet at δ3.59 which is consistent with the proposed structure.

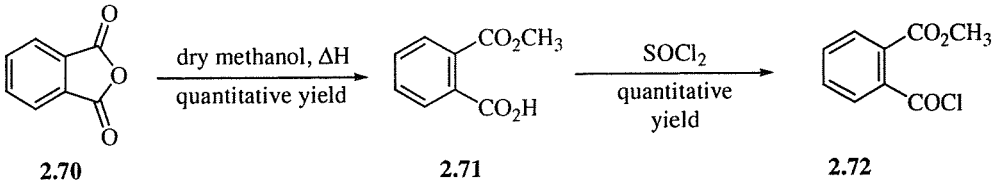

2.70 **2.71** **2.72**

Scheme 2.23

A fine suspension of the ketone **2.73** was treated with NaH in THF, and the addition of MOMCl to the reaction mixture afforded the *N*-MOM ketone **2.74** as a yellow solid in

93% yield. In the penultimate step, lithiation of the *N*-MOM ketone **2.74** under standard conditions gave the desired *N*-MOM benzocarbazoledione (**2.75**) as an orange solid in 88% yield. Finally, removal of the *N*-MOM group form **2.75** was readily achieved by treatment with BBr_3 and $NaHCO_3$ to give the desired benzocarbazoledione (**1.32**) as an orange solid in 57% yield. The melting point of our product was in exellent agreement with the value reported in the literature.[4] The moderate yields are largely due to the difficulty in removing trace organic impurities from the solid. In our experience, removal of traces of normally volatile solvents such acetone required heating the solid under reduced pressure at over 80°C for an extended period of time.

2.6.4 Attempted Synthesis of 5-Methoxymethyl-7,13-dimethyl-12*H*-5,12-diaza-indeno[1,2-b]-phenanthrene (2.57)

The synthesis of the ellipticine analogue 7,13-dimethyl-12*H*-5,12-diaza-indeno[1,2-*b*]-phenanthrene (**2.57**) was attempted following the general methodology developed by Taylor *et al.*[4] [**Scheme 2.24**]. Calothrixin B (**1.27**) was treated with an excess of MeLi in THF. However, the reaction gave a complex mixture which was difficult to purify.

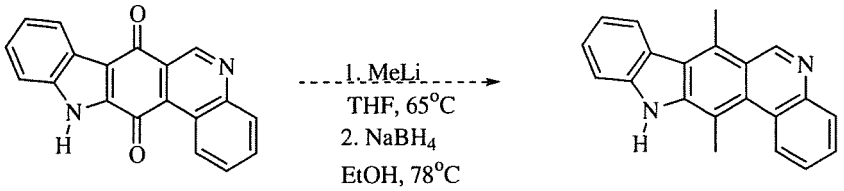

1.27 **2.57** *not isolated*

Scheme 2.24

2.7 Conclusion

We have thus developed a multi-step synthesis of the calothrixins A and B using cheap and readily available starting materials. In spite of some of the difficulties in optimizing reaction steps, a total synthesis of calothrixin B (**1.27**) was achieved with an overall yield of 41% with respect to 3-acetyl-4-carboxyl quinoline **2.38** (69% overall yield with respect to indole). We have also demonstrated the limited flexibility of this methodology by synthesizing a number of calothrixin derivatives, and the carbazoledione analogues ellipticine quinone **1.33** and benzocarbazoledione **1.32**.

With these compounds in hand, we were now poised to carry out the first structure-activity relationship studies of the calothrixins and related carbazolediones.

2.8 Bibliography

(1) Rickards, R. W.; Rothschild, J. M.; Willis, A. C.; de Chazal, N. M.; Kirk, J.; Kirk, K.; Saliba, K. J.; Smith, G. D. *Tetrahedron* **1999**, *55*, 13513-13520.

(2) Chen, X. Graduate Diploma Thesis, The Australian National University, 1999.

(3) Chen, X.; Smith, G. D.; Waring, P. *J. Appl. Phycol.* **2003**, *15*, 269-277.

(4) Taylor, D. A.; Baradarani, M. M.; Martinez, S. J.; Joule, J. A. *J. Chem. Res. (M)* **1979**, 4801-4817.

(5) Saulnier, M. G.; Gribble, G. W. *J. Org. Chem* **1982**, *47*, 2810-2812.

(6) Gribble, G. W.; Saulnier, M. G.; Obaza-Nutaitis, J. A.; Ketcha, D. M. *J. Org. Chem* **1992**, *57*, 5891-5899.

(7) Snieckus, V.; Watanabe, M. *J. Am. Chem. Soc.* **1980**, *102*, 1457-1460.

(8) Kelly, T. R.; Zhao, Y.; Cavero, M.; Torneiro, M. *Org. Lett.* **2000**, *2*, 3735-3737.

(9) Ketcha, D. M.; Gribble, G. W. *J. Org. Chem.* **1985**, *50*, 5451-5457.

(10) Hohenlohe-Oehringen, K.; Rhomberg, A.; Bretschneider, H. *Monatsh. Chem.* **1966**, *97*, 135-144.

(11) Kozmin, S. A.; Janey, J. M.; Rawal, V. H. *J. Org. Chem.* **1999**, *64*, 3039-3052.

(12) Stefanovic, G.; Pavicic-Woss, M.; Lorenc, L.; Mihailovic, M. L. *Tetrahedron* **1959**, *6*, 97-102.

(13) Godard, A.; Queguiner, G. *J. Heterocycl. Chem.* **1980**, *17*, 465-473.

(14) March, J. *Advanced Organic Chemistry: Reactions, Mechanisms, and Structure*; 3rd ed.; John Wiley & Sons: New York, 1985.

(15) Sundberg, R. J. *The Chemistry of Indoles*; Academic Press Inc.: New York, 1970.

(16) Kikugawa, Y. *Synthesis* **1981**, *6*, 460-461.

(17) Okauchi, T.; Itonaga, M. I.; Minami, T.; Owa, T.; Kitoh, K.; Yoshino, H. *Org. Lett.* **2000**, *2*, 1485-1487.

(18) Saulnier, M. G.; Gribble, G. W. *J. Org. Chem* **1982**, *47*, 757-761.

(19) Dieter, R. K. *Tetrahedron* **1999**, *55*, 4177-4236.

(20) Bergman, J.; Venemalm, L. *Tetrahedron* **1990**, *46*, 6061-6066.

(21) Yang, C.; Patel, H. H.; Ku, Y.-Y.; Shah, R.; Sawick, D. *Synth. Commun.* **1997**, *27*, 2125-2132.

(22) Kikugawa, Y. *Synthesis* **1981**, *6*, 461.

(23) Comins, D. L.; Brown, J. D. *J. Org. Chem* **1984**, *49*, 1078-1083.

(24) Sundberg, R. J.; Russell, H. F. *J. Org. Chem* **1973**, *38*, 3324-3330.

(25) Sotelo, E.; Coelho, A.; Raviña, E. *Tetrahedron Lett.* **2001**, *42*, 8633-8636.

(26) Bernardo, P. H.; Chai, C. L. L.; Elix, J. A. *Tetrahedron Lett.* **2002**, *43*, 2939-2940.

(27) Le Guen, M. Honours Thesis, The Australian National University, 2003.

Chapter 3

3.1 Introduction

In Chapter 2, we developed a successful synthetic route to a number of carbazolediones and calothrixin derivatives. With these compounds in hand, we were poised to carry out the first structure-activity relationship (SAR) studies for the calothrixins. However, in order to provide a more detailed study, a large number of calothrixin derivatives and related analogues are desired. A compound library of structurally diverse calothrixin derivatives would serve such a purpose. In theory, such a library can be accessed via combinatorial chemistry using an appropriate multi-step reaction sequence to synthesize a diverse set of compounds based on the core structure of the lead compound, calothrixin B (**1.27**).

Although we have previously demonstrated the versatility of the Friedel-Crafts and metallation approach to the synthesis of carbazolediones in Chapter 2,[1,2] this route is unsuitable for combinatorial synthesis for a number of reasons. Firstly, the synthetic route developed in Chapter 2 employs strong basic conditions and consequently only synthetic precursors with base-stable functional groups can be employed. Secondly, the key lithiation step to form the quinone ring requires low temperatures which must be carefully maintained to ensure good yields. Finally, to obtain the substituted indole and quinoline precursors needed for the synthesis of calothrixin B derivatives would require separate synthetic studies which would be time-consuming. Therefore, in order to synthesize a large number of calothrixin derivatives via combinatorial chemistry, a new synthetic route which employs cheap and readily available starting materials is desirable. Mild reaction conditions in the synthetic sequence should be employed to accommodate a wide range of functional groups. Additionally, a synthetic sequence that incorporates reactions that only require ambient or slightly elevated temperatures would be advantageous as these can later be adapted to solid phase synthesis if desired.

One of the major developments in the field of organic synthesis has been the use of palladium-mediated reactions for the formation of carbon-carbon bonds. These reactions allow the organic chemist to select from a wide range of conditions, many of which are highly tolerant of functional groups and can be carried out at mild or moderately elevated temperatures. An excellent review by Knölker, [3] as well as Bouaziz,[4] outlined examples of palladium-mediated reactions in the syntheses of carbazolediones.

One such example of a palladium-mediated reaction is the key step used in the facile synthesis of murrayaquinone A (**1.40**), shown in **Scheme 3.1**. In studies carried out by Yogo *et al.*[5], the penultimate synthetic intermediate 2-anilino-6-methyl-1,4-benzoquinone (**3.1**) was obtained as the major regioisomer in 60% yield via the Michael addition of aniline to 2-methyl-1,4-benzoquinone (**1.36**). In the key step, the intramolecular cyclization of the benzoquinone **3.1** to form the crucial aryl-aryl bond occurred in the presence of stoichiometric amounts of palladium (II) acetate to give murrayaquinone A (**1.40**) in 64% yield.[5]

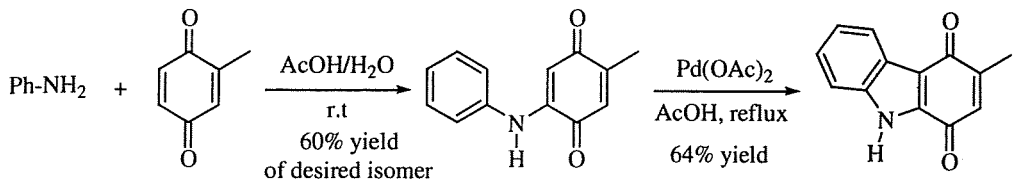

1.36 **3.1** **1.40**

Scheme 3.1

The success of this methodology suggested that a similar approach could be utilized in the synthesis of the indole fragment of calothrixin B via an existing quinone template such as phenanthridine-7,10-dione (**3.2**) **[Scheme 3.2]**. It was envisaged that should regioselective addition of aniline to this quinone template occur to give the desired Michael adduct **3.3**, this adduct can then be cyclized in the presence of palladium (II) acetate to yield calothrixin B (**1.27,** R_1-R_3=H). It is clear, at this point, that diversity may be introduced in the *A*-ring of calothrixin B by using appropriately substituted anilines in the Michael addition step. The economy of this methodology in generating structural diversity can be appreciated if one considers that a single synthetic intermediate **3.3** prepared from substituted anilines can potentially give two regioisomeric calothrixin B derivatives following palladium (II)-mediated cyclization. However, the ratio of regioisomers will depend on the substituted anilines used and thus the outcome cannot be easily predicted beforehand.

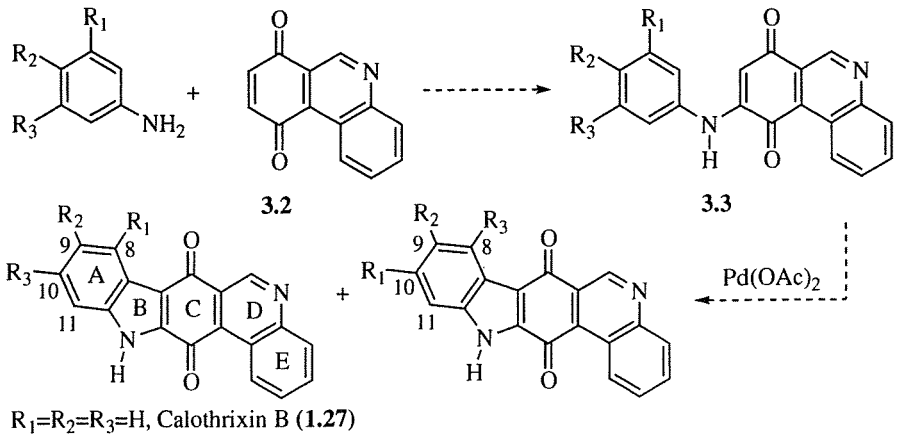

R_1=R_2=R_3=H, Calothrixin B (**1.27**)

Scheme 3.2

The quinone template **3.2**, though not commercially available, can in principle be accessed through the reaction of aniline with 2-formyl-1,4-benzoquinone (**3.4**) followed by the intramolecular cyclization of the resulting Schiff base (**3.5**). However, 2-formyl-1,4-benzoquinone is an unsuitable precursor for the preparation of the phenanthridine-7,10-dione. Studies by Kraus and Zhang[6] as well as Valderrama *et al.*[7] show that the formylbenzoquinone preferentially undergoes Michael addition at the C3-position rather than addition to the carbonyl group of the aldehyde using a range of nucleophiles. Thus the addition of aniline to formylbenzoquinone is likely to give 2-anilino-3-formyl-1,4-benzoquinone (**3.6**) **[Scheme 3.3]** rather than the desired Schiff base **3.5**.

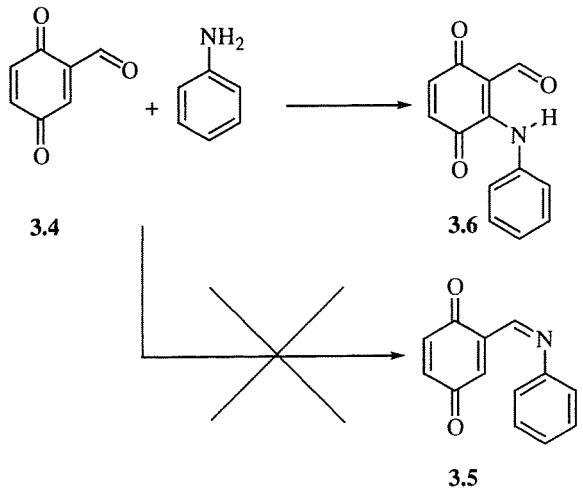

Scheme 3.3

To obtain the desired Schiff base, 2,5-dimethoxybenzaldehyde (**3.7**) may be employed as the synthetic equivalent of 2-formyl-1,4-benzoquinone. Thus the addition of aniline

to the benzaldehyde **3.7** followed by palladium (II)-mediated oxidative aryl-aryl coupling would give 7,10-dimethoxyphenanthridine (**3.9**). The phenanthridine **3.9** can, in principle, be converted to the desired phenanthridine-7,10-dione **3.2** via oxidative demethylation reactions **[Scheme 3.4]**.

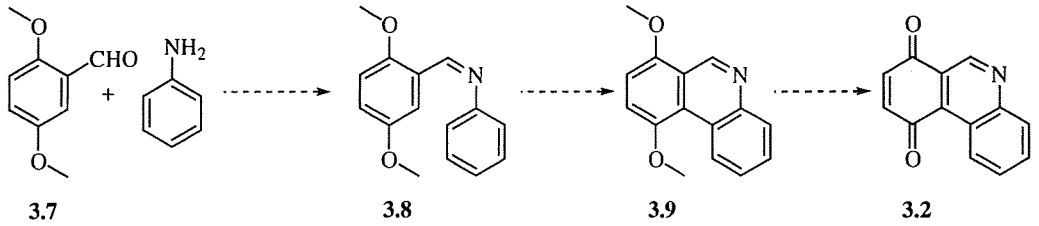

3.7 **3.8** **3.9** **3.2**

Scheme 3.4

The phenanthridine synthesis provides another platform for diversity. For example, the use of substituted anilines in the initial Schiff base formation can in principle lead to polyfunctionalized regioisomeric phenanthridine-7,10-diones (**3.2A**, **3.2B**) **[Scheme 3.5]**. By considering **Scheme 3.2**, this translates to diversity in the *E*-ring of calothrixin B.

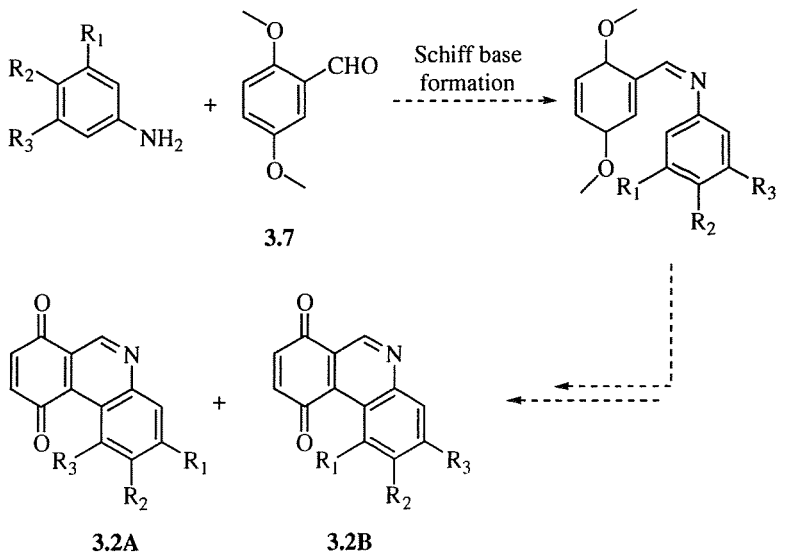

Scheme 3.5

In summary, a reaction sequence employing substituted anilines and 2-formyl-1,4-benzoquinone has the potential to provide a combinatorial library of 1,2,3,4,8,9,10,11-polysubstituted calothrixin B derivatives. As **Scheme 3.6** illustrates, the use of a 3-

substituted aniline alone could give rise to four different isomers if the reaction sequence proceeds as planned. The success of this methodology would consequently lead to a vast number of derivatives for SAR and Quantitative SAR (QSAR) studies.

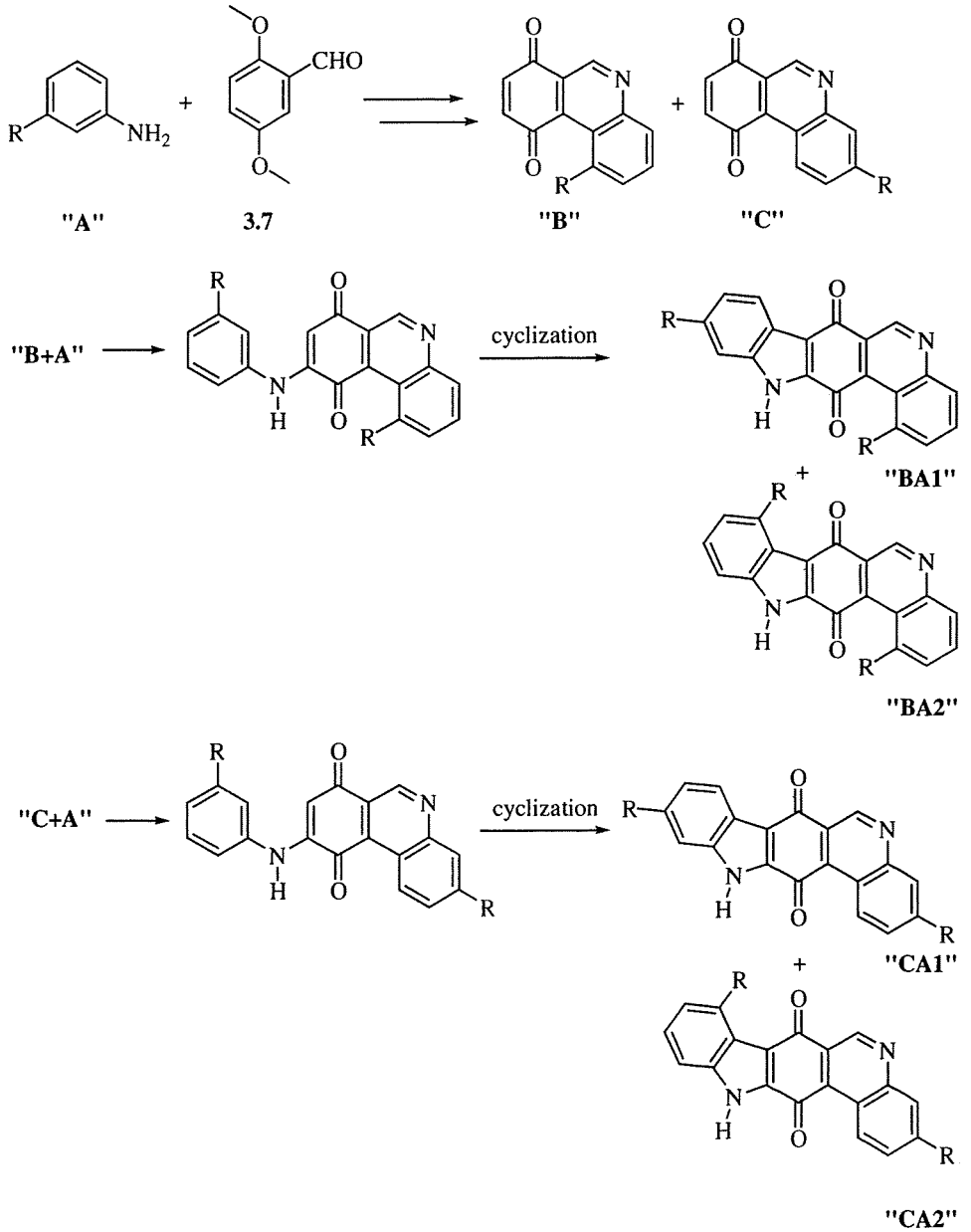

Scheme 3.6

With this new strategy in mind, we proceeded to examine the feasibility of this synthetic route by targeting the parent compound, calothrixin B. The investigations commenced with the synthesis of phenanthridine-7,10-dione (**3.2**).

3.2 Synthesis of the Phenanthridine-7,10-dione (3.2) Template

Preliminary studies into the synthesis of phenanthridine-7,10-dione **(3.2)** was carried out by LeGuen in the Chai group in 2003.[8] In these studies, it was demonstrated that the imine **3.8** derived from the condensation of aniline with 2,5-dimethoxybenzaldehyde **(3.7)** was unstable to purification and thus the subsequent aryl-aryl bond formation to access the phenanthridinedione **3.2** was not attempted. This necessitated the development of an alternative synthetic route to the phenanthridinedione.

Related studies on the synthesis of phenanthridine-based carboskeletons provided crucial leads into the synthesis of the desired phenanthridinedione **3.2.** For example, Harayama *et al.* reported the synthesis of the phenanthridine-based natural product trisphaeridine **(3.10) [Scheme 3.7]**.[9] In their studies, a benzoic acid derivative **3.11** was converted to the corresponding acid chloride using oxalyl chloride in the presence of a catalytic amount of DMF. The acid chloride was then coupled to 2-iodoaniline to yield the benzamide **3.12** in high yields. The benzamide **3.12** was then *N*-protected as the methoxymethyl benzamide **3.13.** Subsequent cyclization of the tertiary benzamide **3.13** using a catalytic amount of palladium (II) acetate and *tris*(*o*-tolyl)phosphine in the presence of sodium carbonate gave the phenanthridin-6-one **3.14** in low yields. The low yield obtained was due to the formation of an undesired regioisomer in 60% yield. Different reaction conditions were employed in order to improve the regioselectivity of the cyclization reaction, but to no avail. However, the phenanthridin-6-one **3.14** was easily converted to trisphaeridine **(3.10)** in 3 steps ~~from the phenanthridin-6-one 3.14~~.[9]

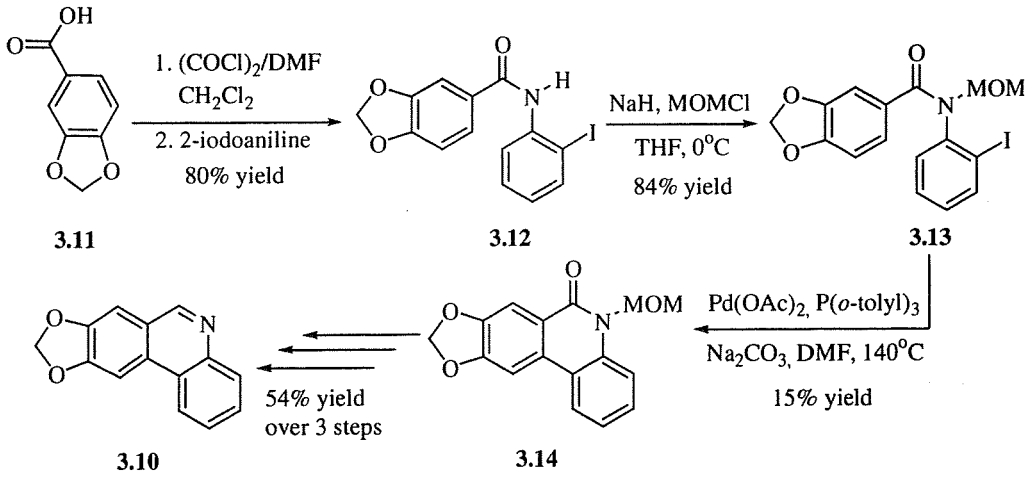

Scheme 3.7

We decided to utilize the approach of Harayama *et al.* for our synthesis of phenanthridine-7,10-dione. Our synthesis commenced with the preparation of 2,5-dimethoxybenzoic acid **3.15** via oxidation of commercially available 2,5-dimethoxybenzaldehyde **3.7** with potassium permanganate following the procedure reported by Azadi-Ardakani and Wallace.[10] The benzoic acid **3.15** was thereby obtained in 62% yield. Treatment of the benzoic acid **3.15** with thionyl chloride generated the acid chloride **3.16**, which upon addition of 2-bromoaniline gave the amide **3.17** as a white solid in quantitative yield **[Scheme 3.8]**.

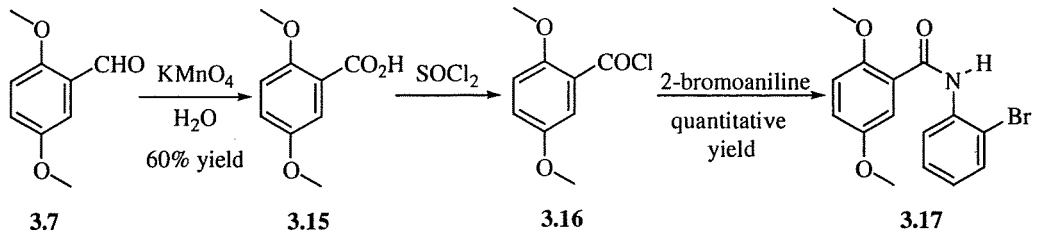

3.7 **3.15** **3.16** **3.17**

Scheme 3.8

Our initial attempts to effect the palladium-mediated biaryl bond formation in the amide **3.17** in the presence of catalytic palladium (II) acetate and *tris*(*o*-tolyl)phosphine with sodium carbonate as base at 140°C failed to yield the desired compound. Studies by Harayama *et al.*[9] as well as Moreno *et al.*[11] on the intramolecular biaryl coupling reactions of benzamides suggest that secondary benzamides will preferentially adopt the minimum energy conformation in which steric interactions are minimized **[Figure 3.1]**. It can be reasoned that of the two extreme conformations shown, unfavorable steric interactions between the aryl substituents in the secondary benzamide **3.17** leads to the *Z*-rotamer **(3.17A)** as the lowest energy rotamer. Clearly, the *Z*-rotamer is not poised for intramolecular biaryl coupling reaction as the aryl groups are *anti* to each other. The *cis* orientation of the aryl groups in the *E*-rotamer **(3.17B)**, on the other hand places the aryl substituents in the proximity required for the desired coupling reaction by palladium-mediated or radical-mediated reactions. Harayama *et al.* therefore hypothesize that the insertion of palladium (0) catalyst in the C-Br bond followed by the free rotation around the C-N bond of the aniline moiety would then allow for the proper orientation required to form the aryl-aryl bond.[9] Similarly, the radical-mediated cyclization utilized by Moreno *et al.*[11] can also proceed when the aryl substituents are in the *cis* configuration in the *E*-rotamer. In view of the failure to obtain the desired product despite the elevated

temperature used, we hypothesized that there is a considerable energy barrier between the *Z*-rotamer **3.17A** and the *E*-rotamer **3.17B**.

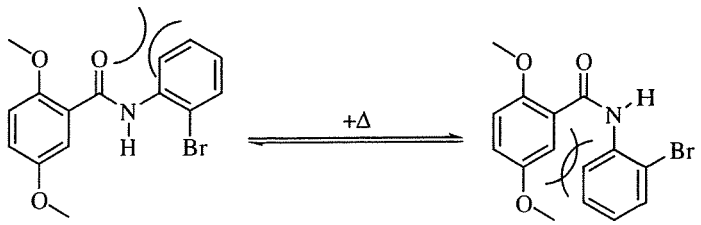

Z-rotamer **3.17A** *E*-rotamer **3.17B**

Figure 3.1

In the strategy of Harayama *et al.* for the synthesis of trisphaeridine outlined previously, the secondary benzamide **3.12** was converted to the tertiary amide **3.13** using sodium hydride and methoxymethyl chloride. Due to competing steric interactions in the tertiary amide **3.13**, the energy barrier between the *E*- and *Z*- rotamers would be much smaller than the corresponding energy barrier in the secondary benzamide. This in turn would facilitate a population shift from the lower energy *E*-rotamer (**3.13A**) to the desired *Z*-rotamer (**3.13B**) which is capable of undergoing intramolecular cyclization [**Figure 3.2**].[9]

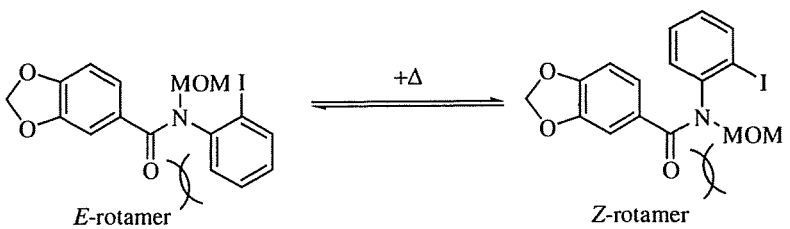

E-rotamer **3.13A** *Z*-rotamer **3.13B**

Figure 3.2

In view of our synthetic requirements in the proposed route, the choice of a protecting group for functionalizing the secondary amide nitrogen atom was important. The protecting group employed must be easily removed so that aromatization of the nitrogen-containing ring can be carried out at later stages in the synthesis. The benzamide **3.16** was therefore treated with sodium hydride and methoxymethyl chloride at a slightly elevated temperature of 30°C to yield the tertiary *N*-MOM benzamide **3.18** as a yellow oil in good yields. Previous attempts to install the MOM group at room

temperature (typically 17-20°C) did not go to completion and starting material was isolated along with the desired *N*-alkylated amide. It was therefore necessary to raise the reaction temperature to 30°C to ensure full conversion of the secondary benzamide to the tertiary product. Upon treatment of *N*-MOM benzamide **3.18** with catalytic palladium (II) acetate and *tris*(*o*-tolyl)phosphine with sodium carbonate at 140°C, the cyclized product **3.19** was obtained in 30% yield **[Scheme 3.9]**.

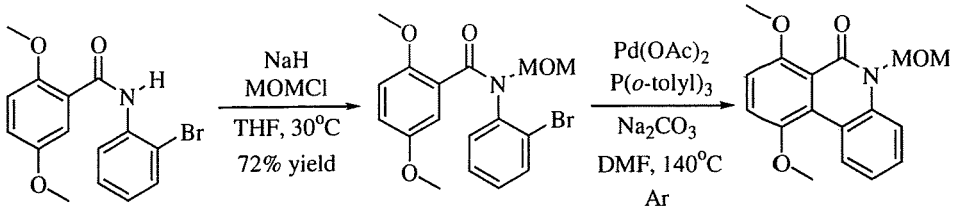

3.17 **3.18** **3.19** 30% yield

Scheme 3.9

The proposed mechanism for the palladium (II)-mediated intramolecular biaryl coupling of the benzamide **3.18** is shown in **Scheme 3.10**. In the first step, palladium (0) is generated *in situ* by the reduction of palladium (II) acetate by triarylphosphines such as the ligand *tris*(*o*-tolyl)phosphine. This is followed by the insertion of the palladium (0) complex into the C-Br bond leading to the formation of the σ-aryl palladium (II) complex **3.20**. Insertion of the palladium (II) complex into the C6-H bond of the amide **3.20** gives the aryl palladium (II) intermediate **3.21** which then rearranges to the σ-alkyl palladium (II) complex **3.22**. Elimination of the palladium group can then occur through two possible mechanisms.[12] In the first proposed mechanism, the palladium group migrates to the amide oxygen via a 1,3-palladotropic shift, and subsequent reductive elimination of palladium (0) gives 7,10-dimethoxy-5*H*-methoxymethylphenanthridin-6-one (**3.19**). In the alternative mechanism, the base-catalyzed abstraction of the proton at the 10a-position generates the anion **3.23** which then reductively eliminates the palladium (0) catalyst to give the product **3.19**. The regenerated palladium (0) catalyst can then react with another molecule of the amide **3.19** to propagate the cycle.

Some font problems in this paragraph.

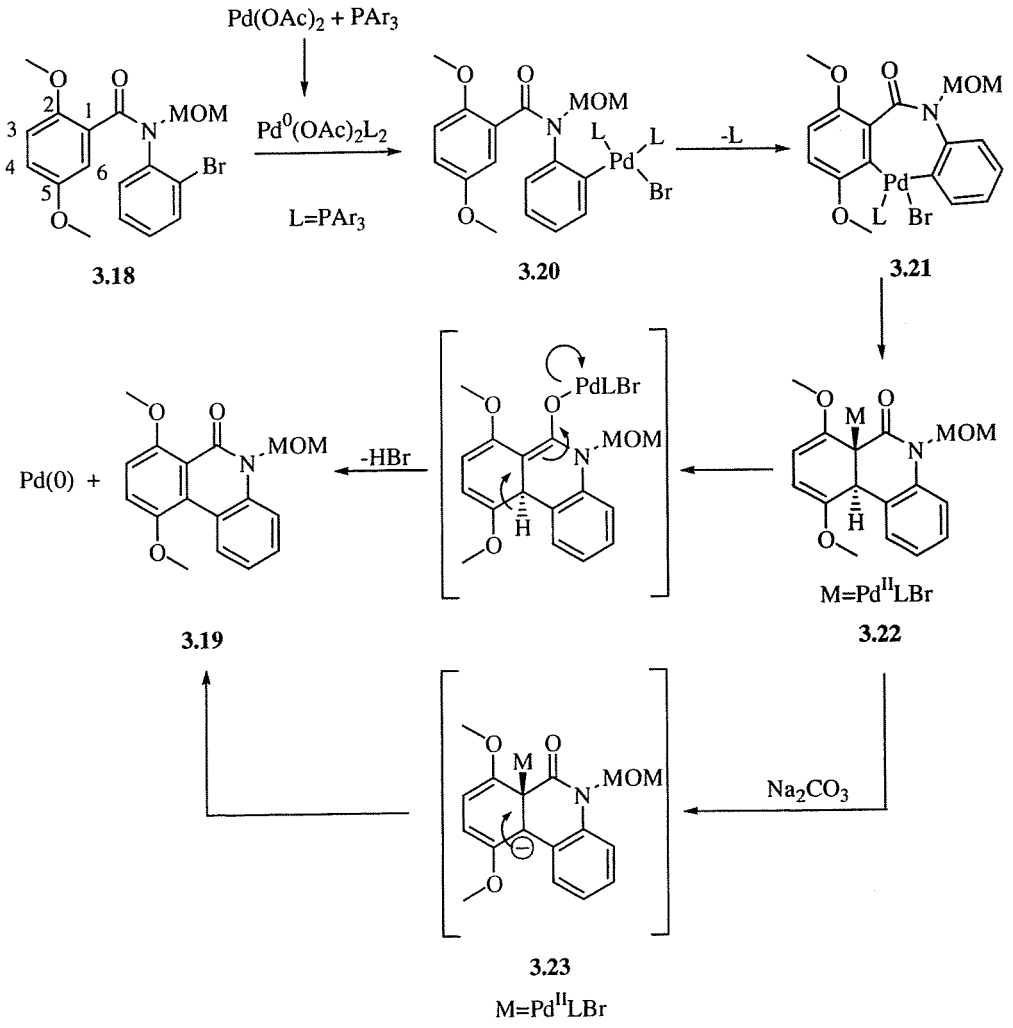

Scheme 3.10

Encouraged by the success of the intramolecular cyclization of the *N*-MOM benzamide **3.18**, the yields of this reaction were optimized by assessing different reaction conditions and reagents. The results are summarized in **Table 3.1**. It was crucial that the palladium-catalyzed reactions were carried out under an atmosphere of argon as the palladium (0) catalysts and the *tris*(*o*-tolyl)phosphine ligands were susceptible to aerial oxidation. When the reaction was carried out using palladium (II) acetate and *tris*(*o*-tolyl)phosphine in a ratio of 1:2 at 100°C, no product formation was observed and the benzamide starting material was recovered **[Entry 4]**. However, when the temperature was raised to 140°C, the desired product was obtained in 30% yield **[Entry 5]**. We attempted to increase the product yield by adding more *tris*(*o*-tolyl)phosphine to the reaction mixture, to no avail. Difficulties were also encountered when *tris*(*o*-

tolyl)phosphine was used as this phosphine ligand readily undergoes oxidation to the corresponding phosphine oxide.

As the palladium (0) species is the active form of the catalyst required for oxidative insertion reactions, we attempted the cyclization reaction of the tertiary benzamide **3.18** in the presence of the commercially available and relatively air-stable palladium (II) *tetrakis*(triphenylphosphine) catalyst. However, the use of the palladium *tetrakis*(triphenylphosphine) catalyst in the absence of phosphine additives failed to react with the tertiary benzamide **3.18** **[Entries 1, 2]**. Interestingly, when triphenylphosphine was added to the palladium (II) *tetrakis*(triphenylphosphine) catalyst in a 1:1 ratio ($Pd[PPh_3]_4$ /PPh_3]), the desired compound was obtained in 10% yield **[Entry 3]**. We therefore attempted to carry out the palladium-catalyzed reaction using palladium (II) acetate and triphenylphosphine as summarized in **Entries 7** and **8**.

It should be noted that in all the reactions that did not occur or did not proceed to completion, the starting material **3.18** was recovered. This suggested that the failure of the palladium-catalyzed reaction to either proceed or go to completion is due to the difficulty or inability to form the σ-aryl palladium (II) complex **3.20**, otherwise the debromination of the tertiary benzamide **3.18** would have been observed.

When the palladium (0) catalyst was generated *in situ* from palladium (II) acetate and triphenylphosphine, the yields of the desired product was greatly improved **[Entry 7]**. Further improvements in the yields was achieved when three equivalents of triphenylphosphine was utilized with 10% palladium (II) acetate **[Entry 8]**.

Reaction Conditions for Pd-Mediated Cyclization of the Tertiary Benzamide **3.18** *to 7,10-Dimethoxy-5H-methoxymethylphenanthridin-6-one* **(3.19)**						
Entry No.	**Catalyst (10% mol)**	**Ligand**	**Catalyst:Ligand Ratio**	**T (°C)**	**Reaction Time (h)**	**% isolated yields**
1	$Pd[PPh_3]_4$	None	-	100	5	0
2	$Pd[PPh_3]_4$	None	-	140	16	0
3	$Pd[PPh_3]_4$	PPh_3	1:1	140	16	10
4	$Pd(OAc)_2$	P(*o*-tolyl)$_3$	1:2	100	5	0
5	$Pd(OAc)_2$	P(*o*-tolyl)$_3$	1:2	140	5	30
6	$Pd(OAc)_2$	P(*o*-tolyl)$_3$	1:4	140	5	30
7	$Pd(OAc)_2$	PPh_3	1:2	140	5	40
8	$Pd(OAc)_2$	PPh_3	1:3	140	5	96
All reactions were carried in dry DMF under argon with 2eq Na_2CO_3 as base.						

Table 3.1

With the compound 7,10-dimethoxy-5-methoxymethyl-5*H*-phenanthridin-6-one **(3.19)** in hand, we were poised to form the quinoline ring system [**Scheme 3.12**]. Following the methodology of Harayama *et al.* [9] and Moreno *et al.*,[11] the reduction of the amide group was carried out by treating the phenanthridin-6-one **3.19** with lithium aluminium hydride in THF. The crude product, presumably **3.24**, was then treated with aqueous hydrochloric acid in THF to remove the MOM group and 7,10-dimethoxyphenanthridine **3.9** was obtained as a pale yellow solid in 90% yield.

To convert the dimethoxyphenanthridine **3.9** to phenanthridine-7,10-dione **(3.2)**, oxidative demethylation was carried out using cerium (IV) ammonium nitrate. The reaction gave the desired phenanthridinedione **3.2** as a yellow solid in 96% yield. The identity of the compound was confirmed by EIMS which showed a molecular ion peak at 209*m/z* which was confirmed by HRMS. Thus the synthesis of the phenanthridine-7,10-dione template required for the proposed synthesis of calothrixin B has been successfully achieved in good overall yields [**Scheme 3.11**].

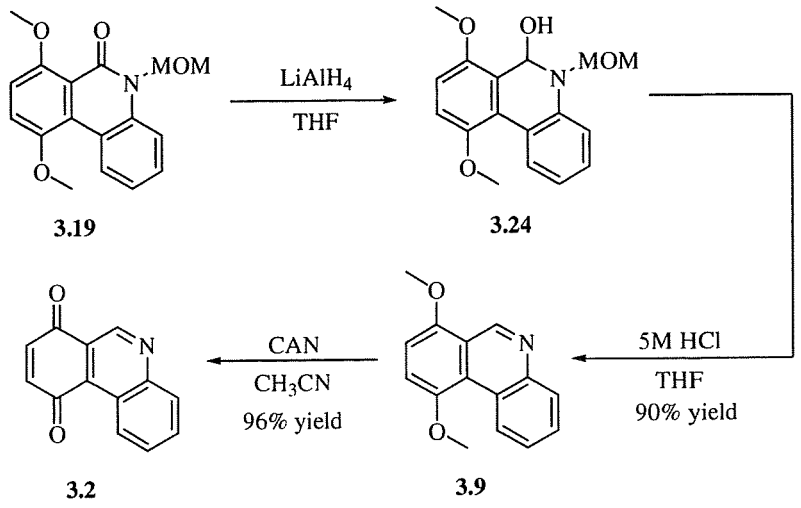

Scheme 3.11

3.3 Model Studies on the Reactivity of the Phenanthridine-7,10-dione (3.2) Template and Related Quinones

The double bonds of quinones are reactive towards addition reactions including radical addition reactions, cycloadditions as exemplified by the Diels-Alder reaction, as well as nucleophilic addition reactions.[13-15] In cases where the quinones are unsymmetrical, regioselectivity issues arise. Various theoretical models have been proposed to predict and rationalize the regioselectivity of addition reactions to quinones. In our proposed synthesis, a key feature in the success of the synthetic route relies on the ability to effect the nucleophilic addition of aniline to a quinone template in a regioselective fashion.

Finley attempted to rationalize the observed regioselectivity of nucleophilic addition reactions to substituted benzoquinones using resonance theory.[14] In this model, Finley classified the substituents present on benzoquinones as electron donating groups (D-groups), electron accepting groups (A-groups), or conjugating substituents (C-groups). As **Figure 3.3** shows, the D-groups are predicted to direct nucleophiles primarily to the C5-position. The A-groups, on the other hand, direct nucleophiles to the C3-position whereas the C-groups direct nucleophiles to the C6, C5 and C3-positions.

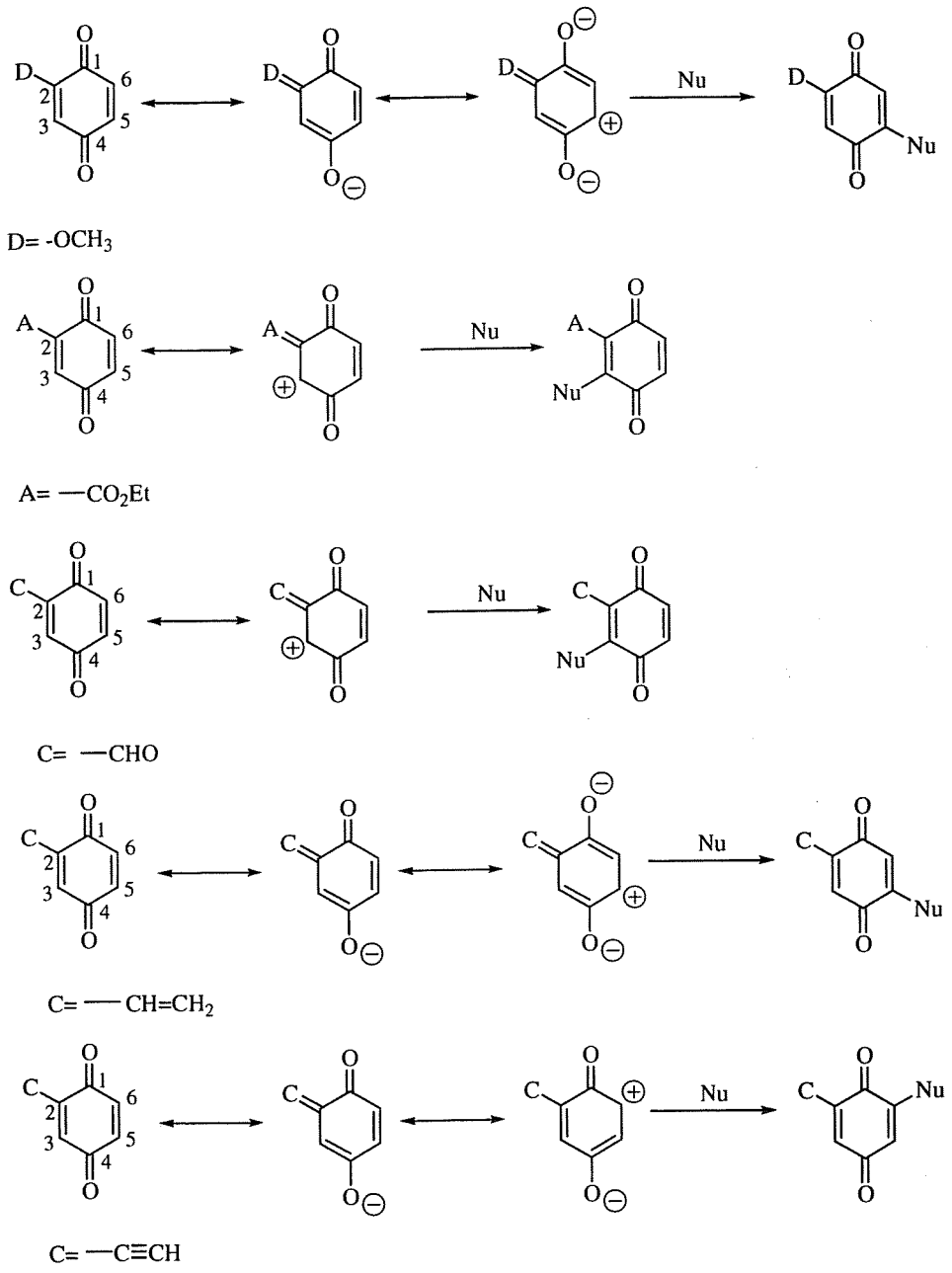

Figure 3.2

These predictions are based on considerations of electrophilic sites on the quinone derived from the examination of resonance structures. For instance, D-groups such as the methoxy substituents reduce the electron-withdrawing ability of the C4-carbonyl through a +R effect **[Figure 3.2]**. This suggests that the C5-position is more susceptible to nucleophilic attack due to the ease of conjugation with the more electron deficient C1 carbonyl group. A-groups such as ester substituents, on the other hand, withdraw electrons through a –R effect leading to an increase in electropositivity on the adjacent

C3-position thereby increasing the electrophilic nature of the adjacent carbon and thus increasing its susceptibility to nucleophilic attack. The effect of C-groups such as the vinyl, acetylene, and formyl substituents is less clear as conjugating substituents can either act as electron donors or electron acceptors. For instance, the vinyl group diminishes the electron-withdrawing ability of the C4-carbonyl by donating electrons to the conjugated system. In contrast, the formyl group withdraws electrons from the C3-position thus increasing its susceptibility to nucleophilic attack. This model, however, ignores the inductive effects of substituents and may therefore fail to predict the experimental outcome.[16] In addition, this theory cannot be used to predict the outcome of more complex polycyclic quinones such as phenanthridine-7,10-dione (**3.2**).

A model based on Frontier Molecular Orbital (FMO) considerations was proposed by Rozeboom *et al.* to predict the outcome of nucleophilic addition reactions to quinones.[16] The FMO approach has been successfully applied in the prediction of the regiochemistry of radical additions, cycloadditions, as well as nucleophilic addition reactions to quinones. The latter occurs when favorable overlap of the Highest Occupied Molecular Orbital (HOMO) of the nucleophile and the Lowest Unoccupied Molecular Orbital (LUMO) of the quinone is achievable. The rate of reaction depends on the energy gap between the HOMO and LUMO, and therefore minimizing the energy gap will increase the reaction rate. In contrast, the regioselectivity of the reaction is governed by the consideration of the size of the orbital coefficients. Consequently, the HOMO of the nucleophile will interact best with the largest LUMO coefficient present on the carbons of the quinone in order to maximize the HOMO-LUMO orbital overlap. This means that the carbon atom on the quinone with the largest orbital coefficient is the most likely position for nucleophilic attack **[Scheme 3.12]**. The size of these orbital coefficients can be calculated computationally thus providing a means of predicting the regioselectivity of addition reactions.

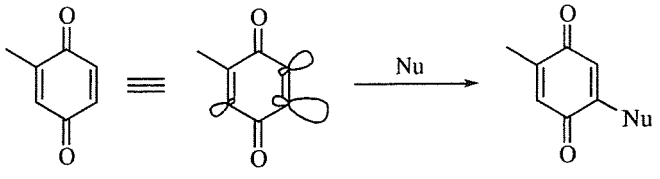

Scheme 3.12

In order to predict the regioselective outcome of nucleophilic additions to various quinones using the FMO theory, it was necessary to determine the LUMO energy and corresponding atomic orbital coefficients for each structure using the SPARTAN 3.0 program. Semi-empirical calculations on various quinones using the Restricted Hartree-Fock method and Slater-Type Orbital (STO-3) basis set were used to determine the molecular LUMO energy from which was derived the atomic orbital coefficients for each atom. The orbital coefficients thus obtained would allow us to predict the site of nucleophilic attack.

To test the reliability of the theoretical predictions, semi-empirical calculations were carried out on phenanthrene-1,4-dione (**3.25**). The calculations predict a slightly larger LUMO coefficient at the C3-position of the phenanthrenedione **3.25** than at the C2-position. As a result, the outcome of the Michael addition of aniline to the phenanthrenedione was predicted to occur preferentially at the C3-position. Experimental results obtained in our group showed that the addition reaction with phenanthridinedione resulted in a 5:1 mixture of 3-anilinophenanthrene-1,4-dione (**3.26**) to 2-anilinophenanthrene-1,4-dione (**3.27**) [**Scheme 3.13**]. These calculations correctly predict the C3-position of the quinone **3.25** as the preferred site of attack. It should be noted that the orbital coefficients of the carbonyl positions were also obtained, and unless noted the values obtained for the orbital coefficients of the carbonyl groups were much smaller than the values for the α-carbon positions.

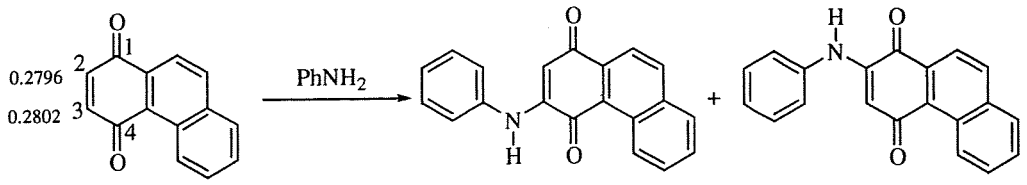

3.25 **3.26** **3.27**

|Δ|=0.0006

Scheme 3.13

Similar calculations were carried out on phenanthridine-7,10-dione (**3.2**) and these calculations predict that a larger orbital coefficient is present at the C8-position (0.2393) as opposed to the C9-position (0.2298) [**Scheme 3.14**]. Thus the calculations predict that the Michael addition of aniline to phenanthridinedione **3.2** would occur preferentially at the C8-position to yield 8-anilinophenanthridine-7,10-dione (**3.28**).

Unfortunately, our synthetic route requires the other regioisomer, 9-anilinophenanthridine-7,10-dione (**3.3**), for synthesizing calothrixin B. The regioisomer that is predicted to form does not lead to calothrixin B but to its isomer, *iso*-calothrixin B (**3.29**).

Experimentally, when the reaction between aniline and phenanthridine-7,10-dione was carried out at 100°C, analysis of the ^{1}H NMR spectrum of the reaction mixture showed that a 1:10 ratio of regioisomers were formed. The products, however, could not be separated by column chromatography. When the mixture was heated in the presence of a catalytic amount of palladium (II) acetate, two products were observed, one which was identified as calothrixin B while the other was the previously unknown *iso*-calothrixin B (**3.29**).

A. Predicted Outcome

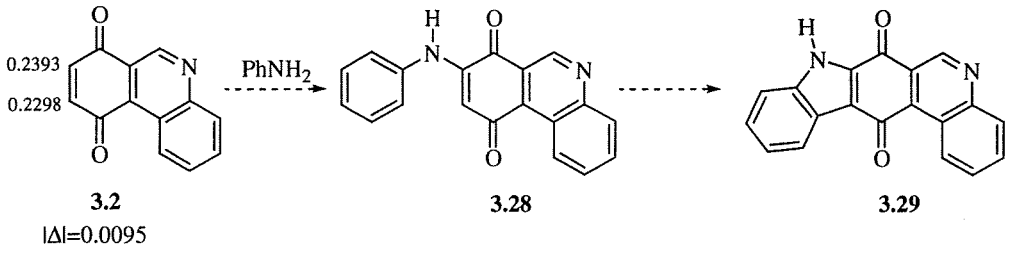

3.2 **3.28** **3.29**

|Δ|=0.0095

B.Experimental Results

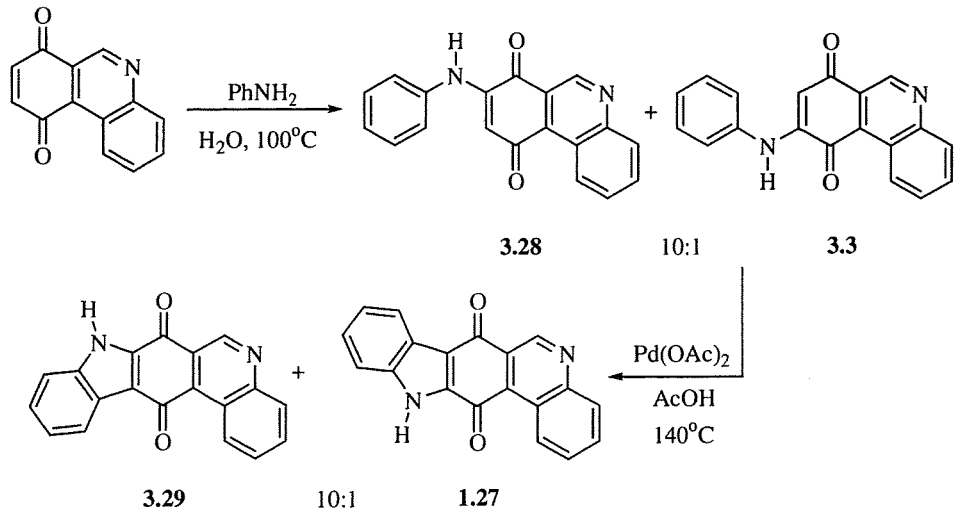

3.28 10:1 **3.3**

3.29 10:1 **1.27**

Scheme 3.14

Interestingly, the calothrixin B isomers had identical retention times when analyzed by thin-layer chromatography and could not be separated using column chromatography.

However, the products could be fractionally recrystallized such that *iso*-calothrixin B precipitates preferentially while calothrixin B remains in solution. A comparison of the ^{1}H NMR spectrum of the *iso*-calothrixin B (**3.29**) with that of authentic calothrixin B (**1.27**) revealed differences in the chemical shifts of the aromatic protons. For example, the most obvious difference in the ^{1}H NMR spectrum is the presence of the singlet resonance at δ9.70 for the proton adjacent to the quinoline nitrogen in *iso*-calothrixin B (**3.29**) as opposed to the characteristic singlet proton at δ9.62 for the proton adjacent to the quinoline nitrogen of calothrixin B (**1.27**). Further evidence for the formation of *iso*-calothrixin B was obtained from the EIMS spectrum which showed a molecular ion peak at 298*m/z* that is consistent with the proposed structure.

We thus serendipitously developed the first synthesis of *iso*-calothrixin B (**3.29**). A previous attempt to synthesize *iso*-calothrixin B using the method developed in Chapter 2 failed to produce the desired product. As the choice of phenanthridinedione **3.2** did not lead to appreciable amounts of the precursor required for the synthesis of calothrixin B, further investigations into more suitable quinone templates were carried out.

Other quinones (**3.30, 3.31**) which were accessible from our synthetic strategy were then considered for the Michael addition reaction with aniline. In particular, we aimed to develop a quinone system that will enable the reversal of the selectivity observed for the Michael addition of aniline to phenanthridine-7,10-dione (**3.2**). Calculations were performed on these quinones to determine the LUMO coefficients which in turn enabled the prediction of the site of nucleophilic attack. The results are summarized in **Scheme 3.15**. The largest LUMO coefficient of 5-methoxymethyl-5*H*-phenanthridine-6,7,10-trione (**3.30**) is at the C8-position, and therefore the predicted product would be 5-methoxymethyl-8-anilino-5*H*-phenanthridine-6,7,10-trione (**3.32**). Calculations on the amide **3.31** showed that the largest LUMO coefficient is at the C6-position of the quinone ring system, which in turn predicts that aniline addition would occur at the C6-position. Since the predicted regioselectivity gives anilino compounds which cannot be converted to calothrixin B (**1.27**), these quinones are not suitable precursors in our proposed synthesis of calothrixin B. Experimentally, the reaction of these quinones with aniline gave complex reaction mixtures.

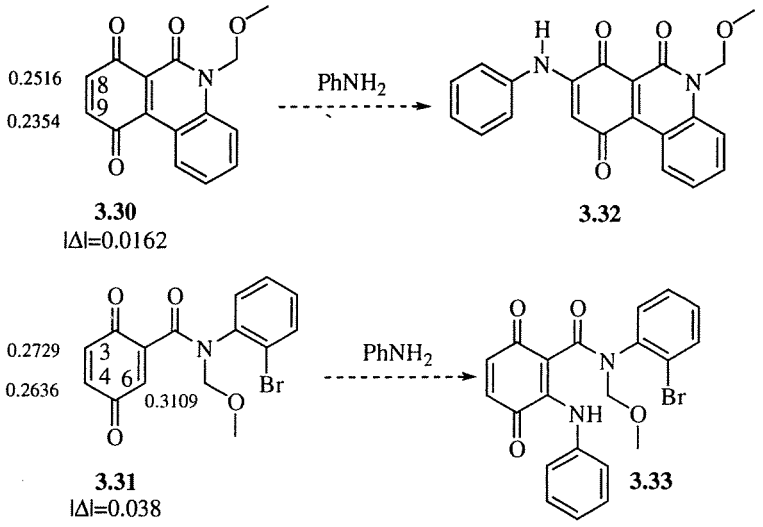

Scheme 3.15

Alternative quinone templates were required for our combinatorial strategy. Fortunately, the work of Yogo *et al.*,[5] and Murphy and Bertrand,[17] provided crucial leads for our synthetic studies. As shown in **Scheme 3.1**, aniline addition to 2-methyl-1,4-benzoquinone (**1.36**) gave 60% of the desired 1-anilino-4-methyl-2,5-benzoquinone (**3.1**) along with 40% of its regioisomer 1-anilino-3-methyl-2,5-benzoquinone. When 1-bromo-3-methyl-2,5-benzoquinone (**3.34**) was reacted with aniline under similar conditions, 6-anilino-1-bromo-3-methyl-2,5-benzoquinone (**3.35**) was exclusively obtained in 90% yield **[Scheme 3.16]**. This was then converted to murrayaquinone A (**1.40**) in an overall 41% yield in 2 steps.

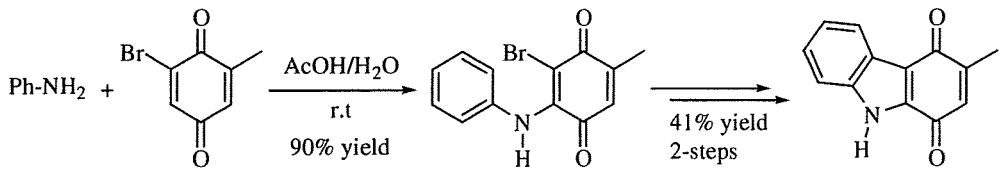

Scheme 3.16

The studies above suggest that 8-bromophenanthridine-7,10-dione (**3.36**) may be a useful template for the addition of aniline to give the desired anilino compound required for the synthesis of calothrixin B. Theoretical calculations, however, show a larger LUMO coefficient at the C8-position as opposed to the C9-position. The calculations thus predict the formation of the undesired anilino compound. However, studies suggest

that in cases where a substituent is present, *ipso* attack is not favorable due to repulsive forces between the attached substituent and the incipient nucleophile.[5,17] Therefore aniline addition to the bromophenanthridine **3.36** should occur at the C9-position to give 9-anilino-8-bromophenanthridine-7,10-dione (**3.37**) [**Scheme 3.17**]. This compound could then be cyclized to yield calothrixin B (**1.27**).

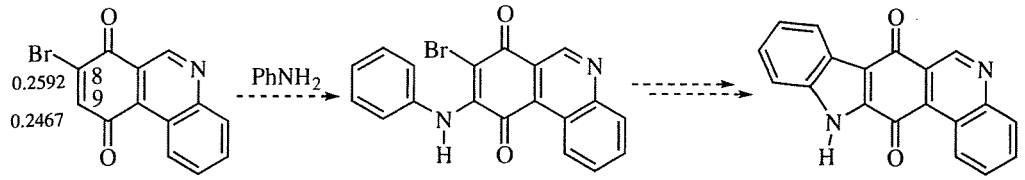

3.36 **3.37** **1.27**

|Δ|=0.0125

Scheme 3.17

In order to test this hypothesis, we embarked on a synthesis of 8-bromophenanthridine-7,10-dione (**3.36**) for our combinatorial strategy.

3.4 Synthesis of the 8-Bromophenanthridine-7,10-dione (3.36) Template

The synthesis of 8-bromophenanthridine-7,10-dione (**3.36**) began with the preparation of 3-bromo-2-hydroxy-5-methoxybenzaldehyde (**3.38**) from 2-hydroxy-5-methoxy benzaldehyde (**3.39**). It has been shown that the 2-hydroxy substituent on the benzaldehyde has a strong *ortho*-directing effect thus resulting in the bromination of the C3-position. Following the procedure of Rubenstein,[18] 2-hydroxy-5-methoxybenzaldehyde (**3.39**) was treated with bromine in buffered acetic acid to give 3-bromo-2-hydroxy-5-methoxybenzaldehyde (**3.38**) in 94% yield. Under these conditions, the formation of the isomer 6-bromo-2-hydroxy-5-methoxybenzaldehyde was not observed. Analysis of the melting point and comparison with the literature melting point confirmed the formation of the desired product.

When the hydroxybenzaldehyde **3.38** was treated with iodomethane and potassium carbonate in dry DMF for 3h, 3-bromo-2,5-dimethoxybenzaldehyde (**1.60**) was obtained in 63% yield. The dimethoxybenzaldehyde **1.60** was then oxidized with a solution of hot potassium permanganate and 3-bromo-2,5-dimethoxybenzoic acid (**3.40**) was

obtained as a white solid in good yields.[10,18] The acid **3.40** was then converted to the tertiary benzamide **3.41** in three steps beginning with the treatment of the acid **3.40** with thionyl chloride. The resulting acid chloride **3.42** was then reacted with 2-iodoaniline to yield the crude benzamide **3.43**, which was then treated with sodium hydride and methoxymethyl chloride in THF at 30°C **[Scheme 3.18]** to yield the tertiary benzamide **3.41**. The 2'-iodobenzamide **3.41** was synthesized in preference to the 2'-bromobenzamide so as to enable differentiation in the reactivities between the two aryl halide ring systems.

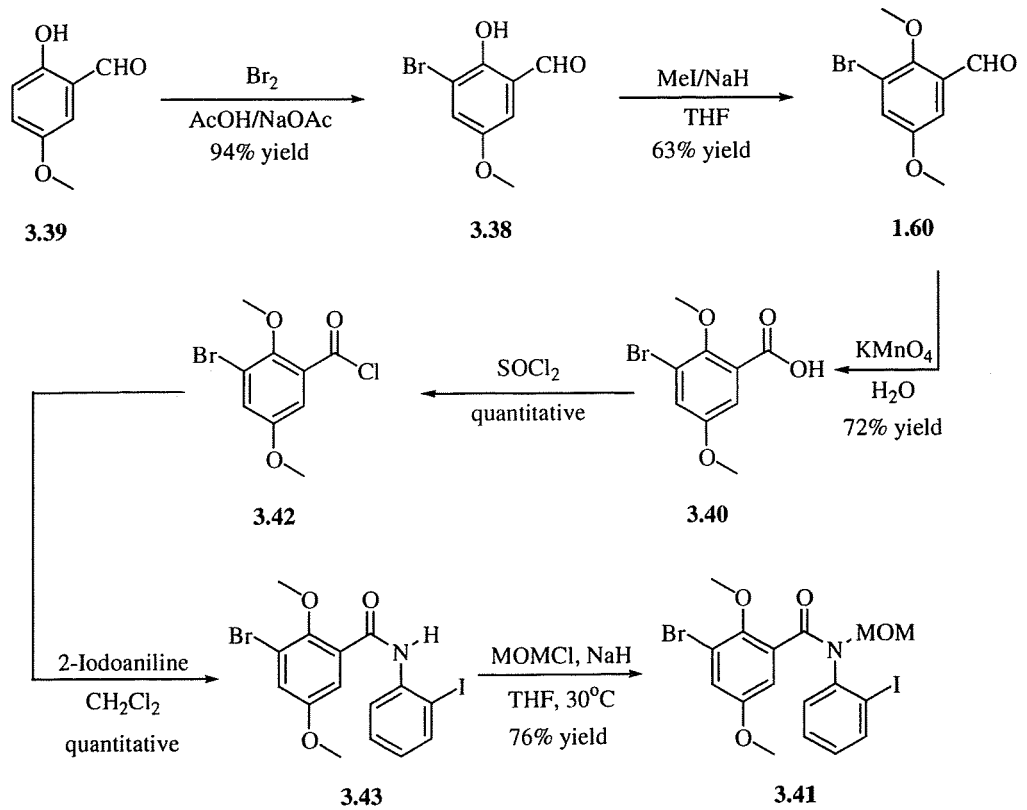

Scheme 3.18

As the insertion of palladium (0) reagents into the C-I bond is more facile than the corresponding insertion into the C-Br bond, the intramolecular biaryl bond formation of the tertiary benzamide **3.41** can be effected under mild conditions. When the benzamide **3.41** was treated with a catalytic amount of palladium (II) acetate and *tris*(*o*-tolyl)phosphine in DMF at 80°C, the desired 8-bromo-7,10-dimethoxy-5*H*-methoxymethylphenanthridin-6-one (**3.44**) was obtained as the exclusive product in 30% yield. The rest of the reaction mixture contained unreacted starting material which

was readily recovered. When triphenylphosphine replaced the *tris*(*o*-tolyl)phosphine ligand, the cyclized product was obtained in 98% yield **[Scheme 3.19]**.

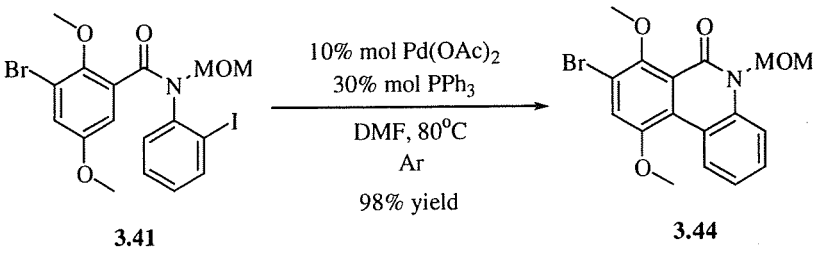

3.41 **3.44**

Scheme 3.19

Due to time constraints, it was not possible to complete the synthesis of 8-bromophenanthridine-7,10-dione (**3.36**). We envisaged that conversion of the bromophenanthridine-6-one **3.44** to 8-bromo-7,10-dimethoxyphenanthridine (**3.36**) can be readily achieved following the procedures developed for the conversion of 7,10-dimethoxy-5-methoxymethyl-5*H*-phenanthrid-6-one (**3.19**) to phenanthridine-7,10-dione **[Scheme 3.11]**. Subsequent Michael addition of aniline to the bromoquinone **3.36** should hopefully afford 8-bromo-9-anilino-phenanthridine-7,10-dione (**3.37**), which is then expected to undergo palladium-mediated cyclization to calothrixin B (**1.27**) **[Scheme 3.20]**.

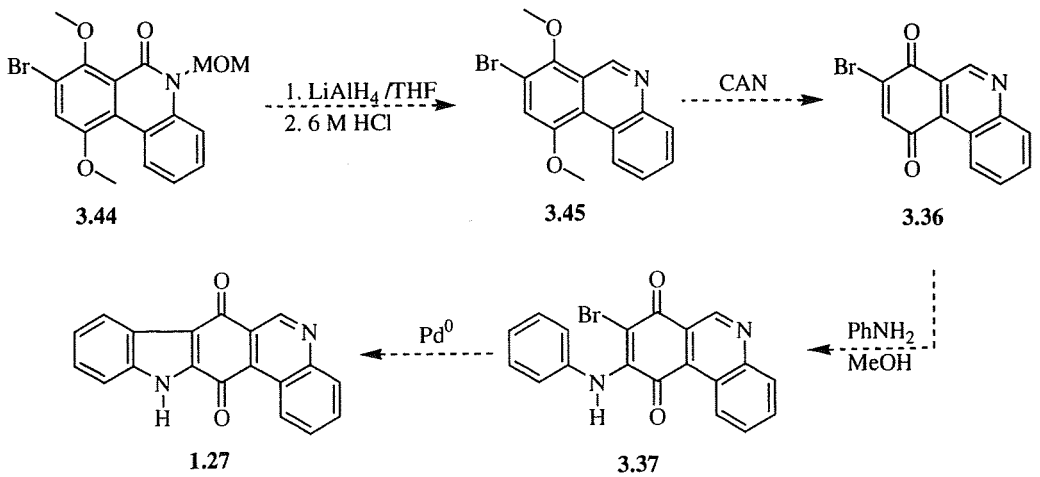

3.44 **3.45** **3.36**

1.27 **3.37**

Scheme 3.20

It is also possible the 8-bromo-7,10-dimethoxyphenanthridine **3.45** may allow for a second strategy towards calothrixin B. This utilizes a Suzuki coupling between the bromophenanthridine **3.45** and 1-amino-2-phenylboronic acid **(3.46)** to install the biaryl linkage in 2-(7,10-dimethoxyphenanthridin-8-yl)phenylamine **(3.47)**. Oxidative demethylation of the phenylamine **3.47** followed by an intramolecular Michael addition of the amino group to the C9-position should then yield calothrixin B **(1.27)** **[Scheme 3.21]**.

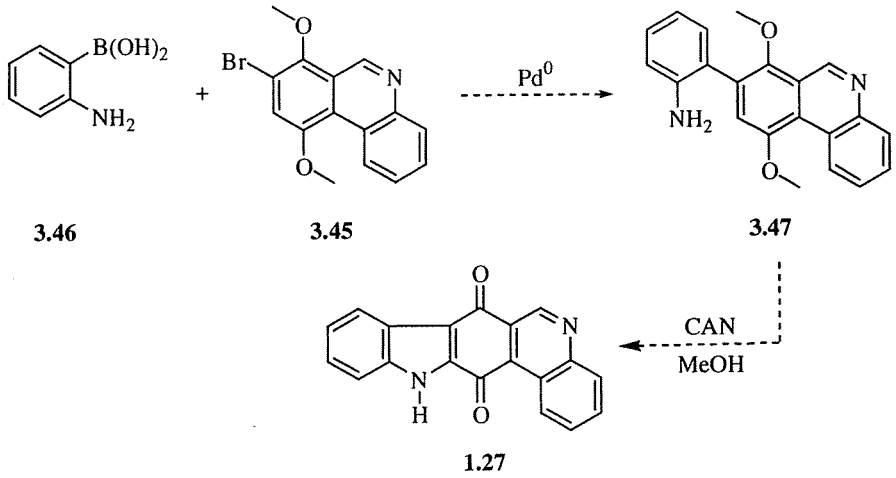

3.46 **3.45** **3.47**

1.27

Scheme 3.21

3.5 Conclusion

The successful synthesis of *iso*-calothrixin B **(3.29)** was achieved for the first time using the phenanthridine-7,10-dione template **3.2**. The mild conditions employed in this synthetic strategy should allow for the combinatorial synthesis of *iso*-calothrixin B derivatives. Due to time constraints, work towards a combinatorial synthesis of calothrixin B employing 8-bromophenanthridine-7,10-dione **(3.36)** remains incomplete. We remain optimistic, however, that this synthesis will work and therefore provide a means of accessing calothrixin B derivatives which can be utilized in a comprehensive QSAR study.

3.6 Bibliography

(1) Bernardo, P. H.; Chai, C. L. L. *J. Org. Chem* **2003**, *68*, 8906-8909.

(2) Bernardo, P. H.; Chai, C. L. L.; Elix, J. A. *Tetrahedron Lett.* **2002**, *43*, 2939-2940.

(3) Knölker, H.-J.; Reddy, K. R. *Chem. Rev.* **2002**, *102*, 4303-4427.

(4) Bouaziz, Z.; Nebois, P.; Poumaroux, A.; Fillion, H. *Heterocycles* **2000**, *52*, 977-999.

(5) Yogo, M.; Ito, C.; Furukawa, H. *Chem. Pharm. Bull.* **1991**, *39*, 328-334.

(6) Kraus, G. A.; Zhang, N. *Tetrahedron Lett.* **2002**, *43*, 9597-9599.

(7) Valderrama, J. A.; Cortés, M.; Pessoa-Mahana, D.; Preite, M.; Benites, J. *Tetrahedron Lett.* **2000**, *41*, 3563-3566.

(8) Le Guen, M. Honours Thesis, The Australian National University, 2003.

(9) Harayama, T.; Akamatsu, H.; Okamura, K.; Miyagoe, T.; Akiyama, T.; Abe, H.; Takeuchi, Y. *J. Chem. Soc. Perkin Trans. 1* **2001**, 523-528.

(10) Azadi-Ardakani, M.; Wallace, T. W. *Tetrahedron* **1988**, *44*, 5939-5952.

(11) Moreno, I.; Teelitu, I.; Etayo, J.; SanMartin, R.; Dominguez, E. *Tetrahedron* **2001**, *57*, 5403-5411.

(12) Beletskaya, I. P.; Cheprakov, A. V. *Chem. Rev.* **2000**, *100*, 3009-3066.

(13) Kutyrev, A. A. *Tetrahedron* **1991**, *47*, 8043-8065.

(14) Finley, K. T. In *The Chemistry of Quinonoid Compounds*; Patai, S., Ed.; Wiley: New York, 1974; Vol. 2, p 877-1144.

(15) Krohn, K. *Tetrahedron* **1990**, *46*, 291-318.

(16) Rozeboon, M. D.; Tegmo-Larsson, I.-M.; Houk, K. N. *J. Org. Chem* **1981**, *46*, 2338-2345.

(17) Murphy, W. S.; Bertrand, M. *J. Chem. Soc. Perkin Trans. 1* **1998**, 4115-4120.

(18) Rubenstein, L. *J. Chem. Soc.* **1925**, 1998-2004.

Chapter 4

4.1 Introduction

With the target carbazolediones synthesized in Chapter 2, we were poised to carry out structure-activity relationship (SAR) studies. The general aim of SAR studies is to determine the structural features in a molecule that gives rise to biological activity. This in turn will enable medicinal chemists to predict and design compounds with optimal biological properties.[1] Furthermore, knowledge of the parameters influencing biological activity can provide mechanistic insights into the interaction of these compounds with biological systems.

Calothrixin B (**1.27**) is considered the lead compound for our SAR studies. For the SAR studies to be useful, a significant number of calothrixin derivatives and related carbazolediones should be available for evaluation. These compounds were prepared using the methodologies outlined in Chapters 2 and 3. Quantitative Structure-Activity Relationship (QSAR) analysis of the physicochemical properties of our test compounds would allow us to determine the parameters that correlate with the measured biological activity. Some important parameters that have been correlated with the biological activity of quinones are outlined below.

4.1.1 The Role of Redox Potentials in the Biological Activity of Quinones

The reduction potential of quinones is an important parameter which has been correlated to the efficacy of quinone-based drugs.[2,3] For example, a study by Kunz *et al.* reported that the antiproliferative properties of mitomycin C analogues were dependent on the propensity of these quinones to undergo one-electron reduction to the reactive semiquinone radical anion. A linear correlation was found between the $\log(1/EC_{50})$ and $E_{1/2}{}^{I}$ for nineteen mitomycin C analogues thereby predicting that a mitomycin C analogue with a lower $E_{1/2}{}^{I}$ value would lead to more potent antiproliferative activity against various cancer cell lines.[4] These results have provided insights into the biological modes of action of mitomycin C (**1.8**). Recent studies have shown that mitomycin C (**1.8**) is enzymatically reduced *in vitro* to the semiquinone radical anion, which in turn produces reactive oxygen species (ROS) through redox cycling.[5] These generated ROS can deplete cellular reductants leading to a loss of cell viability as outlined in Chapter 1. Furthermore, the radical anion of mitomycin C is believed to induce apoptosis, a programmed-form of cell death.[5] The semiquinone radical can

further undergo reduction to the quinol dianion, which has been implicated in the alkylation of DNA. The formation of DNA-mitomycin adducts such as **4.1** interferes with the DNA repair mechanism and can lead to cell death.[6,7]

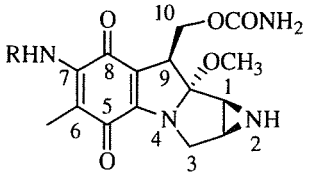

1.8
R=H, mitomycin C

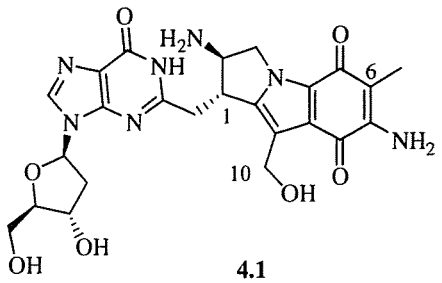

4.1

4.1.2 The Role of Steric Parameters in the Biological Activity of Quinones

The steric parameter molar refractivity (MR), defined as the volume occupied by an atom or molecule, is commonly employed in QSAR studies.[1] The MR parameter is of particular interest when intermolecular binding interactions between a compound and a receptor are important. The size and shape of a compound as well as the charge distribution affects the ability of a compound to bind to receptor sites on biomolecules such as enzymes.

A study by Malta *et al.* attempted to correlate steric factors with the observed trypanocidal activity of naphthoquinone derivatives (**Figure 4.1**).[8] In their studies, fourteen compounds were tested for the ability to kill the parasite *Trypanosoma cruzi*, and of the fourteen compounds, eight were found to be active. The authors then calculated the polarizability factor α expressed as a volume (Å^3). The polarizability factor α is related to molar refractivity (MR) by the equation $\alpha = \frac{3N\text{MR}}{4\pi}$ where N is Avogadro's constant and π=3.14. The results showed that the eight active compounds possessed α values greater than 21 Å^3. In contrast, the six inactive compounds had α values lower than 20 Å^3. The authors argued the observed activity was due to the larger molecules binding to the receptor site on an enzyme, inducing a conformational change which resulted in trypanocidal activity.[8,9] However, the purported enzyme has not been isolated and thus this hypothesis remains speculative.

Active napthoquinones and derivatives

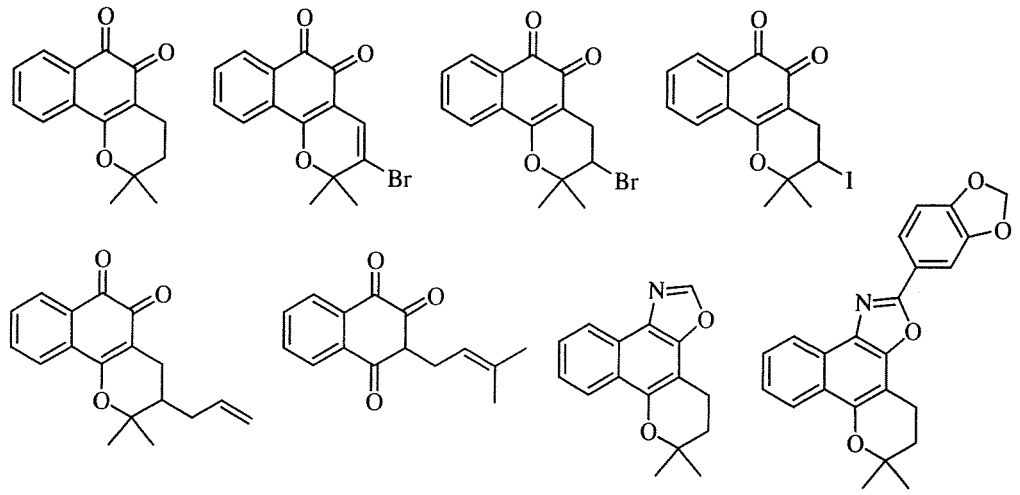

Inactive napthoquinones

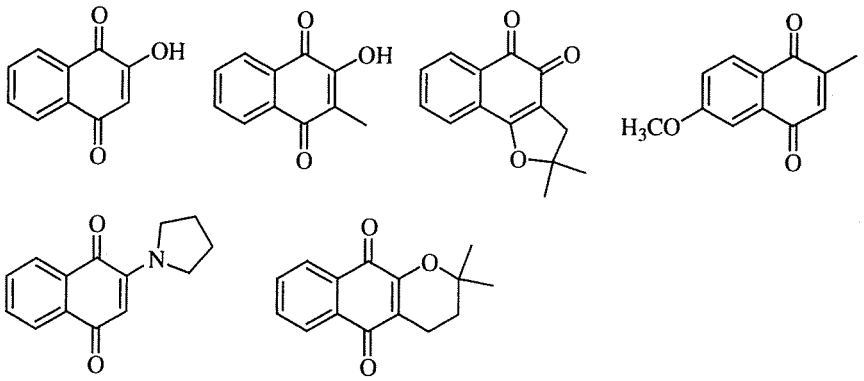

Figure 4.1: *Naphthoquinones tested for trypanocidal activity by Malta et al.*

4.1.3 The Role of Lipophilicity in the Biological Activity of Quinones

Lipophilicity is often an important factor in the determination of the transport of compounds into cells. Originally, lipophilicity was measured as the partition coefficient (P) of a solute in 1-octanol and water, which was used as a model for biological lipid and aqueous phases. The logarithm of the partition coefficient, logP, is the standard measurement for the lipophilicity of a compound in which a negative logP value reflects a greater affinity for the aqueous phase, whereas a positive logP value is indicative of a greater affinity for the lipid phase. The logP value can therefore be used as a measure of the ease with which a compound can diffuse across the lipid bilayer of a cell and enter the cytoplasm. The lipid bilayer which encapsulates most cells is a semi-permeable membrane which excludes many substances.[10,11] Thus compounds that possess a net ionic charge are generally excluded from entering the lipid bilayer but may enter the cell through ion transport channels embedded in the membrane. Highly polar molecules

such as water are also excluded from entering the cell due to unfavorable interactions with the lipophilic membrane, and are generally transported into the cell through porin channels.[12] Highly lipophilic neutral compounds, on the other hand, can enter the lipid bilayer but may fail to diffuse into the cytoplasm due to the polar nature of the aqueous environment within. Thus, for successful diffusion into the cell, a drug must possess sufficient lipophilicity to penetrate the lipid bilayer and also possess enough polar character to enter the cytoplasm. This leads to a diffusion model in which a parabolic relationship between logP and $\log(1/EC_{50})$ is observed.[13]

A study of eleven 7-substituted mitomycin A derivatives showed a weak correlation between lipophilicity and antiproliferative activity in human cancer cells (colon WIDR, ovarian cancer cells, and MCF-7 breast cancer cells). Specifically, bioactivity as measured by the $\log(1/EC_{50})$ showed a linear dependence on the logP values measured and a linear covariance of R^2=0.64 was obtained.[4] It is important to note that a linear trend was observed due to the narrow range of logP values studied (-1.1 to 2.5). Thus as lipophilicity increases, the potency of the mitomycin A derivatives also increases within the logP range tested. One notable exception to the trend, however, was that the parent compound mitomycin A **(1.56)** displayed potent biological activity (EC_{50}=0.30nM) and yet had a low logP value of 0.26. Thus the linear correlation curve of biological activity versus logP predicts less activity for mitomycin A than the actual observed activity.[4] These studies demonstrate that although lipophilicity may be an important factor in determining the antiproliferative activity of mitomycin A derivatives, other parameters must also be influential.

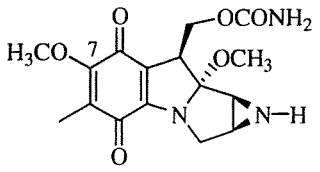

1.56

With these considerations in mind, our SAR and QSAR studies on the calothrixins and carbazolediones focused on the assessment of two of the parameters discussed above (*i.e.*, reduction potentials, and lipophilicity) and their relationship, if any, to biological activity. These studies began with the measurement of the antiproliferative properties of the calothrixins and related carbazolediones.

4.2 Antiproliferative Activity of the Calothrixins and Related Quinones Against HeLa Cells

In these biological experiments, the calothrixins and other carbazolediones were tested against HeLa cervical cancer cells to measure the extent to which cell growth was inhibited. For our studies, the MTT assay was chosen as a measure of the antiproliferative effect of the test compounds. This assay has been shown to give comparable results to the ^{3}H-thymidine incorporation assay, which has the disadvantage of employing radioactive isotopes.[14-17]

The chemical basis for the MTT assay is the reduction of the MTT dye, 3-(4,5-dimethylthiazol-2-yl)-2,5-diphenyl-2*H*-tetrazolium bromide (**4.2**), by the NADH and NADPH of live cells. The yellow MTT dye is metabolized to the dark blue formazan dye **4.3** as shown in **Scheme 4.1**. The concentration of the formazan dye is then measured using spectrophotometric methods at a wavelength of 590nm at which the MTT dye has negligible absorbance.[17,18]

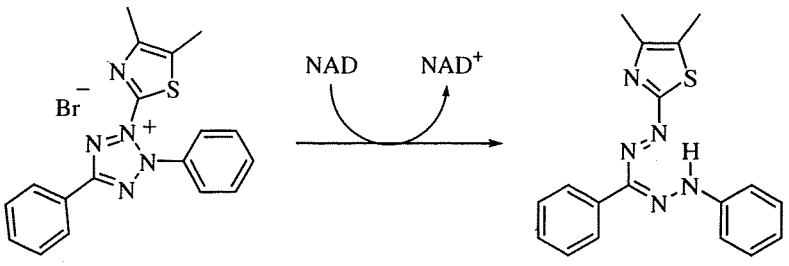

4.2 **4.3**

Scheme 4.1

In a typical procedure, HeLa cells were cultured in RPMI Media with 10% fetal calf serum at a cell density of $0.5x10^{5}$ cells/mL in 96-well plates. All experiments were carried out in quadruplicate and included controls consisting of both untreated cells and media. The test compounds at an initial concentration of 100μM were placed in the wells (first column, rows 1 to 4) of microtitre plates and serial dilutions (1:1) were carried out. Typically, each well contained 5000 cells in a total volume of 100μL, and the concentration of the test compounds ranged from 50μM to 98nM.

The cells were then placed in an incubator at 37°C under an atmosphere of 5% carbon dioxide for a period of three days. As the division time of HeLa cells is between 16 to 20 hours, a three day period allows for approximately four cycles of cell division. A decrease in the number of metabolically active cells relative to the population of untreated cells is a reflection of the antiproliferative properties of the test compounds. To determine the relative populations of metabolically active cells at different concentrations of the test compounds, the MTT colorimetric assay was used.

After three days of incubation, the test solutions were decanted and the live/adherent cells were treated with the MTT dye for 5 hours. The cells were then lysed with a solubilising agent to release the formazan dye. The concentration of the formazan dye per well was obtained by measuring the absorbance at 590nm using an ELISA plate reader. In this manner, the percentage of metabolically-active cells present (% of live cells) can be determined relative to the controls. The dose-response curve (A_{590nm} versus applied concentration of test compound) was generated using the GraphPad Prism Version 2.01 program employing non-linear regression with a sigmoidal variable slope equation.

From the dose-response curve, the EC_{50} values for each test compound was determined. The EC_{50} (Effective Concentration) is defined as the concentration of a compound required to inhibit cell proliferation by 50%. A typical dose-response curve is shown in **Figure 4.2**. The error bars represent differences in the estimated population of live cells for quadruplicate runs. Where the error bars are not visible, the errors lie within the data marker and are too small to be seen.

Thus the EC_{50} values for antiproliferative activity were obtained for the carbazolediones using the MTT assay. The results are presented in the following tables with the relevant discussions.

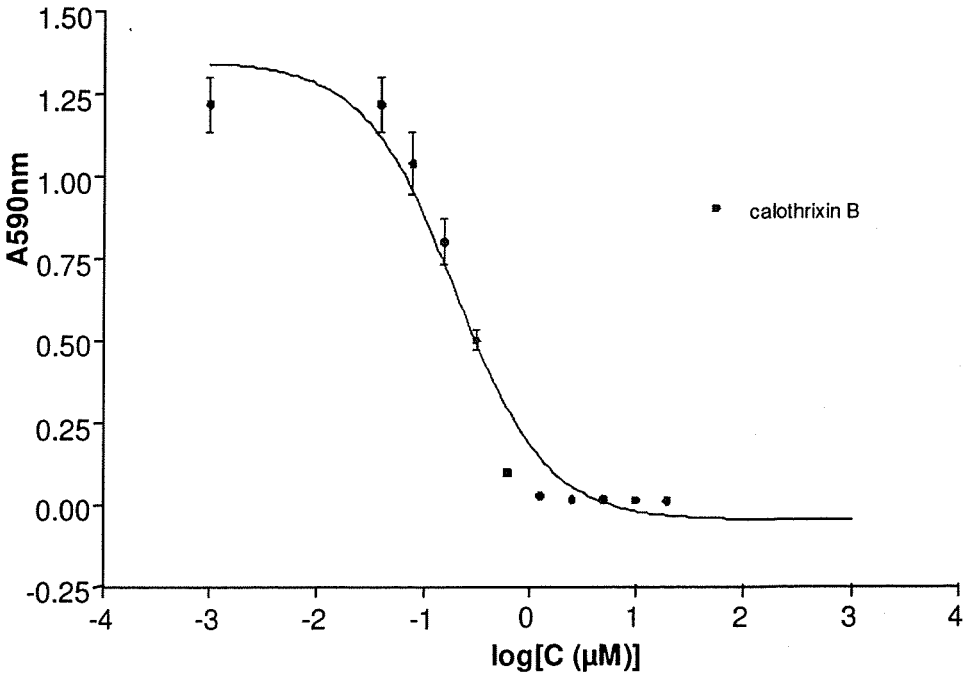

Figure 4.2: *Dose-response curve for the MTT assay of calothrixin B. Where the error bars are not visible, the values lie within the marker.*

4.2.1 Antiproliferative Properties of Calothrixin B and Related Carbazolediones

The results of the MTT assay for calothrixin B (**1.27**) and the carbazolediones **[Figure 4.3]** are shown in **Table 4.1**.

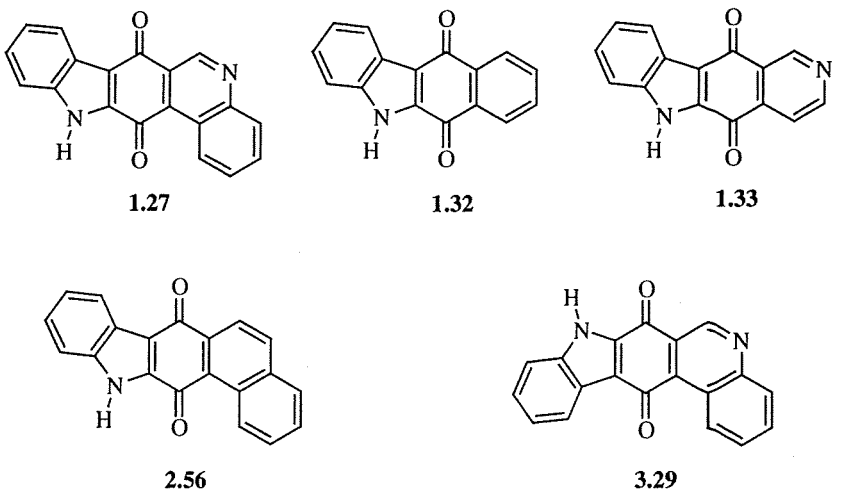

Figure 4.3: *Calothrixins B and related carbazolediones used in the first MTT assay.*

The results showed that all of the quinones tested were active at micromolar concentrations. The tetracyclic ellipticine quinone (**1.33**) was the most active of the carbazolediones with an EC_{50} value of half the value observed for the pentacyclic lead compound, calothrixin B (**1.27**). These compounds differ only in the presence of the *E*-ring in calothrixin B. The greater potency of ellipticine quinone over calothrixin B suggests that the *E*-ring is not crucial for biological activity, and that the *E*-ring can cause the attenuation of biological activity. Similar observations were made when comparing the bioactivity of indolophenanthrenedione (**2.56**) and benzocarbazoledione (**1.32**) where the latter has half the EC_{50} value of the former **[Table 4.1]**.

The constitutional isomer of calothrixin B, *iso*-calothrixin B (**3.29**), was less active than the naturally occurring isomer. The difference in the position of the heteroatom in the *D*-ring and the orientation of the *E*-ring resulted in a two-fold attenuation of antiproliferative activity.

Compound	**EC_{50}(ave)** (μM)	**Std. Dev.** (μM)
Ellipticine quinone (**1.33**)	0.15	±0.01
Calothrixin B (**1.27**)	0.25	±0.02
Benzocarbazoledione (**1.32**)	0.43	±0.01
Iso-calothrixin B (**3.29**)	0.46	±0.01
Indolophenanthrenedione (**2.56**)	1.03	±0.06

Table 4.1

The antiproliferative assay also revealed that the substitution of the heteroaromatic *D*-ring with the corresponding aromatic carbocyclic analogue led to a decrease in potency. This was reflected in the decrease in biological activity of the indolophenanthrenedione (**2.56**) relative to calothrixin B. Similarly, benzocarbazoledione (**1.32**) has weaker antiproliferative activity than ellipticine quinone (**1.33**).

4.2.2 Antiproliferative Activity of Calothrixin B Derivatives

The EC_{50} values for calothrixin A (**1.26**) and various calothrixin derivatives **[Figure 4.4]** are shown in **Table 4.2**.

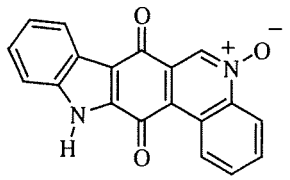

1.26

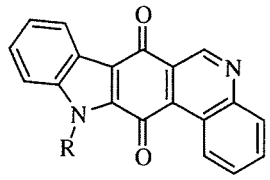

R=CH_3OCH_2-, **2.25**
=$C_6H_5CH_2$-, **2.58**
=CH_3CH_2-, **2.59**

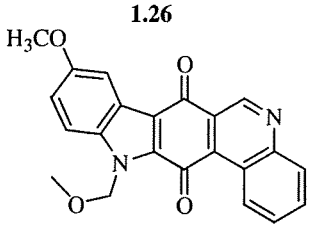

2.64

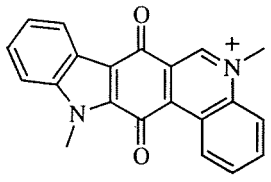

2.63

Figure 4.4: *Calothrixin A and calothrixin derivatives used in the second MTT assay.*

Compound	**EC_{50}(ave)** (μM)	**Std. Dev.** (μM)
Calothrixin A (**1.26**)	0.12	±0.01
Calothrixin B (**1.27**)	0.25	±0.02
N-Benzyl Calothrixin B (**2.58**)	0.38	±0.01
N-MOM Calothrixin B (**2.25**)	0.42	±0.01
N-Ethyl Calothrixin B (**2.59**)	0.45	±0.01
5,12-Dimethyl Calothrixin (**2.63**)	4.68	±0.01
9-Methoxy *N*-MOM-Calothrixin B (**2.64**)	-	-

Table 4.2

It was noted that substitution of the hydrogen atom at the indole nitrogen position of calothrixin B with alkyl substituents resulted in a small decrease in biological activity. This is clearly delineated by comparing the EC_{50} values of the N12-substituted derivatives (**2.25, 2.58, 2.59**) with that of calothrixin B (**1.27**). Interestingly, the N12-substituted calothrixin B derivatives display comparable biological activities, ranging from 0.38μM for *N*-benzyl calothrixin B (**2.58**) to 0.45μM for the *N*-ethyl derivative (**2.59**).

The EC_{50} value for 9-methoxy *N*-MOM calothrixin B (**2.64**) could not be determined from the MTT assay. Although the compound does exhibit antiproliferative properties at concentrations above 0.2μM, the observed activity has a maximum value of only 40% inhibition at 0.8μM. At higher concentrations of the compound (up to 100μM), the percent inhibition does not increase beyond 40%. This result may be due to the very poor solubility of 9-methoxy *N*-MOM calothrixin B in aqueous media.

The results in **Table 4.2** show that the presence of the quinoline *N*-oxide in calothrixin A (**1.26**) enhanced its potency (EC_{50}=0.13μM) twofold relative to that of calothrixin B (**1.27**). In contrast, the cationic species 5,12-dimethyl calothrixin (**2.63**) has a highly attenuated potency of 4.68μM *i.e.*, a 20-fold decrease in antiproliferative activity relative to that observed for calothrixin B. Although the 5,12-dimethyl calothrixin has both indolic *N*-methyl and quinoline *N*-methyl groups, the analysis of the N12-substituted calothrixins suggests that the effect of *N*-substituents on the indole ring would be small, resulting in approximately a two-fold decrease in biological activity. Therefore, the large decrease in the bioactivity of the dimethyl calothrixin **2.63** is probably due to the presence of the charged quinoline *N*-methyl moiety.

It is possible that the differences in observed activity for calothrixin A (**1.26**), calothrixin B (**1.27**) and 5,12-dimethyl calothrixin (**2.63**) may be related to the ability of the compounds to form hydrogen bonds with a donor molecule. The quinoline nitrogen of calothrixin B has a lone pair of electrons which can participate in hydrogen bonding. Similarly, the *N*-oxide of calothrixin A can form hydrogen bonds through the oxygen atom. In contrast, the *N*-methylated quinoline nitrogen atom of 5,12-dimethyl calothrixin (**2.63**) cannot participate in hydrogen bonding. This hydrogen bonding may influence binding to a specific enzyme. For example, it is possible that the calothrixins bind to a receptor site on a biomolecule such as RNA polymerase,[19] and the presence of the nitrogen atom at the 5-position of the calothrixins form a hydrogen bond with an amino or hydroxyl residue in the receptor pocket which strengthens the binding interaction. The position of the quinoline nitrogen atom may be important as *iso*-calothrixin B (**3.29**) is slightly less active than calothrixin B. This hypothesis of hydrogen-bonding assisted receptor binding may also rationalize the greater biological activity observed for ellipticine quinone (**1.33**) relative to benzocarbazoledione (**1.32**),

as well as the greater activity of calothrixin B relative to the indolophenanthrenedione (**2.56**).

The antiproliferative activities of *N*-MOM substituted carbazolediones **[Figure 4.5]** were also measured and compared (**Table 4.3**). The *N*-MOM carbazolediones show a similar order of antiproliferative activity as compared to that observed for the parent compounds. Specifically, the *N*-MOM ellipticine quinone (**2.21**) was the most active compound in this series, followed by *N*-MOM calothrixin B (**2.25**) while the *N*-MOM benzocarbazoledione (**2.75**) was the least active. This result supports the hypothesis that the *E*-ring is not required for bioactivity, while the presence of the nitrogen atom in the *D*-ring contributes to enhanced bioactivity.

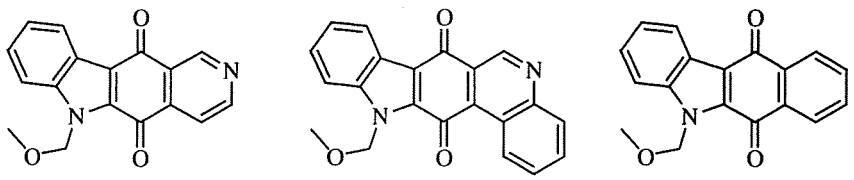

2.21 **2.25** **2.75**

Figure 4.5: N-*MOM substituted carbazolediones tested in the MTT assay.*

It was also observed that the presence of the indolic *N*-MOM group attenuated the bioactivity of these carbazolediones relative to the parent compounds listed previously in **Table 4.1**. The difference in antiproliferative activity between calothrixin B (**1.27**) and *N*-MOM calothrixin B (**2.25**) is only 0.17μM (a two-fold difference), and a similar difference was noted between ellipticine quinone (**1.33**) and *N*-MOM ellipticine quinone (**2.21**). The difference in activity between benzocarbazoledione (**1.32**) and *N*-MOM benzocarbazoledione (**2.75**) is 1.16μM or a four-fold difference.

Compound	**EC_{50}(ave)** (μM)	**Std. Dev.** (μM)
N-MOM ellipticine quinone (**2.21**)	0.37	±0.08
N-MOM Calothrixin B (**2.25**)	0.42	±0.01
N-MOM benzocarbazoledione (**2.75**)	1.59	±0.05

Table 4.3

4.3 Electrochemistry of the Carbazolediones and Correlation of Electrochemical Results to Biological Activity

We set out to measure the redox potentials of the calothrixins and the related carbazolediones in order to determine the influence of redox processes on the observed bioactivity. There are a number of methods for measuring the reduction potentials of quinones. For example, the two-electron reduction potential of quinones can be measured using an enzymatic assay consisting of NADPH and a suitable enzyme such as Quinone Reductase 1 (DT-diaphorase).[20,21] It is more common, however, to measure single-electron reduction potentials for quinones particularly since the semiquinone radical anion has been implicated in several biological mechanisms as discussed earlier.[22-24] These single-electron reductions or half-wave potentials ($E_{1/2}$) can be measured directly using voltammetry. In this work, the half-wave potentials were measured using direct-current (dc) cyclic voltammetry (CV).

A feature of dc-CV is that redox processes can be observed directly, thus allowing determination of the $E_{1/2}$ values as well as demonstrating the reversibility of the electrochemical process. In an electrochemically reversible process, rapid electron transfer occurs in both directions between the oxidized and reduced species. This reversible process is reflected by a consistency in the morphology of the voltammogram over multiple scans **[Figure 4.6]**.

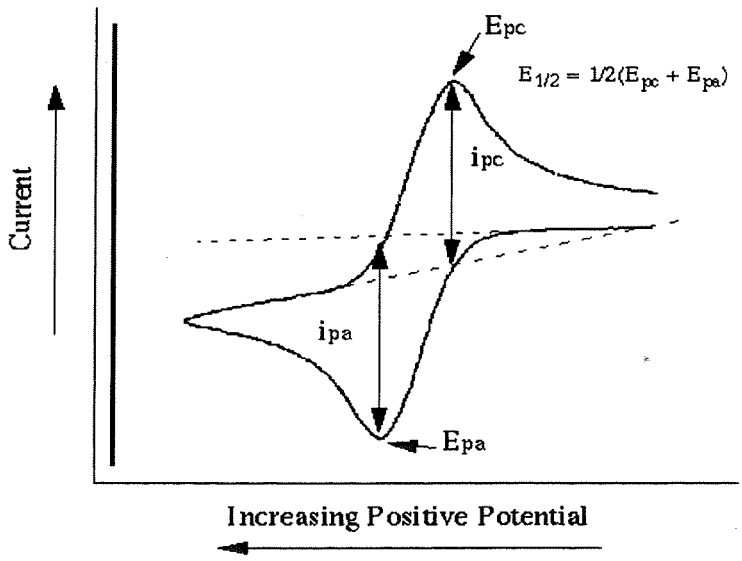

Figure 4.6: *Cyclic Voltammogram of a reversible electrochemical process.*

As the figure shows, there are two peaks for a single electrochemical process. The peak heights are observed at the cathodic peak potential (E_{pc}) for the reduction process, and the anodic peak potential (E_{pa}) for the oxidation process.

In contrast, in an irreversible electrochemical process there is a competing chemical reaction which removes either the oxidized or reduced species at the electrode. This results in the loss of one of the peaks [**Figure 4.7**]. As the figure shows, there is a peak observed at E_{pa} which corresponds to an oxidation process, but the corresponding reduction process is not seen.

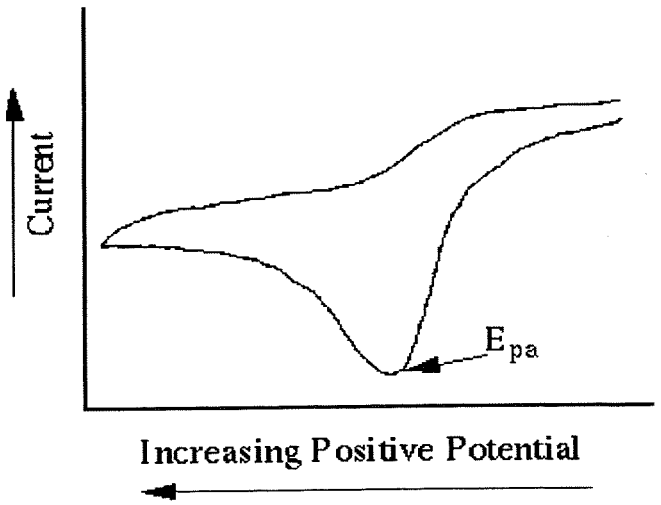

Figure 4.7: *Cyclic Voltammogram of an irreversible electrochemical process.*

In dc-cyclic voltammetry, the working electrode is used to apply a triangular potential ramp to a solution of the test compound. The potential of the working electrode, measured relative to the reference electrode, is varied from the initial potential E_1 to the switching potential E_2 and back at a constant rate. The rate of change in the applied electric potential is known as the scan rate. As the potential changes, the resulting current flow is measured using the auxiliary electrode. The voltammogram is then plotted as the current flow versus applied potential as shown in **Figure 4.8**. The midpoint between the anodic peak potential (E_{pa}) and the cathodic peak potential (E_{pc}) is the half-wave potential $E_{1/2}$. For an electrochemically reversible process, the $E_{1/2}$ value is the potential at which equal concentrations of the reduced and oxidized species of a compound are in the vicinity of the electrode, thus providing a good approximation of the standard reduction potential of the couple.

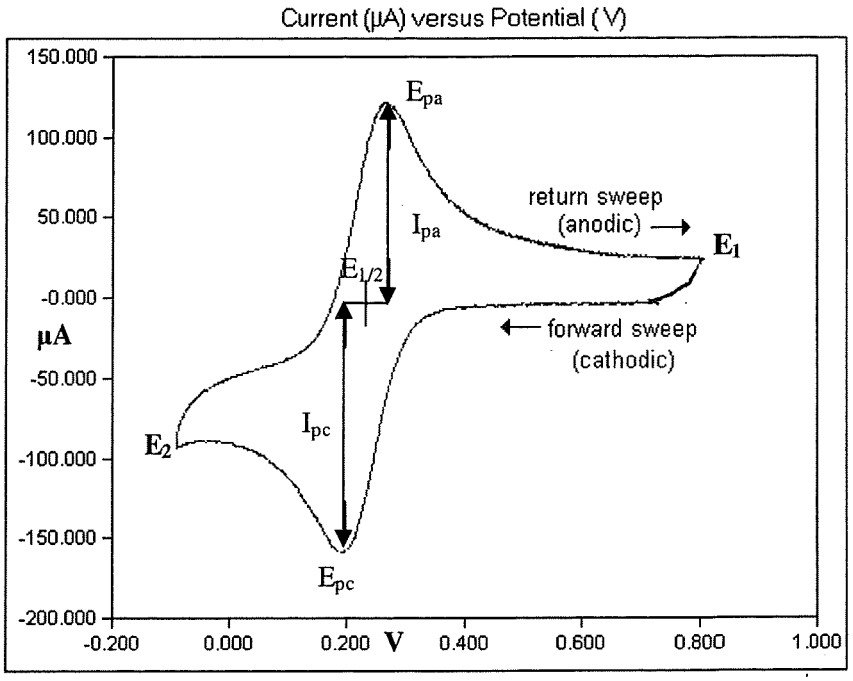

Figure 4.8: *Cyclic Voltammogram of a typical reversible one-electron redox process.*

In a typical procedure, a solution of each test compound was prepared in dry dimethylsulfoxide containing tetra-*n*-butylammonium hexafluorophosphate as a supporting electrolyte. A three-electrode potentiostat consisting of a glassy carbon working electrode, a platinum wire reference electrode, and a platinum auxiliary electrode was then immersed in the solution, and ferrocene (Fc) was added as an internal standard. The ferrocinium/ferrocene couple (Fc^+/Fc) has a standard reduction potential of +0.68V in DMSO relative to the standard hydrogen electrode (SHE). The measurements were then carried out at 20°C using a scan rate of 50mV/s. The cyclic voltammogram of calothrixin B shown in **Figure 4.9** is typical of the CV traces obtained for the other carbazolediones.

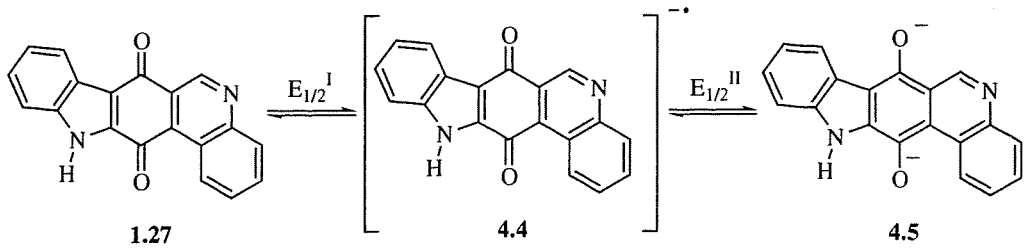

1.27 4.4 4.5

Scheme 4.2

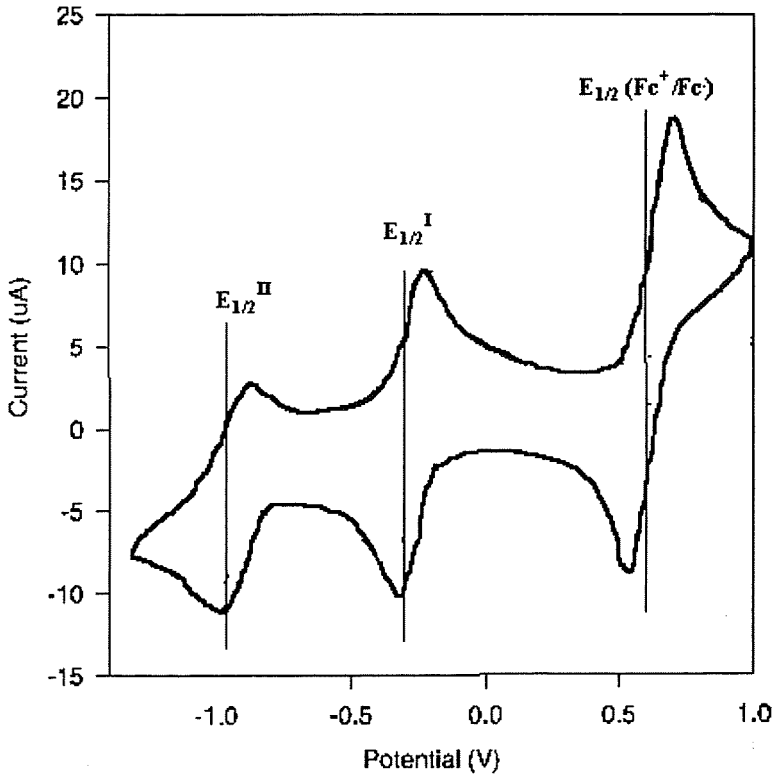

Figure 4.9: *CV trace for calothrixin B along with the ferrocene standard.*

The voltammograms obtained for each of the test compounds showed no changes in the CV trace over multiple scans, which was indicative of reversible electrochemical processes. Thus the quinones were reduced stepwise to the semiquinone radical anion then to the quinol dianion and back without observing any competing chemical reactions within the timescale of these experiments. The $E_{1/2}^{I}$ and $E_{1/2}^{II}$ values were then calculated relative to the ferrocene standard. In addition to the reduction potentials, the difference between the half-wave potentials (ΔE) was also calculated. This difference is proportional to the equilibrium constant for the comproportionation reaction between the quinone **(1.6)** and the quinol dianion **(4.6)** to form the semiquinone radical **(1.12).** The comproportionation and disproportionation reactions will be discussed in more detail in **Section 4.3.3**. The comproportionation reaction is shown in **Scheme 4.3**.

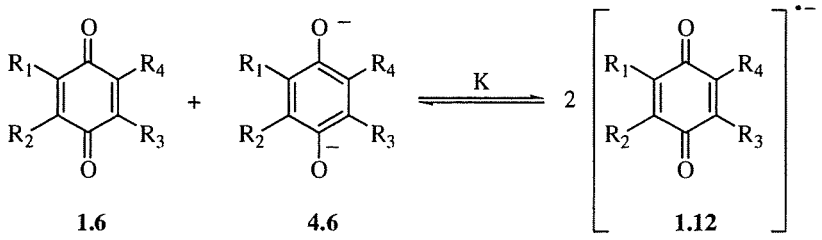

1.6 **4.6** **1.12**

Scheme 4.3

The equilibrium constants were calculated using the Gibbs and Nernst Equations and are reported as the natural logarithm of the equilibrium constant (lnK). A high lnK value is indicative of the stability of the semiquinone radical anion, and thus disproportionation to the quinone and quinol dianion is less likely to occur. The overall reduction potential for the quinone (Q) to the quinol dianion (Q^{2-}) has also been calculated using the equation $E_{Q/Q}^{2-} = (E_{1/2}^{I} + E_{1/2}^{II})/2$.[25] The measured and calculated values are shown in **Table 4.4**. Discussions on the relevance of $E_{1/2}^{I}$, $E_{1/2}^{II}$, lnK and $E_{Q/Q}^{2-}$ values follow.

Compounds	$E_{1/2}^{I}$(V)	$E_{1/2}^{II}$(V)	ΔE	lnK	$E_{Q/Q}^{2-}$ (V)
Calothrixin A (**1.26**)	-0.80	-1.46	0.66	26.1	-1.13
Calothrixin B (**1.27**)	-0.92	-1.54	0.63	25.0	-1.23
N-MOM Calothrixin B (**2.25**)	-0.82	-1.54	0.72	28.5	-1.18
Ellipticine quinone (**1.33**)	-1.09	-1.67	0.58	23.0	-1.38
N-MOM ellipticine quinone (**2.21**)	-0.95	-1.66	0.71	28.1	-1.31
Benzocarbazoledione (**1.32**)	-1.17	-1.84	0.67	26.5	-1.51
N-MOM benzocarbazoledione (**2.75**)	-1.15	-1.86	0.72	28.5	-1.51

lnK=(ΔEF/RT), where $\Delta E=(E_{1/2}^{I}-E_{1/2}^{II})$, F=9.64867x$10^4$ C/mol, R=8.31245 J/(K mol), T=293K. All reduction potentials are relative to Fc^+/Fc.

Table 4.4

4.3.1 Comparison of $E_{1/2}^{I}$ Values of the Calothrixins and Related Carbazolediones

A range of $E_{1/2}^{I}$ values (-0.80V to –1.17V) was observed for the reduction of the carbazolediones to their respective semiquinone radicals. All the $E_{1/2}^{I}$ values calculated were found to be higher (more positive) than –1.18V (-0.50V with respect to SHE), the

putative threshold value for reduction potentials which determines whether or not a compound can accept electrons from biological electron donors.[2] The $E_{1/2}^{I}$ values obtained for these carbazolediones thus predict that these compounds can undergo facile reduction to the semiquinone radical anion in the presence of biological reductants.

As a group, the calothrixin derivatives were found to have similar reduction potentials, displaying relatively early reductions. Calothrixin A (**1.26**) and *N*-MOM calothrixin B (**2.25**) were the easiest to reduce (-0.80 and -0.82V respectively). Calothrixin B (**1.27**), on the other hand, has a half-wave potential of –0.92V which differs by 0.12V from calothrixin A. The greater ease of reduction of calothrixin A may be due to a decrease in the LUMO energy of the molecule at the carbonyl positions through a –I effect exerted by *N*-oxide moiety. Similarly, the *N*-MOM group of calothrixin B may exert a weak –I effect resulting in a greater ease of reduction for *N*-MOM calothrixin B relative to calothrixin B.

A comparison of the $E_{1/2}^{I}$ values obtained for *N*-MOM calothrixin B (**2.25**) and *N*-MOM ellipticine quinone (**2.21**) differ in the ease of reduction by 0.13V. The relative ease of reduction of *N*-MOM calothrixin B as compared to *N*-MOM ellipticine quinone may reflect a lowering of the LUMO energy by -R effects. The extended conjugated π-system in *N*-MOM calothrixin B may provide additional resonance contributions **[Figure 4.10]** for the unpaired electron in the semiquinone radical anion which further stabilize this intermediate relative to the radical anion of *N*-MOM ellipticine quinone **[Figure 4.11]**. A similar argument can be extended to explain the relative ease of reduction of calothrixin B (**1.27**) as compared to ellipticine quinone (**1.33**).

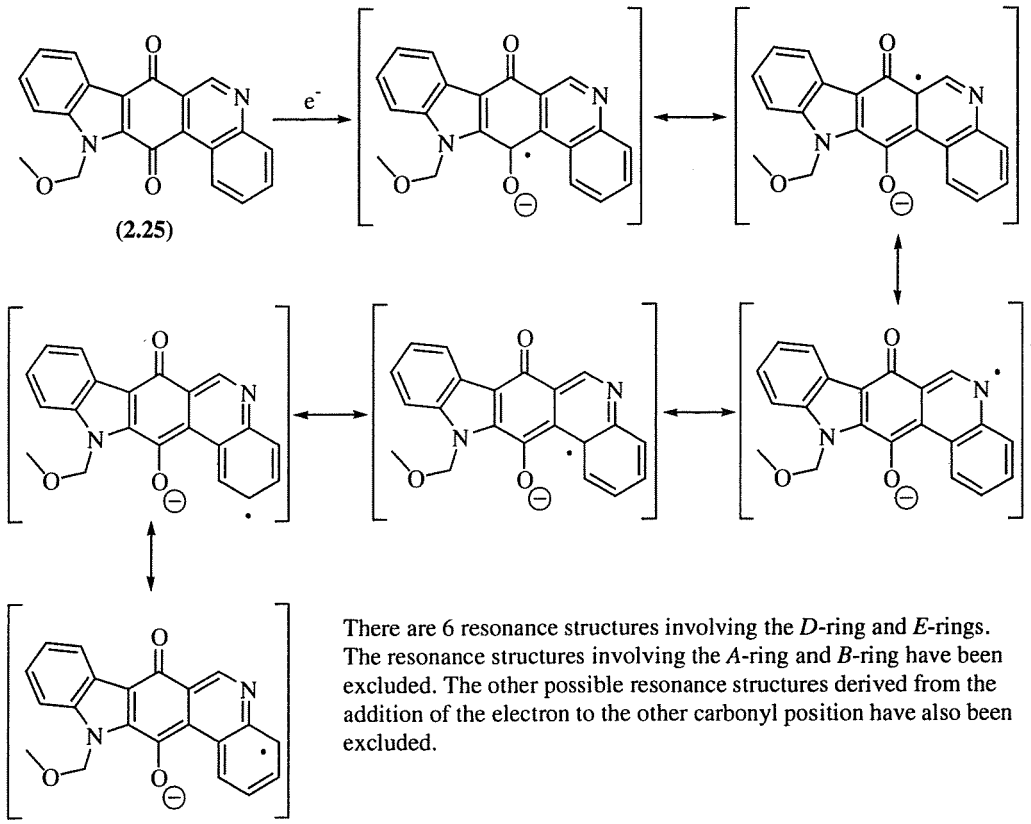

There are 6 resonance structures involving the *D*-ring and *E*-rings. The resonance structures involving the *A*-ring and *B*-ring have been excluded. The other possible resonance structures derived from the addition of the electron to the other carbonyl position have also been excluded.

Figure 4.10: *Selected resonance structures for the semiquinone radical anion of* **2.25**.

The *N*-MOM ellipticine quinone (**2.21**) was found to be significantly easier to reduce than the *N*-MOM benzocarbazoledione (**2.75**) by 0.20V. The difference in $E_{1/2}$ values may reflect the greater stability of the putative radical anion of *N*-MOM ellipticine quinone via delocalization of the unpaired electron onto the nitrogen atom of the pyridine ring system **[Figure 4.11]**.

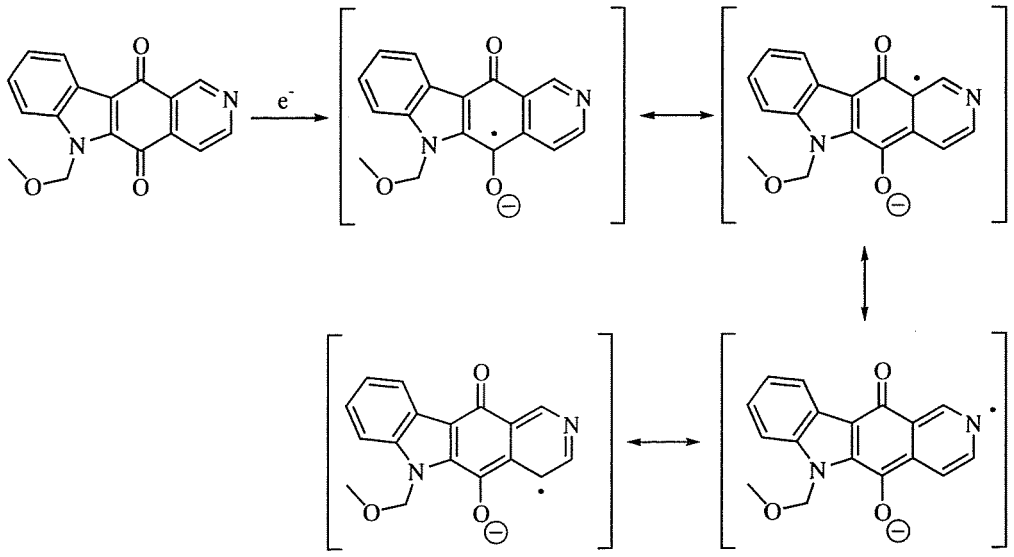

Figure 4.11: *Selected resonance structures for the semiquinone radical anion of* **2.21.**

Benzocarbazoledione (**1.32**) and *N*-MOM benzocarbazoledione (**2.75**) displayed similar $E_{1/2}^{I}$ values and were the most difficult compounds to reduce. It was noted that the presence of the methoxymethyl substituent did not have a significant effect on the reduction potential of *N*-MOM benzocarbazoledione as compared to the parent benzocarbazoledione. The reduction potentials for benzocarbazoledione (**1.32**) were similar to the values reported in the literature ($E_{1/2}^{I}$=-1.188Vand $E_{1/2}^{II}$=-1.778V in acetonitrile with respect to ferrocene).[26]

A graph of the first wave reduction potentials $E_{1/2}^{I}$ against the log($1/EC_{50}$) values is shown in **Figure 4.12**. The results show that there is no simple correlation between the first half-wave potential of these carbazolediones and the antiproliferative activity. Although the first reduction process may be essential for the biological activation of these compounds, the ease of reduction does not reflect an increase in biological activity. This is clearly illustrated with *N*-MOM ellipticine quinone (**2.21**) which has less potent antiproliferative activity than ellipticine quinone (**1.33**) although the latter is more difficult to reduce by 0.14V. Furthermore, benzocarbazoledione (**1.32**) and *N*-MOM benzocarbazoledione (**2.75**) differ in EC_{50} values by a factor of four despite similar $E_{1/2}^{I}$ values for these two compounds. These results suggest that other factors have a greater influence on biological activity.

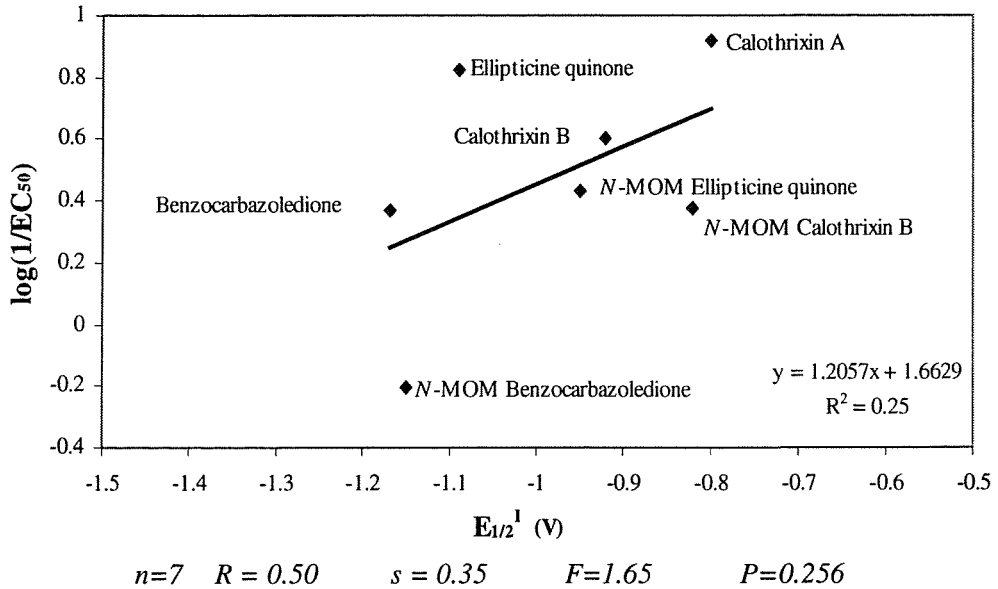

n=7 R = 0.50 s = 0.35 F=1.65 P=0.256

Figure 4.12: *Plot of $E_{1/2}^{I}$ values versus log(1/EC50) of carbazolediones.*

Figure 4.12 includes the statistical parameters *n* (number of data points), *R* (variance), *s* (standard deviation), *F* (Fischer's Test), and *P* (Probability Test). It is beyond the scope of this thesis to discuss the statistical parameters in detail. Therefore, the reliability of the correlation will only be discussed in terms of the covariance, R^2. **Appendix A** includes a brief assessment of these statistical parameters.

4.3.2 Comparison of $E_{1/2}^{II}$ Values of the Calothrixins and Related Carbazolediones

The second wave reduction potential ($E_{1/2}^{II}$) is a measure of the ease of the single-electron reduction of the semiquinone radical anion to the quinol dianion. This second half-wave reduction occurs at more negative potentials ranging from –1.46V to –1.86V. These values are lower than the putative -1.18V threshold required for biological reduction, and therefore this second reduction process will be difficult within the cellular environment.

The semiquinone radical anion of calothrixin A has the least negative $E_{1/2}^{I}$ value at –1.46V, thus it is the easiest semiquinone radical anion to reduce among the test compounds. Calothrixin B (**1.27**) and *N*-MOM calothrixin B (**2.25**) are both reduced from the semiquinone radical anion to the quinol at –1.54V. The two least active compounds have a reduction potential more negative than –1.80V, indicating difficulty in the second reduction.

The graph of $E_{1/2}^{II}$ versus log(1/EC_{50}) is shown in **Figure 4.13**. The correlation between the ease of reduction of the semiquinone radical anion and the biological activity expressed as the log(1/EC_{50}) is weak (R^2=0.52). For example, the *N*-MOM compound have similar $E_{1/2}^{II}$ values to their respective parent compounds despite a two or four-fold difference between the biological activities of the substituted compounds relative to the parent compounds. The poor correlation suggests that other factors may be more important in influencing biological activity.

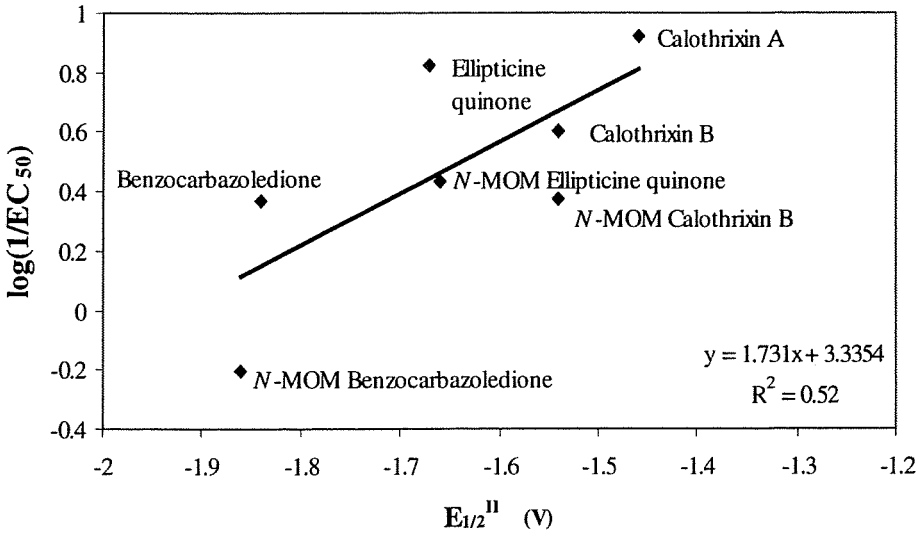

n=7 R = 0.72 s = 0.28 F=5.34 P=0.068

Figure 4.13: *Plot of $E_{1/2}^{II}$ values versus log(1/EC_{50}) of carbazolediones.*

4.3.3 Comparison of lnK Values of the Calothrixins and Related Carbazolediones

The difference between the $E_{1/2}^{I}$ and $E_{1/2}^{II}$ values for each quinone is proportional to the equilibrium constant for the comproportionation reaction between the quinone and quinol dianion which yields the semiquinone radical anion. Due to the large magnitude of the K values, it is more convenient to report the values as the lnK. As mentioned previously, lnK is a measure of the stability of the semiquinone radical anion in the comproportionation reaction, assuming there are no competing reactions involving the semiquinone radical anion. The lnK values are calculated from the reduction potentials using the following reaction equations:

$$Q + e^- \longrightarrow Q^{\cdot -} \qquad E_{1/2}$$

$$Q^{2-} \longrightarrow Q^{\cdot -} + e^- \qquad -E_{1/2}$$

$$Q + Q^{2-} \longrightarrow 2Q^{\cdot -} \qquad \Delta E = E_{1/2}^{I} - E_{1/2}^{II}$$

$$\ln K = \ln\left(\frac{[Q^{\cdot -}]^2}{[Q]\,[Q^{2-}]}\right) \quad ; \quad \ln K = \Delta EF/RT$$

where Q is the quinone, Q^{2-} is the quinol dianion, and $Q^{\cdot -}$ is the semiquinone radical anion, T is temperature, R is the Universal Gas constant, and F is Faraday's constant. These equations show that the stability of the semiquinone radical is determined by the difference in the first and second reduction potentials ($\Delta E = E_{1/2}^{I} - E_{1/2}^{II}$), and not by the ease of the first and second reductions. This can be rationalized by the free energy of the reaction given by the equation $\Delta G = -\Delta EF$. A positive ΔE value therefore reflects a spontaneous comproportionation reaction, and larger ΔE values mean greater semiquinone radical anion stability, as reflected by the lnK values obtained. This is illustrated by the greater stability of the semiquinone radical anion of calothrixin A (**1.26**) relative to the corresponding semiquinone radical anion from calothrixin B (**1.27**).

It has been noted that the greater ease of reduction of calothrixin A is reflected by the higher (more positive) $E_{1/2}^{I}$ and $E_{1/2}^{II}$ values relative to calothrixin B. Furthermore, the ΔE value of calothrixin A is higher than the ΔE value of calothrixin B, which shows that comproportionation reaction for the calothrixin A (**1.26**) and its quinol dianion is more favorable than the corresponding reaction between calothrixin B (**1.27**) and its quinol dianion. Therefore, semiquinone radical anion derived from calothrixin A (**1.26**) is less likely to undergo disproportionation to the quinone and quinol dianion.

The results show that the semiquinone radical anion of ellipticine quinone (**1.33**) is less stable than the corresponding radical anion of benzocarbazoledione (**1.32**) with respect to the comproportionation reaction as reflected by the the lnK difference of 3.5 units. The semiquinone radical anion of *N*-MOM ellipticine quinone (**2.21**) (lnK=28.1) has comparable stability to *N*-MOM benzocarbazoledione (**2.75**) (lnK=28.5) and *N*-MOM calothrixin B (**1.27**) (lnK=28.5). It is interesting to note that the lnK values range from 23 to 29.3, which is indicative of the favorable formation of the radical anions relative to the quinone and quinol dianion species. The results show that most stable

semiquinone radicals (relative to the comproportionation reaction) were formed from the *N*-methoxymethyl carbazolediones (*N*-MOM calothrixin B **(2.25)**, *N*-MOM benzocarbazoledione **(2.75)** and *N*-MOM ellipticine quinone **(2.21)**.

The graph of lnK versus log(1/EC_{50}) is shown in **Figure 4.14**. The correlation obtained is weak with a covariance of R^2=0.50. The graph implies that as the semiquinone radical stability increases, decreasing biological activity should be observed. However, calothrixin A **(1.26)** and *N*-MOM benzocarbazoledione **(2.75)** deviate greatly from the trendline. Upon exclusion of these two data points, a better correlation (log(1/EC_{50}= -0.0781(lnk) + 2.568; R^2=0.84, n=5, R=0.92, s=0.09, F=15.19, P=0.03) is observed. These results suggest that other physicochemical parameters may also be important in influencing the biological activity. Due to the small data set (n=7), more data points are needed in order to confirm this correlation.

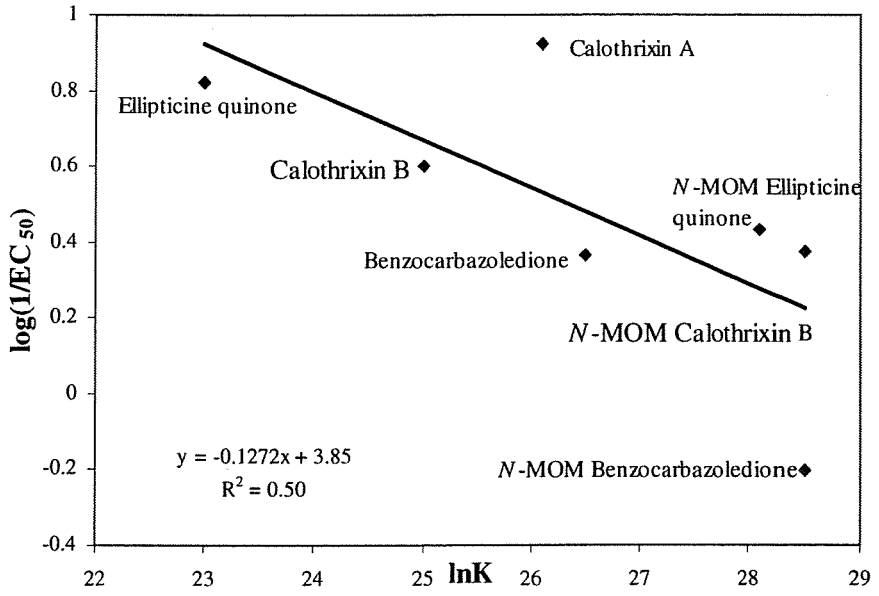

Figure 4.14: *Plot of lnK values versus log(1/EC_{50}).*

4.3.4 Comparison of the Overall Reduction Potential of the Calothrixins and Related Carbazolediones

The two-electron reduction potential of the carbazolediones is a reflection of the overall ability of the quinone to undergo reduction to the quinol dianion. Only calothrixin A **(1.26)** and *N*-MOM calothrixin B **(2.25)** display $E_{Q/Q}^{2-}$ values which meet the threshold

required for the ease of biological reduction. The $E_{Q/Q}^{2-}$ value for calothrixin B (**1.27**) falls 0.05V below the threshold value of -1.18V for biological reduction. The *N*-MOM ellipticine quinone (**2.21**) and ellipticine quinone (**1.33**) had similar reduction potentials with respect to each other, which were below the biological reduction threshold. The benzocarbazolediones **1.32** and **2.75** were the least likely to be reduced as shown by an $E_{Q/Q}^{2-}$ value of –1.51V.

A plot of the log(1/EC_{50}) values and $E_{Q/Q}^{2-}$ values is shown in **Figure 4.15**. The covariance (R^2=0.38) shows that no correlation exists between the overall ease of reduction of the quinone to the dianion and biological activity. This is reflected by the potent activity of ellipticine quinone (**1.33**) and benzocarbazoledione (**1.32**) despite the low (more negative) reduction potentials. This result suggests that the two-electron reduction of the carbazolediones to the corresponding quinol is unlikely to influence biological activity.

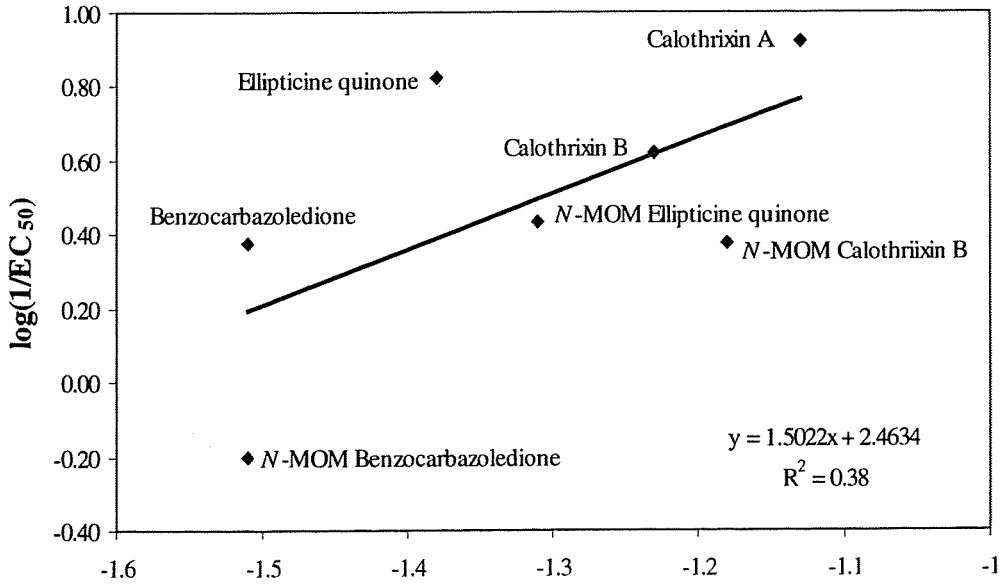

Figure 4.15: *Plot of $E_{Q/Q2-}$ values versus log(1/EC_{50}).*

In summary, this study reports the electrochemical behavior of a number of carbazolediones, including that of the naturally occurring calothrixins A and B. With the exception of the parent benzocarbazoledione (**1.32**), the electrochemical studies are the first to be reported for the carbazolediones. Attempts were made to assess if any

correlation exists between the measured reduction potentials of these quinones and their antiproliferative properties. No correlation was found between the ease of the first one-electron reduction process of the quinones to their respective semiquinone radical anion and their biological activity. The $E_{1/2}^{I}$ values obtained for the compounds were above the reported threshold value of -1.18V for biological reduction, which suggests that facile reduction of these carbazolediones can occur within cells.[2,3] No correlation was found between the $E_{1/2}^{II}$ values corresponding to the reduction of the semiquinone radical anion to the quinol dianion and the antiproliferative properties of these compounds. A weak correlation (R^2=0.50) was found between the relative stability of the semiquinone radical (lnK, calculated for the comproportionation reaction) and biological activity. This suggests that a decrease in the stability of the semiquinone radical anion is reflected by an increase in the biological activity measured. However, it is clear from the poor R^2 values that other parameters can influence biological activity.

4.4 Lipophilicity and Correlation of LogP Values to Biological Activity

The second parameter under investigation is the effect of the lipophilicity of these carbazolediones on their antiproliferative activity against HeLa cervical cancer cells. As discussed earlier, lipophilicity is a key parameter in determining the uptake of a compound into the cell, and can be used to predict if the mode of cellular transport is by passive diffusion or via active uptake.

There are different methods available for measuring logP values. Historically, the logP values were determined using the "shake-flask" method.[27] In this procedure, a compound was placed in a biphasic system of water and 1-octanol and shaken until each layer was saturated with the solute. The concentration of the solute in each layer was then determined using spectrophotometric methods. Poor solubility, the formation of emulsions, and tedious experimental protocols are the general drawbacks to this procedure. The HPLC method is by far the most convenient method for measuring logP values. The main advantage of this method is that only very small quantities of a test compound are required for analysis. Furthermore, analysis by HPLC is rapid and accurate. The experiment is carried out by measuring the retention time of a compound on HPLC using an isocratic solvent program. The retention time of a compound (R_t) is thus proportional to its logP value as it partitions between the mobile solvent phase and

the immobile solid phase of the HPLC column. Thus as logP values increase, solute retention times also increase.

In practice, it is necessary to determine the retention times of standard compounds of known logP values on the HPLC. From the retention time of a compound, the capacity factor k is calculated from the difference between the retention time of the compound and the elution time of an unretained solute (R_0) such that $k=(R_t-R_0)/R_0$. The logarithm of the capacity factor (logk) is linear with respect to the logP value. For our experiment, six standards of known logP values were run with thiourea as the unretained solute, and the linear standard graph of logk against logP was obtained as shown in **Figure 4.16**. The plot of logk versus logP values has a linear coefficient of $R^2=0.98$ thus ensuring the confidence in the logP determinations.

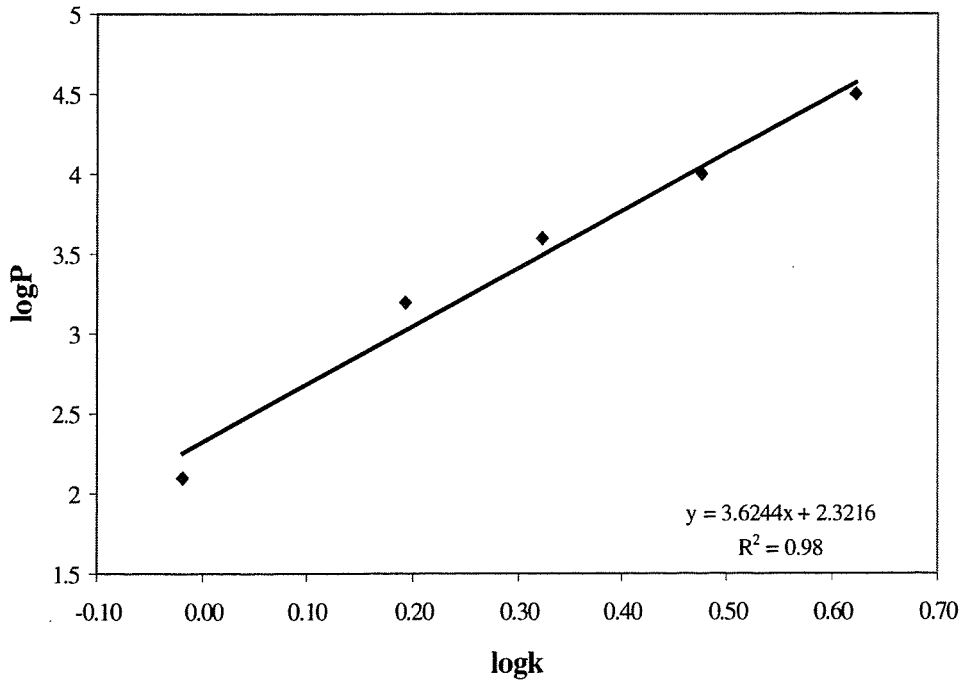

Figure 4.16: *Plot of logk values versus logP for the standards used.*

The test compounds, in the presence of the thiourea internal standard, were then analyzed by HPLC. From the retention times of the calothrixins and carbazolediones, the logk values were calculated. Extrapolation of the logP values from the graph of known standards **(Figure 4.16)** gave the logP values of the test compounds.

Table 4.5 summarizes the logP values for the tetracyclic and pentacyclic carbazolediones. From the qualitative considerations of the structures and the measured logP values, it is difficult to rationalize the observed lipophilicity. The observed logP values for the carbazolediones ranged from 0.12 (low lipophilicity for 5,12-dimethyl calothrixins (**2.63**)) to 5.91 (very high lipophilicity for *N*-benzyl calothrixin B (**2.58**)). The positive logP values indicate that the compounds are more soluble in the lipid phase as compared to the aqueous phase.

Compounds	logP	EC50 (μM)
Calothrixin Analogues		
Benzocarbazoledione (**1.32**)	2.97	0.43
N-MOM ellipticine quinone (**2.21**)	3.45	0.37
Calothrixin B (**1.27**)	3.54	0.25
Ellipticine quinone (**1.33**)	3.95	0.15
N-MOM benzocarbazoledione (**2.75**)	4.05	1.06
iso-Calothrixin B (**3.29**)	4.33	0.47
Indolophenanthrenedione (**2.56**)	4.68	1.19
Calothrixin Derivatives		
5,12-Dimethyl calothrixin (**2.63**)	0.12	4.68
Calothrixin A (**1.26**)	2.56	0.12
N-Ethyl calothrixin B (**2.59**)	4.50	0.45
N-MOM calothrixin B (**2.25**)	4.65	0.42
9-Methoxy-*N*-MOM-calothrixin B (**2.64**)	4.82	-
N-Benzyl calothrixin B (**2.58**)	5.91	0.38

Table 4.5

A wide range of logP values was observed for the calothrixin derivatives. The dimethyl calothrixin **2.63** was the least lipophilic compound (logP=0.12) while the *N*-benzyl calothrixin B (**2.58**) was the most lipophilic (logP=5.91). The N12-substituted calothrixin B derivatives displayed greater lipophilicity than calothrixin B. It is

interesting to note that 9-methoxy *N*-MOM calothrixin B (**2.64**) is less lipophilic than *N*-benzyl calothrixin B (**2.58**), yet the latter is more soluble in both organic and aqueous solvents compared to the former.

To assess if a correlation exists between lipophilicity and antiproliferative properties of these carbazolediones, the Hansch analysis correlating logP values and $\log(1/EC_{50})$ values was employed. Hansch analysis has been successfully employed in many QSAR studies for correlating free energy parameters such as lipophilicity with biological activity. The plot of logP versus $\log(1/EC_{50})$ values of the carbazolediones is shown in **Figure 4.17**.

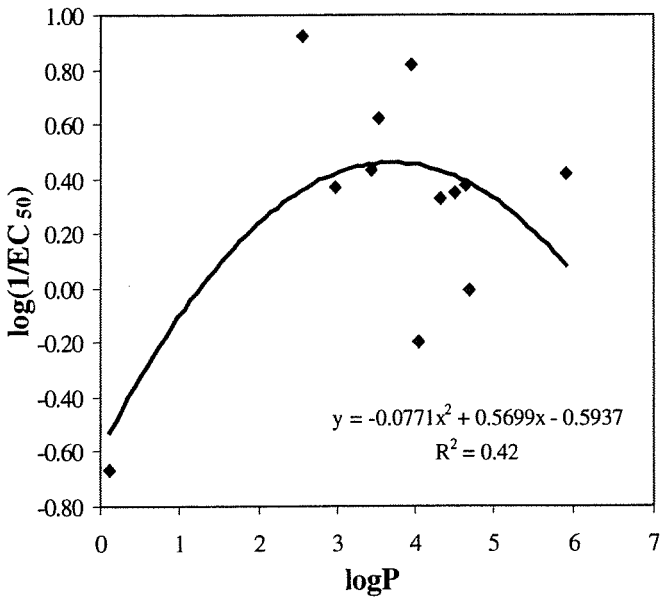

n= 12 *R = 0.65* *s = 0.37* *F=3.31* *P=0.08*

Figure 4.17: *Plot of logP values versus $\log(1/EC_{50})$ of the carbazolediones.*

The most active carbazolediones have logP values in the range of 2.56 to 5.91. The plot shows a weak parabolic relationship between logP and $\log(1/EC_{50})$ with a coefficient of R^2=0.42. This lack of correlation may be due to the structural diversity of the test compounds and thus may not accurately represent a QSAR study. In the following sections, the data was reanalysed to include groupings of test compounds with "similar" structural features.

4.4.1 Correlation of Lipophilicity and Biological Activity for Unsubstituted Carbazolediones

We first examined if a correlation between logP and log(1/EC_{50}) exists for the indolic *N*-unsubstituted carbazolediones calothrixin A (**1.26**), calothrixin B (**1.27**), benzocarbazoledione (**1.32**), ellipticine quinone (**1.33**), indolophenanthrenedione (**2.56**), and *iso*-calothrixin B (**3.29**). The plot is shown in **Figure 4.18**. Unfortunately, the correlation is still weak (R^2=0.53) , and thus it is difficult to interpret the results with confidence.

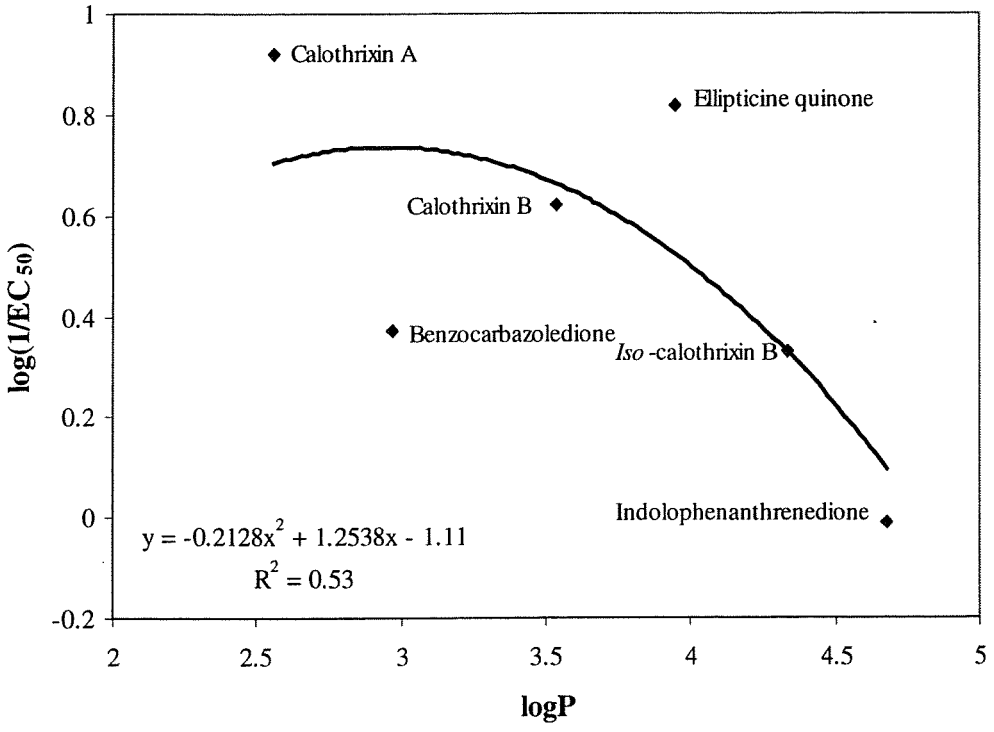

n=6 R = 0.66 s = 0.31 F=1.68 P=0.32

Figure 4.18: *Plot of logP values versus log(1/EC_{50}) of unsubstituted carbazolediones.*

4.4.2 Correlation of Lipophilicity and Biological Activity for *N*-Substituted Carbazolediones

Figure 4.19 shows the plot of logP and log(1/EC_{50}) values for indolic *N*-substituted carbazolediones *N*-MOM ellipticine quinone (**2.21**), *N*-MOM calothrixin B (**2.25**), *N*-benzyl calothrixin B (**2.58**), *N*-ethyl calothrixin B (**2.59**), and *N*-MOM benzocarbazoledione (**2.75**), and it is clear that no correlation is observed. Most of the

data in the graph, however, is for the N12-substituted calothrixin derivatives. There are insufficient data points for a comparison of only the *N*-MOM carbazolediones.

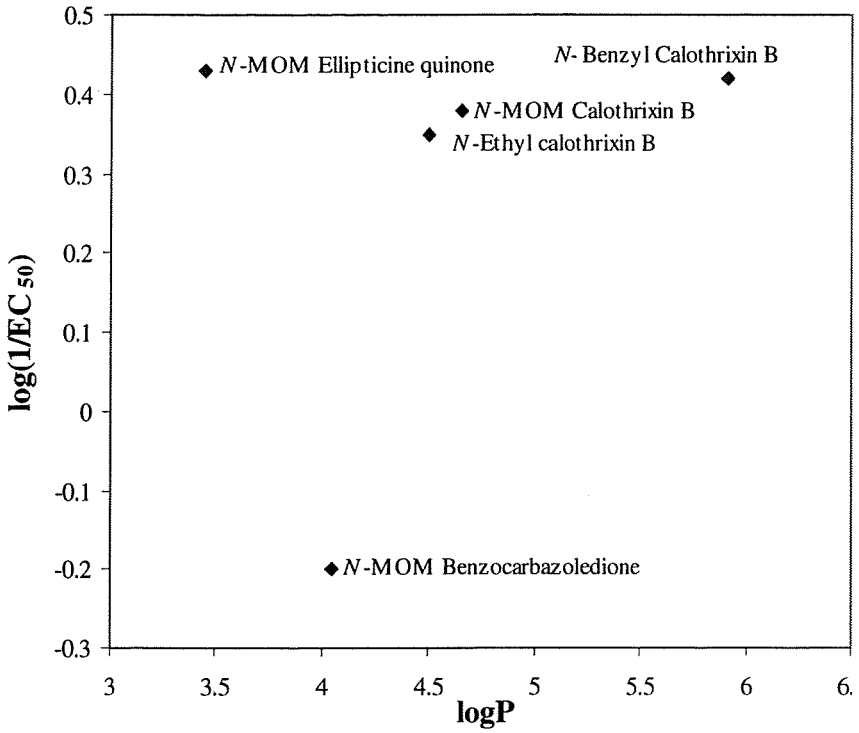

Figure 4.19: *Plot of logP values versus log(1/EC$_{50}$) for indolic* N-*substituted carbazolediones.*

4.4.3 Correlation of Lipophilicity and Biological Activity for the Calothrixins

To minimize structural variation in the QSAR analysis, a plot of logP and log(1/EC$_{50}$) for *N*-substituted calothrixin derivatives was obtained. Unlike the QSAR analysis outlined above, a good correlation (R^2=0.78) was obtained for the calothrixins derivatives **[Figure 4.20]**. The plot shows that as the logP value increases, the biological activity of the test compounds expressed as log(1/EC$_{50}$) also increases until a maximum value is attained, after which increasing logP values will cause a decrease in biological activity. This parabolic curve is typical for the transport of a drug into a cell. The derivative (with respect to logP) of the equation corresponding to the parabolic curve is $\mathbf{D_{logP}}$[log(1/EC$_{50}$)=-0.1928(logP) + 0.7154]. This predicts that the optimal logP value for maximum biological response (EC$_{50}$=0.21μM) will be 3.71. Interestingly, the predicted EC$_{50}$ value of calothrixin A as calculated from the observed logP value is clearly different to the observed EC$_{50}$ value. This suggests that the presence of the *N*-oxide

moiety contributes to the observed biological activity of calothrixin A in a manner that is not solely related to its effect on the lipophilicity of the molecule. Removal of the data point for calothrixin A in the analysis of logP versus $\log(1/EC_{50})$ values results in a better correlation, $\log(1/EC_{50}) = -0.0629(\log P)^2 + 0.5508(\log P) - 0.7186$ with $R^2=0.94$ [n=5, R=0.96, s=0.18, F=14.41, P=0.06]. Due to the limited number of data points, more derivatives need to be assessed in order to confirm this correlation.

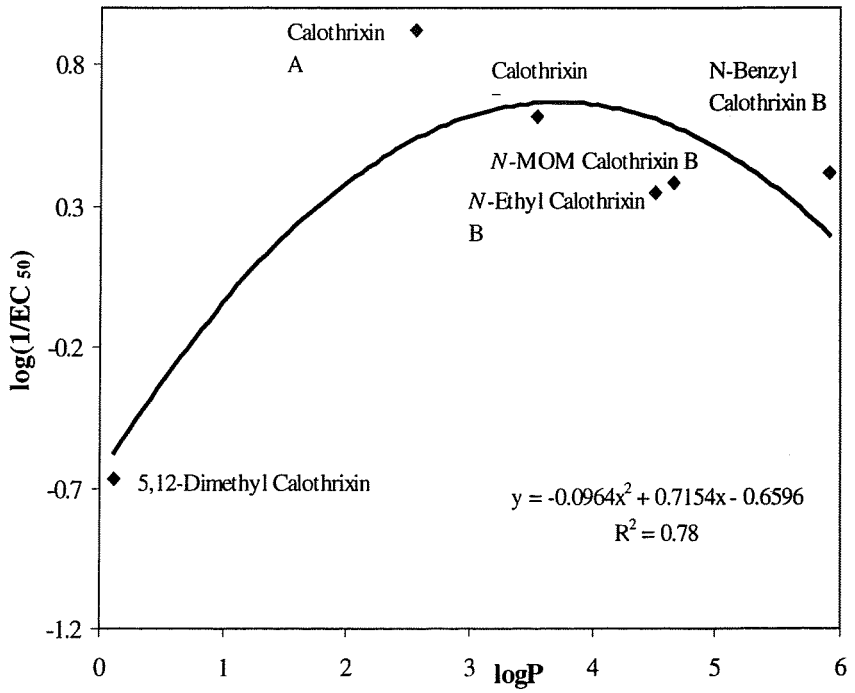

n=6 R = 0.89 s = 0.32 F=5.47 P=0.100

Figure 4.20: *Plot of logP values versus $\log(1/EC_{50})$ for the calothrixin derivatives.*

4.5 Conclusion

The SAR study shows that the presence of the *E*-ring attenuates the antiproliferative activity of the carbazolediones, and therefore is not required for biological activity. The presence of substituents on the indole nitrogen are not essential to the biological activity of these compounds, although the alkyl substituents studied lowered the biological activity observed.

The nitrogen atom in the *D*-ring is also unnecessary for biological activity of carbazolediones although it enhances biological activity, possibly through hydrogen bonding with H-bonding residues in a receptor site of RNA polymerase. This hydrogen-bonding hypothesis is supported by the fact that ellipticine quinone (**1.33**) is more active than benzocarbazoledione (**1.32**), and calothrixin B (**1.27**) is more active than the indolophenanthrenedione (**2.56**). It may also account for the large difference in activity between calothrixin A (**1.26**), which may form hydrogen bonds through the *N*-oxide, and 5,12-dimethyl calothrixin (**2.63**) which cannot form hydrogen bonds through the quinoline nitrogen.

A SAR study within the Chai/Waring group showed that carbazoledione (**4.7**) does not display antiproliferative activity in the MTT assay. Furthermore, the isoquinolinedione (**4.8**) is only weakly active. Murrayaquinone A (**1.40**) and its regioisomer (**4.9**) also display weak activity in the MTT assay.[28]

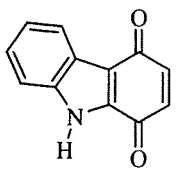

4.7

EC_{50}>50μM

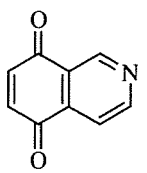

4.8

EC_{50}=12μM

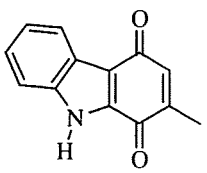

4.9

EC_{50}=7.4μM

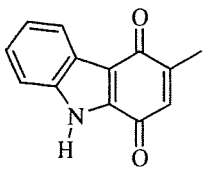

1.40

EC_{50}=13μM

The MTT assay showed that there is an 8-fold difference in the biological activity of ellipticine quinone (**1.33**) relative to ellipticine (**1.70**). A time-dependent MTT assay showed that ellipticine quinone induces its antiproliferative effects in a shorter length of time than ellipticine, which suggests that the mode of action is different for these two compounds.[29] These results suggest that the quinone moiety is essential for biological activity, although the specific mode of action of the carbazolediones has yet to be elucidated. In summary, these SAR studies show that the pharmacophore required for biological activity (below 1μM) is essentially the tetracyclic compound, benzocarbazoledione (**1.32**).

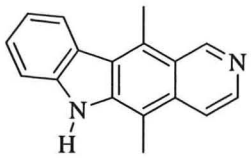

1.70
EC_{50}=1.21μM

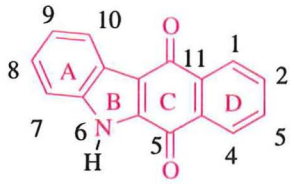

1.32
pharmacophore of the carbazolediones

More experiments are required to determine how the various substitution patterns on the pharmacophore will affect the antiproliferative activity of the carbazolediones. The influence of the *A*-ring on biological activity also requires investigation.

In the QSAR studies, no significant correlation could be established between the different redox potentials ($E_{1/2}^{I}$, $E_{1/2}^{II}$, $E_{Q/Q^{2-}}$) and the antiproliferative activity of the carbazolediones. However, it was noted that the $E_{1/2}^{I}$ values were above the reported threshold required for reduction to occur within cells. Interestingly, the reduction potentials observed are comparable to the values reported for menadione **(1.14)**,[30] which has been shown to undergo one-electron and two-electron reductions within the cellular environment.[21] This suggests that the carbazolediones may be redox-active within the cell.

No direct correlation was found between the lipophilicity and biological activity for all the carbazolediones tested. However, when the data set was limited to the calothrixins, a significant correlation was found between the lipophilicity and biological activity of these compounds. The parabolic correlation between logP and log(1/EC_{50}) suggests that the calothrixins must enter the cytoplasm in order to produce a biological effect. Furthermore, the results predict an optimum logP value for biological activity. In order to confirm this correlation, more calothrixin derivatives are required for testing.

In summarizing the QSAR studies, it is essential to point out that most of the covariance (R^2) values are less than 0.70. This suggests that the correlation is either very poor or no correlation exists. This lack of correlation may be due to the structural diversity of the test compounds. In future work, three separate QSAR studies may be required for the benzocarbazolediones, ellipticines, and calothrixins.

4.6 Bibiliography

(1) Patrick, G. L. *An Introduction to Medicinal Chemistry*; 2nd ed.; Oxford University Press: Oxford, 2001.

(2) De Abreu, F. C.; Ferraz, P. A. d. L.; Goulart, M. O. F. *J. Braz. Chem. Soc.* **2002**, *13*, 19-35.

(3) Kovacic, P.; Osuna Jr., J. A. *Curr. Pharm. Design* **2000**, *6*, 277-309.

(4) Kunz, K. R.; Iyengar, B. S.; Dorr, R. T.; Alberts, D. S.; Remers, W. A. *J. Med. Chem.* **1991**, *34*, 2281-2286.

(5) Abbas, T.; Olivier, M.; Lopez, J.; Houser, S.; Xiao, G.; Kumar, G. S.; Tomasz, M.; Bargonetti, J. *J. Biol. Chem.* **2002**, *277*, 40513-40519.

(6) Paz, M. M.; Das, A.; Palom, Y.; He, Q.-Y.; Tomasz, M. *J. Med. Chem.* **2001**, *44*, 2834-2842.

(7) Penketh, P. G.; Hodnick, W. F.; Belcourt, M. F.; Shyam, K.; Sherman, D. H.; Sartorelli, A. C. *J. Biol. Chem.* **2001**, *276*, 34445-34452.

(8) Malta, V. R. S.; Pinto, A. V.; Molfetta, F. A.; Honorio, K. M.; deSimone, C. A.; Pereira, M. A.; Santos, R. H. A.; daSilva, A. B. F. *J. Mol. Struct. (Theochem)* **2003**, *634*, 271-280.

(9) Cohen, S.; Brif, Z.; Haberman, F.; Liron, Z. In *Computer-Assisted Modeling of Receptor-Ligand Interactions: Theoretical Aspects and Applications to Drug Design*; Rein, R., Golomber, A., Eds.; Alan R. Liss, Inc.: New York, 1989; Vol. 289, p 189-201.

(10) Nikaido, H.; Vaara, M. *Microb. Rev.* **1985**, *49*, 1-32.

(11) Kaback, H. R.; Hong, J.-S. In *CRC Crit. Rev. Microbiol.*; CRC Press Inc.: Boca Raton, 1973, p 333-376.

(12) Hohmann, S.; Nielsen, S.; Agre, P. *Aquaporins*; Academic Press, Inc.: San Diego, 2001; Vol. 51.

(13) Hansch, C. *J. Am. Chem. Soc.* **1969**, *2*, 232-239.

(14) Mosmann, T. *J. Immunol. Methods* **1983**, *65*, 55-63.

(15) Green, L. M.; Reade, J. L.; Ware, C. F. *J. Immunol. Methods* **1984**, *70*, 257-268.

(16) van de Loosdrecht, A. A.; Beelen, R. H. J.; Ossenkoppele, G. J.; Broekhoven, M. G.; Langenhuijsen, M. M. A. C. *J. Immunol. Methods* **1994**, *174*, 311-320.

(17) Ferrari, M.; Fornasiero, M. C.; Isetta, A. M. *J. Immunol. Methods* **1990**, *131*, 165-172.

(18) Bernas, T.; Dobrucki, J. *Cytometry* **2002**, *47*, 236-242.

(19) Doan, N. T.; Stewart, P. R.; Smith, G. D. *FEMS Microbiol. Lett.* **2001**, *196*, 135-139.

(20) Lind, C.; Cadenas, E.; Hochstein, P.; Ernster, L. In *Methods in Enzymology*; Packer, L., Glazer, A. N., Eds.; Academic Press Inc.: San Diego, 1990; Vol. 186, p 92-105.

(21) Gutierrez, P. L. *Free Radical Biol. Med.* **2000**, *29*, 263-275.

(22) Weiner, L. M. In *Methods in Enzymology*; Packer, L., Ed.; Academic Press Inc.: San Diego, 1994; Vol. 233, p 92-105.

(23) Bolton, J. L.; Trush, M. A.; Penning, T. M.; Dryhurst, G.; Monks, T. J. *Chem. Res. Toxicology* **2000**, *13*, 135-160.

(24) Inbaraj, J. J.; Gandhidasan, R.; Murugesan, R. *Free Radical Biol. Med.* **1999**, *26*, 1072-1078.

(25) Brunmark, A.; Cadenas, E. *Free Radical Biol. Med.* **1989**, *7*, 435-477.

(26) Macías-Ruvalcaba, N.; Cuevas, G.; González, I.; Aguilar-Martínez, M. *J. Org. Chem* **2002**, *67*, 3673-3681.

(27) Tute, M. S. In *Comprehensive Medicinal Chemistry*; Sammes, P. G., Taylor, J. B., Eds.; Pergamon Press: Oxford, 1990; Vol. 4, p 1-31.

(28) Le Guen, M. Honours Thesis, The Australian National University, 2003.

(29) Wilkes, B. A. Honours Thesis, The Australian National University, 2002.

(30) Bernardo, P. H.; Chai, C. L. L.; Heath, G. A.; Mahon, P. J.; Smith, G. D.; Waring, P. W.; Wilkes, B. A. *J. Med. Chem.* **2004**, *47*, 4958-4963.

Chapter 5

5.1 Introduction

It is clear from the studies outlined in Chapter 4 that the biological activity of the calothrixins and related carbazolediones are dependent on the lipophilicity of the compounds. It was noted that the $E_{1/2}^{1}$ values corresponding to the reduction of the quinones to the semiquinone radical anion were greater (more positive) than the threshold value of -0.5 V (versus the SHE), which suggests that intracellular reduction of the quinones would be facile. Furthermore, calothrixin A has been shown to undergo redox cycling in both *in vitro* studies and cell-free systems,[1] and therefore it is likely that the other carbazolediones are redox-active in the biological environment. In the past years, the Chai/Waring group has been interested in the study of a bioactive class of compounds known as the epidithiopiperazine-2,5-diones (ETP compounds).[2] Although the calothrixins and the ETP compounds have vastly different chemical motifs, the activities of both types of compounds are likely to be related to the propensity to undergo oxidation and reduction reactions. It is for this reason that SAR studies of the ETP compounds were undertaken. It is hoped that possible conclusions on the mechanism of biological action of ETP compounds may provide some insights on the mechanism of action of the calothrixins.

The general structure of the ETP compounds contains an internal disulfide linkage at the α,α'-positions of the piperazinedione ring system **(5.1)** which is the essential pharmacophore for biological activity.[3-5] These compounds are of considerable interest due to the potent biological activities displayed by several naturally occurring ETP compounds. For example, the fungal metabolite sporidesmin **(5.2)** from *Pithomyces chartarum* displays potent antiviral properties by inhibiting the function of RNA polymerase.[6,7] Sporidesmin is the causative agent of facial eczema, a disease which affects sheep and cattle in parts of Australia and New Zealand.[4] The mycotoxin chetomin **(5.3)** from various *Chaetomium* species displays antibacterial, antiviral and immunosuppressive properties.[2,3] Arguably, the most widely studied ETP compound is the fungal metabolite gliotoxin **(5.4)**. Gliotoxin has been isolated from a variety of fungi including *Aspergillus fumigatus, Penicillium* and *Gliocladium* species.[3-5,8] Gliotoxin exhibits potent biological activities such as antibacterial, antiviral, antitumor, and immunosuppressive properties.[5-7,9-14] The systemic toxicity of the ETP compounds on the whole, however, precludes any clinical application.[3]

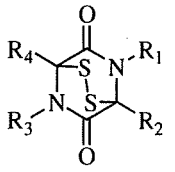

5.1

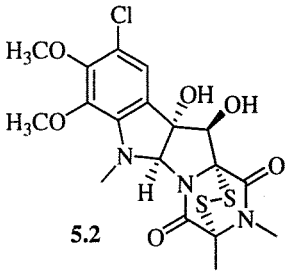

5.2

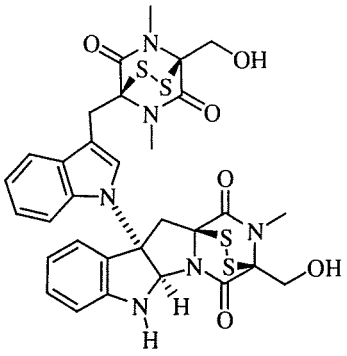

5.3

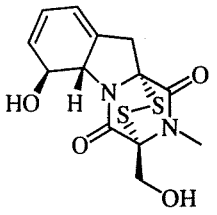

5.4

Studies have shown that the disulfide linkage is essential to the biological activity of most ETP compounds. For example, dimercaptogliotoxin **5.5**, its methyl thioether **5.6**, and its monosulfide **5.7** do not display cytotoxic activity.[15] It has been proposed that the biological activity of the ETP compounds arises from the ability of the disulfide linkage to undergo reduction to the dithiol form *in vivo*. Two mechanisms have been proposed to account for the biological activity of ETP compounds: the redox cycling mechanism, and the thiol-disulfide exchange mechanism.

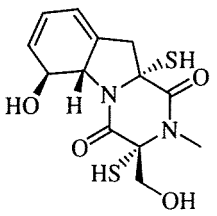

5.5

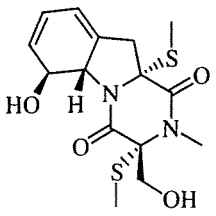

5.6

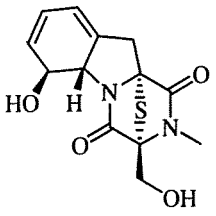

5.7

In the redox cycling mechanism outlined in **Scheme 5.1**, the ETP compound **(5.1)** is reduced by cellular reductants to the dimercaptopiperazinedione **(5.8)**. The dimercaptopiperazinedione **5.8** can then undergo auto oxidation in the presence of oxygen to yield the superoxide radical anion and the ETP compound. The superoxide radical anion can, in turn, give rise to other reactive oxygen species (ROS) which can

then lead to lipid peroxidation, DNA strand breaks, and oxidation of protein thiol residues.[16]

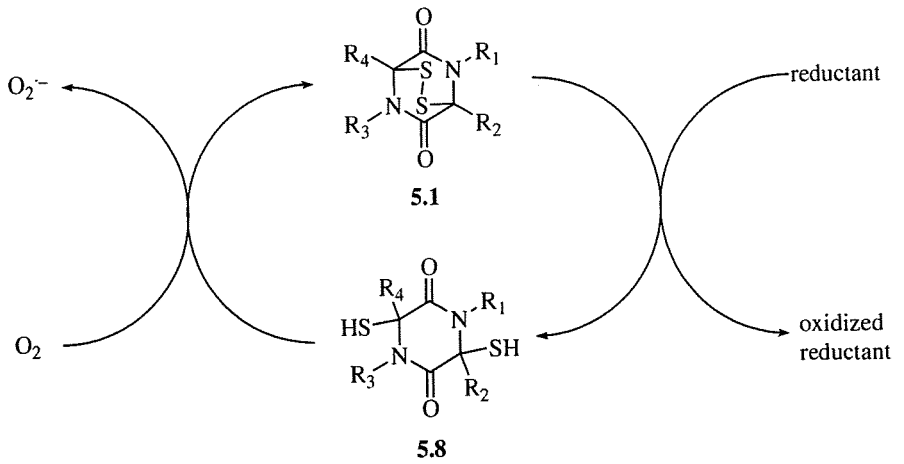

Scheme 5.1

The main evidence in support of the redox cycling mechanism is the detection of these ROS associated with the auto oxidation process of the dimercaptopiperazinediones.[16] For example, *in vitro* studies have shown that the reduced form of sporidesmin (**5.9**) auto oxidizes to the ETP compound in the presence of a suitable metal catalyst, producing superoxide radical anions and hydrogen peroxide. *In vitro* studies involving erythrocytes and sporidesmin also led to the detection of ROS. The addition of strong thiol chelators such as zinc and nickel inhibited ROS generation, possibly through the formation of stable mercaptides with the dimercaptopiperazinediones.[17,18]

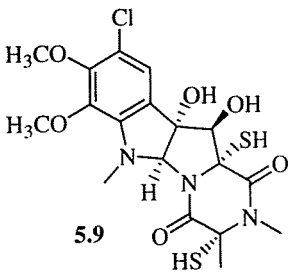

The second mechanism which may account for the biological activities of ETP compounds is the thiol-disulfide exchange mechanism. The first step in this mechanism involves an S_N2 reaction between the ETP compound and a thiol (RSH) to form a mixed disulfide intermediate **5.10**. The mixed disulfide can react further with a thiol to give the

dimercaptopiperazinedione **5.8**, and the disulfide RSSR. The reactions are reversible and therefore an equilibrium is established.[19]

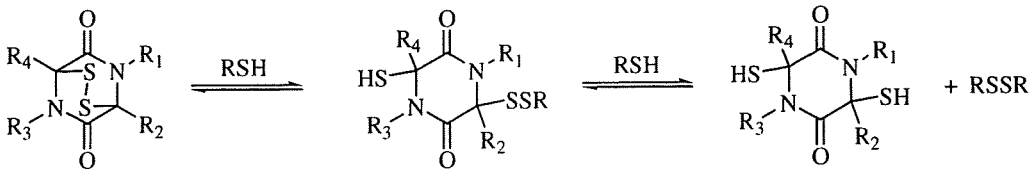

5.1 **5.10** **5.8**

Scheme 5.2

The QSAR studies of selected ETP compounds were carried out in order to attain additional insights into the mode of action of the ETP compounds and thus aid in the elucidation of the mechanism of action. In order to carry out these studies, the biological activity, redox potential, and lipophilicity of these compounds were measured.

5.2 Measurement of the Lipophilicities of the ETP Compounds

Several *N,N'*-disubstituted ETP compounds (**5.11-5.14**) were synthesized following literature procedures.[7,20,21] The compound 3,6-epidithio-L-prolyl-L-proline anhydride (diprolyl ETP, **5.15**) was synthesized following the procedure developed by Ohler *et al.*[22]

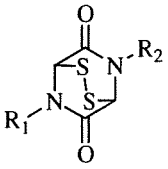

(5.11) R_1=R_2=CH_3
(5.12 R_1=R_2=CH_2CH_3
(5.13) R_1=R_2=$CH_2C_6H_5$
(5.14) R_1=CH_3, R_2=$CH_2C_6H_5$

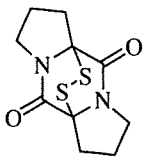

5.15

The logP values for the ETP compounds were obtained using the HPLC methodology outlined in Chapter 4. The results are shown in **Table 5.1**. The EC_{50} values listed below were obtained from a short-term (8hr) killing assay using murine thymocytes during the author's graduate diploma studies,[21] and these values reflect the cytotoxicity of the ETP compounds.

Compound	LogP	EC_{50} (μM)
N,N'-dimethyl ETP (**5.11**)	0.43	0.85
diprolyl ETP (**5.15**)	0.95	20.63
N,N'-diethyl ETP (**5.12**)	1.09	2.52
gliotoxin (**5.4**)	1.30	0.61
N-benzyl-*N'*-methyl ETP (**5.14**)	1.78	7.95
N,N'-dibenzyl ETP (**5.13**)	2.99	2.25

The EC_{50} values listed were obtained from the author's graduate diploma studies.[21]

Table 5.1

The results show that the *N,N'*-dimethyl ETP (**5.11**) is the least lipophilic and the second most potent cytotoxic compound in the series of compounds studied. The *N,N'*-dibenzyl ETP (**5.13**) is the most lipophilic compound which still shows some activity. In contrast, the diprolyl ETP compound displays poor cytotoxicity and has low lipophilicity. Gliotoxin (**5.4**), the only naturally occurring ETP compound tested in this series, has the most potent cytotoxicity and displays lipophilicity between that of the *N,N'*-diethyl ETP (**5.12**) and *N*-benzyl-*N'*-methyl ETP (**5.14**).

The graph of logP versus $\log(1/EC_{50})$ was obtained for these ETP compounds [**Figure 5.1**]. The results show that there is no correlation between the lipophilicity of the ETP compounds and their cytotoxic activity. It is therefore likely that other parameters may influence the biological activity of the ETP compounds.

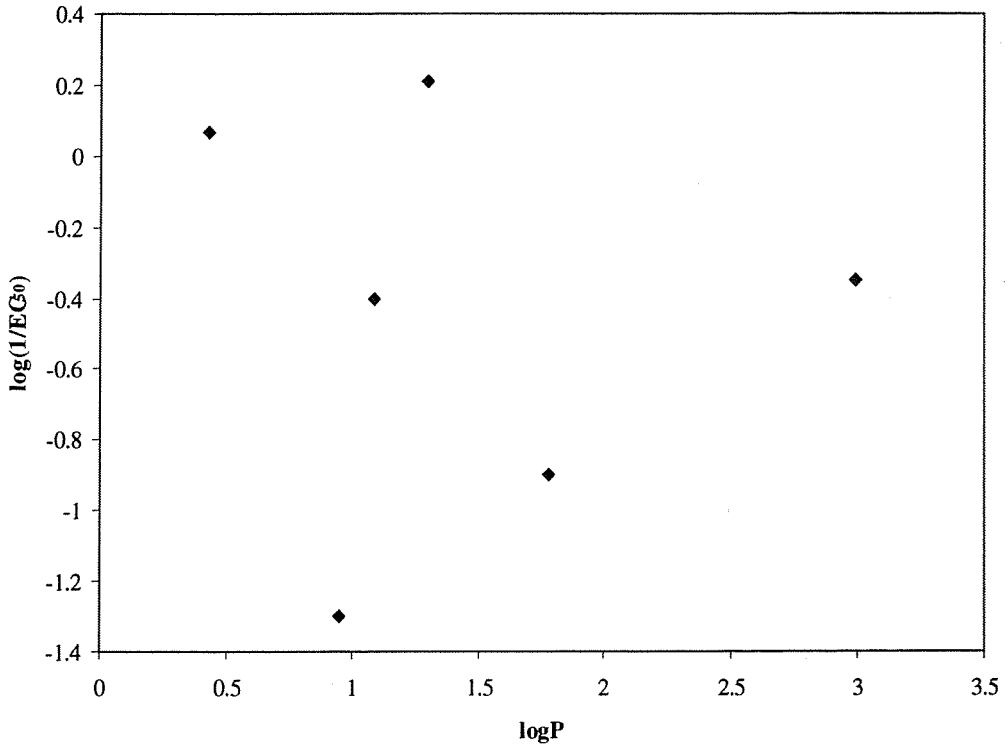

Figure 5.1: *Plot of logP values versus log(1/EC$_{50}$) for the ETP compounds*

5.3 Measurement of ETP Reduction Potentials via Thiol-Disulfide Exchange Reactions

The reduction potential of disulfides is often difficult to measure under standard electrochemical conditions such as cyclic voltammetry as sulfur-containing compounds interact with the metal electrodes and form metal-sulfur complexes.[23] The use of enzyme-coupled redox reactions to measure the reduction potential of disulfides is limited by problems relating to enzyme-substrate binding and enzyme stability.[24]

Another method for measuring the redox potential of a disulfide is through the thiol-disulfide exchange reaction as shown in **Scheme 5.3**.[19] In this method, the disulfide is reacted with a thiol (RSH) of known concentration and redox potential ($E_{RSSR/RSH}$). The reaction is monitored over time until no further change is noted in the concentrations of the thiols and disulfides, thus indicating that equilibrium has been established. The equilibrium constant (K_{eq}) is then calculated by using the measured concentrations of the thiols (RSH and **5.8**) and disulfides (RSSR and **5.1**).

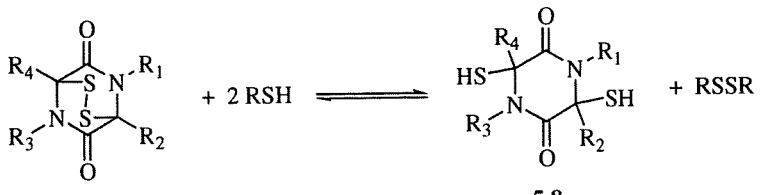

5.1 **5.8**

dimercaptopiperazinedione or "dithiol"

Scheme 5.3

The Nernst Equation is then used to calculate the reduction potential of the disulfide. For an ETP compound the equation corresponding to the thiol-disulfide exchange reaction with a thiol is shown below:

$$K_{eq} = \frac{[ETP^{red}][RSSR]}{[ETP^{ox}][RSH]^2} \text{ and } E_{ETP} = E_{RSSR/RSH} + \frac{RT}{2F}\ln(K_{eq})$$

where $[ETP^{red}]$ and $[ETP^{ox}]$ are the molar concentrations of the dimercaptopiperazinedione and ETP compound respectively, E_{ETP} is the reduction potential of the ETP compound, R is the Gas Constant and F is Faraday's Constant.

In the author's graduate diploma studies,[21] the equilibrium constant for the thiol-disulfide exchange reaction between gliotoxin **(5.4)** and glutathione **(1.15)** was measured. Standard curves were prepared for both gliotoxin and its reduced form in order to facilitate the measurement of the equilibrium mixture using HPLC. The thiol-disulfide exchange reaction was then carried out in aqueous buffer (pH= 7.00, 25°C) in order to mimic biological conditions. To prevent the auto oxidation of thiols, the reactants were prepared in degassed solvents and the reaction mixture was kept under an atmosphere of argon. To minimize errors due to auto oxidation, EDTA was added to sequester metal ions such as Fe^{2+} which can catalyze the auto-oxidation of thiols. A large concentration of the redox buffer, glutathione and oxidized glutathione (GSH/GSSG), was employed to minimize errors due to auto oxidation as well as to minimize the time required for equilibration. The reaction mixture was analyzed at intervals of time by high performance liquid chromatography (HPLC) to determine the concentration of gliotoxin **(5.4)** and dimercaptogliotoxin **(5.5)**.[21,25]

GSH= 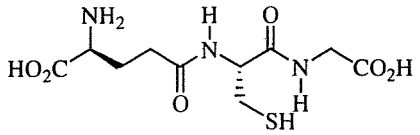

1.15

In this study, a similar methodology was applied to measure the reduction potentials of some selected ETP compounds. The initial efforts were directed towards the determination of the retention times of both the oxidized (disulfide) and reduced (dimercapto) forms of the selected ETP compounds to ensure that the concentration of each species can be measured in the equilibrium studies. Of the ETP compounds selected, the *N,N'*-diethyl ETP (**5.12**) and its reduced form were inseparable on HPLC. The *N,N'*-dibenzyl derivative (**5.13**) was poorly soluble and thus gave rise to unreliable standard curves. The remaining compounds (and their dimercapto forms) comprised of *N,N'*-dimethyl **5.11**, *N*-benzyl-*N'*-methyl **5.14**, and diprolyl ETP **5.15** were subjected to equilibrium measurements. In these experiments, the GSH/GSSG redox buffer ($E_{GSSG/GSH}$=-252mV)[24] was employed. Aliquots of the reaction mixture were analyzed on HPLC at time intervals until no further change was noted in the peak areas of each component, thus establishing equilibrium.

The studies with *N,N'*-dimethyl ETP (**5.11**) and GSH (**1.15**) gave complex HPLC traces which prevented the measurement of the equilibrium constant and hence the redox potential of *N,N'*-dimethyl ETP. The HPLC traces showed that in addition to the presence of GSH, GSSG, *N,N'*-dimethyl ETP, and traces of the dimercapto form, two other peaks were also observed. The first peak is likely to result from the establishment of a pseudo-equilibrium between GSH and *N,N'*-dimethyl ETP (**5.11**) such that one of the peaks could be due to the mono mixed disulfide (MMD) **5.16**. The formation of mono mixed disulfide intermediates have been reported in the literature for thiol-disulfide exchange reactions under analogous reaction conditions, most notably between protein disulfide residues and GSH.[2,25-28] The second peak may be that of the double mixed disulfide (DMD) **5.17**, which can be formed by the reaction of the mono mixed disulfide intermediate with GSSG **[Scheme 5.4]**. Other thiols were employed in order to minimize mono and double mixed disulfide formation. Unfortunately, it was difficult to find a suitable thiol which would minimize the formation of MMDs and DMDs. The cysteine/cystine redox buffer (CySH/CySSCy, $E_{CySSCy/CySH}$=-327mV)[24] was employed, but this gave complex HPLC traces, while the use of dithiothreitol (DTT) led to

quantitative reduction of the ETP compound. An attempt was made to react the dithiol of *N,N'*-dimethyl ETP with gliotoxin, but only complex mixtures were obtained.

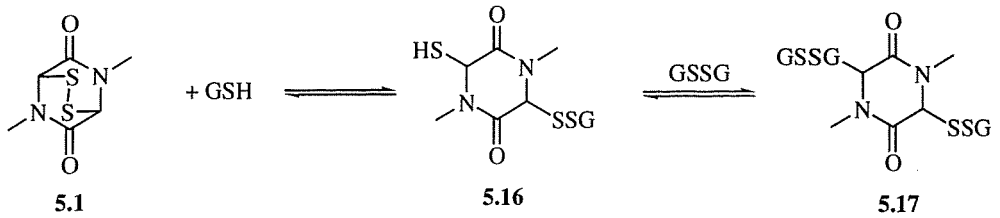

5.1 **5.16** **5.17**

Scheme 5.4

However, the equilibrium measurements for the reaction of *N*-benzyl-*N'*-methyl ETP (**5.14**) and diprolyl ETP (**5.15**) respectively with GSH were successfully carried out. The equilibrium constants for the reactions and the calculated reduction potentials are shown in **Table 5.2**.

Compound	K_{eq} (M^{-1})	E_{ETP} (mV)	EC_{50} (μM)
Gliotoxin (**5.4**)	1200±200	-162±2	0.61
N-benzyl-*N*-methyl ETP (**5.14**)	11±4	-222±4	7.95
Diprolyl ETP (**5.15**)	6.8±0.5	-228±1	20.63

Reduction potentials relative to the Standard Hydrogen Electrode. Results for gliotoxin obtained in the author's graduate diploma studies.

Table 5.2

The results show that the most active compound, gliotoxin (**5.4**), has the highest reduction potential. The *N*-benzyl-*N*-methyl ETP (**5.14**) was more difficult to reduce, and the diprolyl ETP (**5.15**) was the least likely to undergo reduction. All three compounds have reduction potentials above the putative -0.50 V (versus SHE) threshold for biological reduction.[29,30] The reduction potentials for the ETP compounds show that the common cellular reductant GSH can easily reduce these compounds. Following the measurement of the reduction potentials as summarized above, Bernardo *et al.*[31] have subsequently shown that the intracellular concentrations of gliotoxin (**5.4**) and diprolyl ETP (**5.15**) are proportional to the reduction potential of these toxins. Furthermore, the biological accumulation of these ETP compounds appears to be mediated by the

presence of cellular glutathione. This led to the hypothesis of a redox-driven accumulation of the ETP compounds in cells.[31]

In the theory of redox-driven accumulation of the ETP compounds, it is assumed that the ETP compound (**5.1**) enters the cell in order to establish an equilibrium between the extracellular concentration and intracellular concentrations of the compound. However, the intracellular ETP compound is reduced to the cell-impermeable dimercapto form (**5.8**). This results in an influx of the ETP compound into the cell in an attempt to establish the equilibrium between intracellular and extracellular concentrations of the disulfide. The process continues until the equilibrium is established.[31] A simplified diagram for this mechanism of accumulation is shown in **Scheme 5.5**.

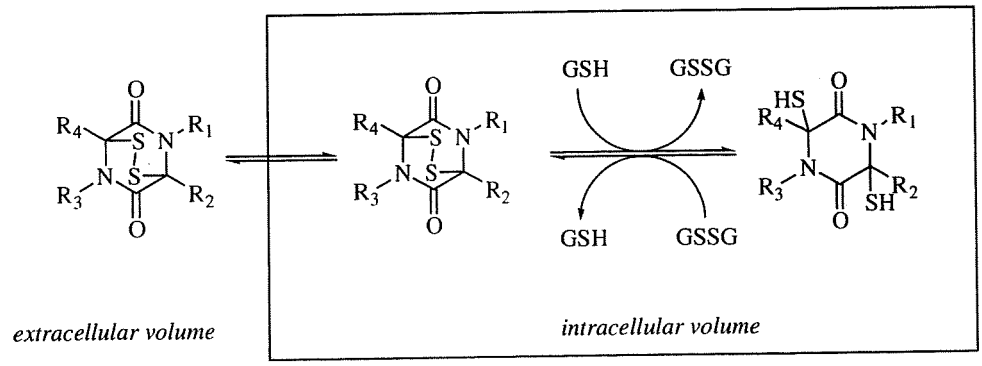

Scheme 5.5

From this model, it is possible to calculate the total intracellular concentration [ETP_I] of the ETP compound and its reduced form using the equation:

$$[ETP_I] = \frac{[ETP_{Applied}](1+P)}{(1+V_C+PV_C)} \quad ;P = K_{eq}\frac{[GSH]^2}{[GSSG]}$$

where [$ETP_{Applied}$] is the applied concentration of the ETP compound, V_C is the total volume of the cells, and K_{eq} is the equilibrium constant for the thiol-disulfide exchange reaction between the ETP compound and glutathione.[31]

We were therefore interested in studying the biological accumulation of the redox-active calothrixins in order to determine if the redox potential is proportional to the intracellular concentration of these quinones. The $E_{1/2}^1$ value (-0.80V referenced to

ferrocene) for calothrixin A (**1.26**) suggest that the compound was concentrated in the cell as the semiquinone radical anion. An initial investigation was therefore carried out using calothrixin A (**1.26**) as the test compound.

5.4 Biological Accumulation of Calothrixin A

The purpose of the uptake studies is to determine if the biological accumulation of the test compound, calothrixin A (**1.26**) is redox-driven. This can be assessed by measuring the intracellular concentration of calothrixin A relative to the applied concentration in the bulk media.

The biological accumulation experiment was carried out using P388 murine macrophages. The total cell volume (V_C) of one million P388 cells is approximately 1.3μL.[31] This volume is essential for calculating the molar concentration of the test compound, assuming uniform distribution of the test compound throughout the cell. A standard curve was prepared for measuring the concentration of calothrixin A via HPLC based on the peak area observed. The standard curve is shown in **Figure 5.2**.

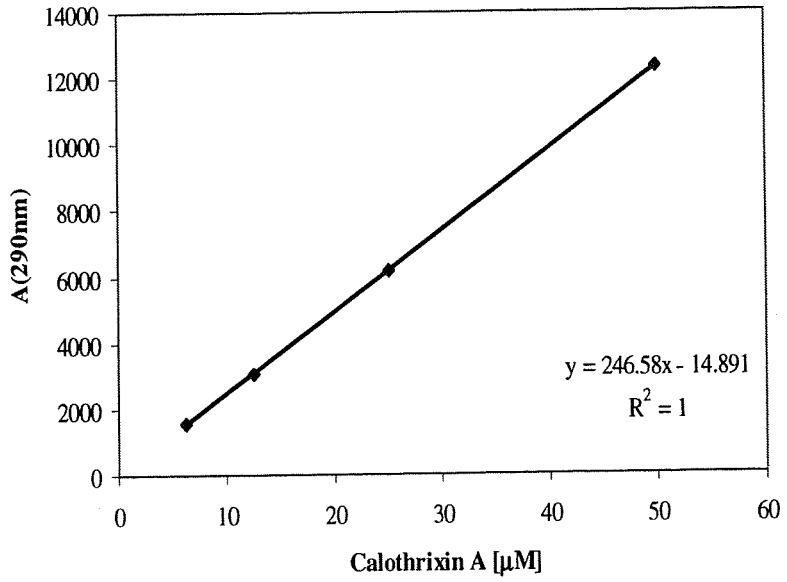

Figure 5.2: *Standard curve for calothrixin A*

For the first experiment, 50 million cells were placed in 50mL Hanks Buffered Saline solution containing 10% horse serum at 37°C. This gave a cell suspension at a density of $1x10^6$ cells/mL. The cells were then incubated with calothrixin A at an applied concentration of 6μM for two hours. It is important to note that the time interval

employed was insufficient for cell death to occur so that whole live cells could be obtained for analysis. After two hours, the cells were pelleted and the media was discarded. The cells were resuspended in fresh media, transferred to a clean Eppendorf tube, then re-pelleted and the medium was discarded to remove extracellular calothrixin A.

The cells were then lysed in phosphate-buffered saline (PBS) containing 1% trifluoroacetic acid (1mL). The cellular debris was pelleted, and the supernatant was analysed via HPLC. The intracellular concentration of calothrixin A [Calothrixin A_I] was calculated from the concentration of the aliquot using the equation

$$[\text{Calothrixin } A_I] = ([\text{Calothrixin } A_{Aliquot}]\ V_{Aliquot})/V_C$$

where [Calothrixin $A_{Aliquot}$] is the concentration of calothrixin A in the aliquot, $V_{Aliquot}$ is the volume of the aliquot (1mL), and V_C is the total cell volume.

However, the concentration of calothrixin A in the aliquot fell below the detection limit of the instrument. Fortunately, it was noted that the cellular debris was highly colored (orange), and therefore it was deduced that an aqueous extraction was likely to be inadequate for removing calothrixin A from the cellular debris. A second extraction of the cellular debris was therefore carried out using acetonitrile. An analysis of the aliquot via HPLC showed that acetonitrile fraction contained 15.7μM of calothrixin A. Using the equation above, the intracellular concentration of calothrixin A was calculated at 242μM. This reflects a 40-fold increase in cell-associated calothrixin A versus the initial applied concentration.

To corroborate these results, a second experiment was carried out using 20 million P388 cells in 200mL of media. This would give a cell density of $1x10^5$ cells/mL. The experiment was carried out as outlined previously, using an applied concentration of 6μM of calothrixin A. The HPLC analysis of the aliquot from the aqueous extraction again fell below the detection limit. However, the acetonitrile aliquot contained calothrixin A at a concentration of 18.17μM, which corresponds to an intracellular concentration of 699μM. The intracellular concentration measured was 175-times greater than the initial concentration.

These results show that the intracellular concentration of calothrixin A is much larger than the applied concentration. This large difference in intracellular versus extracellular concentrations of calothrixin A may account for the difference observed between an *in vivo* antiproliferative assay and an *in vitro* RNA polymerase inhibition assay. A study by Doan *et al.*[32] showed that the growth of *Bacillus subtilis* was strongly inhibited by calothrixin A with an EC_{50} of 8μM. However, an *in vitro* study showed that a calothrixin A concentration of 200μM is required to inhibit RNA polymerase (10 units/mL) by 91%. Our results show that an applied concentration of 6μM is sufficient to produce an intracellular concentration of 242μM (at a cell density of 10^6 cells/mL) of calothrixin A in P388 cells. If the mode of accumulation in *B. subtilis* is similar to what has been observed in P388 cells, then the applied concentration corresponding to the EC_{50} value should be sufficient to produce the concentration of calothrixin A required to abrogate RNA polymerase activity.

The results also show that a decrease in cell density is reflected by an increase in the intracellular concentration of calothrixin A. Furthermore, the results indicate that the intracellular concentration of calothrixin A greatly exceeds the applied concentration. This suggests that calothrixin A is concentrated within the cell, possibly through redox-driven accumulation.

Recent unpublished work[33] by Dr. Paul Waring has shown that the antiproliferative activity of calothrixin A (measured using the MTT assay) is dependent on cell density. A graph of cell density versus EC_{50} values **[Figure 5.3]** shows that the EC_{50} value decreases with lower cell densities until it approaches a minimum EC_{50} value (3.7nM) when the cell density approaches zero. This observation is predicted by the redox-uptake mechanism.[31]

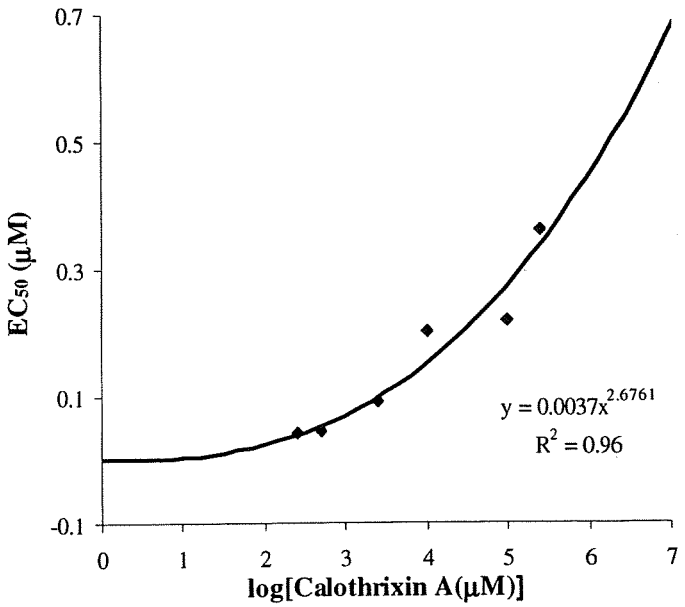

Figure 5.3: *Dependence of calothrixin A EC_{50} values on cell density of P388 cells [data from Dr. Paul Waring].*

It should be noted that there is no direct evidence to show that calothrixin A is concentrated within the cytoplasm and not simply concentrated in the cell membrane. However, the QSAR analysis of the calothrixin derivatives in Chapter 4 suggests that there is a parabolic relationship between lipophilicity and $\log(1/EC_{50})$, which implies that the calothrixins must enter the cytoplasm. If the calothrixins were merely bound to the cell membrane, then the relationship between lipophilicity and $\log(1/EC_{50})$ would be linear.

Further tests are required, however, to prove that the large cell-associated concentration of calothrixin A **(1.26)** is a result of redox-driven accumulation. One such test would be to determine if reduced calothrixin A can be found in the cytoplasm. An indirect method would be to measure the concentration of calothrixin A in GSH-depleted P388 cells to determine if the loss of cellular reductants attenuates the uptake of this redox active quinone.

5.5 Conclusions

A limited QSAR study of the ETP compounds was carried out, and the results show that the cytotoxicity of the ETP compounds does not correlate with lipophilicity. The

reduction potentials of the ETP compounds were measured using the thiol-disulfide exchange mechanism, but the data is insufficient for QSAR analysis. However, it has been shown in following studies[31] that the uptake of ETP compounds is facilitated by the ease of reduction to the dimercapto form.

Studies have shown that calothrixin A undergoes redox cycling *in vitro,*[1] which may be facilitated by its ease of reduction. The result of the uptake studies showed that intracellular concentrations of calothrixin A increases with decreasing cell density. Furthermore, the intracellular concentrations are much higher than the applied concentrations. These results show that EC_{50} value reported for the inhibition of *B. subtilis* may be sufficient to give rise to the intracellular concentration of calothrixin A required to inhibit RNA polymerase. The results indicate that redox cycling or RNA polymerase inhibition are possible modes of action for calothrixin A.

Other experiments are required, however, to assess other possible biological modes of action. For example, the possibility of DNA intercalation is currently under investigation. Furthermore, as many cellular quinones are associated with the mitochondria, it would be interesting to determine if calothrixin A disrupts the mitochondrial electron transport chain.

5.6 Bibliography

(1) Chen, X.; Smith, G. D.; Waring, P. *J. Appl. Phycol.* **2003**, *15*, 269-277.

(2) Chai, C. L. L.; Waring, P. *Redox Rep.* **2000**, *5*, 257-264.

(3) Waring, P.; Eichner, R. D.; Müllbacher, A. *Med. Res. Rev.* **1988**, *8*, 499-524.

(4) Taylor, A. In *Microbial Toxins Part VII: Algal and Fungal Toxins*; Kaids, S., Ciegler, A., Ajl, S., Eds.; Academic Press: 1971, p 337-371.

(5) Sammes, P. G. *Fortschr. Chem. Org. Naturst* **1975**, *32*, 51-118.

(6) Brewer, D.; Hannah, D. E.; Taylor, A. *Can. J. Microbiol.* **1966**, *12*, 1187-1195.

(7) Trown, P. W. *Biochem. Biophys. Res. Comm.* **1968**, *33*, 402-407.

(8) Seigle-Murandi, F.; Krivobok, S.; Steiman, R.; Marzin, D. *J. Agric. Food Chem.* **1990**, *38*, 1854-1856.

(9) Brewer, D.; Taylor, A. *Can. J. Microbiol.* **1967**, *13*, 1577-1589.

(10) Miller, P. A.; Milstrey, K. P.; Trown, P. W. *Science* **1968**, *159*, 431-432.

(11) Waring, P.; Eichner, R. D.; Müllbacher, A.; Sjaarda, A. *J. Biol. Chem.* **1988**, *263*, 18493-18499.

(12) Sutton, P.; Moreland, A.; Hutchinson, I. V.; Müllbacher, A. *Transplantation* **1995**, *60*, 900-902.

(13) De Clercq, E.; Billiau, A.; Ottenheijm, C. J.; Herscheid, J. D. M. *Biochem. Pharmacol.* **1978**, *27*, 635-639.

(14) Waring, P.; Newcombe, N.; Edel, M.; Lin, Q. H.; Jiang, H.; Sjaarda, A.; Piva, T.; Müllbacher, A. *Toxicon* **1994**, *32*, 491-504.

(15) Trown, P. W.; Bilello, J. A. *Antimicrob. Agents Chemother.* **1972**, *2*, 261-266.

(16) Munday, R. *Free Radical Biol. Med.* **1989**, *7*, 659-673.

(17) Munday, R. *J. Appl. Toxicol.* **1984**, *4*, 176-181.

(18) Munday, R. *J. Appl. Toxicol.* **1984**, *4*, 182-186.

(19) Gilbert, H. F. In *Advances in Enzymology*; Meister, A., Ed.; John Wiley & Sons: Orlando, 1990; Vol. 63, p 69-172.

(20) Jiang, H.; Newcombe, N.; Sutton, P.; Lin, Q. H.; Müllbacher, A.; Waring, P. *Aust. J. Chem.* **1993**, *46*, 1743-1754.

(21) Bernardo, P. H. Graduate Diploma Thesis, The Australian National University, 2001.

(22) Ohler, E.; Poisel, H.; Tataruch, F.; Schmidt, U. *Chem. Ber.* **1972**, *105*, 635-641.

(23) Jocelyn, P. C. *Biochemistry of the SH group; The Occurence, Chemical Properties, Metabolism and Biological Function of Thiols and Disulphides*; Academic Press Inc.: London, 1972.

(24) Lees, W.J.; Whitesides, G. M. *J. Org. Chem.* **1993**, *58*, 642-647.

(25) Bernardo, P. H.; Chai, C. L. L.; Deeble, G. J.; Liu, X. M.; Waring, P. *Bioorg. Med. Chem. Lett.* **2001**, *11*, 483-485.

(26) Rabenstein, D. L.; Yeo, P. L. *J. Org. Chem.* **1994**, *59*, 4223-4229.

(27) Rabenstein, D. L.; Yeo, P. L. *Anal. Chem.* **1993**, *65*, 3061-3066.

(28) Rabenstein, D. L.; Weaver, K. H. *J. Org. Chem.* **1996**, *61*, 7391-7397.

(29) Kovavic, P.; Osuna Jr., J. A. *Curr. Pharm. Design* **2000**, *6*, 277-309.

(30) De Abreu, F. C.; Ferraz, P. A. d. L.; Goulart, M. O. F. *J. Braz. Chem. Soc.* **2002**, *13*, 19-35.

(31) Bernardo, P. H.; Brasch, N.; Chai, C. L. L.; Waring, P. *J. Biol. Chem.* **2003**, *278*, 46549-46555.

(32) Doan, N. T.; Rickards, R. W.; Rothschild, J. M.; Smith, G. D. *J. Appl. Phycol.* **2000**, *12*, 409-416.

(33) Waring, P., personal communication.

Chapter 6

6.1 General Experimental

^{1}H NMR and ^{13}C NMR spectra were acquired on a Varian Gemini 2 Spectrometer operating at 300 MHz and 75.4 MHz respectively, unless stated otherwise. The probe temperature used was generally room temperature (25°C) unless otherwise noted. NMR spectra were recorded in deuterated solvents with chemical shifts (δ) reported as shifts in parts per million from tetramethylsilane (TMS, 0.00 ppm). Proton spectra recorded in $CDCl_3$ were referenced to either the residual solvent peak at δ7.26 or TMS. Carbon spectra recorded in $CDCl_3$ were referenced to the central peak of the $CDCl_3$ triplet at δ77.0. Proton spectra recorded in D_2O were referenced to the residual solvent peak at δ4.79. Proton spectra recorded in *d*-DMSO were referenced to the residual solvent peak at δ2.50. Carbon spectra recorded in *d*-DMSO were referenced to the central peak of the heptet at δ39.5. Proton spectral data are reported as follows: chemical shift (δ), multiplicity (s-singlet, d-doublet, t-triplet, q-quartet, m-multiplet, app. t-apparent triplet, br. s-broad singlet *etc.*), relative integral (number of protons), coupling constants (*J* in Hz), and assignments where possible. Carbon spectral data are reported as follows: chemical shift (δ) and assignment where possible.

UV-Visible spectroscopy data were recorded using Carey 4G UV-Visible spectrophotometer at 25°C. Samples were prepared at 3mg/mL concentrations and referenced against the solvent indicated. The data is reported as the absorption coefficient (absorption units per Molar concentration) at the wavelength (in nm) of maximum absorbance.

Infrared (IR) spectra were measured on a Perkin Elmer 1800 Spectrum One FTIR or Shimadzu FTIR-8400 Fourier Transform Infrared Spectrometer. Samples were analyzed as KBr discs for solids or as thin liquid films on NaCl plates for liquids. The absorption spectra for characteristic peaks are reported in the following format: frequency (ν_{max} cm^{-1}) and peak intensity (w-weak, m-medium, s-strong, br-broad).

Electron impact mass spectra (EIMS) and high resolution mass spectra (HRMS) were measured by the Research School of Chemistry Mass Spectrometry Unit, ANU, using a VG Micromass 7070F double focusing mass spectrometer, using positive ion impact

techniques. Mass spectral data are listed as mass-to-charge ratios (*m/z*) and relative intensity (% of base peak).

Elemental Analyses were carried out by the Micro Analysis Unit of the Research School of Chemistry using a Carlo Erba 1106 CHN Analyzer.

Column chromatography was carried out using Merck Silica gel (Kieselgel 60, 0.040-0.063mm), with positive pressure applied by nitrogen flow. Thin layer chromatography was carried out using Merck Silica gel 60 F_{254} precoated aluminum plates analyzed under a 254 nm UV lamp. TLC plates were also developed using a solution of ammonium molybdate/ ceric ammonium nitrate/ sulfuric acid/ and water (10g: 0.4g: 5.6mL: 200mL). Melting points were measured using a Reichert hot-stage microscope and have been corrected using calibration standards.

Analytical grade solvents were used without further purification unless otherwise stated. Ethyl acetate, light petroleum and methanol were purchased from BDH and were distilled following standard purification methods.[1] TMEDA was purchased from Aldrich and distilled over KOH and stored over sodium wire. Sodium hydride (60% suspension in mineral oil) was purified by adding *n*-hexane to make a suspension, followed by vacuum filtration to obtain a grey powder. The solid was stored under an atmosphere of dry nitrogen when not in use. Commercial reagents were purchased from Aldrich, Merck, or BDH. All reactions were carried out under an atmosphere of dry nitrogen unless otherwise specified. Reactions involving moisture-sensitive reagents were carried out using oven-dried glassware and dry solvents.

6.2 Experimental Procedures and Data for Chapter 2

6.2.1 Procedures for the Synthesis of Quinoline-3,4-anhydride (2.30)

Quinoline-3-Acetyl-4-Carboxylic Acid **(2.38)**

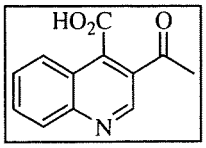

The title compound was prepared using a modification of the literature procedure.[2] Isatin (5g, 34mmol) was dissolved in a solution of 35% KOH (14mL) and stirred until a clear yellow solution was formed. The reaction mixture was neutralized with 6N HCl, followed by the addition of solid Na_2CO_3 to adjust the pH to pH=9. 3-Ketobutyraldehyde dimethyl acetal (6.4mL, 48mmol) was then added and the reaction mixture was stirred for 1h at 20°C. After 1h, the temperature was raised to 75°C and the solution was stirred for a further 30min following which the reaction mixture was cooled to 0°C and acidified with 6N HCl to pH=0. The resulting enamine precipitated as a yellow solid which was subsequently filtered and dried. The enamine was then redissolved in 7% NaOH (14mL), stirred for 30min at 75°C then cooled to 0°C and acidified with 6N HCl to obtain the crude 3-acetyl-quinoline-4-carboxylic acid as a brown solid. Recrystallization from ethanol followed by trituration with ether yielded the pure product as brown crystals (6.8g, 32mmol, 94% yield).

R_f 0.53 (EtOH).

Mp 225-228°C (lit. 228-230°C).[2]

^{1}H-NMR (D_2O +Na_2CO_3): δ2.74 (s, 3H, CH_3), 7.69 (app. t, J_{app}= 8Hz, 1H, Ar-**H**), 7.93 (app. t, J_{app}= 8Hz, 1H, Ar-**H**), 7.95 (d, J= 8Hz, 1H, Ar-**H**), 8.00 (d, J= 8Hz, 1H, Ar-**H**), 9.24 (s, 1H, Ar-**H**).

Quinoline-3,4-dicarboxylic acid **(2.39)**

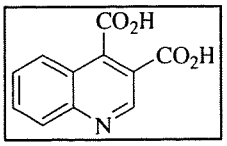

The title compound was prepared using a modification of the literature procedure.[3] A basic solution of 6% NaOCl was prepared by adding NaOH (9.2g, 0.23mol) to commercially available 12.5% NaOCl solution (66mL) and water (66mL). This solution was cooled to 0°C and slowly added to the solid quinoline-3-acetyl-4-carboxylic acid **(2.38)** (6.0g, 28mmol). When the addition was completed, the reaction mixture was stirred for 30min at 70°C, then cooled to 0°C and excess solid $NaHSO_3$ (2.0g) was added portionwise. The cold solution was carefully acidified with 6N HCl until pH=2 to precipitate the title

compound. The precipitate was filtered and the solid obtained was washed with acetone (20mL) and ether (20mL) to give the title compound as a white solid (5.6g, 26mmol, 93% yield).

Mp 255°C (lit. 250-255°C).[2]

^{1}H-NMR (D_2O +Na_2CO_3): δ7.68 (app. t, J_{app}= 8Hz, 1H, Ar-**H**), 7.82 (app. t, J_{app}= 8Hz, 1H, Ar-**H**), 7.94 (d, J= 8Hz, 1H, Ar-**H**), 8.03 (d, J= 8Hz, 1H, Ar-**H**), 9.09 (s, 1H, Ar-**H**).

Quinoline-3,4-anhydride **(2.30)**

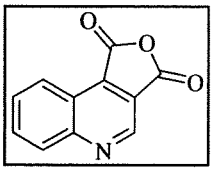

To quinoline-3,4-dicarboxylic acid **(2.39)** (3.0g, 14mmol) was added acetic anhydride (25mL) and the reaction mixture was refluxed for 30 min. The resulting clear solution was then cooled to room temperature, and the solvent was removed under reduced pressure. The title compound was obtained as a white solid in quantitative yield (2.75g). The product could be recrystallized from acetone, or alternatively the unpurified product could be used in the next synthetic step.

R_f 0.80 (acetone).

Mp 170-171°C (lit. 170-171°C).[2]

^{1}H-NMR ($CDCl_3$): δ7.96 (app. t, J_{app}= 8Hz, 1H, Ar-**H**), 8.08 (app. t, J_{app}= 8Hz, 1H, Ar-**H**), 8.38 (d, J= 8Hz, 1H, Ar-**H**), 8.80 (d, J= 8Hz, 1H, Ar-**H**), 9.50 (s, 1H, Ar-**H**).

^{13}C-NMR ($CDCl_3$): δ121.1, 123.6, 124.9, 130.7, 131.2, 134.1, 135.8, 144.5, 152.1, 161.6 (CO), 162.2 (CO).

6.2.2 General Procedure for the Methanolysis of Anhydrides

The appropriate anhydride (typically 0.50g) was dissolved in dry distilled methanol (50mL) and the reaction mixture was refluxed for 30min. The solvent was then removed under reduced pressure to yield the crude product.

3-Carboxy-4-methoxycarbonylquinoline **(2.29)**

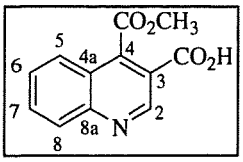

The title compound was prepared from quinoline-3,4-anhydride **(2.30)** (0.50g, 2.5mmol) using the methodology outlined above. Recrystallization from hot acetone yielded the desired compound as a pale yellow compound (0.41g, 1.8mmol, 70% yield). The proton and carbon

assignments were made using HMBC and HMQC experiments performed on an INOVA 500 MHz spectrometer.

R_f 0.24 (MeOH).

Mp 230-232°C, decomp.

^{1}H NMR (*d*-DMSO): δ4.00 (s, 3H, OCH_3), 7.78 (app. t, J_{app}= 7Hz, 1H, C6-**H**), 7.87 (d, *J*= 7Hz, 1H, C8-**H**), 7.99 (app. t, J_{app}= 7Hz, 1H, C7-**H**), 8.18 (d, *J*= 8Hz, 1H, C5-**H**), 9.36 (s, 1H, C2-**H**).

^{13}C NMR (*d*-DMSO): δ53.1 (CH_3), 120.2 (**C**3), 122.4 (**C**8), 125.8 (**C**7), 128.9 (**C**5), 129.4 (**C**4a), 132.4 (**C**6), 141.4 (**C**4), 148.9 (**C**8a), 150.0 (**C**2), 165.4 (**C**-O_2H), 166.8 (**C**-O_2CH_3).

UV-Vis (MeOH) ε_{235nm}= 32611 M^{-1}.

IR (KBr disk) ν_{max} cm^{-1} 765 s, 1256 s, 1316 s, 1732 s, 2427 br.

EIMS *m/z* (rel. A): 231 ($M^{+\cdot}$, 100), 200 ([**M**-OCH_3]$^+$, 99), 187 ([**MH**-CO_2H]$^+$, 42), 172 (14), 155 (87), 127 (92), 116 (22), 101 (30), 89 (32), 74 (35), 63 (26).

HRMS Calculated 231.0532 for $C_{12}H_9NO_4$ found 231.0534.

Analytical Anal. Calcd for $C_{12}H_9NO_4$: C, 62.34; H, 3.92; N, 6.06. Found: C, 62.06; H, 3.80; N, 5.92.

2-Carboxy-1-methoxycarbonylbenzene **(2.71)**

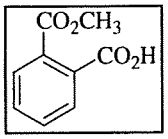

The title compound was prepared from commercially available phthalic anhydride (0.50g, 3.4mmol) using the methodology outlined above. The product was obtained in quantitative yield (0.61g, 3.3mmol).

Mp 84°C (lit. 84°C).[4]

^{1}H NMR (*d*-DMSO): δ3.93 (s, 3H, OCH_3), 7.60 (m, 2H, Ar-**H**), 7.68 (m, 1H, Ar-**H**), 7.94 (d, *J*= 9Hz, 1H, Ar-**H**).

3-Carboxy-4-methoxycarbonylpyridine **(2.14)**

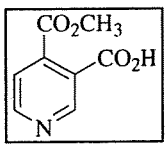

The title compound was prepared from commercially available pyridine-3,4-anhydride (0.50g, 3.4mmol) using the methodology outlined above. Recrystallization from hot acetone yielded the desired compound as a pale yellow solid (0.43g, 2.4mmol, 70% yield).

Mp 172°C. (lit. 172°C).[5]

^{1}H NMR (*d*-DMSO): δ4.26 (s, 3H, OCH_3), 8.05 (d, *J*= 5Hz, 1H, Ar-**H**), 9.29 (d, *J*= 5Hz, 1H, Ar-**H**), 9.45 (s, 1H, Ar-**H**).

6.2.3 Procedure for the Preparation of Indole Derivatives

N-*Tosylindole* [6] **(2.46)**

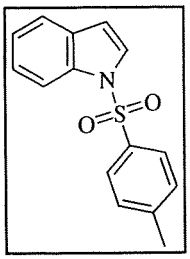

To a solution of indole (1.27g, 11mmol) in dry THF (45mL) at 0°C under nitrogen was added powdered KOH (3.05g, 54mmol). After 5 min, tosyl chloride (2.28g, 12mmol) was added to the suspension with vigorous stirring. The reaction mixture was allowed to stir for 20min at room temperature following which benzene (70mL) was added. The combined organic layers were filtered by gravity to remove insoluble materials, and the organic layer was washed with saturated NaCl solution (20mL). The organic layer was then dried with $MgSO_4$ and the solvent was removed under reduced pressure to obtain the crude product. Recrystallization from hot ethanol gave the desired product as white crystals (2.86g, 10mmol, 96% yield).

Mp 86°C (lit. 86°C).[7]

^{1}H NMR ($CDCl_3$): δ2.34 (s, 3H, CH_3), 6.64 (d, *J*= 4Hz, 1H, Ar-**H**), 7.20-7.33 (m, 4H, Ar-**H**), 7.53 (d, *J*= 8Hz, 1H, Ar-**H**), 7.56 (d, *J*= 4Hz, 1H, Ar-**H**), 7.76 (d, *J*= 8Hz, 2H, Ar-**H**), 7.99 (d, *J*= 8Hz, 1H, Ar-**H**).

N-*Tosyl-3-iodoindole* **(2.47)**

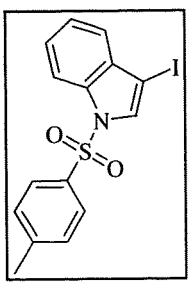

To a solution of indole (5g, 43mmol) and NaOH (1.75g, 44mmol) in methanol (150mL) under nitrogen was added a solution of I_2 (10.75g, 42mmol) and KI (21.25g, 128mmol) in methanol (40mL) which resulted in a cloudy suspension. When the reaction mixture became clear, water was added (250mL) to quench the reaction and to precipitate 3-iodoindole. The precipitate was filtered and washed with cold water. The precipitate was then dissolved in ether and dried with Na_2SO_4, filtered and concentrated *in vacuo* to yield 3-iodoindole as a white solid (8.5g, 35mmol, 81% yield). The solid was dissolved in benzene (100mL), and tosyl chloride (9.7g, 51mmol) was added. To this solution was then added to a solution of tetrabutylammonium sulfate (1.16g, 3.4mmol) and NaOH (15.5g, 0.39mol) in water (31mL). The reaction mixture was stirred for 2h after which the benzene layer was separated, washed with water (100mL), and the organic layer was filtered through a short column of silica to remove

TsOH. The solvent was removed *in vacuo* and recrystallization from hexane yielded the title compound as a white solid (9.94g, 25mmol, 57% overall yield).

Mp 240°C (lit. 238-239°C).[8]

^{1}H NMR ($CDCl_3$): δ2.35 (s, 3H, CH_3), 7.24 (d, *J*= 9Hz, 2H, Ar-**H**), 7.30 (m, 3H, Ar-**H**), 7.70 (s, 1H, Ar-**H**), 7.78 (d, *J*= 8Hz, 2H, Ar-**H**), 7.96 (d, *J*= 9Hz, 1H, Ar-**H**).

6.2.4 General Procedure for the Preparation of Acid Chlorides

The appropriate carboxylic acid (typically 1g) was dissolved in $SOCl_2$ (15mL) and the reaction mixture was refluxed for 30min until a clear yellow solution was obtained. The mixture was cooled to room temperature and the solvent was removed under reduced pressure to yield the crude acid chloride as a yellow gum. The crude acid chloride was then dried over K_2CO_3 in a dessicator under vacuum. Due to its instability, the crude acid chloride was used in the next synthetic step without further purification.

3-Chlorocarbonyl-4-methoxycarbonylquinoline (**2.28**)

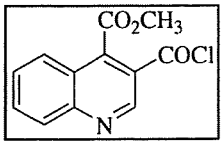

The title compound was prepared from 3-carboxy-4-methoxycarbonylquinoline (**2.29**) (1.85g, 8mmol) using the procedure outlined above. The product was obtained in quantitative yield. The $CDCl_3$ utilized for NMR analysis was passed through anhydrous Na_2SO_4 as the acid chloride is sensitive to traces of H_2O.

^{1}H-NMR ($CDCl_3$): δ4.20 (s, 3H, OCH_3), 8.19 (s, 2H, Ar-**H**), 8.40 (br s, 1H, Ar-**H**), 9.00 (d, *J*= 8Hz, 1H, Ar-**H**), 9.87 (s, 1H, Ar-**H**).

^{13}C-NMR ($CDCl_3$): δ54.5 (OCH_3), 122.4, 123.2, 124.3, 127.5, 132.5, 138.6, 139.8, 144.9, 148.9, 163.0 (**C**O), 163.1 (**C**O).

2-Chlorocarbonyl-1-methoxycarbonylbenzene (**2.72**)

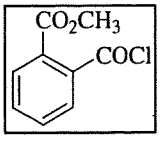

The compound was prepared from 2-carboxy-1-methoxycarbonyl benzene (**2.71**) (1.1g, 6mmol) using the procedure outlined above. Due to the instability of the acid chloride, the compound was utilized in the next step without further characterization.

3-Chlorocarbonyl-4-methoxycarbonylpyridine **(2.13)**

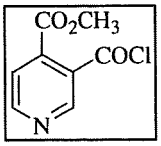

The compound was prepared from 3-carboxy-4-methoxycarbonyl pyridine **(2.14)** (0.50g, 2.8mmol) using the procedure outlined above. Due to the instability of the acid chloride, the compound was utilized in the next step without further characterization.

6.2.5 Procedures for the Coupling of Indole Derivatives to Acid Chlorides

3-(3-Indolyl)carbonyl-4-methoxycarbonylquinoline **(2.26)**

Method 1

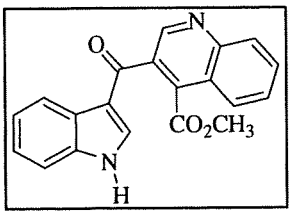

To a suspension of $AlCl_3$ (0.20g, 1.5mmol) in dry CH_2Cl_2 (10mL) at room temperature under a nitrogen atmosphere was added a solution of 3-chlorocarbonyl-4-methoxycarbonyl quinoline **(2.28)** (0.10g, 0.40mmol). The reaction mixture was stirred for 10min, and a yellow-orange solution formed. To this colored solution was carefully added *N*-tosylindole **(2.46)** (0.16g, 0.59mmol). The reaction mixture was stirred for 16h under an atmosphere of dry nitrogen. The reaction mixture was poured into ice-water mixture (2g), and the organic layer was separated. The aqueous layer was further extracted with CH_2Cl_2 (10mL), and the combined organic layers were washed successively with brine (10mL), saturated $NaHCO_3$ solution (10mL), and distilled water (10mL). The organic layer was dried with Na_2SO_4, filtered, and the solvent removed to obtain a dark brown solid. Purification of the solid via flash chromatography on silica ($CHCl_3$) gave only *N*-tosylindole **(2.46)** and a complex mixture which could not be separated further.

Method 2

To a stirred solution of *N*-tosyl-3-iodoindole **(2.47)** (0.15g, 0.38mmol) in dry THF (10mL) at -100°C was added a solution of *n*-butyl lithium (1M solution in hexane, 0.38mL, 0.38mmol). The reaction mixture was stirred for 1h at -100°C, then a cold solution of the acid chloride **2.28** (0.12g, 0.48mmol) in dry THF (10mL) was carefully added to the reaction mixture and stirred for a further 2h. The reaction mixture was then warmed to room temperature, and saturated $NaHCO_3$ solution (20mL) was added to quench the reaction. The organic layer was separated, and the aqueous layer was further extracted with ethyl acetate (10mL). The combined organic layers were dried with Na_2SO_4, filtered, and the solvent was removed under reduced pressure to yield a brown

solid. Flash chromatography of the product on silica (EtOAc) yielded a yellow solid. Analysis of the solid via ^{1}H NMR spectroscopy showed only the presence of *N*-tosylindole (**2.46**).

Method 3

To a solution of *N*-tosyl-3-iodoindole (**2.47**) (0.1g, 0.25mmol) in dry THF (5mL) at -30°C was added MeMgCl (2.4M in THF, 0.14mL, 0.34mmol). The reaction mixture was stirred for 1h, then a solution of the acid chloride **2.28** (0.12g, 0.48mmol) in dry THF (5mL) was carefully added. The reaction mixture was stirred further for 1h, then warmed to room temperature and stirred for 16h. The reaction was stopped by the addition of saturated NH_4Cl solution (10mL), and the organic layer was separated. The aqueous layer was extracted with ethyl acetate (10mL), and the combined organic layers were dried with Na_2SO_4, filtered, and the solvent was removed *in vacuo* to obtain a brown solid. Analysis of the ^{1}H NMR spectrum of the crude solid showed a complex mixture. The solid was purified by flash chromatography on silica (EtOAc) and *N*-tosylindole (**2.46**) was isolated as a pale yellow solid. The desired product was not obtained.

Method 4

To a cold solution of indole (0.10g, 0.85mmol) in dry CH_2Cl_2 (5mL) was added Et_2AlCl (1M in hexane, 0.71mL, 0.71mmol). The reaction mixture was stirred for 1h at 0°C, following which a solution of the acid chloride **2.28** (0.30g, 1.3mmol) in dry CH_2Cl_2, (5mL) was added and the mixture was stirred further for 1h. The reaction was then quenched by the addition of saturated $NaHCO_3$ solution (5mL) and the aqueous layer was extracted with CH_2Cl_2 (2x5mL). The combined organic layers were dried with $MgSO_4$ and the solvent was removed under reduced pressure to yield the crude product. Purification of the product via column chromatography on silica (1:1 EtOAc/light petroleum) yielded the desired product **2.26** as a pale yellow solid (76mg, 27% yield).

Method 5

To a solution of $ZnCl_2$ (0.24g, 1.8mmol) in dry THF (5mL) was added *N*-tosyl-3-iodoindole (**2.47**) (0.17g, 0.43mmol). The solution was cooled to -78°C and a solution of *n*-butyl lithium (0.43mL, 1M in hexane, 0.43mmol) was added dropwise. The

reaction mixture was warmed to room temperature and stirred for 1h, after which a solution of the acid chloride **2.28** (0.13g, 0.43mmol) in dry THF (5mL) was added. The reaction mixture was stirred for 16h after which saturated $NaHCO_3$ solution (10mL) was added to quench the reaction. The organic layer was separated, and the aqueous layer was thrice extracted with ethyl acetate (3x10mL). The combined organic layers were dried with $MgSO_4$, filtered and the solvent removed *in vacuo* to afford the crude product **2.26**. The product was purified using column chromatography on silica (1:1 EtOAc/light petroleum) to yield the desired product as a pale yellow solid (66mg, 47% yield).

Method 6

To a mixture of indole (0.50g, 4.3mmol) and anhydrous zinc chloride (1.16g, 8.6mmol) in dry CH_2Cl_2 (20mL) under nitrogen was added dropwise a solution of methyl magnesium chloride (1.43mL of 3M solution in THF, 4.3mmol). The reaction mixture was stirred for 2h at room temperature in order to generate *N*-(chlorozinc)indole **(2.52)** *in situ.* The resulting suspension was then quickly added to a solution of 3-chlorocarbonyl-4-methoxycarbonylquinoline **(2.28)** (2.0g, 7.9mmol) in dry CH_2Cl_2 (20mL) and the reaction mixture was stirred at room temperature for 16h. The reaction was quenched by the addition of saturated NH_4Cl solution (5mL) followed by the extraction of the reaction mixture with three portions of CH_2Cl_2 (15mL each). The combined organic layers were then washed with saturated aqueous $NaHCO_3$ (5mL), saturated NaCl (5mL), and dried with $MgSO_4$. The organic layer was then filtered and the solvent was removed *in vacuo.* Column chromatography on silica (1:1 ethyl acetate: light petroleum) followed by recrystallization in acetone/*n*-hexane afforded 3-(3-indolyl)carbonyl-4-methoxycarbonylquinoline as a fine yellow powder (1.28g, 3.9mmol, 90% yield).

R_f 0.38 (1:1 EtOAc/ light petroleum).

Mp 196°C.

^{1}H-NMR ($CDCl_3$): δ3.75 (s, 3H, OCH_3), 7.29 (m, 2H, Ar-**H**), 7.39 (d, *J*= 8Hz, 1H, Ar-**H**), 7.48 (s, 1H, Ar-**H**), 7.68 (app. t, J_{app}= 8Hz, 1H, Ar-**H**), 7.84 (app. t, J_{app}=8Hz, 1H, Ar-**H**), 8.12 (d, *J*= 8Hz, 1H, Ar-**H**), 8.19 (d, *J*= 8Hz, 1H, Ar-**H**), 8.39 (d, *J*= 8Hz, 1H, Ar-**H**), 9.19 (s, 1H, Ar-**H**), 9.69 (s, 1H, N**H**).

^{13}C-NMR ($CDCl_3$): δ53.1 (OCH_3), 111.7, 117.5, 122.3, 123.2, 123.6, 124.4, 125.7, 125.8, 128.6, 129.7, 131.2, 131.8, 134.8, 136.5, 138.1, 148.8, 148.9, 167.2 (CO_2CH_3), 188.1 (CO).

UV-Vis (CH_2Cl_2) $\varepsilon_{244\ nm}$= 41570 M^{-1}.

IR (KBr disk) ν_{max} cm^{-1} 1238 s, 1433 s, 1514 s, 1580 s, 1596 s, 1726 s, 2951 w, 3253 s.

EIMS *m/z* (rel. A): 330 ($M^{+\cdot}$, 85), 299 (25), 270 ([M-OCH_3]$^+$, 60), 242 (35), 214 (25), 144 (100), 116 (37), 89 (26).

HRMS Calculated 330.1004 for $C_{20}H_{14}N_2O_3$, found 330.1008.

Analytical Anal. Calcd for $C_{20}H_{14}N_2O_3$: C, 72.72; H, 4.27; N, 8.48. Found: C, 72.44; H, 4.26; N, 8.18.

3-(5-Methoxyindol-3-yl)carbonyl-4-methoxycarbonylquinoline **(2.66)**

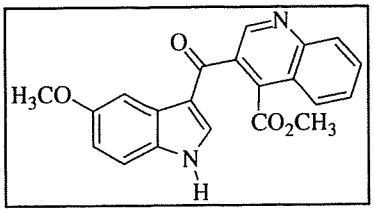

To a mixture of 5-methoxyindole (0.50g, 3.4mmol) and anhydrous zinc chloride (0.93g, 6.8mmol) in dry CH_2Cl_2 (10mL) under nitrogen was added dropwise a solution of methyl magnesium chloride (1.13mL of 3M solution in THF, 3.4mmol). The reaction mixture was stirred for 2h at room temperature in order to generate *N*-(chlorozinc)indole **(2.65)** *in situ.* The resulting suspension was then quickly added to a solution of 3-chlorocarbonyl-4-methoxycarbonylquinoline **(2.28)** (1.08g, 4.3mmol) in dry CH_2Cl_2 (10mL) and was stirred at room temperature for 16h. The reaction was quenched with the addition of saturated NH_4Cl solution (20mL), and the organic layer was separated. The aqueous layer was then extracted with three portions of EtOAc (15mL each). The combined organic layers were successively washed with saturated aqueous $NaHCO_3$ (10mL) and distilled water (10mL), and then dried with $MgSO_4$. The organic layer was filtered and the solvent was removed under reduced pressure to yield the crude product. Column chromatography on silica (1:1 ethyl acetate: light petroleum) afforded 3-(5-methoxyindol-3-lyl)carbonyl-4-methoxycarbonylquinoline as a pale yellow powder (1.12g, 3.2mmol, 94% yield). The ^1H and ^{13}C NMR spectra were obtained in a mixed solvent system consisting of 0.5mL $CDCl_3$ and 10μL *d*-DMSO.

R_f 0.21 (1:1 EtOAc/light petroleum); 0.69 (EtOAc).

Mp 213°C.

^1H-NMR ($CDCl_3$ +*d*-DMSO): δ3.79 (s, 3H, OCH_3), 3.92 (s, 3H, OCH_3), 6.99 (dd, *J*= 3Hz and 9Hz, 1H, Ar-**H**), 7.34 (d, *J*= 9Hz, 1H, Ar-**H**), 7.47 (d, *J*= 3Hz, 1H, Ar-**H**), 7.71 (app. t, J_{app}= 7Hz, 1H, Ar-**H**), 7.87 (app. t, J_{app}= 7Hz, 1H, Ar-

H), 7.96 (d, *J*= 3Hz, 1H, Ar-**H**), 8.15 (d, *J*= 8Hz, 1H, Ar-**H**), 8.24 (d, *J*= 8Hz, 1H, Ar-**H**), 8.98 (s, 1H, N**H**), 9.22 (s, 1H, Ar-**H**).

^{13}C-NMR ($CDCl_3$ +*d*-DMSO): δ52.9 (OCH_3), 55.7 (OCH_3), 103.3, 112.7, 114.4, 116.8, 125.7, 126.6, 128.5, 129.3, 131.1, 131.6, 135.2, 138.1, 156.5, 166.9 (CO_2CH_3), 187.5 (**C**O).

EIMS *m/z* (rel. A): 360 ($M^{+\cdot}$, 100), 174 (81), 112 (39).

IR (KBr disk) ν_{max} cm^{-1} 1214 m, 1268 m, 1433 s, 1465 m, 1584 m, 1597 s, 1728 s, 2950 w, 3198 br.

HRMS Calculated 360.1110 for $C_{21}H_{16}N_2O_4$ found 360.1099.

Analytical Anal. Calcd for $C_{21}H_{16}N_2O_4$: C, 69.99; H, 4.47; N, 7.77; Found C, 70.03; H, 4.56; N, 7.48.

3-(1-Methoxycarbonylbenzene-2-yl)carbonylindole **(2.73)**

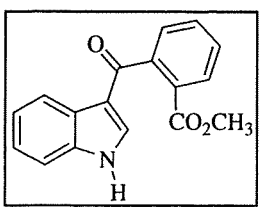

To a stirred mixture of indole (0.86g, 7.3mmol) and anhydrous zinc chloride (2.0g, 14.6mmol) in dry CH_2Cl_2 (40mL) at room temperature under nitrogen, was added dropwise a solution of MeMgCl (2.6mL of 3.0M solution in THF, 7.8mmol). After stirring for 1h, the reaction mixture was added in one portion to a solution of 2-chlorocarbonyl-1-methoxycarbonylbenzene **(2.72)** (1.21g, 6mmol) in dry CH_2Cl_2 (20mL). The reaction mixture was stirred for 16h at room temperature under nitrogen before being quenched by the addition of saturated NH_4Cl solution (20mL). The reaction mixture was extracted with $CHCl_3$ (3 x 20mL) and the combined organic layers were washed with saturated $NaHCO_3$ solution (25mL) and brine (25mL). The organic layer was then dried over $MgSO_4$, filtered and the solvent removed *in vacuo* to give an orange solid. The crude product was triturated with hot ether to yield the pure product as a fine white powder (1.30g, 4.6mmol, 76% yield).

R_f 0.48 (1:1 EtOAc/light petroleum).

Mp 197-198°C.

^{1}H-NMR (*d*-DMSO): δ3.59 (s, 3H, OCH_3), 7.24 (m, 2H, Ar-**H**), 7.49-7.73 (m, 5H, Ar-**H**), 7.90 (d, *J*= 8Hz, 1H, Ar-**H**), 8.13 (d, *J*= 8Hz, 1H, Ar-**H**), 12.01 (s, 1H, N**H**).

^{13}C-NMR (*d*-DMSO): δ52.1 (OCH_3), 112.3, 116.4, 121.2, 121.9, 123.1, 125.6, 128.0, 129.43, 129.46, 129.52, 132.0, 135.4, 136.8, 142.6, 166.8 (CO_2CH_3), 190.1 (CO).

IR (KBr disk) ν_{max} cm^{-1} 756 s, 1273 s, 1433 s, 1520 m, 1580 m, 1604 s, 1720 s, 3213 br.

EIMS *m/z* (rel. A): 279 ($M^{+\cdot}$, 60), 248 ($[M-OCH_3]^+$, 9), 144 (100).

HRMS Calculated 279.0895 for $C_{17}H_{13}NO_3$, found 279.0900.

Analytical Anal. Calcd for $C_{17}H_{13}NO_3$: C, 73.11; H, 4.69; N, 5.02. Found: C, 72.82; H, 4.70; N, 4.99.

3-(4-Methoxycarbonylpyridine-3-yl)carbonylindole **(2.68)**

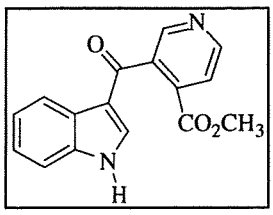

To a stirred mixture of indole (0.39g, 3.3mmol) and anhydrous zinc chloride (0.91g, 6.6mmol) in dry CH_2Cl_2 (50mL) under nitrogen was added dropwise a solution of MeMgCl (1.11mL of 3.0M solution in THF, 3.3mmol). After stirring for 1h, the reaction mixture was added in one portion to a solution of 3-chlorocarbonyl-4-methoxycarbonylpyridine **(2.13)** (0.55g, 2.8mmol) in dry CH_2Cl_2 (50mL). The reaction mixture was stirred for 16h at room temperature under nitrogen, following which the reaction mixture was quenched by addition of saturated NH_4Cl solution (50mL). The reaction mixture was extracted with CH_2Cl_2 (2 x 20mL) and the combined organic layers were washed with saturated aqueous $NaHCO_3$ and brine (50mL). The organic layer was then dried over $MgSO_4$, filtered and the solvent removed to leave a solid residue. Trituration with ether gave the desired product as a white solid (0.56g, 2.0mmol, 72% yield).

Mp 173-5°C.

^{1}H-NMR ($CDCl_3$): δ3.44 (s, 3H, OCH_3), 7.20-7.30 (m, 2H, Ar-**H**), 7.41 (m, 1H, Ar-**H**), 7.65 (d, *J*= 4Hz, 1H, Ar-**H**), 7.85 (dd, *J*= 2Hz and 9Hz, 1H, Ar-**H**), 8.79 (d, *J*= 5Hz, 1H, Ar-**H**), 8.94 (s, 1H, N**H**), 9.16 (s, 1H, Ar-**H**).

^{13}C-NMR ($CDCl_3$): δ53.0 (OCH_3), 111.7, 118.1, 122.3, 123.2, 124.4, 125.4, 134.2, 136.5, 137.9, 148.3, 150.5, 165.7 (CO_2CH_3), 188.0 (CO).

IR (KBr disk) ν_{max} cm^{-1} 1306 m, 1432 s, 1524 s, 1626 s, 1726 s, 3109 w, 3351 br.

EIMS *m/z* (rel. A): 281 ($M^{+\cdot}$, 27), 280 ($[M-H]^+$, 71), 144 (100), 116 (32), 89 (27).

HRMS Calculated 280.0848 for $C_{16}H_{12}N_2O_3$, found 280.0854.

Analytical Anal. Calcd for $C_{16}H_{12}N_2O_3$: C, 68.57; H, 4.32; N, 9.99. Found: C, 68.53; H, 4.52; N, 9.61.

6.2.6 General Procedure for the *N*-MOM Protection of the Indole Derivatives

To a solution of the selected unprotected indole derivatives (3mmol) in dry THF (100mL) at 0°C under nitrogen was added NaH (86mg, 3.6mmol). The suspension was warmed to room temperature over 30min and a bright red colour was observed. The suspension was then cooled to 0°C and methoxymethyl chloride (0.21mL, 3.6mmol) was added. The reaction mixture was warmed to room temperature and stirred for 16 h. The resulting suspension was then poured into a saturated $NaHCO_3$ solution (50mL) and the organic layer was separated. The product was further extracted from the aqueous layer with CH_2Cl_2 (3x10mL). The combined organic layers were then dried with $MgSO_4$ and filtered, and the solvent was removed *in vacuo* to yield the desired compound. After purification, the product was dried for 24h over solid K_2CO_3 under vacuum before proceeding to the next synthetic step.

3-(1-Methoxymethylindol-3-yl)carbonyl-4-methoxycarbonylquinoline **(2.55)**

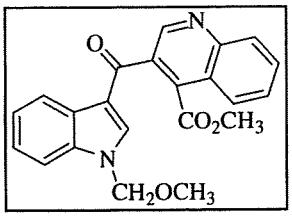

The title compound was prepared from **2.26** using the general procedure outlined above. Purification *via* column chromatography (1:1 EtOAc/light petroleum) followed by recrystallization from acetone/*n*-hexane gave the desired compound as a white powder (1.0g, 2.7mmol, 90% yield).

R_f 0.45 (1:1 EtOAc/light petroleum).

Mp 163°C.

^{1}H NMR ($CDCl_3$): δ3.18 (s, 3H, OCH_3), 3.64 (s, 3H, OCH_3), 5.33 (s, 2H, NCH_2), 7.30 (m, 2H, Ar-**H**), 7.44 (m, 2H, Ar-**H**), 7.60 (app. t, J_{app}= 8Hz, 1H, Ar-**H**), 7.77 (app. t, J_{app}= 8Hz, 1H, Ar-**H**), 8.05 (d, J= 8Hz, 1H, Ar-**H**), 8.13 (d, J= 8Hz, 1H, Ar-**H**), 8.36 (d, J= 8Hz, 1H, Ar-**H**), 9.13 (s, 1H, Ar-**H**).

^{13}C NMR ($CDCl_3$): δ52.9 (OCH_3), 56.3 (OCH_3), 78.3 (NCH_2), 110.6, 117.1, 122.6, 123.5, 123.6, 124.6, 125.7, 126.7, 128.5, 129.7, 131.1, 131.6, 136.8, 137.3, 137.8, 148.8, 166.9 (CO_2CH_3), 187.8 (**C**O).

UV-Vis (CH_2Cl_2) $\varepsilon_{247\ nm}$= 33008 M^{-1}.

IR (KBr disk) ν_{max} cm^{-1} 752 m, 1027 m, 1094 s, 1120 m, 1222 s, 1266 s, 1389 s, 1525 s, 1619 s, 1728 s, 2951 w, 3119 w, 3435 br.

EIMS *m/z* (rel. A): 374 ($\mathbf{M^{+\cdot}}$, 100), 343 ($[\mathbf{M}\text{-}OCH_3]^+$, 27), 188 (55), 143 (52), 128 (19), 100 (49).

HRMS Calculated 374.1267 for $C_{22}H_{18}N_2O_4$, found 374.1266.

Analytical Anal. Calcd for $C_{22}H_{18}N_2O_4$: C, 70.58; H, 4.85; N, 7.48. Found: C, 70.52; H, 4.80; N, 7.28.

3-(1-Methoxymethyl-5-methoxyindol-3-lyl)carbonyl-4-methoxycarbonylquinoline (**2.67**)

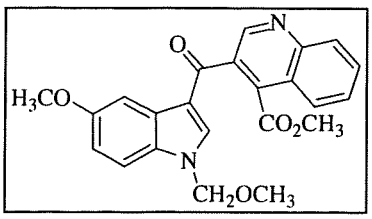

The title compound was prepared from **2.66** using the general procedure outlined above. Purification *via* column chromatography using two solvent systems (100mL of 1:1 EtOAc/light petroleum, then 99:1 EtOAc/MeOH) followed by recrystallization from hot ether gave the desired compound as a white powder (1.19g, 2.9mmol 98% yield).

R_f 0.30 (1:1 EtOAc/light petroleum); 0.74 (EtOAc).

Mp 67-68°C.

^{1}H-NMR ($CDCl_3$): δ3.28 (s, 3H, OCH_3), 3.78 (s, 3H, OCH_3), 3.94 (s, 3H, OCH_3), 5.41 (s, 2H, NCH_2), 7.03 (dd, *J*= 2Hz and 9Hz, 1H, Ar-**H**), 7.45 (d, *J*= 9Hz, 1H, Ar-**H**), 7.47 (s, 1H, Ar-**H**), 7.74 (app. t, J_{app}= 8Hz, 1H, Ar-**H**), 7.90 (app. t, J_{app}= 8Hz, 1H, Ar-**H**), 7.97 (d, *J*= 2Hz, 1H, Ar-**H**), 8.17 (d, *J*= 8Hz, 1H, Ar-**H**), 8.31 (d, *J*= 9Hz, 1H, Ar-**H**), 9.25 (s, 1H, Ar-**H**).

^{13}C-NMR ($CDCl_3$): δ53.2 (OCH_3), 55.8 (OCH_3), 56.4 (OCH_3), 78.6 (NCH_2), 103.76, 103.79, 103.83, 111.6, 115.2, 116.6, 123.8, 125.9, 127.7, 129.0, 131.6, 137.4, 138.9, 147.8, 148.1, 157.2, 166.7 ($\mathbf{CO_2}CH_3$), 187.2 (**CO**).

EIMS *m/z* (rel. A): 404 ($\mathbf{M^{+\cdot}}$, 100), 373 ($[\mathbf{M}\text{-}OCH_3]^+$,18), 218 (25), 214 (30), 45 (61)

IR (KBr disk) ν_{max} cm^{-1} 798 m, 1034 m, 1094 s, 1219 m, 1268 s, 1486 m, 1624 s, 1772 s, 2834 w, 1938 w, 2938 w, 3431 br.

HRMS Calculated 404.1372 for $C_{23}H_{20}N_2O_5$ found 404.1372.

Analytical Anal. Calcd for $C_{23}H_{20}N_2O_5$ C, 68.31; H, 4.98; N, 6.93; Found C, 68.15; H, 5.16; N, 6.75.

1-Methoxymethyl-3-(1-methoxycarbonylbenzene-2-lyl)carbonylindole **(2.74)**

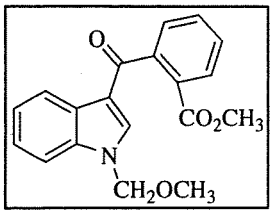

The title compound was prepared from **2.73** using the general procedure outlined above. Purification *via* column chromatography (1:1 EtOAc/light petroleum) followed by recrystallization from acetone/*n*-hexane gave the desired compound as a white powder in 93% yield.

R_f 0.52 (1:1 EtOAc/light petroleum).

Mp 128°C.

^{1}H NMR ($CDCl_3$): δ3.23 (s, 3H, OCH_3), 3.62 (s, 3H, OCH_3), 5.41 (s, 2H, NCH_2), 7.31 (m, 3H, Ar-**H**), 7.50-7.65 (m, 4H, Ar-**H**), 8.01 (d, *J*= 6Hz, 1H, Ar-**H**), 8.34 (m, 1H, Ar-**H**).

^{13}C NMR ($CDCl_3$): δ52.2 (OCH_3), 56.2 (OCH_3), 78.1 (NCH_2), 110.4, 118.0, 122.6, 123.2, 124.1, 126.8, 127.8, 129.3, 129.4, 130.1, 132.0, 136.3, 137.0, 142.8, 167.1 (**C**O), 191.3 (**C**O).

EIMS *m/z* (rel. A): 323 ($M^{+\cdot}$, 100), 292 ($[M-OCH_3]^+$, 51), 188 (74), 163 (42), 158 (23), 77 (18).

IR (KBr disk) ν_{max} cm^{-1} 759 m, 1041 m, 1102 m, 1179 m, 1228 m, 1275 s, 1388 m, 1458 w, 1528 m, 1640 s, 1712 s, 22937 w, 2996 w, 3092 w.

HRMS Calculated 323.1158 for $C_{19}H_{17}NO_4$, found 323.1153.

Analytical Anal. Calcd for $C_{19}H_{17}NO_4$: C, 70.58; H, 5.30; N, 4.33. Found: C, 70.34; H, 5.54; N, 4.16.

1-Methoxymethyl-3-(4-methoxycarbonylpyridine-3-yl)carbonylindole **(2.69)**

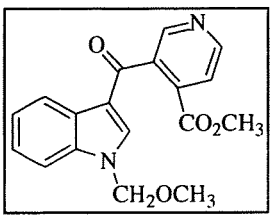

The title compound was prepared from **2.68** using the general procedure outlined above. Concentration of the filtrate gave a pale brown solid, which upon flash chromatography with EtOAc gave the title compound as a fine white solid in 90% yield.

R_f 0.24 (1:1 EtOAc/light petroleum); 0.40 (EtOAc).

Mp 126°C.

^{1}H-NMR ($CDCl_3$): δ3.26 (s, 3H, OCH_3), 3.71 (s, 3H, OCH_3), 5.41 (s, 2H, NCH_2), 7.38 (m, 3H, Ar-**H**), 7.51 (m, 1H, Ar-**H**), 7.80 (d, *J*= 5Hz, 1H, Ar-**H**), 8.37 (app. t, J_{app}= 4Hz, 1H, Ar-**H**), 8.85 (br s, 2H, Ar-**H**).

^{13}C-NMR ($CDCl_3$): δ52.9 (OCH_3), 56.3 (OCH_3), 78.2 (NCH_2), 110.5, 117.7, 122.6, 123.1, 123.5, 124.5, 126.6, 136.1, 136.7, 137.0, 137.3, 148.9, 151.2, 165.7 (CO_2CH_3), 188.2 (**C**O).

EIMS *m/z* (rel. A): 324 ($M^{+\cdot}$, 100), 293 ($[M-OCH_3]^+$, 48), 188 (72), 164 (26).

IR (KBr disk) ν_{max} cm^{-1} 661 m, 757 m, 880 w, 1092 s, 1120 m, 1190 w, 1228 m, 1286 s, 1383 s, 1533 s, 1642 s, 1733 s, 2941 w, 3115 w.

HRMS Calculated 324.1110 for $C_{18}H_{16}N_2O_4$, found 324.1112.

Analytical Anal. Calcd for $C_{18}H_{16}N_2O_4$: C, 66.66; H, 4.97; N, 8.64. Found: C, 66.46; H, 4.93; N, 8.51.

6.2.7 Procedures for *N*-Acylation and *N*-Sulfonation of the Indole Derivatives

3-(1-Acetylindol-3-yl)carbonyl-4-methoxycarbonylquinoline **(2.53)**

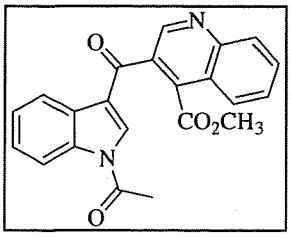

To a solution of 3-(3-indolyl)carbonyl-4-methoxycarbonyl quinoline (**2.26**) (0.50g, 1.5mmol) in dry THF (50mL) at 0°C was added NaH (72mg, 3mmol). The suspension was warmed to room temperature over 30min and a bright red colour was observed. The suspension was then cooled to 0°C and acetyl chloride (0.21mL, 3.6mmol) was added. The suspension was warmed to room temperature and stirred for 16 h. The reaction mixture was then poured into a saturated $NaHCO_3$ solution (50mL) and the organic layer was separated. The product was further extracted from the aqueous layer with CH_2Cl_2 (3x10mL). The combined organic layers were then dried with $MgSO_4$ and filtered, and the solvent was removed *in vacuo* to yield the desired compound in quantitative yield. Purification via silica chromatography (1:1 EtOAc/light petroleum) gave the desired compound as an orange solid (0.10g, 0.27mmol, 18% yield). The product is unstable and readily undergoes hydrolysis to 3-(3-indolyl)carbonyl-4-methoxycarbonylquinoline (**2.26**).

R_f 0.61 (1:1 EtOAc/light petroleum).

MP 50-53°C.

^{1}H NMR ($CDCl_3$): δ2.63 (s, 3H, CH_3), 3.72 (s, 3H, OCH_3), 7.49 (m, 2H, Ar-**H**), 7.76 (m, 2H, Ar-**H**), 7.91 (app. t, J_{app}= 8Hz, 1H, Ar-**H**), 8.17 (d, *J*= 8Hz, 1H, Ar-**H**), 8.25 (d, *J*= 8Hz, 1H, Ar-**H**), 8.38 (d, *J*= 8Hz, 1H, Ar-**H**), 8.47 (d, *J*= 8Hz, 1H, Ar-**H**), 9.23 (s, 1H, Ar-**H**).

^{13}C NMR ($CDCl_3$): δ23.9 (**CH_3**), 53.1 (**OCH_3**), 116.4, 121.1, 122.3, 123.4, 125.6, 126.0, 126.9, 127.1, 128.8, 129.9, 130.6, 131.7, 133.6, 136.1, 138.3, 148.6, 149.3, 166.8 (**NCO**), 168.7 (**CO_2CH_3**), 188.7 (**CO**).

3-(1-Phenylsulfonylindol-3-yl)carbonyl-4-methoxycarbonylquinoline **(2.54)**

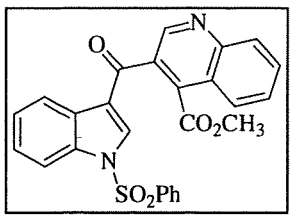

To a cold solution of **2.26** (0.10g, 0.3mmol) in dry THF (15mL) was added NaH (16mg, 0.67mmol). The reaction mixture was stirred at room temperature for 30 min, and then cooled to 0°C prior to the addition of phenylsulfonyl chloride (77μL, 0.6mmol). The reaction mixture was stirred for 16 hours at room temperature, then poured into an ice-water mixture (15mL). The organic layer was separated, and the aqueous layer was further extracted with CH_2Cl_2 (10mL). The combined organic layers were washed with saturated NaCl solution (10mL), dried with Na_2SO_4 and filtered. The solvent was then removed under reduced pressure, and the product was purified via column chromatography on silica (1:1 EtOAc/light petroleum). The product was obtained as a pale green oil (0.122g, 0.26mmol, 87% yield).

R_f 0.61 (1:1 EtOAc/light petroleum).

^{1}H NMR ($CDCl_3$): δ3.62 (s, 3H, **OCH_3**), 7.45 (m, 3H, Ar-**H**), 7.55 (app. t, J_{app}=7Hz, 1H, Ar-**H**), 7.63 (d, J= 7Hz, 1H, Ar-**H**), 7.93 (app. t, J_{app}= 7Hz, 1H, Ar-**H**), 8.00 (d, J= 5Hz, 2H, Ar-**H**), 8.20-8.28 (m, 2H, Ar-**H**), 8.39 (m, 1H, Ar-**H**), 9.20 (s, 1H, Ar-**H**).

^{13}C NMR ($CDCl_3$): δ52.9 (**OCH_3**), 113.2, 120.9, 123.0, 123.4, 125.2, 126.0, 126.4, 127.3, 127.5, 128.8, 129.7, 130.0, 130.5, 131.6, 134.2, 134.7, 134.9, 137.1, 138.1, 148.5, 149.4, 166.5 (**CO_2CH_3**), 188.5 (**CO**).

3-(1-Phenylsulfonylindol-3-yl)carbonyl-4-methoxycarbonylpyridine **(2.15)**

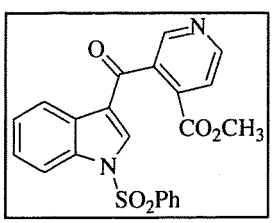

To a stirred solution of 3-(4-methoxycarbonylpyridine-3-yl) carbonylindole **(2.68)** (0.25g, 0.89mmol) in dry THF (50mL) at 0°C was added NaH (26mg, 1.1mmol). The reaction mixture was stirred for 30min prior to the addition of phenylsulfonyl

chloride (0.14ml, 1.1mmol). The reaction mixture was warmed to room temperature and stirred for a further 16h. The reaction mixture was then poured into cold saturated $NaHCO_3$ solution (50mL) and the organic layer was separated. The aqueous layer was further extracted with ethyl acetate (3x10mL). The combined organic layers were dried with Na_2SO_4, filtered, and the solvent removed *in vacuo*. The solid was purified using column chromatography on silica (2:3 EtOAc/light petroleum) to yield the product as a white solid (0.30g, 0.71mmol, 80% yield)

R_f 0.53 (2:3 EtOAc/light petroleum).

MP 147-149°C (lit. 146-149°C). [5]

^{1}H NMR ($CDCl_3$): δ3.51 (s, 3H, OCH_3), 7.40-8.39 (m, 14H, Ar-**H**).

6.2.8 General Lithiation of *N*-MOM Protected Quinone Precursors

Lithium hexamethyldisilazide (LHMDS) was prepared immediately prior to use by adding *n*-BuLi (0.60mL, 2.6M in THF, 1.57mmol) to a solution of hexamethyldisilazane (0.33mL, 1.57mmol) in dry ether (10mL) and stirring for 1h at room temperature. The LHMDS precipitated as white crystals in ether. The solvent was then removed using a stream of dry nitrogen, and the solid was dissolved in cold dry THF (10mL) at 0°C to produce a 0.15M solution of LHMDS. The general lithiation procedure is as follows:

To a solution of the quinone precursors (typically 0.2 to 0.4g, 0.72mmol) in dry THF (60mL) and TMEDA (0.11mL, 0.72mmol) at –78°C under nitrogen was added a solution of LHMDS (10mL, 0.15M, 1.5mmol). The reaction mixture was stirred for 2h at –78°C then slowly warmed to 0°C over 30 min and stirred for a further 2h. The reaction was quenched by the addition of saturated $NaHCO_3$ solution (50mL). The organic layer was separated and the aqueous layer was further extracted with EtOAc (2x50mL portions). The combined organic layers were washed with saturated NaCl solution (50mL) then dried with $MgSO_4$ and filtered. The solvent was removed under reduced pressure to yield the desired crude product.

N-*Methoxymethyl Calothrixin B* (**2.25**)

The title compound was prepared from 3-(1-methoxymethyl-5-methoxyindol-3-yl)carbonyl-4-methoxycarbonylquinoline

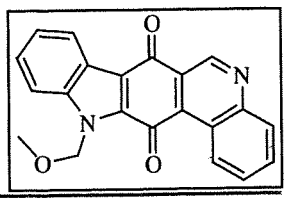

(**2.55**) following the general procedure above. Column chromatography on silica (2:3 EtOAc/*n*-hexane) followed by recrystallization from hot EtOAc and hexane gave the desired product as an amorphous orange solid (0.23g, 0.67 mmol, 92% yield). The spectroscopic data obtained are similar to the values reported in the literature.

R_f 0.59 (2:3 EtOAc/*n*-hexane).

Mp 233-234°C (lit. 234-235°C).[9]

^{1}H NMR ($CDCl_3$): δ3.44 (s, 3H, OCH_3), 6.16 (s, 2H, NCH_2), 7.45 (app. t, J_{app}= 8Hz, 1H, Ar-**H**), 7.53 (app. t, J_{app} = 8Hz, 1H, Ar-**H**), 7.65 (d, J= 9Hz, 1H, Ar-**H**), 7.79 (app. t, J_{app}= 7Hz, 1H, Ar-**H**), 7.86 (app. t, J_{app}= 7Hz, 1H, Ar-**H**), 8.24 (d, J= 8Hz, 1H, Ar-**H**), 8.44 (d, J= 8Hz, 1H, Ar-**H**), 9.60 (d, J= 8Hz, 1H, Ar-**H**), 9.79 (s, 1H, Ar-**H**).

^{13}C-NMR ($CDCl_3$): δ56.7 (OCH_3), 75.5 (NCH_2), 111.9, 118.6, 123.1, 123.2, 123.9, 124.2, 125.4, 127.7, 128.3, 130.279, 130.337, 131.6, 133.4, 135.5, 140.2, 147.7, 152.1, 181.3 (**C**O), 182.1 (**C**O).

EIMS *m/z* (rel. A): 342 ($M^{+\cdot}$, 100), 327 ($[M-CH_3]^+$, 45), 299 (64).

HRMS Calculated 342.1004 for $C_{21}H_{14}N_2O_3$, found 342.1000.

Analytical Anal. Calcd for $C_{21}H_{14}N_2O_3$: C, 73.68; H, 4.12; N, 8.18. Found: C, 73.67; H, 4.16; N, 8.41.

9-Methoxy-N-*methoxymethyl Calothrixin B* (**2.64**)

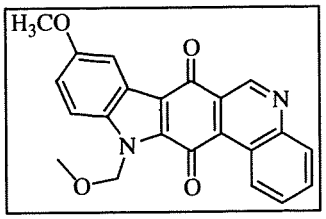

The title compound was prepared from 3-(1-methoxy methyl-5-methoxyindol-3-yl)-carbonyl-4-methoxycarbonyl quinoline (**2.67**) following the general procedure above with the following modifications: To a solution of **2.67** (90mg, 0.22mmol) in dry ether (20mL) at –78°C under nitrogen was added a suspension of LHMDS (2eq) in dry ether (5mL). The reaction mixture was slowly warmed to room temperature. After stirring for a further 1h, the reaction mixture was quenched by the addition of saturated $NaHCO_3$ solution (10mL). The organic layer was separated and the aqueous layer was further extracted thrice with EtOAc (20mL each). The combined organic layers were washed with brine (50mL) and dried with $MgSO_4$. The solvent was removed *in vacuo* to obtain the crude product. Column chromatography on silica (2:3 EtOAc/*n*-hexane) gave the desired product as a dark red solid (42mg, 0.11mmol, 51% yield).

R_f 0.48 (2:3 EtOAc/*n*-hexane).

Mp 238°C.

^{1}H-NMR (*d*-DMSO, 90°C, 500MHz): δ3.38 (s, 3H, OC**H**$_3$), 3.90 (s, 3H, OC**H**$_3$), 6.10 (s, 2H, NC**H**$_2$), 7.21 (d, *J*= 9Hz, 1H, Ar-**H**), 7.73 (s, 1H, Ar-**H**), 7.76 (d, *J*= 9Hz, 1H, Ar-**H**), 7.85 (br s, 1H, Ar-**H**), 7.93 (br s, 1H, Ar-**H**), 8.16 (d, *J*= 8Hz, 1H, Ar-**H**), 9.49 (d, *J*= 8Hz, 1H, Ar-**H**), 9.61 (s, 1H, Ar-**H**).

^{13}C-NMR (*d*-DMSO, 90°C, 125MHz): δ55.3 (OCH$_3$), 55.7 (OCH$_3$), 74.9 (NCH$_2$), 102.6, 113.5, 118.6, 126.9, 129.5, 129.6, 131.1, 133.1, 151.2, 157.5, 180.5. Due to poor solubility and poor S/N ratio, the other carbon signals could not be detected.

UV-Vis (CH_2Cl_2) $\varepsilon_{284\ nm}$= 42624 M^{-1}.

IR (KBr disk) ν_{max} cm^{-1} 771 m, 1030 m, 1061 m, 1081 s, 1120 m, 1198 m, 1260 m, 1400 w, 1458 m, 1479 m, 1496 m, 1520 s, 1568 w, 1643 s, 2930 w, 3433 br.

EIMS *m/z* (rel. A): 372 ($M^{+\cdot}$, 100), 357 ($[M-CH_3]^+$, 27), 341 (16), 329 (43).

HRMS Calculated 372.1110 for $C_{22}H_{16}N_2O_4$ found 372.1109.

Analytical Anal. Calcd for $C_{22}H_{16}N_2O_4$: C, 70.96; H, 4.33; N, 7.52. Found: C, 70.63; H, 4.59; N, 7.32.

N-*Methoxymethyl-5H-benzo[b]carbazole-6,11-dione* (**2.75**)

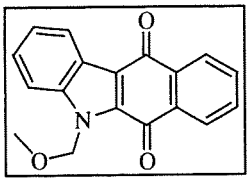

The title compound was prepared from 1-methoxymethyl-3-(1-methoxycarbonylbenzene-2-yl)carbonylindole (**2.74**) following the general procedure. Column chromatography on silica (1:2 EtOAc/light petroleum) followed by recrystallization from Et_2O/*n*-hexane gave the desired compound as a yellow solid (0.174g, 0.60mmol, 88% yield).

R_f 0.58 (1:2 EtOAc/light petroleum).

Mp 143-145°C.

^{1}H-NMR ($CDCl_3$): δ3.39 (s, 3H, OC**H**$_3$), 6.18 (s, 2H, NC**H**$_2$), 7.43 (app. t, J_{app}= 7Hz, 1H, Ar-**H**), 7.51 (app. t, J_{app}= 7Hz, 1H, Ar-**H**), 7.65 (d, *J*= 8Hz, 1H, Ar-**H**), 7.73 (m, 2H, Ar-**H**), 8.17-8.24 (m, 2H, Ar-**H**), 8.49 (d, *J*= 8Hz, 1H, Ar-**H**).

^{13}C-NMR ($CDCl_3$): 56.5 (OCH$_3$), 75.3 (NCH$_2$), 111.9, 120.2, 123.9, 124.0, 124.9, 126.3, 126.6, 127.9, 133.0, 133.5, 133.7, 133.9, 135.1, 139.8, 179.0 (**C**O), 181.6 (**C**O).

IR (KBr disk) ν_{max} cm^{-1} 714 m, 746 m, 1061 w, 1080 w, 1117 w, 1230 s, 1260 m, 1522 m, 1658 s, 2930 w, 3436 br.

EIMS *m/z* (rel. A): 291 ($M^{+\cdot}$, 93), 276 ($[M-CH_3]^+$, 91), 260 ($[M-OCH_3]^+$, 31), 248 (100), 190 (24).

HRMS Calculated 291.0895 for $C_{18}H_{13}NO_3$, found 291.0897.

Analytical Anal. Calcd for $C_{18}H_{13}NO_3$: C, 74.22; H, 4.50; N, 4.81. Found: C, 74.21; H, 4.45; N, 4.61.

N-*Methoxymethyl-6H-pyrido[4,3-b]carbazole-5,11-dione* (**2.21**)

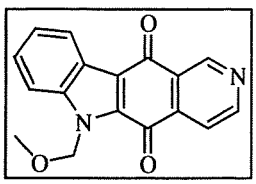

The title compound was prepared from 1-methoxymethyl-3-(4-methoxycarbonylpyridine-3-yl)carbonylindole (**2.69**) (0.35g, 1.1mmol) following the general procedure. Column chromatography (1:1 EtOAc/light petroleum followed by pure EtOAc) afforded pure *N*-MOM-ellipticine quinone as a yellow solid (0.11g, 0.38mmol, 35% yield).

R_f 0.47 (2:1 EtOAc/light petroleum).

Mp 195°C (lit. 196-7°C).[10]

^{1}H-NMR ($CDCl_3$): δ3.39 (s, 3H, OCH_3), 6.15 (s, 2H, NCH_2), 7.47 (app. t, J_{app}= 6Hz, 1H), 7.56 (app. t, J_{app}= 6Hz, 1H, Ar-**H**), 7.67 (d, *J* =9Hz, 1H, Ar-**H**), 7.99 (d, *J*= 9Hz, 1H, Ar-**H**), 8.49 (d, *J*= 8Hz, 1H, Ar-**H**), 9.06 (d, *J*= 5Hz, 1H, Ar-**H**), 9.46 (s, 1H, Ar-**H**).

^{13}C-NMR ($CDCl_3$): δ56.6 (OCH_3), 75.4 (NCH_2), 112.0, 120.3, 123.7, 124.1, 125.4, 128.7, 134.4, 139.4, 140.2, 148.2, 154.9, 177.7 (**C**O), 180.9 (**C**O).

IR (KBr disk) ν_{max} cm^{-1} 759 w, 1029 m, 1119 m, 1223 m, 1242 m, 1263 m, 1336 w, 1400 w, 1470 m, 1511 m, 1586 w, 1652 s, 1668 s, 3433 br.

EIMS *m/z* (rel. A): 292 ($M^{+\cdot}$, 100), 277 ($[M-CH_3]^+$, 53), 262 (46), 249 (61).

HRMS Calculated 292.0842 for $C_{17}H_{12}N_2O_3$, found 292.0843.

Analytical Anal. Calcd for $C_{17}H_{12}N_2O_3$: C, 69.86; H, 4.14; N, 9.58. Found C, 69.68; H, 3.89; N, 9.82.

6.2.9 Procedures for the Synthesis of *N*-Unsubstituted Carbazolediones

Most of the *N*-unsubstituted carbazolediones were synthesized by removing the *N*-MOM group of the respective *N*-MOM carbazolediones. The individual procedures for

the deprotection of the *N*-MOM group of the carbazolediones are reported below. Procedures for the synthesis of the parent carbazolediones by cyclization of the *N*-phenylsulfonyl precursors are also given. The purity of the samples were determined either by elemental analysis or HPLC under two different solvent systems. Where HPLC is the method for assessing purity, the conditions are as follows:

System 1: For HPLC, a Hewlett Packard HP 1050 Series System with a Phenomenex Hypersil 5μ C18 column (250x4.60mm) and a spectroscopic detector operating at 254nm with a flow rate of 1mL/min was used. Two solvent systems were employed: 1% aqueous orthophosphoric acid and methanol in a ratio of 7:3 (A) and methanol (B). The samples were eluted starting with 100%A which was lowered to 42% A (58% B) over 15min, then to 100%B within a further 15min followed by isocratic elution in 100% B for a further 10 min.

HPLC Solvent Program for System1

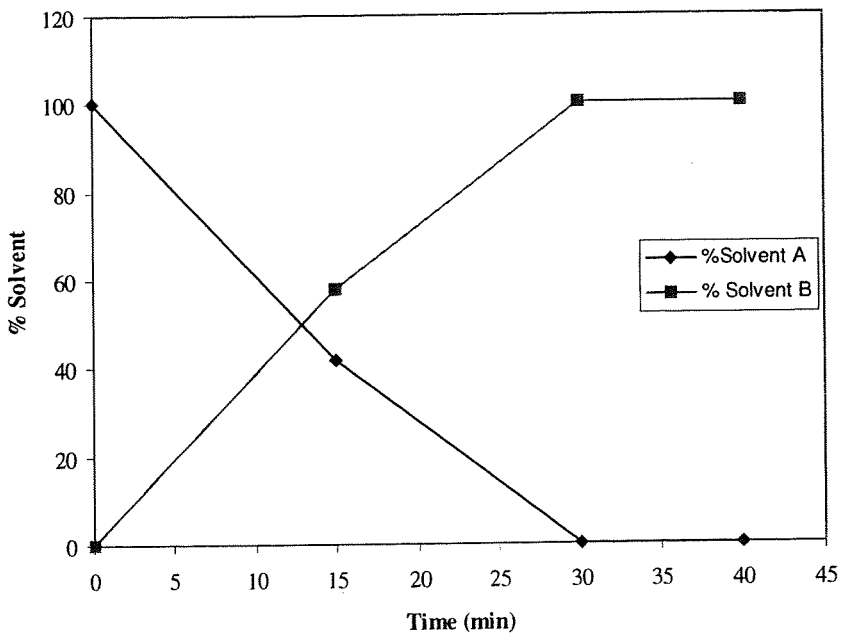

System 2: For HPLC, an Agilent 1100 Series HPLC machine using a Phenomenex Hypersil 5μ C18 column (250x4.60mm) and a spectroscopic detector operating at 254nm with a flow rate of 1mL/min was used. Two solvent systems were used, Solvent A was 0.1% trifluoroacetic acid and Millipore H_2O and Solvent B was 0.1%

trifluoroacetic acid and HPLC-grade CH_3CN. The solvent was run at 5% B for 5min and then raised to 95% B within 55 min, followed by isocratic elution in 95% B for a further 10min, and finally lowered to 5% B over 10 min.

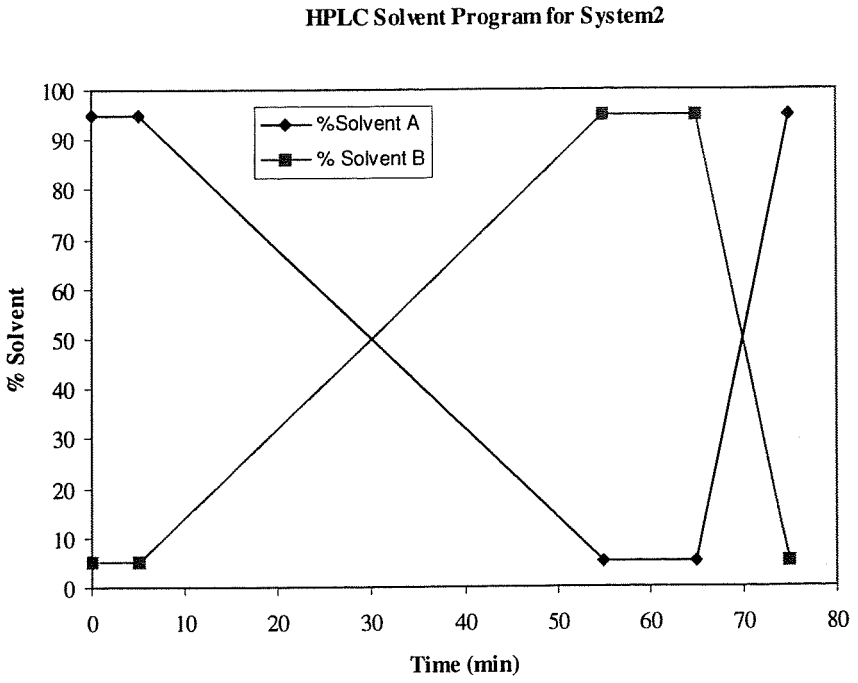

Calothrixin B **(1.27)**

Method 1: Attempted Synthesis of Calothrixin B from **2.54**

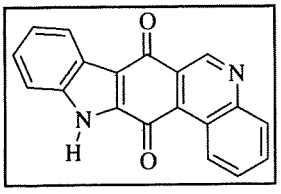

To a stirred solution of 3-(1-phenylsulfonylindol-3-yl) carbonyl -4-methoxycarbonylquinoline **(2.54)** (0.10g, 0.21mmol) in dry THF (20mL) was added TMEDA (32μL, 0.21mmol). The solution was cooled to -78°C, and a solution of LDA (1.8M in hexane, 0.26mL, 0.47mmol) was added. The reaction mixture was stirred for 1h at -78°C, then warmed to room temperature and stirred further for 4h. The reaction was quenched by the addition of saturated $NaHCO_3$ solution (20mL) and the organic layer was separated. The aqueous layer was further extracted with ethyl acetate (20mL), and the combined organic layers were dried with Na_2SO_4, filtered, and the solvent removed *in vacuo*. ^1H NMR analysis of the crude product in $CDCl_3$ showed only the presence of 3-(3-indolyl)carbonyl-4-methoxycarbonylquinoline **(2.26)**. Analysis of the crude

product by TLC against authentic calothrixin B also showed no trace of the desired product.

Method 2: Attempted Synthesis of Calothrixin B from **2.25**

An attempt was made to prepare the title compound following the procedure reported by Kelly.[9] To a solution of *N*-methoxymethyl calothrixin B (**2.25**) (7mg, 0.02mmol) in THF (3mL) was added concentrated hydrochloric acid (12M, 1mL) at room temperature. The reaction mixture was stirred at 55°C for 48h. Analysis of the reaction mixture by TLC, however, showed only starting material.

Method 3: Synthesis of Calothrixin B from **2.25**

To a solution of *N*-methoxymethyl calothrixin B (**2.25**) (7mg, 0.02mmol) in DMSO (1mL) was added concentrated hydrochloric acid (12M, 1mL) at room temperature. The reaction mixture was stirred at 100°C for 16h. The reaction mixture was then cooled to room temperature, and the solvent was removed *in vacuo* to obtain a brown solid. The solid was purified via flash chromatography on silica (1:2 EtOAc/light petroleum) to obtain calothrixin B as a red solid (5mg, 0.016mmol, 83% yield). This result, however, was not reproducible as variable yields were obtained on larger scales.

Method 4: Synthesis of Calothrixin B from **2.25**

To a solution of *N*-methoxymethyl calothrixin B (**2.25**) (55mg, 0.16mmol) in dry CH_2Cl_2 (10mL) at 0°C under nitrogen was added a solution of BBr_3 (1M solution in hexanes, 190μL, 0.19mmol). The solution was warmed to room temperature and stirred for 30min. To the reaction mixture was added saturated $NaHCO_3$ solution (10mL), and the mixture was stirred vigorously at 55°C for 1h. The organic layer was separated, and the aqueous layer was extracted with $CHCl_3$ (50mL). The combined organic layers were dried with $MgSO_4$ and the solvent was removed *in vacuo*. Flash chromatography (EtOAc) gave the desired product as a red solid. The product was recrystallised from hot acetone as a red powder (41mg, 0.14mmol, 85% yield). Comparison of the product with authentic calothrixin B using thin layer chromatography in various solvent systems (1:2 EtOAc/light petroleum, 1:1 EtOAc/light petroleum, and MeOH) showed the compounds were identical. The purity of the sample was confirmed by HPLC in 2 different solvent systems.

R_f 0.47 (1:2 EtOAc/light petroleum).

Mp ≥300°C (lit.≥300°C).[11]

^{1}H NMR (*d*-DMSO): δ7.39 (app. t, J_{app}= 7Hz, 1H, Ar-**H**), 7.47 (app. t, J_{app}= 7Hz, 1H, Ar-**H**), 7.62 (d, *J*= 7Hz, 1H, Ar-**H**), 7.89 (app. t, J_{app}= 7Hz, 1H, Ar-**H**), 7.96 (app. t, J_{app}= 7Hz, 1H, Ar-**H**), 8.17 (d, *J*= 9Hz, 2H, Ar-**H**), 9.58 (d, *J*= 9Hz, 1H, Ar-**H**), 9.62 (s, 1H, Ar-**H**).

EIMS *m/z* (rel. A): 298 (**M**$^{+\cdot}$, 100), 270 ([**M**-CO]$^+$, 17), 242 (12), 214 (10), 149.1 (10).

HRMS Calculated 298.0742 for $C_{19}H_{10}N_2O_2$, found 298.0741.

Purity **System 1: Retention time:** 28.3min.

System 2: Retention time: 39.5min.

5H-Benzo[b]carbazole-6,11-dione **(1.32)**

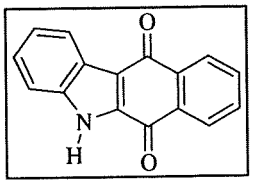

To a stirred solution of *N*-methoxymethyl-5*H*-benzo[b] carbazole-6,11-dione **(2.75)** (42mg, 0.14mmol) in CH_2Cl_2 (10mL) at -78°C under nitrogen was added BBr_3 (1.0M solution in hexanes, 0.28mL, 0.28mmol). The reaction mixture was stirred at room temperature for 1h following which saturated $NaHCO_3$ solution (10mL) was added to the reaction mixture. The reaction mixture was stirred vigorously at 60°C for 1h during which the organic layer had completely evaporated. The aqueous layer was extracted with EtOAc (3x20mL) and the combined organic layers were dried over Na_2SO_4, filtered and the solvent was removed *in vacuo* to give an orange solid. Purification by column chromatography (1:2 EtOAc/light petroleum) followed by recrystallization from ether/*n*-hexane afforded the desired compound as a fine orange solid (20mg, 0.078mmol, 57% yield).

R_f 0.34 (1:2 EtOAc/light petroleum).

Mp 300-303°C (lit. 307-310°C).[12]

^{1}H-NMR (*d*-DMSO): δ7.36 (app. t, J_{app}= 7Hz, 1H, Ar-**H**), 7.48 (app. t, J_{app}= 7Hz, 1H, Ar-**H**), 7.59 (d, *J*= 8Hz, 1H, Ar-**H**), 7.84 (m, 2H, Ar-**H**), 8.10 (app. t, J_{app}= 7Hz, 2H, Ar-**H**), 8.21 (d, *J*= 8Hz, 1H, Ar-**H**), 13.09 (s, 1H, N**H**).

^{13}C-NMR (*d*-DMSO): 113.9, 117.4, 122.4, 123.9, 124.0, 126.0, 126.1, 127.0, 132.6, 133.2 , 134.1 , 134.3 , 137.2 , 138.2 , 177.6 (**C**O), 180.4 (**C**O).

EIMS *m/z* (rel. A): 247 (**M**$^{+\cdot}$, 100), 219 ([**M**-CO]$^+$, 32), 190 (23).

HRMS Calculated 247.0633 for $C_{16}H_9NO_2$, found 247.0633.

Purity **System 1: Retention time:** 23.9min.

System 2: Retention time: 37.8min.

6H-Pyrido[4,3-b]carbazole-5,11-dione **(1.33)**

Method 1: Synthesis of Ellipticine Quinone from **2.21**

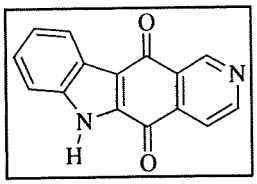

The compound was synthesized from *N*-methoxymethyl-6*H*-pyrido[4,3-*b*]carbazole-5,11-dione **(2.21)** following the methodology used in the synthesis of 5*H*-benzo[*b*]carbazole-6,11-dione **(1.32)**. Column chromatography on silica (1:2 EtOAc/ light petroleum) gave the desired compound as an orange solid (60mg, 0.24mmol, 71% yield).

Method 2: Synthesis of Ellipticine Quinone using **2.15**

To a stirred solution of 3-(1-phenylsulfonylindol-3-yl)carbonyl-4-carbomethoxy pyridine **(2.15)** (35mg, 0.08mmol) in dry THF (1mL) was added TMEDA (13μL, 0.08mmol). The solution was cooled to -78°C, and a solution of LHMDS (5M in THF, 32μL, 0.16mmol) was added. The reaction mixture was stirred for 2h at -78°C, then warmed to room temperature and stirred overnight. The reaction was quenched by the addition of saturated $NaHCO_3$ solution (5mL). The product was extracted from the aqueous layer with ethyl acetate (10mL), and the organic layer was dried with Na_2SO_4, filtered, and the solvent was removed under reduced pressure. Purification via column chromatography on silica (1:2 EtOAc/light petroleum) gave the desired product as an orange solid (10mg, 0.04mmol, 47% yield).

R_f 0.29 (1:2 EtOAc/light petroleum).

Mp ≥300°C (lit.315-316°C).[12]

^{1}H-NMR (*d*-DMSO): δ7.40 (app. t, J_{app}= 7Hz, 1H, Ar-**H**), 7.49 (app. t, J_{app}= 7Hz, 1H, Ar-**H**), 7.62 (d, *J*= 8Hz, 1H, Ar-**H**), 7.95 (d, *J*= 5Hz, 1H, Ar-**H**), 8.23 (d, *J*= 8Hz, 1H, Ar-**H**), 9.08 (d, *J*= 5Hz, 1H, Ar-**H**), 9.27 (s, 1H, Ar-**H**).

Analytical Anal. Calcd for $C_{17}H_{12}N_2O_3$: C, 72.58; H, 3.25; N, 11.28. Found: C, 71.95; H, 3.49; N, 11.25.

6.2.10 Synthesis of Calothrixin A (1.26)

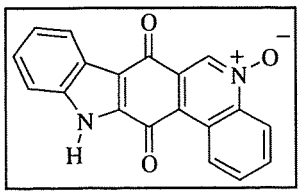

The title compound was prepared following the literature procedure.[9] To a solution of calothrixin B **(1.27)** (69mg, 0.23mmol) in CH_2Cl_2 (100mL) was added a solution of *m*-CPBA (600mg, 3.5mmol) in CH_2Cl_2 (100mL). The reaction mixture was refluxed for 14h. The resulting suspension was further diluted with CH_2Cl_2 (500mL) to obtain a bright red solution. The reaction mixture was then washed with saturated Na_2CO_3 solution (3x15mL), and distilled H_2O (15mL portions) until the pH of the aqueous layer was neutral. The organic layer was dried with Na_2SO_4 and the solvent was removed *in vacuo* to yield the crude product. Purification by column chromatography (1:2 EtOAc/light petroleum) followed by trituration with ether and recrystallization from methanol gave the title compound as a red solid (53mg, 0.17mmol, 73% yield).

R_f 0.47 (1:1 EtOAc/light petroleum).

Mp ≥280°C (lit.≥280°C).[11]

^{1}H NMR (*d*-DMSO): δ7.38 (app. t, J_{app}= 7Hz, 1H, Ar-**H**), 7.45 (app. t, J_{app}= 7Hz, 1H, Ar-**H**), 7.60 (d, *J*= 8Hz, 1H, Ar-**H**), 7.98 (app. t, *J*= 4Hz, 2H, Ar-**H**), 8.12 (d, *J*= 8Hz, 1H, Ar-**H**), 8.60 (d, *J*= 9Hz, 1H, Ar-**H**), 8.88 (s, 1H, Ar-**H**), 9.68 (d, *J*= 9Hz, 1H, Ar-**H**).

Analysis Anal. Calcd for $C_{19}H_{10}N_2O_3$: C, 72.61; H, 3.21; N, 8.91. Found C, 72.79; H, 3.33; N, 8.58.

6.2.11 Preparation of *N*-Substituted Calothrixins from Calothrixin B

N-Benzyl Calothrixin B **(2.58)**

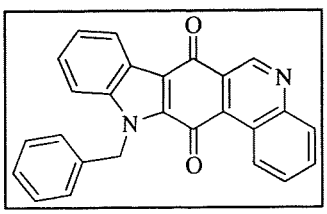

To a solution of calothrixin B **(1.27)** (55mg, 0.18mmol) in dry DMF (5mL) at 0°C under nitrogen was added NaH (9mg, 0.38mmol). After stirring for 1h at 0°C, benzyl bromide (44μL, 0.37mmol) was added, and the reaction mixture was warmed to room temperature. After stirring for 16h, the reaction was quenched by the addition of distilled water (5mL), and the solvent was removed *in vacuo*. The crude product was redissolved in ethyl acetate (30mL) and washed successively with saturated $NaHCO_3$ solution (10mL) and brine (10mL). The organic layer was dried with $MgSO_4$ and the solvent was removed under reduced pressure to

yield the crude product. Column chromatography on silica (1:1 EtOAc/light petroleum) yielded *N*-benzyl calothrixin B as an orange solid (61mg, 0.16mmol, 88% yield).

R_f 0.71 (1:1 EtOAc/light petroleum).

Mp 251-3°C.

^{1}H-NMR (*d*-DMSO, 80°C, 500 MHz): δ6.04 (s, 2H, NC**H**$_2$), 7.31 (m, 5H, Ar-**H**), 7.45 (app. t, J_{app}= 8Hz, 1H, Ar-**H**), 7.51 (app. t, J_{app}= 8Hz, 1H, Ar-**H**), 7.74 (d, *J*= 8Hz, 1H, Ar-**H**), 7.83 (app. t, J_{app}= 9Hz, 1H, Ar-**H**), 7.93 (app. t, J_{app}= 8Hz, 1H, Ar-**H**), 8.16 (d, *J*= 9Hz, 1H, Ar-**H**), 8.31 (d, *J*= 8Hz, 1H, Ar-**H**), 9.45 (d, *J*= 9Hz, 1H, Ar-**H**), 9.62 (s, 1H, Ar-**H**).

^{13}C-NMR (*d*-DMSO, 80°C, 125 MHz): δ47.7 (N**C**H$_2$), 112.2, 116.3, 122.2, 122.3, 123.9, 124.6, 126.3, 126.9, 127.1, 127.2, 128.2, 129.5, 129.7, 131.1, 133.0, 135.3, 136.4, 139.3, 146.8, 151.1, 180.1 (**C**O), 181.1 (**C**O).

EIMS *m/z* (rel. A): 388 (**M**$^{+\cdot}$, 96), 91 (100).

HRMS Calculated 388.1212 for $C_{26}H_{16}N_2O_2$, found 388.1209.

UV-Vis (CH_3CN) $\varepsilon_{284\ nm}$= 38230 M^{-1}.

IR (KBr disk) ν_{max} cm^{-1} 1078 m, 1244 m, 1466 m, 1496 m, 1525 m, 1653 s, 2925 w, 3431 br.

Analytical Anal. Calcd for $C_{26}H_{16}N_2O_2$: C, 80.40; H, 4.15; N, 7.21. Found: C, 80.33; H, 4.17; N, 7.31.

N-*Ethyl Calothrixin B* (**2.59**)

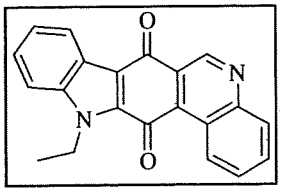

Sodium hydride (1mg, 0.042mmol) was added to a solution of calothrixin B (**1.27**) (5mg, 0.017mmol) in dry DMF (5mL) at 0°C under nitrogen. After stirring for 1h at 0°C, ethyl bromide (2.5μL, 0.033mmol) was added, and the reaction mixture was warmed to room temperature and stirred for 16h. The reaction was quenched by the addition of distilled water (5mL), and the solvent was removed *in vacuo*. The residue was redissolved in ethyl acetate (10mL) and washed successively with saturated $NaHCO_3$ solution (5mL) and brine (5mL). The organic layer was dried with $MgSO_4$ and the solvent was removed under reduced pressure to yield the crude product. Column chromatography on silica (1:1 EtOAc/light petroleum) gave the desired product as a red solid (3mg, 0.009mmol, 54% yield). The quantity obtained was insufficient to obtain a ^{13}C NMR spectrum.

R_f 0.74 (1:1 EtOAc/light petroleum).

Mp 269-270°C

^{1}H-NMR ($CDCl_3$): δ1.62 (m, 3H, CH_3), 4.80 (m, 2H, NCH_2), 7.41-7.54 (m, 3H, Ar-H), 7.78-7.88 (s, 2H, Ar-**H**), 8.20 (app. t, J_{app}= 7Hz, 1H, Ar-**H**), 8.43-8.51 (m, 1H, Ar-**H**), 9.72 (s, 1H, Ar-**H**), 9.82 (m, 1H, Ar-**H**).

EIMS *m/z* (rel. A): 326 ($M^{+\cdot}$, 100), 311 ($[M-CH_3]^+$, 68), 298 ($[M-CH_2CH_3]^+$, 27).

HRMS Calculated 326.1055 for $C_{21}H_{14}N_2O_2$ found 326.1053.

UV-Vis (CH_3CH) $\varepsilon_{289\ nm}$= 34237 M^{-1}.

IR (KBr disk) ν_{max} cm^{-1} 751 w, 779 w, 803 m, 1090 s, 1228 m, 1259 s, 1476 w, 1497 w, 1523 m, 1648 s, 1954 w, 2923 m, 3436 br.

Purity **System 1: Retention time:** 33.8min.

System 2: Retention time: 41.3min.

5,12-Dimethyl Calothrixin **(2.63)**

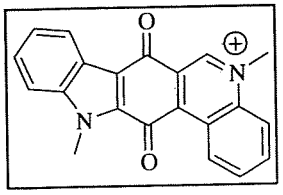

To a solution of calothrixin B **(1.27)** (55mg, 0.18mmol) in dry DMF (5mL) at 0°C under nitrogen was added NaH (9mg, 0.38mmol). After stirring for 1h at 0°C, iodomethane (23μL, 0.37mmol) was added, and the reaction mixture was warmed to room temperature. After stirring for 16h, the reaction was quenched by the addition of distilled water (5mL), and the solvent was removed *in vacuo*. The crude product was redissolved in ethyl acetate (30mL) and washed successively with saturated $NaHCO_3$ solution (10mL) and brine (10mL). The organic layer was dried with $MgSO_4$ and the solvent was removed under reduced pressure to yield the crude product. Column chromatography on silica (1:1 EtOAc/light petroleum) yielded 5,12-dimethyl calothrixin B as an orange solid (61mg, 0.16mmol, 88% yield).

R_f 0.63 (1:1 EtOAc/light petroleum).

Mp 69-70°C.

^{1}H-NMR ($CDCl_3$): δ3.03 (s, 3H, NCH_3), 4.14 (s, 3H, NCH_3), 7.45-7.53 (m, 3H, Ar-**H**), 7.78-7.85 (m, 2H, Ar-**H**), 8.23 (d, *J*= 8Hz, 1H, Ar-**H**), 8.52 (d, *J*= 8Hz, 1H, Ar-**H**), 9.41 (s, 1H, Ar-**H**), 9.99 (d, *J*= 8Hz, 1H, Ar-**H**).

^{13}C-NMR ($CDCl_3$): δ31.0 (NCH_3), 52.2 (NCH_3), 98.0, 110.1, 117.5, 122.5, 123.7, 124.2, 124.5, 125.2, 127.7, 129.0, 129.7, 130.8, 131.9, 135.9, 138.7, 140.2, 148.2, 181.9 (**C**O).

EIMS *m/z* (rel. A): 327 ($M^{+\cdot}$, 100), 313 ($[M-CH_3]^+$, 40), 283 (12), 255 (12), 86 (25), 84 (40).

HRMS Calculated 327.1134 for $C_{21}H_{15}N_2O_2$, found 327.1137.
Calculated 312.0899 for $C_{20}H_{12}N_2O_2$, found 312.0889.

UV-Vis (CH_3CN) $\varepsilon_{254\ nm}$= 32904 M^{-1}.

IR (KBr disk) ν_{max} cm^{-1} 718 w, 734 w, 774 m, 811 m, 967 w, 1016 m, 1074 m, 1112 m, 1247 s, 1304 m, 1340 m, 1372 w, 1432 m, 1455 m, 1610 m, 2837 w, 2934 w, 2960 w, 3436 br.

Purity **System 1: Retention time:** 27.9min.
System 2: Retention time: 45.1min.

Attempt Synthesis of N-*Acetyl calothrixin B* **(2.61)**

To a solution of calothrixin B **(1.27)** (20mg, 0.07mmol) in dry THF (5mL) at 0°C was added NaH (10mg, 0.42mmol). After stirring for 1h at 0°C, acetyl chloride (10μL, 0.14mmol) was added, and the reaction mixture was warmed to room temperature. After stirring for 16h, the reaction was quenched by the addition cold saturated $NaHCO_3$ solution (5mL), and the organic layer was separated. The aqueous layer was further extracted with ethyl acetate (10mL). The organic layer was dried with $MgSO_4$ and the solvent was removed under reduced pressure to yield the crude product. Column chromatography on silica (1:1 EtOAc/light petroleum) yielded *N*-acetyl calothrixin B as an orange solid (11mg, 0.03mmol, 47% yield). The product slowly hydrolyzed to calothrixin B and acetic acid and could not be characterized further. The synthesis of this compound was consequently abandoned.

R_f 0.70 (1:1 EtOAc/light petroleum).

MP 230-235°C.

^{1}H NMR ($CDCl_3$): δ2.84 (s, 3H, CH_3), 7.54-7.66 (m, 2H, Ar-**H**), 7.81-7.95 (m, 2H, Ar-**H**), 8.09 (d, *J*= 9Hz, 1H, Ar-**H**), 8.26 (d, *J*= 9Hz, 1H, Ar-**H**), 8.48 (d, *J*= 9Hz, 1H, Ar-**H**), 9.33 (d, *J*= 9Hz, 1H, Ar-**H**), 9.77 (s, 1H, Ar-**H**).

EIMS *m/z* (rel. A): 340 ($M^{+\cdot}$, 2), 298 ([M-Ac]$^+$, 78), 91 (100).

Attempted Synthesis of N-*Phenylsulfonyl Calothrixin B* **(2.62)**

To a solution of calothrixin B **(1.27)** (50mg, 0.17mmol) in dry THF (5mL) at 0°C was added NaH (8mg, 0.33mmol). After stirring for 1h at 0°C, phenylsulfonyl chloride (42μL, 0.33mmol) was added, and the reaction mixture was warmed to room temperature. After stirring for 16h, the reaction was quenched by the addition cold saturated $NaHCO_3$ (5mL), and the organic layer was separated. The aqueous layer was

further extracted with ethyl acetate (10mL). The organic layer was dried with $MgSO_4$ and the solvent was removed under reduced pressure to yield the crude product as a pale yellow solid. The solid turned dark red on prolonged exposure to air. The ^1H NMR spectrum of the solid was identical to that of calothrixin B. Due to the instability of the product, no further attempts were made to synthesize this compound.

6.2.12 Deuterium Labeling Studies of Metallated Indoles

Deuterium-labeling studies were carried out in order to determine the efficiency of the metallation reactions of *N*-tosyl-3-iodoindole. The metallated indoles were generated according to the procedures outlined below, and were consequently treated with D_2O. The level of deuterium incorporation was measured in the product, *N*-tosylindole **(2.46)**, via ^1H NMR spectroscopy by comparing the integral for the C3-H signal (δ6.60) and C2-H signal (δ7.55) to the integral of the methyl signal (3H at δ2.35). Deuteration of the C3- or C2- positions is reflected by a corresponding decrease in the integral for δ6.60 or δ7.55 respectively.

Lithiation of N-*Tosyl-3-iodoindole* **(2.47)**

To a solution of *N*-tosyl-3-iodoindole **(2.47)** (0.15g, 0.38mmol) in dry THF (15mL) at -100°C under nitrogen was added *n*-butyl lithium (0.30mL, 2.5M in THF, 0.76mmol). The reaction mixture was stirred for 10min before D_2O (1mL) was rapidly added to quench the reaction. The reaction mixture was warmed to room temperature and saturated $NaHCO_3$ solution (10mL) was added. The organic layer was separated and the aqueous layer was further extracted with CH_2Cl_2 (20mL). The combined organic layers were dried with Na_2SO_4, filtered, and the solvent removed *in vacuo* to obtain the crude product, *N*-tosylindole **(2.46)**. Integration of the ^1H-NMR spectrum of the product showed 75% D-incorporation at C3 and 25% D-incorporation at C2.

Lithiation of N-*Tosyl-3-iodoindole and Metal Exchange with* $ZnCl_2$

To a solution of *N*-tosyl-3-iodoindole **(2.47)** (0.15g, 0.38mmol) in dry THF (15mL) with anhydrous $ZnCl_2$ (0.20g, 1.5mmol) at –78°C under nitrogen was added *n*-butyl lithium (0.30mL, 2.5M in THF, 0.76mmol). The reaction mixture was stirred at room temperature for 1h before D_2O (1mL) was added rapidly to quench the reaction. Saturated $NaHCO_3$ solution (10mL) was then added to the reaction mixture and the organic layer was separated. The aqueous layer was further extracted with CH_2Cl_2

(20mL). The combined organic layers were dried with Na_2SO_4, filtered, and the solvent was removed *in vacuo* to obtain the crude product, *N*-tosylindole (**2.46**). Integration of the appropriate signals in the ^{1}H-NMR spectrum of the crude product showed 25% D-incorporation at C3 and no D-incorporation at C2.

Halogen-Metal Exchange of N-Tosyl-3-iodoindole and MeMgCl Followed by Deuterium Labeling

A solution of MeMgCl (0.25mL, 3M solution in THF, 0.75mmol) was added to a solution of *N*-tosyl-3-iodoindole (**2.47**) (0.15g, 0.38mmol)) in dry THF (15mL) at –30°C under nitrogen. The reaction mixture was stirred for 1h at –30°C before D_2O (1mL) was added rapidly to quench the reaction. The reaction was quenched by the addition of saturated $NaHCO_3$ solution(10mL) to the reaction mixture, and the organic layer was separated. The aqueous layer was further extracted with CH_2Cl_2 (20mL). The combined organic layers were dried with Na_2SO_4, filtered, and the solvent was removed *in vacuo* to obtain the crude product, *N*-tosylindole (**2.46**). Integration of the appropriate signals in the ^{1}H-NMR spectrum of the product showed ≥90% D-incorporation at C3 and no D-incorporation at C2.

6.3 Experimental Procedures and Data for Chapter 3

6.3.1 Procedures for the Synthesis of 3-Bromo-2, 5-Dimethoxybenzaldehyde (1.60)

3-Bromo-2-hydroxy-5-methoxybenzaldehyde **(3.38)**

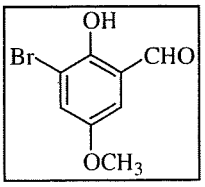

The title compound was prepared following the literature procedure.[13] 2-Hydroxy-5-methoxybenzaldehyde (6g, 40mmol) was dissolved in glacial acetic acid (30mL) and powdered anhydrous sodium acetate (3.6g, 44mmol) was added. The suspension was cooled to 5°C and a solution of bromine (6g, 38mmol) in glacial acetic acid (12mL) was added dropwise. A fine yellow-orange suspension quickly formed. After stirring for a further 2h, the reaction mixture was diluted with water (10mL) and the solid formed was filtered under vacuum and dried. Recrystallization of the collected precipitate from hot ethanol gave the desired product as a white powder (8.6g, 38mmol, 94% yield).

Mp 106-107°C (lit. 107°C).[13]

^{1}H NMR ($CDCl_3$): δ3.83 (s, 3H, OCH_3), 7.04 (s, 1H, Ar-**H**), 7.43 (s, 1H, Ar-**H**), 9.83 (s, 1H, **CHO**), 11.14 (s, 1H, **OH**).

3-Bromo-2,5-dimethoxybenzaldehyde **(1.60)**

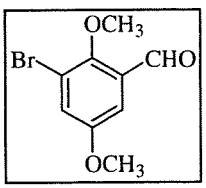

The title compound was prepared using a modification of the literature procedure.[13] Anhydrous K_2CO_3 (2.76g, 20mmol) was added to a solution of 3-bromo-2-hydroxy-5-methoxybenzaldehyde **(3.38)** (5g, 20mmol) in dry DMF (50mL) under nitrogen. To this reaction mixture was added iodomethane (2.5mL, 40mmol). The reaction mixture was stirred for 3h before H_2O (10mL) was added to quench the reaction. The solvent was removed under reduced pressure, and the residue was dissolved in $CHCl_3$ (50mL). The organic layer was washed with H_2O (20mL) and then the organic layer was dried with $MgSO_4$, filtered and the solvent removed *in vacuo* to yield the crude product. Recrystallization of the resulting solid from hot ether gave the desired product as pale yellow crystals (2.82g, 12mmol, 53% yield).

Mp 63°C (lit. 63°C).[13]

^{1}H NMR ($CDCl_3$): δ3.82 (s, 3H, OCH_3), 3.94 (s, 3H, OCH_3), 7.28 (s, 1H, Ar-**H**), 7.39 (s, 1H, Ar-**H**), 10.32 (s, 1H, **CHO**).

6.3.2 Procedures for the Synthesis of 2,5-Dimethoxybenzoic Acid (3.15) and 3-Bromo-2,5-dimethoxybenzoic Acid (3.40)

2,5-Dimethoxybenzoic acid **(3.14)**

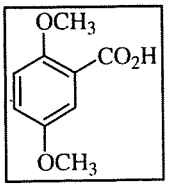

The title compound was synthesized using the procedure of Azadi-Ardakani and Wallace.[14] To a suspension of finely powdered 2,5-dimethoxybenzaldehyde **(3.7)** (5g, 30mmol) in water (80mL) at 80°C was added dropwise a solution of $KMnO_4$ (6.76g, 43mmol) in H_2O (130mL). The reaction mixture was stirred for 1h at 80°C. To the hot reaction mixture was added aqueous NaOH (2.5M) until the reaction mixture was alkaline to litmus paper. The hot suspension was then filtered through Celite, and the precipitate was further washed with aliquots of hot water (3x25mL). The combined filtrate and washings were combined and cooled to room temperature. The basic solution was washed with aliquots of CH_2Cl_2 (3x40mL) to remove traces of unreacted benzaldehyde. The aqueous solution was carefully acidified by the addition of concentrated HCl (12M) until a white precipitate formed. The product was then extracted from the aqueous phase with CH_2Cl_2 (3x50mL). The organic layers were collected, dried with $MgSO_4$, and filtered and removed under reduced pressure to yield a white solid. Recrystallization from ethyl acetate and light petroleum gave the desired product as white crystals (3.27g, 60% yield).

R_f 0.16 (1:1 EtOAc/light petroleum).

Mp 74-75°C (lit. 74-75°C).[14]

^{1}H-NMR ($CDCl_3$): δ 3.82 (s, 3H, OCH_3), 4.04 (s, 3H, OCH_3), 7.00 (d, J= 9Hz, 1H, Ar-**H**), 7.12 (dd, J_{app}= 9Hz and 3Hz, 1H, Ar-**H**), 7.68 (d, J= 3Hz, 1H, Ar-**H**), 11.00 (br s, 1H, O**H**).

3-Bromo-2,5-dimethoxybenzoic Acid **(3.40)**

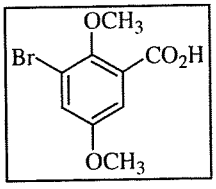

The title compound was prepared following the procedure of Rubenstein.[13] To a suspension of finely powdered 3-bromo-2,5-dimethoxybenzaldehyde **(1.60)** (2.8g, 11mmol) in H_2O (27mL) at room temperature was added a solution of $KMnO_4$ (2.7g, 17mmol) in H_2O (40mL). The reaction mixture was then heated to 80°C and stirred for 1h. To the hot reaction mixture was added 10% NaOH solution until the reaction mixture was alkaline to litmus paper. The hot suspension was then filtered to remove the brown

precipitate. The precipitate was washed with hot water (20mL) and the combined supernatant was cooled to room temperature. The basic solution was washed with CH_2Cl_2 (2x20mL) to remove unreacted benzaldehyde **1.60**. The aqueous solution was then carefully acidified with concentrated HCl (12M) until a white suspension was formed. The product was then extracted from the aqueous phase with $CHCl_3$ (3x20mL). The organic layer was separated, dried with $MgSO_4$, filtered and the solvent removed *in vacuo* to obtain the crude product as a white solid. Recrystallization from ethanol and water gave the desired product as white crystals (4.1g, 16mmol, 73% yield).

Mp 133°C (lit. 132°C).[13]

^{1}H NMR ($CDCl_3$): δ3.84 (s, 3H, OCH_3), 4.00 (s, 3H, OCH_3), 7.36 (s, 1H, Ar-**H**), 7.56 (s, 1H, Ar-**H**).

6.3.3 Preparation of Secondary Benzamides

N-(2-Bromophenyl)-2,5-dimethoxybenzamide **(3.17)**

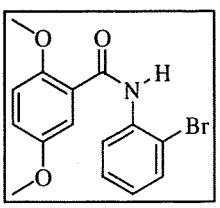

2,5-Dimethoxybenzoic acid **(3.15)** (1.24g, 6.8mmol) was dissolved in $SOCl_2$ (10mL) and the reaction mixture was refluxed for 30min under dry nitrogen. The reaction mixture was then cooled to room temperature and the excess $SOCl_2$ was carefully removed under reduced pressure to yield the acid chloride **3.16** as the crude product. The acid chloride was then dissolved in dry CH_2Cl_2 (20mL) following which a solution of 2-bromoaniline (1g, 5.8mmol) in dry CH_2Cl_2 (5mL) and NaH (0.16g, 6.8mmol) were added. The mixture was stirred for 2h at room temperature before saturated $NaHCO_3$ solution (10mL) was added to quench the reaction. The organic layer was separated and the aqueous layer was further extracted with CH_2Cl_2 (3x15mL). The combined organic layers were dried with $MgSO_4$, and the solvent was removed under reduced pressure to yield the product in quantitative yields. Purification of the compound via column chromatography (1:3 EtOAc/light pertroleum) gave the desired product as a white solid (1.89g, 5.6mmol, 97% yield). The ^{1}H NMR spectrum shows 4 methoxy signals due to rotamers in approximately 4:1 ratio, but the other proton signals are equivalent for both rotamers.

R_f 0.43 (1:3 EtOAc/light petroleum).

Mp 82-83°C (lit. 82-83°C).[15]

^{1}H-NMR ($CDCl_3$): δ3.83 and 3.86 (s, 3H, rotamer OCH_3,), 3.94 and 4.06 (s, 3H, rotamer OCH_3), 6.93-7.05 (m, 2H, Ar-**H**), 7.36 (app. t, J_{app}= 8Hz, 1H, Ar-

H), 7.58 (d, *J*= 8Hz, 1H, Ar-**H**), 7.86 (d, *J*= 3Hz, 1H, Ar-**H**), 8.67 (d, *J*= 8Hz, 1H, Ar-**H**), 10.65 (s, 1H, N**H**).

EIMS *m/z* (rel. A): 337 ($M^{+\cdot}$, 100), 335 ($M^{+\cdot}$, 100), 319 (78), 317 (78).
Two molecular ion peaks ($M^{+\cdot}$) were observed due to ^{81}Br and ^{79}Br isotopes.

HRMS Calculated 335.0157 for $C_{15}H_{13}{}^{79}BrINO_3$ found 335.0162.
Calculated 337.0137 for $C_{15}H_{13}{}^{81}BrINO_3$ found 337.0136.

IR (KBr disk) 663 w, 739 m, 809 w, 877 w, 1023 m, 1045 m, 1177 m, 1213 m, 1281 m, 1317 m, 1435 s, 1496 s, 1538 s, 1580 s, 1667 s, 2831 w, 2952 w, 3302 m, 3436 br.

*3-Bromo-*N*-(2-iodophenyl) -2,5-dimethoxybenzamide* **(3.43)**

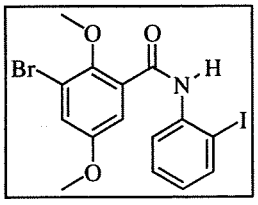

To a solution of 3-bromo-2,5-dimethoxybenzoic acid **(3.40)** (0.50g, 1.9mmol) in dry CH_2Cl_2 (20mL) at 0°C was added oxalyl chloride (0.20mL, 2.3mmol), a catalytic amount of DMF (10μL), and NaH (0.05g, 1.9mmol). The reaction mixture was stirred for 2h under nitrogen at room temperature following which the excess oxalyl chloride was removed *in vacuo* to obtain the crude acid chloride **3.42**. The residue was dissolved in dry CH_2Cl_2 (20mL) and 2-iodoaniline (0.46g, 2.1mmol) was quickly added in one portion. The reaction mixture was stirred for another 2h after which saturated $NaHCO_3$ solution (10mL) was added to quench the reaction. The organic layer was separated and the aqueous layer was further extracted with CH_2Cl_2 (20mL). The combined organic layers were separated and dried with $MgSO_4$, filtered, and the solvent was removed *in vacuo* to obtain the crude product. Flash chromatography on silica (2:3 EtOAc/light petroleum) gave the title compound as a cream colored solid (0.68g, 1.5mmol, 77% yield).

R_f 0.83 (2:3 EtOAc/light petroleum).

Mp 99-101°C.

^{1}H-NMR ($CDCl_3$): δ3.82 (s, 3H, OCH_3), 3.96 (s, 3H, OCH_3), 6.91 (m, 1H, Ar-**H**), 7.30-7.43 (m, 2H, Ar-**H**), 7.66 (s, 1H, Ar-**H**), 7.86 (m, 1H, Ar-**H**), 8.49 (d, *J*= 8Hz, 1H, Ar-**H**), 10.11 (s, 1H, N**H**).

^{13}C-NMR ($CDCl_3$): δ55.8 (OCH_3), 62.8 (OCH_3), 99.6, 111.9, 117.8, 121.0, 126.0, 129.5, 130.4, 132.1, 139.9, 140.4, 147.3, 155.3, 168.0 (**C**O).

(rotamer): δ55.9, 62.7, 89.4, 115.0, 118.2, 122.4, 123.6, 128.0, 129.0, 130.0, 139.2, 139.3, 148.6, 156.3, 162.4.

EIMS *m/z* (rel. A): 463 ($M^{+\cdot}$, 25), 460 ($M^{+\cdot}$, 100), 459 ($[M-H]^+$, 95), 458 ($[M-H]^+$, 90), 446 (68), 444 (68).

Two molecular ion peaks ($M^{+\cdot}$) and two $[M-OCH_3]^+$ peaks were observed due to ^{81}Br and ^{79}Br isotopes.

HRMS Calculated 460.9124 for $C_{15}H_{13}BrINO_3$ found 460.9127.

IR (KBr disk) ν_{max} cm^{-1} 724 w, 755 w, 784 w, 863 w, 992 m, 1042 m, 1239 m, 1295 m, 1420 m, 1471 s, 1525 m, 1599 m, 1678 m, 1713 m, 2853 m, 2925 m, 3436 br.

6.3.4 Preparation of Tertiary Benzamides

N-(2-Bromophenyl)-2,5-dimethoxy-N-methoxymethylbenzamide **(3.18)**

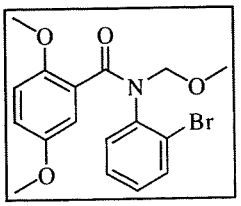

To a solution of *N*-(2-bromophenyl)-2,5-dimethoxybenzamide **(3.16)** (1.95g, 6.8mmol) in dry THF (20mL) under nitrogen was added methoxymethyl chloride (0.88mL, 12mmol) and NaH (0.30g, 13mmol). The reaction mixture was stirred for 16h at 30°C, following which the reaction mixture was poured into saturated $NaHCO_3$ solution (20mL). The organic layer was separated, and the aqueous layer was further extracted with CH_2Cl_2 (3x15mL). The combined organic extracts were dried with $MgSO_4$, and the solvent removed under reduced pressure to yield the crude product. Column chromatography on silica (2:3 EtOAc/light petroleum) gave the desired compound as a yellow viscous oil (1.55g, 4.1mmol, 60% yield).

R_f 0.32 (1:2 EtOAc/light petroleum).

^{1}H-NMR ($CDCl_3$): δ3.59 (s, 3H, OCH_3), 3.68 (s, 3H, OCH_3), 3.75 (s, 3H, OCH_3), 4.63 (d, *J*= 10Hz, 1H, CH_aH_b), 5.82 (d, *J*= 10Hz, 1H, CH_aH_b), 6.57-6.91 (m, 2H, Ar-**H**), 6.98 (d, *J*= 3Hz, 1H, Ar-**H**), 7.04 (app. t, J_{app}= 6Hz, 1H, Ar-**H**), 7.13 (app. t, J_{app}= 6Hz, 1H, Ar-**H**), 7.29 (app. t, J_{app}= 8Hz, 1H, Ar-**H**), 7.47 (d, *J*= 8Hz, 1H, Ar-**H**).

^{13}C-NMR ($CDCl_3$): δ55.5 (OCH_3), 55.6 (OCH_3), 56.7 (OCH_3), 77.3 (CH_2), 111.5, 111.7, 116.0, 123.0, 126.3, 127.3, 129.5, 131.3, 132.8, 139.3, 148.7, 152.6, 169.5 (CO).

EIMS *m/z* (rel. A): 383 ($M^{+\cdot}$, 45), 381 ($M^{+\cdot}$, 45), 350 ($[M-OCH_3]^+$, 10), 348 ($[M-OCH_3]^+$,10), 276 (18), 274 (18), 245 (98), 243 (100), 105 (34), 45 (40).

Two molecular ion peaks ($M^{+\cdot}$) and two $[M\text{-}OCH_3]^+$ peaks were observed due to ^{81}Br and ^{79}Br isotopes.

HRMS Calculated 379.0419 for $C_{17}H_{18}{}^{79}BrNO_4$ found 379.0408.

Analytical Anal. Calcd for $C_{17}H_{18}BrNO_4$: C, 53.70; H, 4.77; N, 3.68. Found C, 53.64; H, 4.90; N, 3.69.

*3-Bromo-*N*-(2-iodophenyl) -2,5-dimethoxy-*N*-methoxymethylbenzamide* **(3.41)**

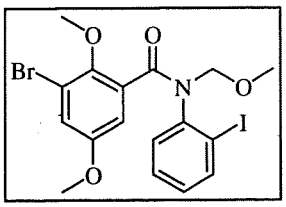

To a solution of 3-bromo-*N*-(2-iodophenyl)-2,5-dimethoxy benzamide (**3.43**) (0.88g, 1.9mmol) in dry THF (10mL) under nitrogen was added methoxymethyl chloride (0.30mL, 3.9mmol) and NaH (0.10g, 4.1mmol). The reaction mixture was stirred for 16h at 30°C following which the reaction mixture was poured into saturated $NaHCO_3$ solution (20mL) to quench the reaction. The organic layer was separated and the aqueous layer was further re-extracted with CH_2Cl_2 (3x15mL). The combined organic layers were dried with $MgSO_4$, filtered and the solvent removed *in vacuo* to yield the crude product. Column chromatography on silica (2:3 EtOAc/light petroleum) gave the desired compound as a viscous yellow oil which solidified upon standing (0.65g, 1.3mmol, 68% yield). Two distinct sets of methoxy signals (three methoxy signals per set) in a ratio of 4:1 were observed in the ^1H NMR spectrum which suggests the presence of rotamers, but the aromatic hydrogen signals overlapped. The ^{13}C NMR spectrum in contrast shows distinct sets of signals for each rotamer; the carbon resonances of each rotamer is reported below.

R_f 0.72 (2:3 EtOAc/light petroleum).

MP 40-42°C.

^1H-NMR ($CDCl_3$): δ3.62 (s, 3H, OCH_3), 3.66 and 3.78 (s, 3H, OCH_3), 3.80 and 3.93 (s, 3H, OCH_3), 4.60 (d, *J*= 10Hz, 1H, CH_aH_b), 5.87 (d, *J*= 10Hz, 1H, CH_aH_b), 6.88-6.91 (m, 2H, Ar-**H**), 7.00-7.08 (m, 1H, Ar-**H**), 7.20 (m, 1H, Ar-**H**), 7.36-7.39 (m, 1H, Ar-**H**), 7.74 (d, *J*= 8Hz, 1H, Ar-**H**).

^{13}C-NMR ($CDCl_3$): [rotamer 1] δ55.6 (OCH_3), 56.7 (OCH_3), 62.3 (OCH_3), 76.6 (CH_2), 99.5, 109.5, 117.1, 119.9, 128.8, 129.9, 131.3, 132.7, 139.2, 141.8, 146.1, 155.3, 168.2 (**C**O).

[rotamer 2] δ55.6 (OCH_3), 56.7 (OCH_3), 62.8 (OCH_3), 76.6 (CH_2), 99.5, 111.7, 112.5, 117.6, 120.8, 129.3, 129.9, 131.6, 132.0, 139.7, 147.1, 155.2, 167.8 (**C**O).

EIMS *m/z* (rel. A): 507 ($\mathbf{M}^{+\cdot}$, 15), 505 ($\mathbf{M}^{+\cdot}$, 15), 380 ($[\mathbf{M}\text{-I}]^+$, 42), 378 ($[\mathbf{M}\text{-I}]^+$, 42), 245 (97), 243 (100), 45 (92).

Two molecular ion peaks ($\mathbf{M}^{+\cdot}$) and two $[M\text{-I}]^+$ peaks were observed due to ^{81}Br and ^{79}Br isotopes.

HRMS Calculated 504.9386 for $C_{17}H_{17}{}^{79}BrINO_4$ found 504.9380.

IR (KBr disk) ν_{max} cm^{-1} 648 w, 681 w, 725 w, 747 w, 856 w, 911 w, 994 m, 1018 m, 1044 s, 1082 s, 1225 s, 1278 m, 1306 m, 1374 m, 1420 s, 1473 s, 1562 w, 1598 m, 1669 s, 2831 w, 2937 m, 3436 br.

Analytical Anal. Calcd for $C_{17}H_{17}BrINO_4$: C, 40.34; H, 3.39; N, 2.77. Found C, 40.66; H, 3.48; N, 2.48.

6.3.5 Palladium-Mediated Cyclization of Tertiary Benzamides

7,10-Dimethoxy-5-methoxymethyl-5H-phenanthridin-6-one **(3.19)**

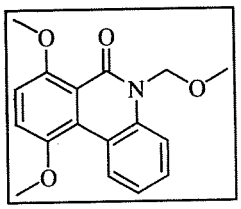

To a solution of *N*-(2-bromophenyl)-2,5-dimethoxy-*N*-methoxy methylbenzamide **(3.18)** (0.72g, 1.89mmol) in dry degassed DMF (15mL) was added PPh_3 (0.15g, 0.56mmol), anhydrous Na_2CO_3 (0.40g, 3.77mmol) and $Pd(OAc)_2$ (43mg, 0.19mmol). The reaction mixture was stirred at 140°C under an argon atmosphere, following which the reaction mixture was cooled to room temperature and filtered through Celite. A volume of acetone (10mL) was filtered through the Celite and the combined filtrate was concentrated under reduced pressure to yield the crude product. The crude product was purified by flash chromatography on silica (EtOAc) to yield the desired compound as a white solid (0.55g, 1.84mmol, 96% yield).

R_f 0.35 (4:1 EtOAc/light petroleum).

Mp 117-118°C (lit. 117-118C).[15]

^{1}H-NMR ($CDCl_3$): δ3.51 (s, 3H, OCH_3), 4.00 (s, 6H, 2x OCH_3), 5.78 (br. s, 2H, CH_2), 7.06 (d, *J*= 9Hz, 1H, Ar-**H**), 7.25-7.32 (m, 2H, Ar-**H**), 7.48 (app. t, J_{app}= 8Hz, 1H, Ar-**H**), 7.59 (d, *J*= 9Hz, 1H, Ar-**H**), 9.25 (d, *J*= 10Hz, 1H, Ar-**H**).

8-Bromo-7,10-Dimethoxy-5-methoxymethyl-5H-phenanthridin-6-one **(3.44)**

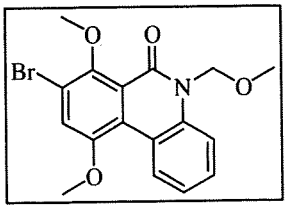

To a solution of 3-bromo-*N*-(2-iodophenyl)-2,5-dimethoxy- *N*-methoxymethylbenzamide **(3.41)** (0.18g, 0.35mmol) in dry degassed DMF (15mL) was added PPh_3 (28mg, 0.11mmol), anhydrous Na_2CO_3 (74mg, 0.70mmol) and $Pd(OAc)_2$ (8mg, 0.035mmol). The reaction mixture was stirred at 80°C under an argon atmosphere for 5h following which the reaction mixture was cooled to room temperature and filtered through Celite. An aliquot of acetone (10mL) was filtered through the Celite, and the combined filtrates were removed under reduced pressure to yield the crude product. Purification via column chromatography on silica (EtOAc) gave the desired compound as a brown solid (0.12g, 0.32mmol, 92% yield).

R_f 0.74 (1:1 EtOAc/light petroleum).

Mp 102-104°C.

^{1}H-NMR ($CDCl_3$): δ3.51 (s, 3H, OCH_3), 3.95 (s, 3H, OCH_3), 4.03 (s, 3H, OCH_3), 5.77 (s, 2H, CH_2), 7.25-7.29 (m, 2H, Ar-**H**), 7.49 (s, 1H, Ar-**H**), 7.52-7.58 (m, 1H, Ar-**H**), 9.13 (d, *J*= 8Hz, 1H, Ar-**H**).

^{13}C-NMR ($CDCl_3$): δ56.4 (OCH_3), 56.7 (OCH_3), 61.7 (OCH_3), 74.2 (CH_2), 115.1, 118.1, 118.4, 119.9, 121.3, 122.5, 125.4, 128.7, 129.3, 136.7, 152.0, 153.4, 159.5 (**C**O).

EIMS *m/z* (rel. A): 379 ($M^{+\cdot}$, 90), 377 ($M^{+\cdot}$, 86), 347 (50), 345 (48), 336 (52), 334 (68), 319 (100), 317 (88), 304 (73).

Two molecular ion peaks ($M^{+\cdot}$) were observed due to ^{81}Br and ^{79}Br isotopes.

HRMS Calculated 377.0263 for $C_{17}H_{16}{}^{79}BrNO_4$ found 377.0265.

Calculated 379.0242 for $C_{17}H_{16}{}^{81}BrNO_4$ found 379.0252.

IR (KBr disk) ν_{max} cm^{-1} 758 w, 1052 s, 1076 s, 1224 m, 1276 w, 1297 w, 1363 w, 1458 s, 1655 s, 2824 w, 2932 w, 2962 w, 3435 br.

6.3.6 Preparation of 7,10-Dimethoxyphenanthridine (3.9)

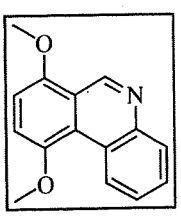

$LiAlH_4$ (44mg, 0.36mmol) from freshly crushed pellets was added to a solution of 7,10-dimethoxy-5-methoxymethyl-5*H*-phenanthridin-6-one **(3.19)** (0.10g, 0.33mmol) in dry THF (10mL). The reaction mixture was stirred for 1h at room temperature following which wet ether (9:1 ether/H_2O, 10mL) was carefully added to decompose the excess $LiAlH_4$. The organic layer was separated and washed with distilled water (10mL aliquots) until the aqueous

layer was neutral. To the organic solvent was added hydrochloric acid (6M, 30mL), and the resulting clear orange solution was stirred for 1h at room temperature following which the reaction mixture was carefully neutralized by the addition of solid $NaHCO_3$. The organic layer was separated and the product was further extracted from the aqueous layer with $CHCl_3$ (2x20mL). The combined organic layers were then washed with brine (20mL), dried with $MgSO_4$, filtered and concentrated under reduced pressure to yield the crude product as an orange oil. Column chromatography using silica (2:3 EtOAc/light petroleum) gave the desired compound as a yellow solid (72mg, 0.30mmol, 90% yield).

R_f 0.31 (2:3 EtOAc/light petroleum).

Mp 167-169°C.

^{1}H-NMR ($CDCl_3$): δ4.02 (s, 3H, OCH_3), 4.08 (s, 3H, OCH_3), 7.01 (d , *J*= 9Hz, 1H, Ar-**H**), 7.25 (d, *J*= 5Hz, 1H, Ar-**H**), 7.65 (app. t, J_{app}= 8Hz, 1H, Ar-**H**), 7.75 (app. t, J_{app}= 8Hz, 1H, Ar-**H**), 8.22 (d, *J*= 8Hz, 1H, Ar-**H**), 9.51 (d, *J*= 8Hz, 1H, Ar-**H**), 9.73 (s, 1H, Ar-**H**).

^{13}C-NMR ($CDCl_3$): δ56.0 (OCH_3), 56.1 (OCH_3), 106.9, 112.5, 118.5, 123.6, 123.7, 126.8, 128.1, 128.3, 129.4, 144.9, 148.0, 151.1, 151.6.

EIMS *m/z* (rel. A): 239 (**$M^{+\cdot}$**, 98), 224 ([**M**-CH_3]$^+$,100), 209 (15), 153 (25).

HRMS Calculated 239.0946 for $C_{15}H_{13}NO_2$ found 239.0950.

IR (KBr disk) ν_{max} cm^{-1} 718 w, 734 m, 774 m, 802 w, 811 m, 962 w, 1016 m, 1075 m, 1112 m, 1214 w, 1247 s, 1304 m, 1341 m, 1372 m, 1399 w, 1432 m, 1455 m, 1479 m, 1595 w, 1610 w, 1667 br, 2835 w, 2934 w, 2959 w, 3435 br.

6.3.7 Preparation of Phenanthridine-7,10-dione (3.2)

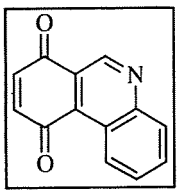

To a stirred solution of 7,10-dimethoxyphenanthridine (**3.9**) (0.30g, 1.25mmol) in acetonitrile (50mL) was added a solution of cerium ammonium nitrate (2.1g, 3.83mol) in H_2O (50mL). The reaction mixture was stirred for 2h at room temperature after which solid $NaHCO_3$ was carefully added to adjust the pH to 7. The reaction mixture was concentrated *in vacuo* and the residue obtained was partitioned in H_2O (20mL) and CH_2Cl_2 (20mL). The organic layer was separated, and aqueous layer was extracted with portions of CH_2Cl_2 (2x20mL). The combined organic extracts were dried with $MgSO_4$, filtered, and the solvent removed under reduced pressure to yield the crude product as a

yellow solid. Flash chromatography using silica (CH_2Cl_2) gave the desired product as a yellow solid (0.25g, 1.20mmol, 96% yield).

R_f 0.32 (1:3 EtOAc/light petroleum).

Mp 169-170°C (lit. 169-171).[15]

^{1}H-NMR ($CDCl_3$): δ7.04 (m, 2H, Ar-**H**), 7.81 (app. t, *J*= 7Hz, 1H, Ar-**H**), 7.91 (app. t, *J*= 7Hz, 1H, Ar-**H**), 8.22 (d, *J*= 8Hz, 1H, Ar-**H**), 9.42 (d, *J*= 8Hz, 1H, Ar-**H**), 9.63 (s, 1H, Ar-**H**).

EIMS *m/z* (rel. A): 209 ($M^{+\cdot}$, 100), 153 (50), 127 (32).

HRMS Calculated 209.0477 for $C_{13}H_7NO_2$ found 209.0480.

6.3.8 Preparation of Anilinophenanthridine-7,10-dione and Palladium-Catalyzed Cyclization to Calothrixin B (1.27) and *Iso*-calothrixin B (3.29)

A suspension of the phenanthridine-7,10-dione **3.2** (13mg, 0.06mmol) in distilled water (50mL) was heated to 100°C until a yellow solution was formed. To the hot solution was added a solution of aniline (13μL, 0.14mol) in 1% acetic acid (1mL). The reaction mixture was refluxed for 16h before the solution was cooled, and the solvent was removed *in vacuo*. The residue was resuspended in CH_2Cl_2 (10mL), washed with saturated NH_4Cl solution (5mL), dried with $MgSO_4$, filtered and the solvent was removed *in vacuo* to obtain a gray solid in quantitative yield. The crude mixture of regioisomeric anilinophenanthridinediones (**3.3, 3.28**) was then dissolved in glacial acetic acid (5mL), and a catalytic amount of palladium (II) acetate (1 mg) was added. The reaction mixture was stirred for 16h at 140°C following which the reaction mixture was cooled to room temperature and the solvent removed *in vacuo*. The residue was redissolved in $CHCl_3$ and filtered through a column of silica. The solvent was removed under reduced pressure to yield a mixture of calothrixin B and *iso*-calothrixin B in a 1:10 ratio (quantitative yield). Fractional recrystallization of the mixture from $CHCl_3$ gave pure *iso*-calothrixin B as a dark red solid (16mg, 0.05mmol, 90% yield). The calothrixin B obtained was identical to the product previously obtained.

Iso-*Calothrixin B* (**3.29**)

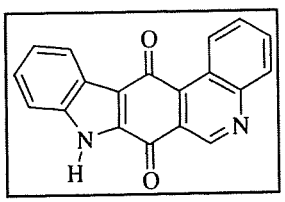

^{1}H-NMR (*d*-DMSO): δ7.40 (app. t, J_{app}= 7Hz, 1H, Ar-**H**), 7.47 (app. t, J_{app}= 7Hz, 1H, Ar-**H**), 7.61 (d, *J*= 8Hz, 1H, Ar-**H**), 7.86 (m, 1H, Ar-**H**), 7.95 (m, 1H,

Ar-**H**), 8.14 (d, *J*= 8Hz, 1H, Ar-**H**), 8.25 (d, *J*= 8Hz, 1H, Ar-**H**), 9.55 (s, 1H, Ar-**H**), 9.70 d, *J*= 8Hz, 1H, Ar-**H**).

The N-**H** peak was not observed in the range of δ0-10 ppm.

^{13}C-NMR (*d*-DMSO): δ114.0, 118.6, 122.4, 123.1, 124.1, 124.2, 124.3, 127.2, 127.9, 129.8, 130.0, 131.9, 134.2, 135.5, 138.4, 146.9, 151.8, 177.8 (**C**O), 184.1 (**C**O).

EIMS *m/z* (rel. A): 298 ($\mathbf{M}^{+\cdot}$, 58), 270 ($[\mathbf{M}\text{-CO}]^+$, 20), 78 (C_6H_6, 90), 63 (100), 45 (55).

HRMS Calculated 298.0742 for $C_{19}H_{10}N_2O_2$ found 298.0747.

IR (KBr disk) ν_{max} cm^{-1} 752 w, 769 w, 780 w, 1060 m, 1245 m, 1245 m, 1329 w, 1399 w, 1534 s, 1647 s, 3248 s, 3436 br.

Purity **System 1: Retention time:** 31.1min.

System 2: Retention time: 43.6min.

6.4 Experimental Procedures and Data for Chapter 4

6.4.1 Lipophilicity Measurements via High Performance Liquid Chromatography

All HPLC experiments were performed on an Agilent 1100 Series HPLC machine using a 250x4.60mm Phenomenex Hypersil C18 reverse-phase column with a 5μm pore size. All experiments were run isocratically at 25°C using degassed 60% acetonitrile and 40% H_2O containing 0.1% trifluoroacetic acid, and the HPLC detector was set to monitor the eluent at 254nm, 290nm and 300nm wavelengths.

Test samples were prepared as stock solutions at 4mM concentration in HPLC-grade acetonitrile. These samples were further diluted to 100μM concentrations in HPLC-grade acetonitrile which contained thiourea (1mg/mL) as an internal standard. All samples were filtered through Millipore™ Millex-HN 4.5μm pore size nylon filters prior to injection. The injection volume used was 10uL for each run.

Standard compounds of known logP values were run on the HPLC to measure the retention time of the compound (R_t) relative to the dead volume marked by thiourea (R_0). The capacity factor k was then calculated using the equation $k=(R_t-R_0)/R_0$. The logarithm of the capacity factor (logk) was then graphed against the logP values of the standard compounds to obtain a linear graph. This linear graph (logk versus logP) is then used to extrapolate the logP values of the test compounds based on the calculated logk value of the test compounds.

6.4.2 Experimental Protocols for Biological Experiments

Antiproliferative Assays for the Calothrixins and Related Compounds using the MTT Colorimetric Assay

HeLa cervical cancer cells were cultured in HEPES-buffered RPMI 1640 Media with 10% fetal calf serum. The cells were incubated at 37°C under an atmosphere of 5% carbon dioxide.

Effects of compounds on HeLa cell proliferation and viability were measured using the colorimetric MTT Assay. Standard solutions of the test compounds were prepared in Aldrich Hybrimax™ DMSO at 4mM concentrations. Stock solutions of each compound

for biological studies were prepared at 100μM concentrations by placing 25μL of the standard solution in 1mL of fresh media. The experiments were carried out in 96-well microtitre plates divided into 8 rows and 12 columns. The following procedure was carried out for the first row (wells 1 to 12), and were applied to the next three rows as well to obtain quadruplicate results.

To wells 2 to11 of a 96-well flat-bottom microtitre plate was added 50μL of fresh media, while 100μL of fresh media was added to well 12. To well 1 was added 100μL of 100μM stock solution of the test compound. Serial dilutions (1:1) were carried out by placing 50μL of the solution from well 1 into well 2 and mixing thoroughly, then taking 50μL of the solution from well 2 and placing it in well 3. This process was continued down the plate until well 10, and a volume of 50μL from well 10 was discarded. Wells 11 (for untreated cells) and 12 (blank) were the controls for the experiment.

To wells 1-11 was then added 50μL of the cell suspension (100,000 cells/mL) to achieve a final concentration of $5x10^3$ cells per well in 100μL media for the 3-day assay. The concentrations of the test compound employed were 50μM, 25μM, 12.5μM, 6.25μM, 3.12μM, 1.56μM, 0.78μM, 0.39μM, 0.20μM, and 0.098μM. The cells were then incubated for 3 days at 37°C under an atmosphere of 5% CO_2. After the specified time, the media in the plates were decanted to remove dead cells and 100μL of cold PBS was added to each well. The PBS solution was decanted, and 100μL of fresh media was placed in each well. To each well was then added 10μL of MTT solution (5mg/mL in PBS). The cells were then incubated for a further 5h, after which 100μL of lysing solution (10% w/v sodium dodecyl sulfate in 0.01M HCl) was added to each well. The lysed cells were then incubated at 37°C for 16h. After the incubation period, the absorbances of each plate was analyzed at 590nm using a μQuant automated spectrophotometric plate reader from Bio-Tek Instruments Inc. The results were expressed as percentages of control (untreated cells) and were analyzed using GraphPad Prism 2.0 software. All measurements were made in quadruplicate and the results presented are typical of multiple independent experiments.

6.5 Experimental Procedures for Chapter 5

6.5.1 Thiol-Disulfide Exchange Studies for the ETP Compounds *via* HPLC

Glutathione (GSH), oxidized glutathione (GSSG), cysteine (CySH) and cystine (CySSCy) were purchased from Sigma. The ETP compounds were obtained within the Chai group.[16] The reduced form of the ETP compounds were generated *in situ* by reduction with sodium borohydride. The concentrations of GSH and CySH were measured using the method of Ellman.[17] Specifically, the quantitative reaction of 5,5'-dithio*bis*(2-nitrobenzoic) acid (DTNB) with the thiols produces 2-nitro-5-thiobenzoic acid, which is measured *via* UV Visible spectroscopy (ϵ_{412nm}=14150 M^{-1} cm^{-1}) to determine the concentration of the thiol used. The concentration of the solutions were found to be accurate and reproducible (within 3% error).

All aqueous solutions were prepared in argon-degassed Tris buffer (0.05M Tris at pH 7.0 in deionized water) containing EDTA (1mM). All solutions were filtered through Millipore™ Millex-HN 4.5μm pore size nylon filters prior to injection on the HPLC instrument.

HPLC measurements were performed on a Beckman System Gold HPLC instrument using a 250x4.60mm Phenomenex Hypersil C18 reverse-phase column with a 5μm pore size. All experiments were run at 25°C and the HPLC traces were recorded at 260nm wavelength. The solvents used were HPLC grade acetonitrile with 0.1% TFA (Solvent A) and MilliQ deionized H_2O with 0.1% TFA (Solvent B). The test compounds were eluted with a solvent gradient as follows:

The solvent gradient was run at 85% A and 15% B for 2min and then raised to 95% B within 10 min, followed by isocratic elution in 95% B for a further 2min, and finally lowered to 15% B over 2min followed by isocratic elution at 15%B for 12min.

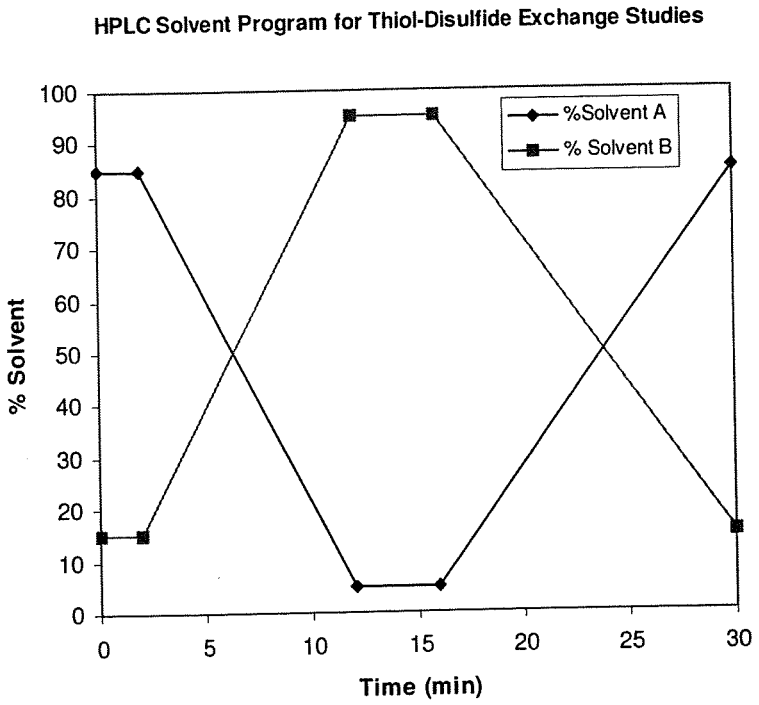

Standard solutions of the ETP compound and the corresponding reduced form (dithiol) were prepared using the argon-degassed Tris buffer. All solutions were filtered through Millipore™ Millex-HN 4.5μm pore size nylon filters prior to injection. Standard solutions of the ETP compound and the dithiol were prepared at 380μM, 190μM, 95μM, 48μM, and 24μM concentrations. The standard solutions were used to determine the individual standard curves for the ETP compound and dithiol. The standard curves showed a linear correlation between the concentration and corresponding peak area with linear coefficients of R^2=0.99 for each graph.

Thiol-disulfide exchange studies between the ETP compound (100μM initial concentration), GSH (2.8mM initial concentration) and GSSG (2.8mM) were carried out in Teflon-sealed Reacti-vials™ containing argon-degassed Tris buffer (0.5mM). The solutions were kept under an atmosphere of argon to minimize the auto-oxidation of thiols.

At hourly intervals, aliquots of the reaction mixture were removed from the Reacti-vials™ via syringe, filtered, and immediately injected onto the HPLC. From analysis of the HPLC graphs at 1h, 2h,and 3h it was noted that no further change was noted in the

peak areas corresponding to the ETP compound and its reduced form thereby establishing that the system was at equilibrium (typically within 1h). From the peak areas of the ETP compound and reduced ETP compound, the equilibrium concentrations were determined for each component using their respective calibration curves. The equlilibrium constants were then calculated using the following equation:

$$K_{eq} = \frac{[ETP^{red}][RSSR]}{[ETP^{ox}][RSH]^2}$$

The reduction potential of the ETP compounds were then calculated using the Nernst Equation:

$$E_{ETP} = E_{GSSG/GSH} + \frac{RT}{2F}\ln(K_{eq})$$

where $[ETP^{red}]$ and $[ETP^{ox}]$ are the molar concentrations of the dimercaptopiperazinedione and ETP compound respectively, E_{ETP} is the reduction potential of the ETP compound, $E_{GSSG/GSH}$ is the reduction potential of oxidized glutathione (-252mV), R is the Gas Constant (8.3145J/mol K), T is the temperature (298K) and F is Faraday's Constant (9.64867×10^4 C/mol).

Confirmation of the results for the reduction potentials of the ETP compounds was obtained using the thiol-disulfide exchange reaction between the ETP compound and the CySH/CySSCy redox buffer. The reaction was carried out using the procedure outlined above, and the equilibrium constants were determined by HPLC.

From the equilibrium constants obtained for the ETP compound and the thiols, the theoretical equilibrium constant (K_{eq3}) for the thiol-disulfide exchange reaction between CySSCy and GSH was calculated using the following equations:

$$K_{eq1} = \frac{[ETP^{red}][GSSG]}{[ETP^{ox}][GSH]^2}, \quad K_{eq2} = \frac{[ETP^{red}][CySSCy]}{[ETP^{ox}][CySH]^2};$$

$$CySSCy + 2\,GSH \rightleftharpoons GSSG + 2\,CySH$$

$$K_{eq3} = \frac{[CySH]^2\,[GSSG]}{[CySSCy][GSH]^2} = K_{eq1}/K_{eq2}$$

The calculated K_{eq3} values were between 3.2 to 3.5, which is in excellent agreement with the experimental value.[18] This ensures the accuracy of the K_{eq} values obtained for the thiol-disulfide exchange reactions of the ETP compounds.

6.5.2 Uptake Studies of Calothrixin A Measured by HPLC

P388 murine macrophages were cultured in Hanks Buffered Saline Solution with 10% horse serum at 37°C under an atmosphere of 5% CO_2. All HPLC experiments were performed on an Agilent 1100 Series HPLC machine using a 250x4.60mm Phenomenex Hypersil C18 reverse-phase column with a 5μm pore size. All experiments were run isocratically at 25°C using degassed 40% acetonitrile and 60% H_2O containing 0.1% trifluoroacetic acid. HPLC data were recorded at 260nm wavelength.

In Set A, a cell suspension in media (50mL) at a density of 10^6 cells/mL was placed in a culture flask. In Set B, a cell suspension of P388 cells in media (200mL) at a density of 10^5 cells/mL was placed in a separate culture flask. To Set A was added a solution of calothrixin A in Aldrich Hybrimax™ DMSO (100μL, 4mM solution) and to Set B was added 400μL of the calothrixin A solution. The final concentration of calothrixin in each flask was 10μM. Upon addition of calothrixin A, the flasks were placed in an incubator at 37°C with 5% carbon dioxide for 2h. After the incubation period, the cell suspensions were transferred to sterile Eppendorf™ tubes and centrifuged at 1000 rpm for 5min. The supernatant was then decanted, and the cell pellet was resuspended in cold phosphate buffer and transferred to a sterile Eppendorf™ tube. The cell suspensions were then centrifuged and the supernatant was decanted.

The cell pellets were then lysed with phosphate buffer containing 1% trifluoroacetic acid (1mL). The suspension was placed in a sonicator for 1h at 37°C. The cell suspension then centrifuged to pellet cellular debris. An aliquot of the supernatant (100μL) was then injected on the HPLC instrument without prior filtration to determine the concentration of calothrixin A.

The aqueous supernantant was then decanted. Analysis of the pellets by confocal microscopy showed that Set A was slightly orange whereas Set B was a deeper red color. Thin needles of calothrixin A were evident in the pellet of Set B. To extract calothrixin A from the cell debris, acetonitrile (1mL) was added to the pellet and the suspension placed in a sonicator for 1h at 37°C. An aliquot of the supernatant was removed, filtered through a Millipore™ Millex-HN 0.45μm pore size 4mm filter, then analyzed using HPLC.

6.6 Bibliography

(1) Armarego, W. L. F.; Perrin, D. D. *Purification of Laboratory Chemicals*; 4th ed.; Butterworth-Heinemann: Oxford, 1997.

(2) Hohenlohe-Oehringen, K.; Rhomberg, A.; Bretschneider, H. *Monatsh. Chem.* **1966**, *97*, 135-144.

(3) Stefanovic, G.; Pavicic-Woss, M.; Lorenc, L.; Mihailovic, M. L. *Tetrahedron* **1959**, *6*, 97-102.

(4) Veibel, S.; Pedersen, C. *Acta Chim. Scand.* **1955**, *9*, 1674-1684.

(5) Ketcha, D. M.; Gribble, G. W. *J. Org. Chem.* **1985**, *50*, 5451-5457.

(6) Kikugawa, Y. *Synthesis* **1981**, *6*, 460-461.

(7) Illi, V. O. *Synthesis* **1979**, 136.

(8) Witulski, B.; Buschmann, N.; Bergsträßer, U. *Tetrahedron* **2000**, *56*, 8473-8480.

(9) Kelly, T. R.; Zhao, Y.; Cavero, M.; Torneiro, M. *Org. Lett.* **2000**, *2*, 3735-3737.

(10) Snieckus, V.; Watanabe, M. *J. Am. Chem. Soc.* **1980**, *102*, 1457-1460.

(11) Rickards, R. W.; Rothschild, J. M.; Willis, A. C.; de Chazal, N. M.; Kirk, J.; Kirk, K.; Saliba, K. J.; Smith, G. D. *Tetrahedron* **1999**, *55*, 13513-13520.

(12) Taylor, D. A.; Baradarani, M. M.; Martinez, S. J.; Joule, J. A. *J. Chem. Res. (M)* **1979**, 4801-4817.

(13) Rubenstein, L. *J. Chem. Soc.* **1925**, 1998-2004.

(14) Azadi-Ardakani, M.; Wallace, T. W. *Tetrahedron* **1988**, *44*, 5939-5952.

(15) Le Guen, M. Honours Thesis, The Australian National University, 2003.

(16) Bernardo, P. H. Graduate Diploma Thesis, The Australian National University, 2001.

(17) Ellman, G. L. *Arch. Biochem. Biophys.* **1959**, *82*, 70-77.

(18) Gorin, G.; Doughty, G. *Arch. Biochem. Biophys.* **1968**, *126*, 547-551.

Appendices

Appendix A

The following are truncated output files obtained from SigmaPlot which contain the relevant data analyses and statistical tests.

1. Correlation of $E_{1/2}^{I}$ values versus $\log(1/EC_{50})$ [Figure 4.12]

[Variables]

$x = E_{1/2}^{I}$

$y = \log(1/EC_{50})$

[Equation]

f=y0+a*x

$n=7$ $R = 0.50$ $R^2 = 0.25$ $s= 0.35$

	Coefficient	Std. Error	t	P
y0	1.6629	0.9353	1.7779	0.1356
a	1.2057	0.9393	1.2837	0.2555

Analysis of Variance:

	DF	SS	MS	F	P
Regression	1	0.2026	0.2026	**1.65**	**0.256**
Residual	5	0.6148	0.1230		
Total	6	0.8174	0.1362		

Durbin-Watson Statistic = 2.3619

Normality Test: Passed (P = 0.7842)

Constant Variance Test: Passed (P = 0.6019)

Power of performed test with alpha = 0.0500: 0.1930

The power of the performed test (0.1930) is below the desired power of 0.8000.

You should interpret the negative findings cautiously.

2. Correlation of $E_{1/2}^{II}$ values and $\log(1/EC_{50})$ [Figure 4.13]

[Variables]

$x = E_{1/2}^{II}$

$y = \log(1/EC_{50})$

[Equation]

f=y0+a*x

$n=7$ $R = 0.72$ $R^2 = 0.52$ $s= 0.28$

	Coefficient	Std. Error	t	P
y0	3.3354	1.2422	2.6851	0.0436
a	1.7310	0.7488	2.3117	0.0688

Analysis of Variance:

	DF	SS	MS	F	P
Regression	1	0.4223	0.4223	**5.34**	**0.068**
Residual	5	0.3951	0.0790		
Total	6	0.8174	0.1362		

Durbin-Watson Statistic = 2.6518

Normality Test: Passed (P = 0.7071)

Constant Variance Test: Passed (P = 0.2550)

Power of performed test with alpha = 0.0500: 0.4405

The power of the performed test (0.4405) is below the desired power of 0.8000.

You should interpret the negative findings cautiously.

2. Correlation of lnK values and log(1/EC_{50}) [Figure 4.14]

x = lnK

y = log(1/EC_{50})

[Equation]

f=y0+a*x

$n=7$ $R = 0.71$ $R^2 = 0.50$ $s= 0.29$

	Coefficient	Std. Error	t	P
y0	3.8500	1.5152	2.5409	0.0518
a	-0.1272	0.0570	-2.2335	0.0758

Analysis of Variance:

	DF	SS	MS	F	P
Regression	1	0.4082	0.4082	**4.99**	**0.076**
Residual	5	0.4092	0.0818		
Total	6	0.8174	0.1362		

Durbin-Watson Statistic = 1.3666

Normality Test: Passed (P = 0.5283)

Constant Variance Test: Passed (P = 0.0956)

Power of performed test with alpha = 0.0500: 0.4212

The power of the performed test (0.4212) is below the desired power of 0.8000.

You should interpret the negative findings cautiously.

3. Correlation of $E_{Q/Q}^{2-}$ values and log(1/EC_{50}) [Figure 4.15]

x = $E_{Q/Q}^{2-}$

y = log(1/EC_{50})

[Equation]

f=y0+a*x

n=7 R = 0.62 R^2= 0.39 s = 0.32

	Coefficient		Std. Error	t	P
y0	2.4603	1.1239	2.1891	0.0802	
a	1.4997	0.8457	1.7733	0.1364	

Analysis of Variance:

	DF	SS	MS	F	P
Regression	1	0.3142	0.3142	**3.14**	**0.136**
Residual	5	0.4995	0.0999		
Total	6	0.8137	0.1356		

Durbin-Watson Statistic = 2.6287

Normality Test: Passed (P = 0.7573)

Constant Variance Test: Passed (P = 0.2965)

Power of performed test with alpha = 0.0500: 0.3066

The power of the performed test (0.3066) is below the desired power of 0.8000.

You should interpret the negative findings cautiously.

4. Correlation of logP values and log(1/EC_{50}) of the Carbazolediones[Figure 4.17]

x = logP

y = log(1/EC_{50})

[Equation]

f=y0+a*x+b*x^2

n= 12 R = 0.65 R^2 = 0.42 s = 0.37

	Coefficient		Std. Error	t	P
y0	-0.5937	0.3798	-1.5632	0.1524	
a	0.5699	0.2322	2.4550	0.0365	
b	-0.0771	0.0374	-2.0627	0.0692	

Analysis of Variance:

	DF	SS	MS	F	P
Regression	2	0.8848	0.4424	**3.31**	**0.084**
Residual	9	1.2032	0.1337		
Total	11	2.0881	0.1898		

Durbin-Watson Statistic = 2.4669

Normality Test: Passed (P = 0.3500)

Constant Variance Test: Passed (P = 0.5877)

Power of performed test with alpha = 0.0500: 0.6447

The power of the performed test (0.6447) is below the desired power of 0.8000.

You should interpret the negative findings cautiously.

5. Correlation of logP values and log(1/EC_{50}) of unsubstituted carbazolediones[Figure 4.18]

x = logP

y = log(1/EC_{50})

[Equation]

f=y0+a*x+b*x^2

n=6 R = 0.73 R^2 = 0.53 s= 0.31

	Coefficient		Std. Error	t	P
y0	-1.1100	3.6085	-0.3076	0.7785	
a	1.2538	2.0602	0.6086	0.5858	
b	-0.2128	0.2842	-0.7488	0.5083	

Analysis of Variance:

	DF	SS	MS	F	P
Regression	2	0.3162	0.1581	**1.68**	**0.32**
Residual	3	0.2824	0.0941		
Total	5	0.5987	0.1197		

Durbin-Watson Statistic = 2.3324

Normality Test: Passed (P = 0.7089)

Constant Variance Test: Passed (P = 0.0600)

Power of performed test with alpha = 0.0500: 0.3582

The power of the performed test (0.3582) is below the desired power of 0.8000.

You should interpret the negative findings cautiously.

6. Correlation of logP values and log(1/EC_{50}) of the calothrixins[Figure 4.20]

x = logP

y = log(1/EC_{50})

[Equation]

f=y0+a*x+b*x^2

n=6 R = 0.89 R^2 = 0.78 s= 0.3218

	Coefficient		Std. Error	t	P
y0	-0.6596	0.3369	-1.9576	0.1452	
a	0.7154	0.2349	3.0453	0.0556	

b	-0.0964	0.0384	-2.5113	0.0868

Analysis of Variance:

	DF	SS	MS	F	P
Regression	2	1.1324	0.5662	**5.47**	**0.100**
Residual	3	0.3106	0.1035		
Total	5	1.4429	0.2886		

Durbin-Watson Statistic = 2.0342

Normality Test: Passed (P = 0.3317)

Constant Variance Test: Passed (P = 0.0600)

Power of performed test with alpha = 0.0500: 0.6805

The power of the performed test (0.6805) is below the desired power of 0.8000.

You should interpret the negative findings cautiously.

Appendix B

Selected NMR Spectra of Synthetic Intermediates and Products

Figure 1. ^{1}H NMR spectrum of compound **2.29**..... 196

Figure 2. ^{13}C NMR spectrum of compound **2.29**..... 197

Figure 3. ^{1}H NMR spectrum of compound **2.28**..... 198

Figure 4. ^{13}C NMR spectrum of compound **2.28**..... 199

Figure 5. ^{1}H NMR spectrum of compound **2.26**..... 200

Figure 6. ^{13}C NMR spectrum of compound **2.26**..... 201

Figure 7. ^{1}H NMR spectrum of compound **2.55**..... 202

Figure 8. ^{13}C NMR spectrum of compound **2.55**..... 203

Figure 9. ^{1}H NMR spectrum of compound **2.25**..... 204

Figure 10. ^{1}H NMR spectrum of compound **1.27**..... 205

Figure 11. ^{1}H NMR spectrum of compound **1.26**..... 206

Figure 12. ^{1}H NMR spectrum of compound **3.29**..... 207

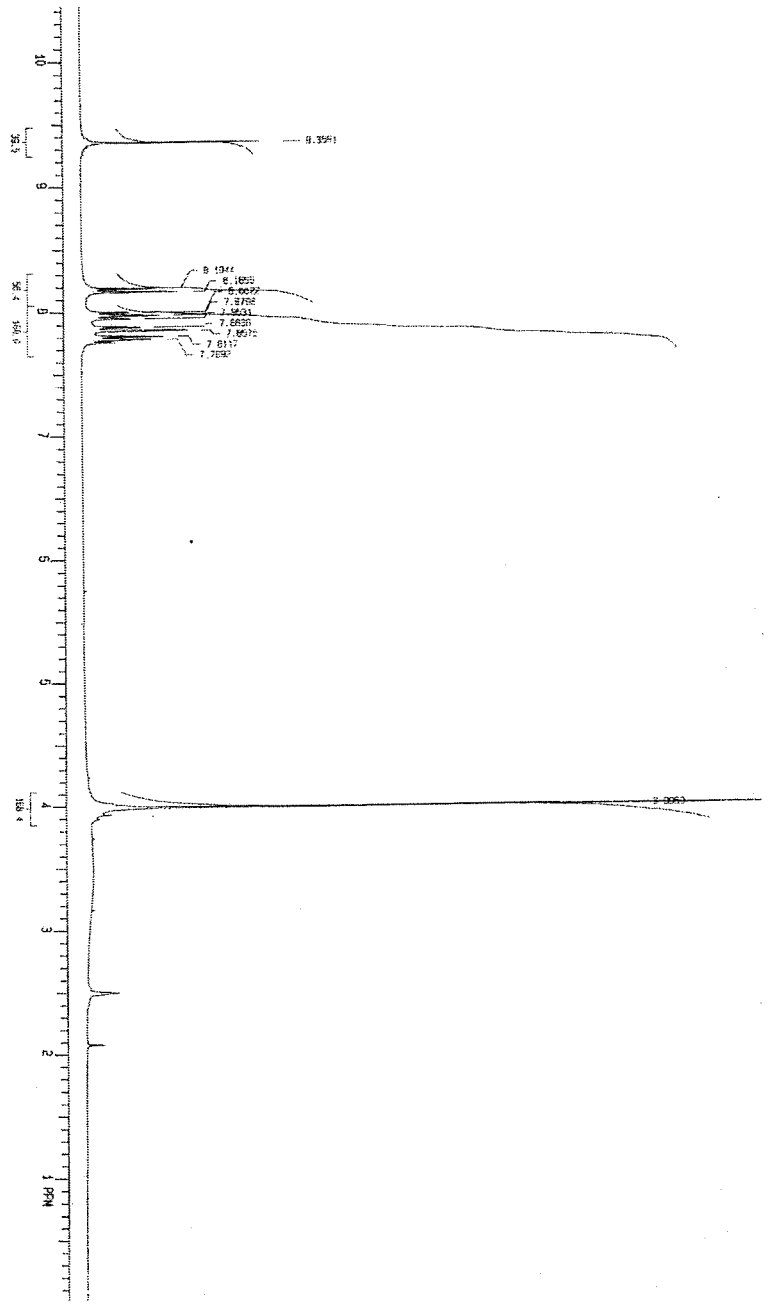

Figure 1. ^{1}H NMR spectrum of compound **2.29**

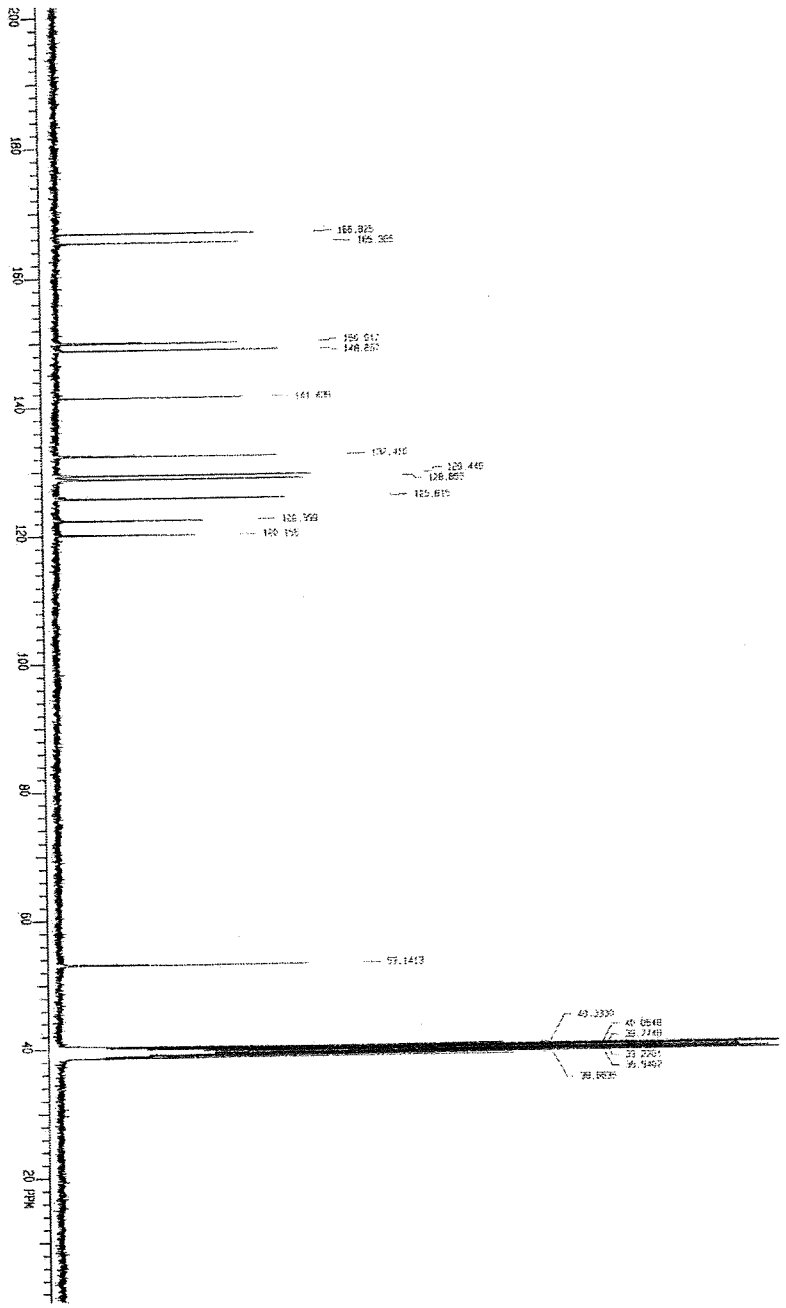

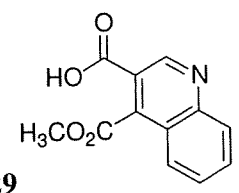

Figure 2. ^{13}C NMR spectrum of compound **2.29**

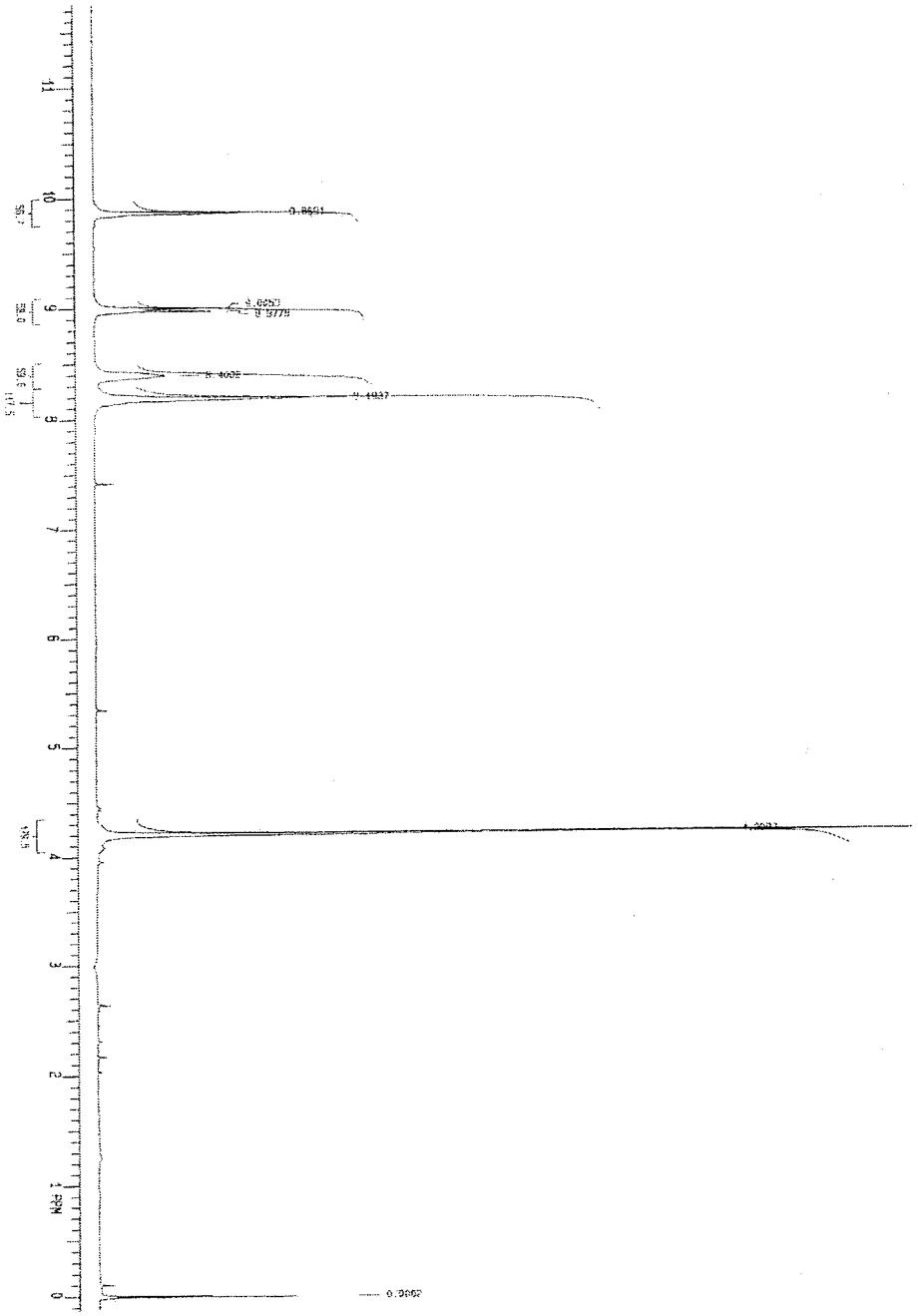

Figure 3. ^{1}H NMR compound **2.28**

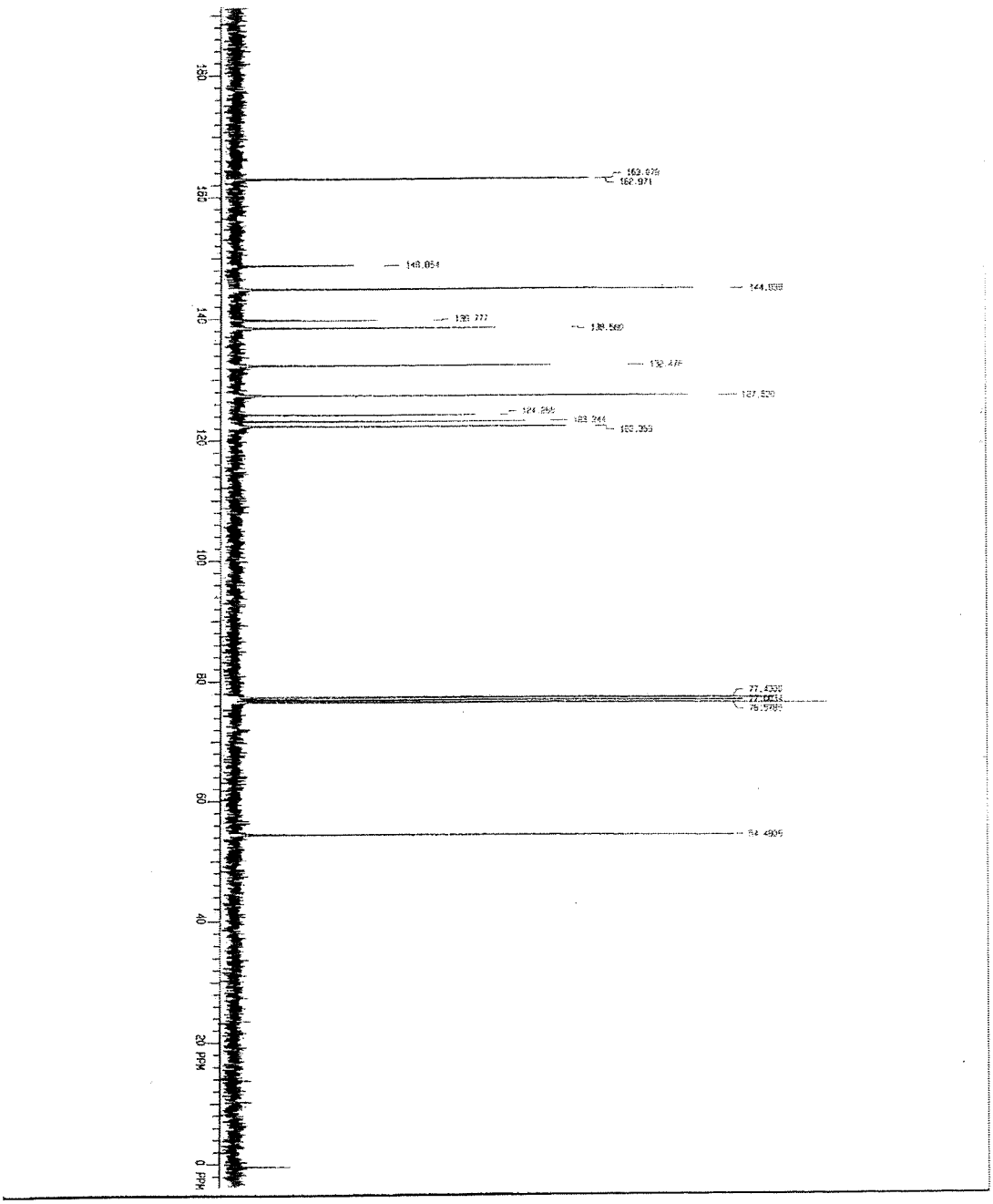

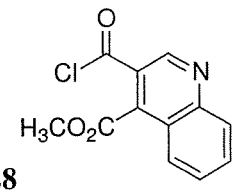

Figure 4. ^{13}C NMR compound **2.28**

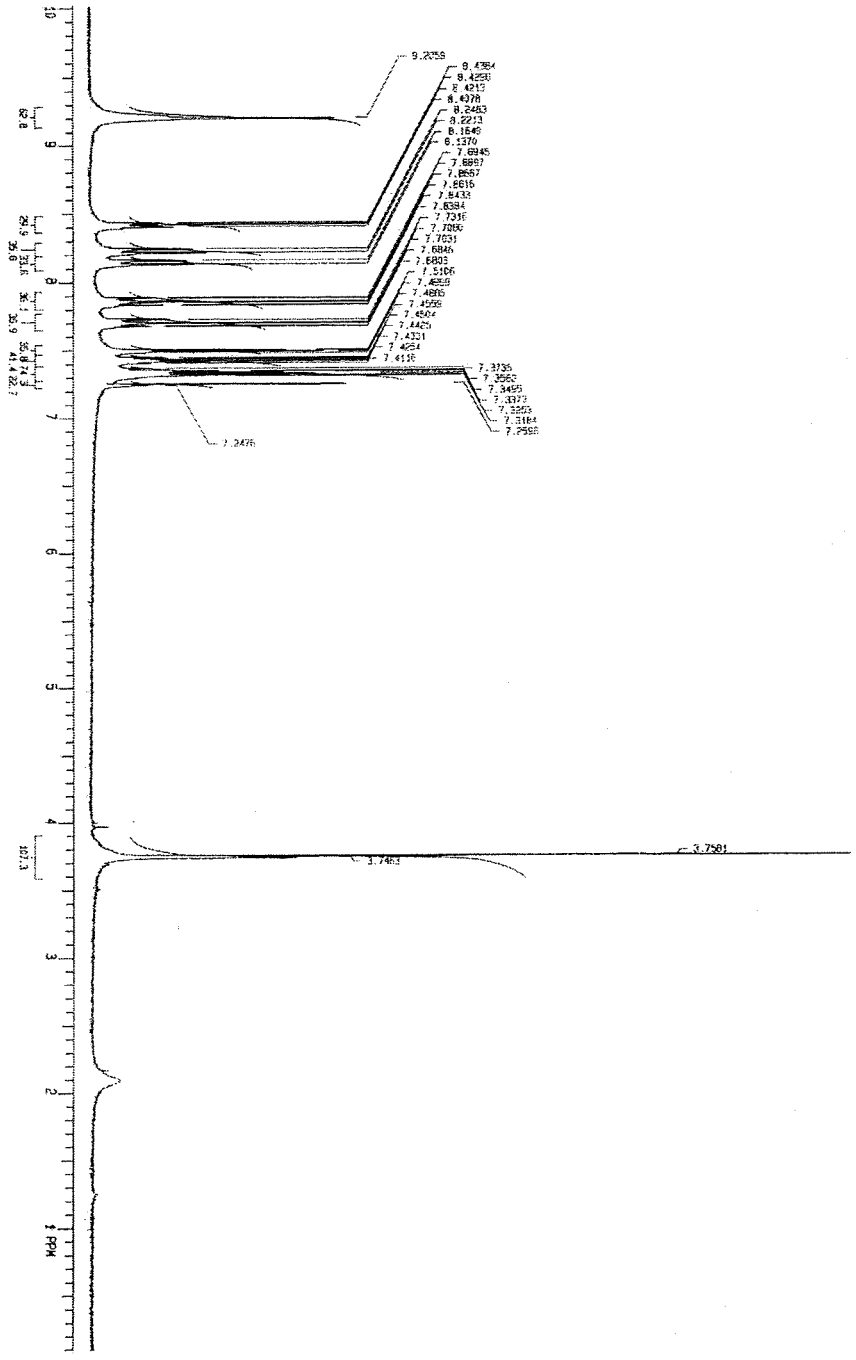

Figure 5. ^{1}H NMR compound **2.26**

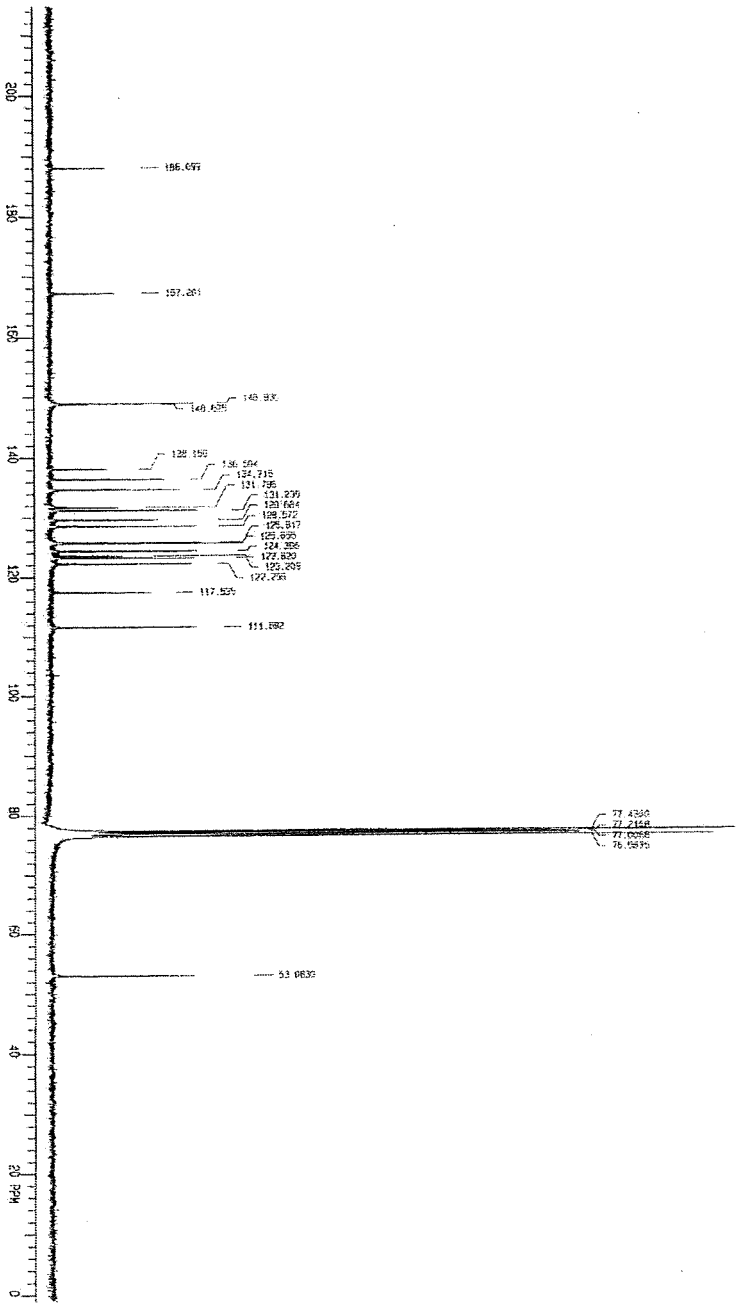

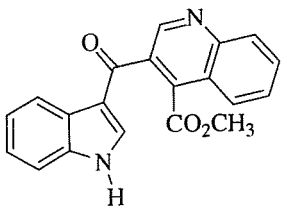

Figure 6. ^{13}C NMR compound **2.26**

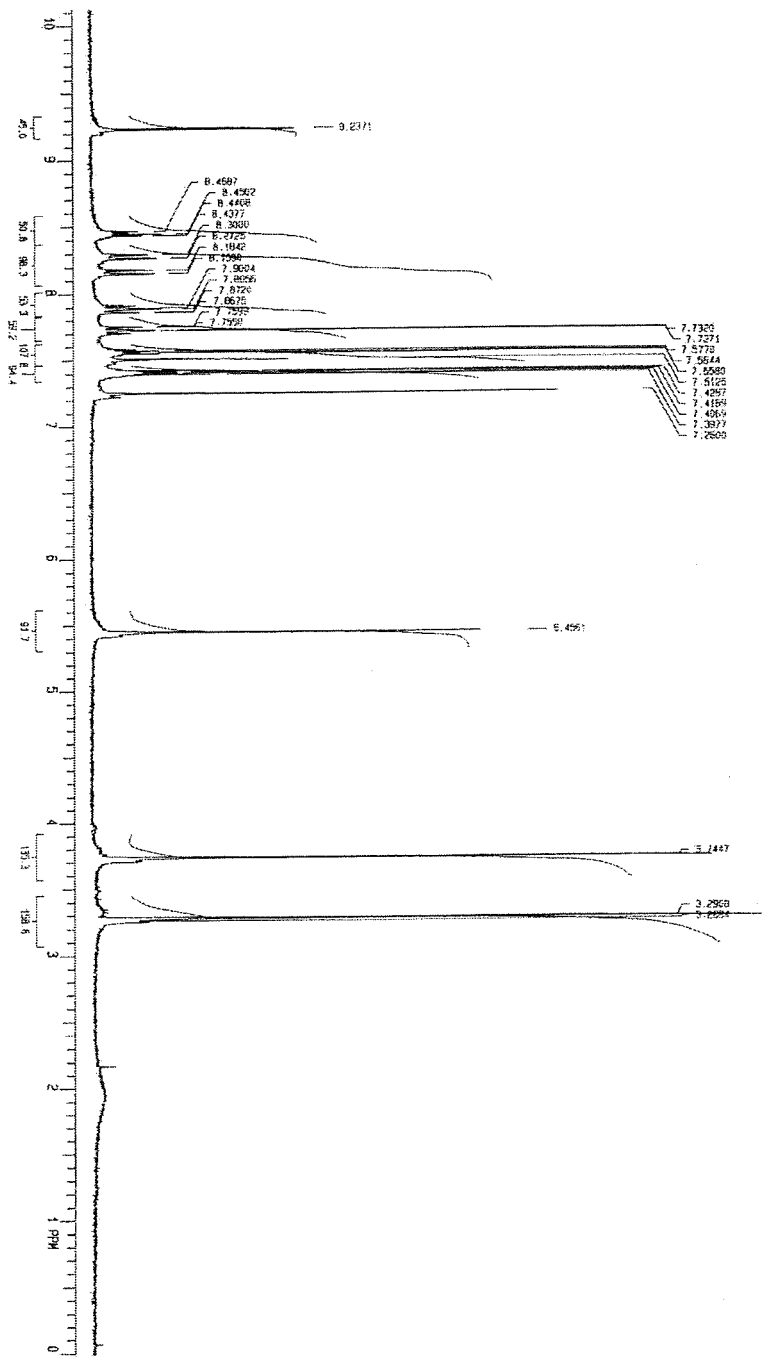

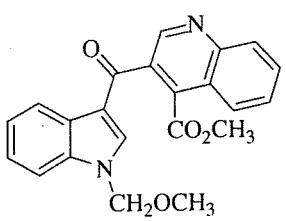

Figure 7. ^{1}H NMR compound **2.55**

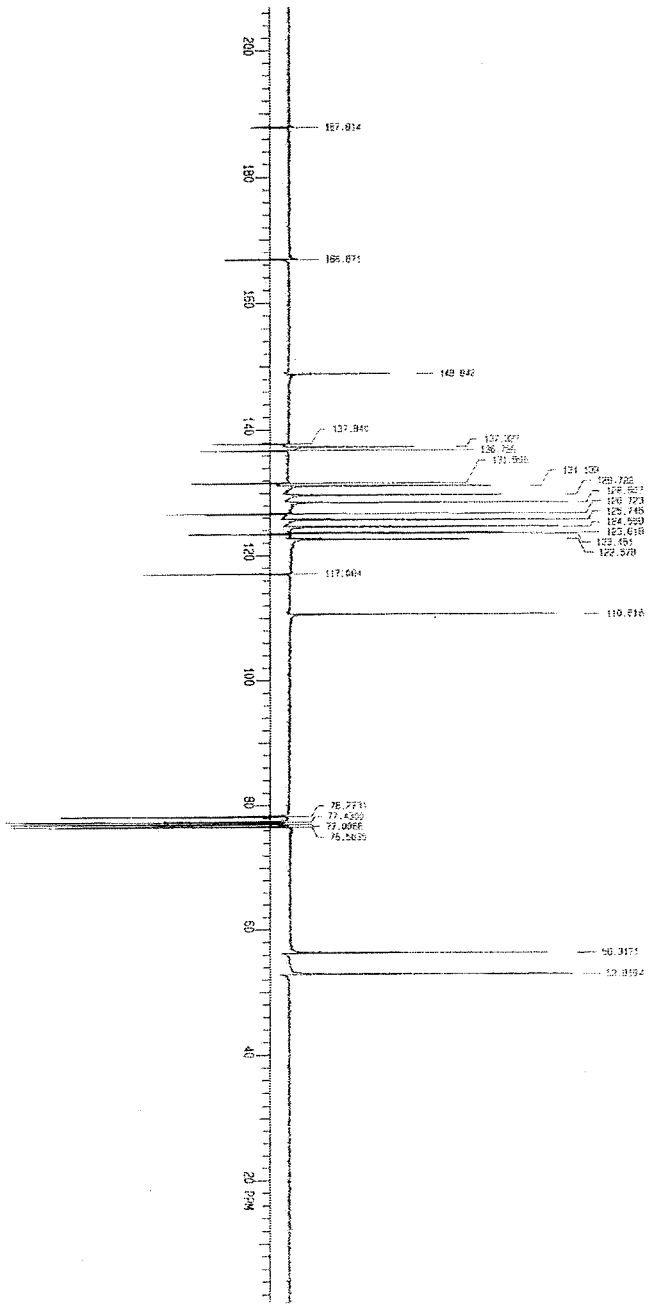

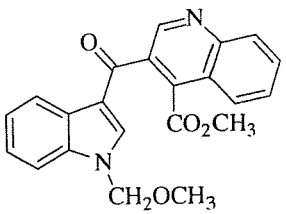

Figure 8. ^{13}C NMR (APT sequence) compound **2.55**

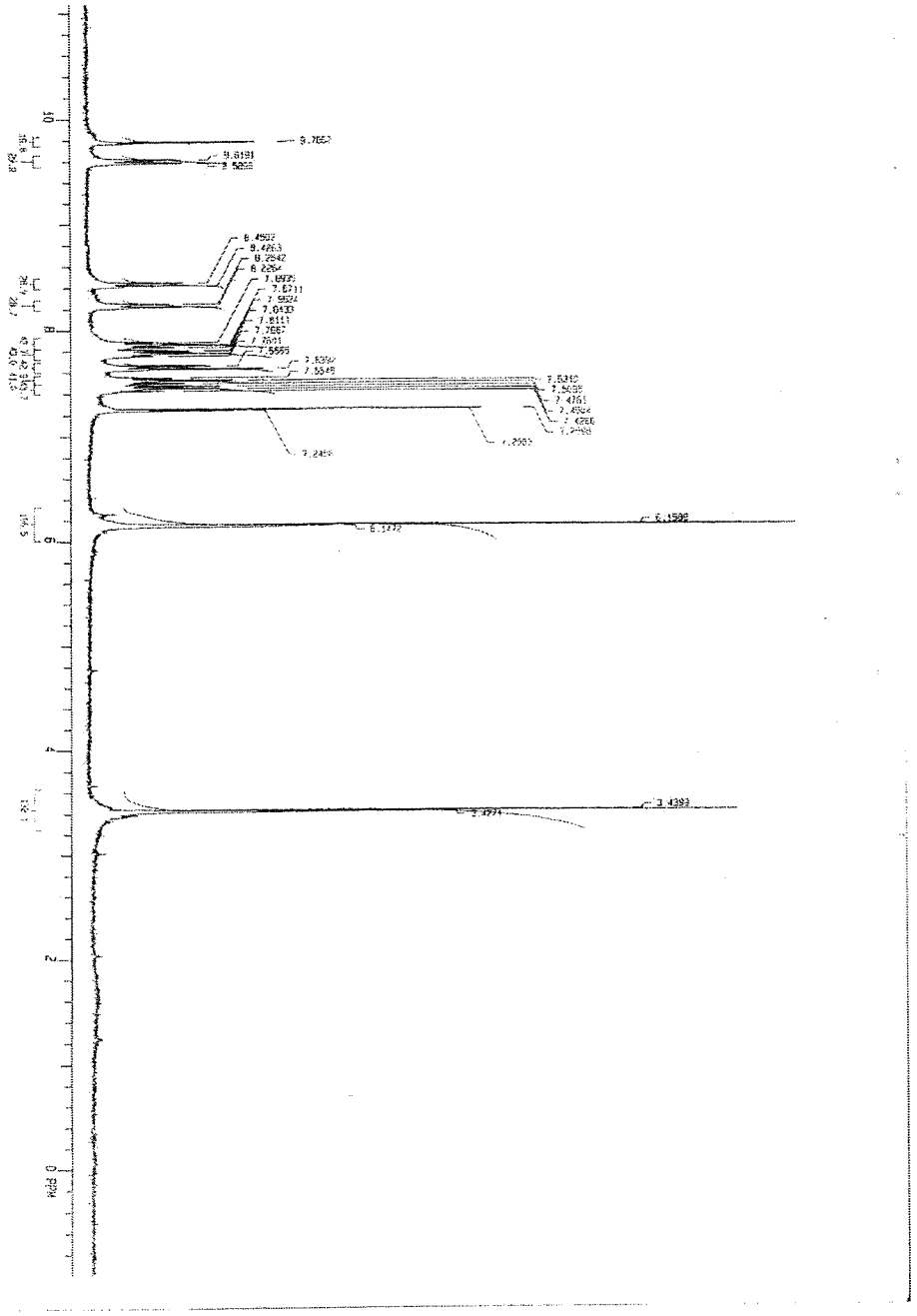

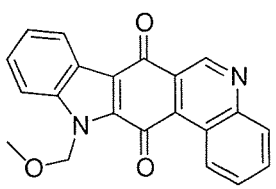

Figure 9. ^{1}H NMR compound **2.25**

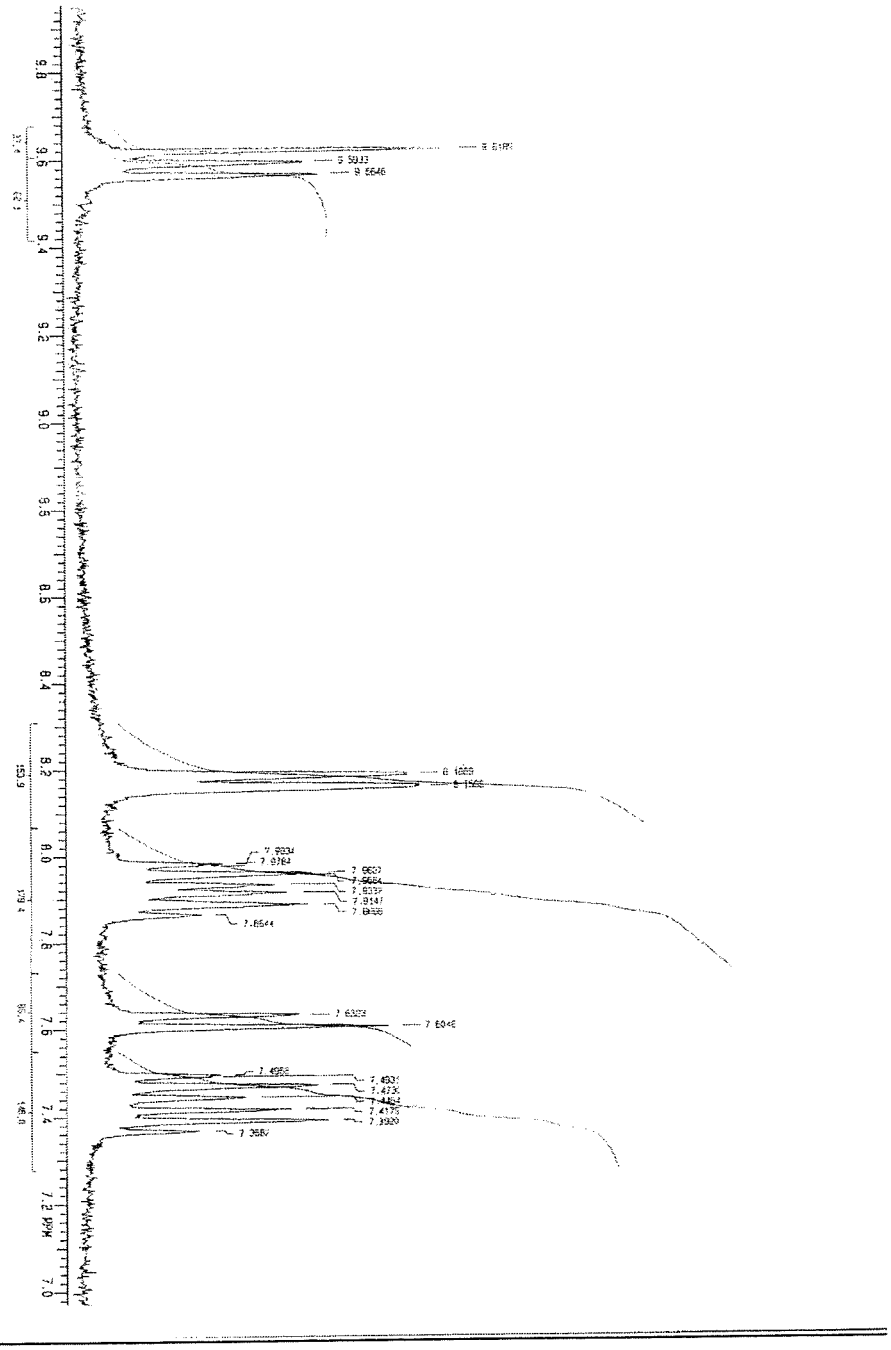

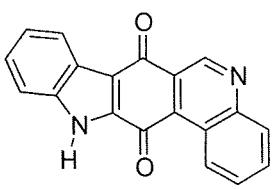

Figure 10. ^{1}H NMR compound **1.27**

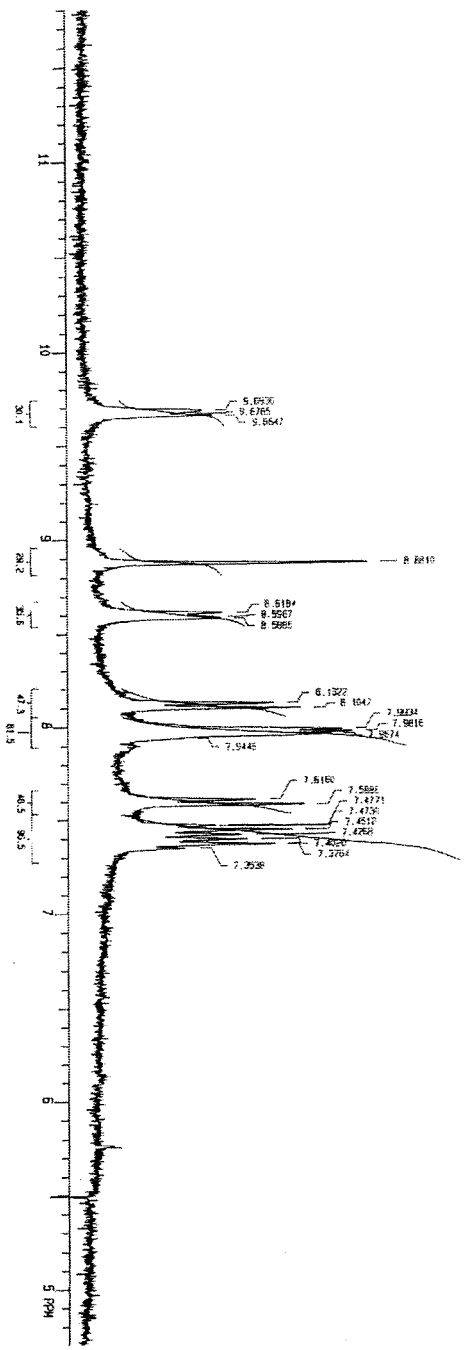

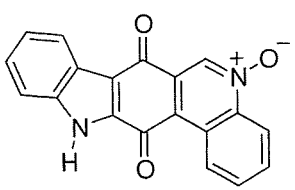

Figure 11. ^{1}H NMR compound **1.26**

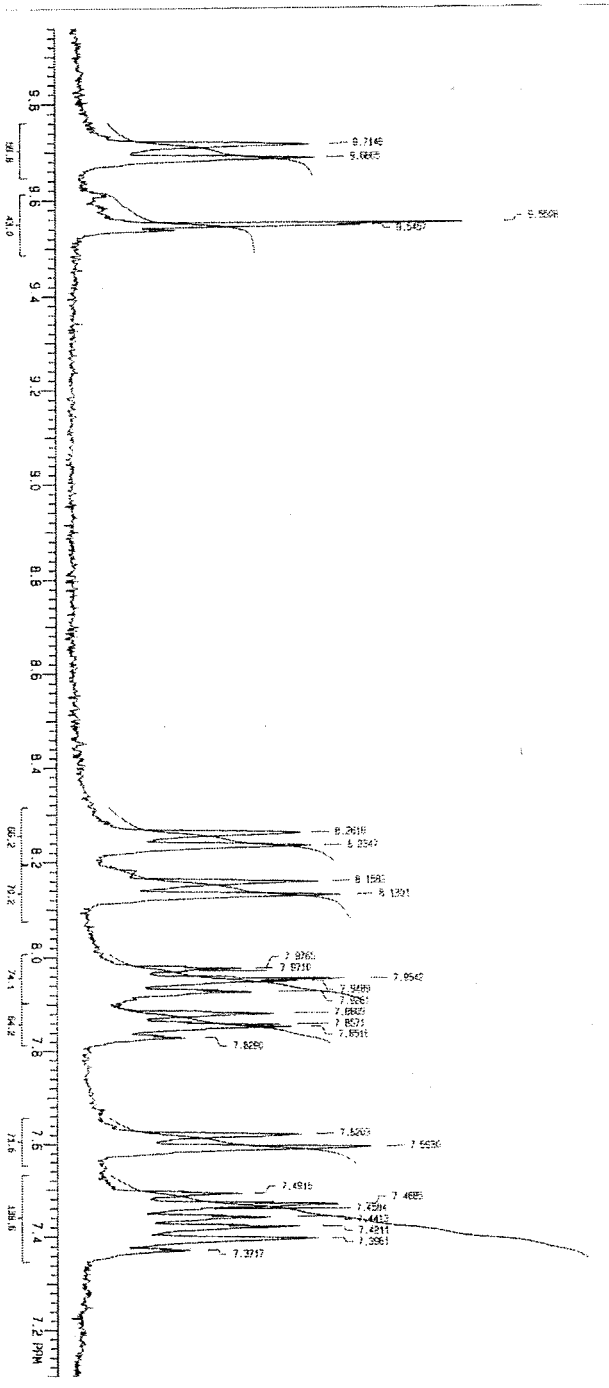

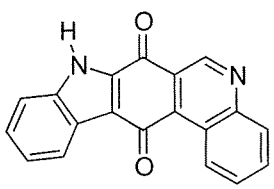

Figure 12. ^{1}H NMR compound **3.29**

2234512
A.N.U. LIBRARY

NOT FOR LOAN